Study and control of the production of 3-hydroxypropionic acid by an acetic acid bacterium in the context of extractive bioconversion

Claire Saulou-Berion, Florence De Fouchécour, Henri-Eric Spinnler

université PARIS-SACLAY

NNT : 2019SACLAXXX

Thèse de doctorat

AgroParisTech
INSTITUT DES SCIENCES ET INDUSTRIES DU VIVANT ET DE L'ENVIRONNEMENT
PARIS INSTITUTE OF TECHNOLOGY FOR LIFE, FOOD AND ENVIRONMENTAL SCIENCES

Étude et contrôle de la production de l'acide 3-hydroxypropionique par une bactérie acétique dans un contexte de bioconversion extractive

Thèse de doctorat de l'Université Paris-Saclay
préparée à AgroParisTech

Ecole doctorale n°581
Agriculture, Alimentation, Biologie, Environnement et Santé (ABIES)
Spécialité de doctorat: Biotechnologies

Thèse présentée et soutenue à Paris, le 3 décembre 2019, par

FLORENCE DE FOUCHÉCOUR

Composition du Jury :

Jean-Roch MOURET — **Rapporteur**
Chargé de Recherches, INRA, UMP Sciences pour l'Œnologie, Montpellier (France)
Heleen DE WEVER — **Rapporteur**
Project Manager, Flemish Institute for Technological Research (VITO), Mol (Belgique)

Carole MOLINA-JOUVE — **Examinatrice**
Professeur, INSA Toulouse, Toulouse Biotechnology Institute (TBI), Toulouse (France)
Nicolas BERNET — **Examinateur**
Directeur de Recherches, INRA, UR Laboratoire de Biotechnologies de l'Environnement (LBE), Narbonne (France)
Théodore BOUCHEZ — **Examinateur**
Directeur de Recherches, Irstea, UR Procédés Biotechnologiques au Service de l'Environnement (PROSE), Antony (France)

Henry-Éric SPINNLER — **Directeur de thèse**
Professeur, AgroParisTech, UMR Génie et Microbiologie des Procédés Alimentaires (GMPA)
Claire SAULOU-BÉRION — **Encadrante de thèse**
Maître de Conférences, AgroParisTech, UMR Génie et Microbiologie des Procédés Alimentaires (GMPA)

Université Paris-Saclay

AgroParisTech
ED n°581 ABIES

Étude et contrôle de la production de l'acide 3-hydroxypropionique par une bactérie acétique dans un contexte de bioconversion extractive

Study and control of the production of 3-hydroxypropionic acid by an acetic acid bacterium in the context of extractive bioconversion

Florence DE FOUCHÉCOUR

THÈSE PRÉSENTÉE POUR L'OBTENTION DU GRADE DE DOCTEUR DE L'UNIVERSITÉ PARIS-SACLAY
A THESIS SUBMITTED FOR THE DEGREE OF DOCTOR OF PHILOSOPHY OF UNIVERSITÉ PARIS-SACLAY

Superviseurs de la thèse **Thesis Advisors**
Pr. Henry-Éric SPINNLER (Directeur de thèse)
Pr. Ioan Cristian TRELEA
Dr. Claire SAULOU-BÉRION

Travaux menés au sein de **Works were carried out in**
UMR n°782 Génie et Microbiologie des Procédés Alimentaires
AgroParisTech, INRA
F-78550 Thiverval-Grignon, France

Page left blank intentionally

« Quelle étrange circonstance ! C'est à peine si l'imagination trouve à hasarder de ce fait une explication hypothétique ayant une base expérimentale quelconque. »

— **Louis PASTEUR**, février 1880,
Comptes-rendus des séances de l'Académie des Sciences 90:239-248

« La dernière démarche de la raison est de reconnaître qu'il y a une infinité de choses qui la surpassent. »

— **Blaise PASCAL**, 1670 (posthume),
Pensées

Page left blank intentionally

CONTENTS

Publications and Communications **v**

Acronyms and Symbols **vii**

List of figures **xi**

List of tables **xiii**

Introduction **1**

1 Literature review **5**
1.1 Attractiveness of 3-hydroxypropionic acid for the chemical industry 7
1.2 3-hydroxypropionic acid as microbial product: various routes with various hurdles 10
1.3 Overcoming hurdles to 3-hydroxypropionic acid commercial production through process engineering 26
1.4 Downstream processes for 3-hydroxypropionic acid recovery 33
1.5 Conclusion and outlooks 40

2 Material and methods **43**
2.1 Overall methodology 44
2.2 Materials 46
2.3 Batch cultures in shake-flasks (Chapter 3) 50
2.4 Fed-batch bioconversion of 1,3-propanediol in bioreactor (Chapter 3) 52
2.5 Extractive bioconversion of 1,3-propanediol (Chapter 4) 54
2.6 Analytical methods 58
2.7 Calculations 61
2.8 Modelling approach (Chapter 5) 63

3 An easy feeding strategy, based on pH control, for highly efficient production of 3-hydroxypropionic acid by *Acetobacter* sp. CIP 58.66 **65**
3.1 Introduction 66
3.2 Experimental approach 67
3.3 Results and discussion 69
3.4 Conclusion 81

4 Integrated production of 3-hydroxypropionic acid using non-dispersive extraction during bioconversion with *Acetobacter* sp. CIP 58.66 **83**
4.1 Introduction 84
4.2 Experimental approach 85
4.3 Results and discussion 87
4.4 Conclusion 98

5 Kinetic modelling of 3-hydroxypropionic acid production by *Acetobacter* sp. CIP 58.66 for further understanding and optimisation of the process **99**
5.1 Introduction 100
5.2 Experimental methods 101
5.3 Modelling methods 106
5.4 Results and discussion 114
5.5 Conclusion 128

Conclusion and perspectives **131**

References **139**

Appendices **155**
Appendix A 16S rRNA gene analysis of *Acetobacter* sp. CIP 58.66 155
Appendix B O_2 transfer characterisation in the bioreactor: k_La estimation 159
Appendix C Python script for parameter estimation 163

PUBLICATIONS AND COMMUNICATIONS

Patent

A patent is currently under study by the INRA department in charge of technology transfer:

Spinnler, H.E., **de Fouchécour, F.**, Sánchez-Castañeda, A.K., Trelea, C., Athès, V., Saulou-Bérion, C., Moussa, M., Production par *Acetobacter* sp. d'acide 3-hydroxypropionique et extraction en ligne par un contacteur membranaire.

Articles published in a international peer-reviewed journal

de Fouchécour, F., Sánchez-Castañeda, A.K., Saulou-Bérion, C., Spinnler, H.E., (2018) Process engineering for microbial production of 3-hydroxypropionic acid, *Biotechnology Advances* **(36)** 4, 1207-1222, doi: 10.1016/j.biotechadv.2018.03.020 (IF 2016: 10.597)

Articles to be submitted after the patent is published:

de Fouchécour, F., Lemarchand, A., Spinnler, H.E., Saulou-Bérion, C., An easy feeding strategy, based on pH control, for highly efficient production of 3-hydroxypropionic acid by an acetic acid bacterium (To be submitted to *Bioresource Technology*).

de Fouchécour, F.[1], Sánchez-Castañeda, A.K.[1], Ghorbal, S., Saulou-Bérion, C., Moussa, M., Athès, V., Trelea, C., Spinnler, H.E., Experimental demonstration of a non-dispersive extractive bioconversion for 3-hydroxypropionic acid production using an acetic acid bacterium (To be submitted to *Bioresource Technology*).
[1] These authors contributed equally

Communications orales sans actes

* speaker

de Fouchécour, F.*, Saulou-Bérion, C., Spinnler, H.E., (2018). Better characterising growth of Acetobacter aceti for its use in an integrated biotechnological process dedicated to 3-hydroxypropionic acid production. Journées des Doctorants ABIES, Paris, France (19/04/2018 – 20/04/2018),

(This presentation was rewarded with a bursary for international mobility)

de Fouchécour, F.*, Görge, J., Saulou-Bérion, C., Spinnler, H.E. (2018). Alleviating 3-hydroxypropionic acid production related stresses through an integrated process strategy. 4th Microbial Stress Meeting, Kinsale, Ireland (23/04/2018 – 25/04/2018)

de Fouchécour, F.*, Lemarchand, A., Saulou-Bérion, C., Spinnler, H.E. (2018). Étude de la production d'une molécule plateforme, l'acide 3-hydroxypropionique, par la bactérie acétique *Acetobacter aceti* pour sa mise en œuvre dans un procédé biotechnologique intégré. Congrès annuel de la Société Française de Microbiologie, Paris, France (01/10/2018 – 03/10/2018)

de Fouchécour, F.*, Lemarchand, A., Saulou-Bérion, C., Spinnler, H.E. (2019). Kinetic study of fed-batch production of 3-hydroxypopanoic acid (3-HP) by *Acetobacter aceti* within an integrated process. 5th European Congress of Applied Biotechnology, Florence, Italy (15/09/2019 – 19/09/2019)

Participation in a Young Scientist Panel

Béfort, N., **de Salivet de Fouchécour, F.**, de Rouffignac, A., Holt, C. A., Leclère, M., Loth, T., Moscoviz, R., Pion, F., Ruault, J.-F., Thierry, M. (2017). Toward a European bioeconomic transition: is a soft shift enough to challenge hard socio-ecological issues?. Youth scientist panel Position Paper - YSPPP - bioeconomy. Presented at European Workshop on Bioeconomy, Paris, France (2017-06-28 – 2017-06-29), doi : 10.15454/1.5087523122132947E12

ACRONYMS AND SYMBOLS

Molecules

1,3-PDO	1,3-propanediol
3-HP	3-hydroxypropionic acid
3-HPA	3-hydroxypropanal
3-HPAm	3-hydroxypropionamide
3-HPN	3-hydroxypropionitrile
4-HB	4-hydroxybutyrate
ATP	adenosine triphosphate
Cas9	CRISPR-associated endonuclease 9
cFDA	carboxyfluorescein diacetate
CoA	coenzyme A
CRISPR	Clustered Regularly Interspaced Short Palindromic Repeats
DDMA	didodecylmethylamine
DHA	dihydroxyacetone
DNA	desoxyribonucleic acid
IPTG	isopropyl β-D-1-thiogalactopyranoside
MCR	malonyl-CoA reductase
MSA	malonate semi-aldehyde
PEI	polyethyleneimine
PI	propidium iodide
PQQ	pyrroquinoline quinone
PVA	polyvinyl alcohol
rRNA	ribosomal ribonucleic acid
SAP	super absorbent polymers
TCA	tricarboxylic acid
TOA	trioctylamine

Organisms

A. lovaniensis	*Acetobacter lovaniensis*
B. subtilis	*Bacillus subtilis*
C. glutamicum	*Corynebacterium glutamicum*
E. coli	*Escherichia coli*
G. oxydans	*Gluconobacter oxydans*
I. orientalis	*Issatechenkia orientalis*
K. pneumoniae	*Klebsiella pneumoniae*
L. reuteri	*Lactobacillus reuteri*
S. cerevisiae	*Saccharomyces cerevisiae*

Other abbreviations

CC	Cell Count
CDW	Cell Dry Weight
e^-	electron
EU	European Union
HFMC	Hollow Fibres Membrane Contactor
HPLC	High Performance Liquid Chromatography
ISPR	*In Situ* or In Stream Product Recovery
MIC	Minimal Inhibitory Concentration
MTS	Microbial Transition State
OD	Optical Density
ODE	Ordinary Differential Equation
RO	Reverse Osmosis
rpm	Rotations Per Minute
vvm	Vessel Volume Per Minute

Symbols

ΔrG	Gibbs free energy of reaction	J mol^{-1}
ΔrG°	standard Gibbs free energy of reaction	J mol^{-1}
μ	specific growth rate	h^{-1}
μ_{max}	maximal specific growth rate	h^{-1}
π_0	3-HPA production rate	h^{-1}
π_1	3-HP production rate	h^{-1}
τ_{90}	duration for which $q_{\text{3-HP}} > 0.90 \cdot q_{\text{3-HP,max}}$	h
D_{in}	dilution rate due to feeding	h^{-1}
D_{out1}	dilution rate due to volume loss (aeration)	h^{-1}
D_{out2}	dilution rate due to volume loss (sampling)	h^{-1}
$f_{I,0}$	3-HP inhibition factor on 3-HPA production	*no unit*
$f_{I,1}$	3-HP inhibition factor on 3-HP production	*no unit*
$f_{I,X}$	3-HP inhibition factor on bacterial growth	*no unit*

$f_{L,0}$	1,3-PDO limitation factor on 3-HPA production	*no unit*
$f_{L,1}$	3-HPA limitation factor on 3-HP production	*no unit*
$f_{L,X}$	1,3-PDO limitation factor on bacterial growth	*no unit*
K_D	distribution (or partition) coefficient	*no unit*
K_{iX}	3-HP inhibition constant for biomass formation	mol L^{-1}
K_{i0}	3-HP inhibition constant for 3-HPA production	mol L^{-1}
K_{i1}	3-HP inhibition constant for 3-HP production	mol L^{-1}
K_{OW}	octanol/water partition coefficient	*no unit*
K_{sX}	1,3-PDO saturation constant for biomass formation	mol L^{-1}
K_{s0}	1,3-PDO saturation constant for 3-HPA production	mol L^{-1}
K_{s1}	3-HPA saturation constant for 3-HP production	mol L^{-1}
n_0	exponent coefficient of the 3-HP inhibition factor on 3-HPA production	*no unit*
n_1	exponent coefficient of the 3-HP inhibition factor on 3-HP production	*no unit*
N_g	number of generations	*no unit*
n_X	exponent coefficient of the 3-HP inhibition factor on bacterial growth	*no unit*
P_0	3-HPA concentration	mol L^{-1}
P_1	3-HP concentration	mol L^{-1}
pO_2	partial dioxygen pressure	% of saturation
$q_{\text{3-HP}}$	specific 3-HP productivity	$g_{\text{3-HP}}$ g_{CDW}^{-1} h^{-1}
$q_{\text{3-HP,max}}$	maximal specific 3-HP productivity	$g_{\text{3-HP}}$ g_{CDW}^{-1} h^{-1}
Q_{in}	inlet flow rate	L h^{-1}
Q_{out1}	flow rate of volume loss due to aeration	L h^{-1}
Q_{out2}	flow rate of volume loss due to sampling	L h^{-1}
$r_{\text{3-HP}}$	volumetric 3-HP productivity	$g_{\text{3-HP}}$ L^{-1} h^{-1}
$r_{\text{3-HP,max}}$	maximal volumetric 3-HP productivity	$g_{\text{3-HP}}$ L^{-1} h^{-1}
S_1	1,3-PDO concentration	mol L^{-1}
$S_{1,in}$	1,3-PDO concentration in the feeding solution	mol L^{-1}
t	time	h
V	working volume	L
w_i	weight attributed to variable i during the model's parameter optimisation	*no unit*
X	biomass concentration	Cmol L^{-1}
$Y_{P_0S_1}$	3-HPA yield from 1,3-PDO	mol mol^{-1}
$Y_{P_1P_0}$	3-HP yield from 3-HPA	mol mol^{-1}
Y_{XS_1}	Biomass yield from 1,3-PDO	Cmol mol^{-1}

Page left blank intentionally

LIST OF FIGURES

Chapter 1

1.1 Skeletal formula of 3-HP 7
1.2 The potential of 3-hydroxypropionic acid as building-block 8
1.3 Evolution over the years of the number of articles and patents on 3-HP 10
1.4 Main heterotrophic routes for 3-HP acid synthesis 14
1.5 Microbial agents under investigation for 3-HP production and their carbon source . 24
1.6 Multi-step strategies for 3-HP acid production from glycerol 31
1.7 Selection of the appropriate ISPR technique for 3-HP recovery 36
1.8 Schematic representation of reactive liquid-liquid extraction of 3-HP using tertiary amines 36

Chapter 2

2.1 Schematic representation of the overall methodology implemented in the present thesis 45
2.2 Picture of *Acetobacter* sp. 58.66 (Phase contrast microscope) 46
2.3 Schematic representation of a hollow fibre membrane contactor (HFMC) 49
2.4 Follow up of the growth of *Acetobacter* sp. CIP 58.66 from stock cultures, for inoculum preparation 51
2.5 Process and Instrumentation Diagram of the pH control-based fed-batch process . . 53
2.6 Process and instrumentation diagram of the extractive bioconversion 55
2.7 Correlation between optical density and cell dry weight of *Acetobacter* sp. CIP 58.66 58
2.8 Example of a cytogram of dual cFDA/PI staining for a sample from extractive bioconversions 59

Chapter 3

3.1 Putative metabolic pathway of 1,3-PDO oxidation into 3-HP by acetic acid bacteria 67
3.2 Experimental design of Chapter 3 68
3.3 Single-step, pH control-based fed-batch of *Acetobacter* sp. CIP 58.66 on 1,3-propanediol 72

3.4 Growth of *Acetobacter* sp. CIP 58.66 and glycerol consumption during the sequential process . . . 76
3.5 Bioconversion of 1,3-PDO into 3-HP by growing cells of *Acetobacter* sp. CIP 58.66 in a pH-based fed-batch, preceded by a first growth step on glycerol in batch mode . . . 79

Chapter 4

4.1 Experimental design of Chapter 4 . . . 86
4.2 Growth characteristics of *Acetobacter* sp. CIP 58.66 during extractive bioconversion 88
4.3 Evolution of the medium's composition during extractive bioconversion . . . 92
4.4 Total 3-HP and its distribution among the three phases (bioconversion medium, organic phase and back-extraction phase) . . . 95

Chapter 5

5.1 Schematic representation of the data sets used for modelling . . . 102
5.2 Example of the computation of volumes and flow-rates for one of the fed-batch experiments . . . 105
5.3 Schematic representation of the system being modelled . . . 108
5.4 Illustration of the variations of the 3-HP inhibition factor depending on the exponent value . . . 110
5.5 Results of the parameter optimisation . . . 115
5.6 Analysis of the residuals . . . 117
5.7 Representation of the model's limiting and inhibiting factors . . . 119
5.8 Model validation on the data from fed-batch bioconversion at pH 4.5 . . . 121
5.9 Comparison of the cumulative fed volumes of the different experimental conditions of sequential fed-batchs . . . 122
5.10 Model evaluation on the data from extractive bioconversions . . . 124
5.11 Model simulations for single-step fed-batch bioconversions . . . 125
5.12 Model simulations for batch cultures in shake-flasks with different initial 1,3-PDO concentrations . . . 127

Appendices

A.1 Phylogenetic tree of genus *Acetobacter* based on 16S rRNA gene sequences . . . 158
B.2 Schematic representation of the variations of O_2 concentration during its transfer . 159
B.3 Illustration of k_La calculation for one set of stirring and air flow conditions . . . 161
B.4 Results of the multivariate linear regression of k_La as a function of stirring and air flow rates . . . 162

LIST OF TABLES

Chapter 1

1.I Properties of 3-HP 7
1.II Best 3-hydroxypropionic acid production performances listed by type of metabolic pathway 12
1.III Extractive fermentations for microbial production of organic acids, using reactive liquid-liquid ISPR 38

Chapter 2

2.I List of chemicals with suppliers and purities 47
2.II Characteristics of the membrane contactor modules 49
2.III Media composition for cultures of *Acetobacter* sp. CIP 58.66 51
2.IV Operating conditions of the membrane contactor modules 56
2.V Conditions of analysis for HPLC quantifications 60

Chapter 3

3.I Index of methods used in Chapter 3 68
3.II Comparison of growth and bioconversion for different initial 1,3-PDO concentrations in shake-flasks cultures 70
3.III Growth comparison of *Acetobacter* sp. CIP 58.66 with glycerol as substrate, at different intial pH 74
3.IV Bioconversion characteristics of *Acetobacter* sp. CIP 58.66, after its growth on glycerol 80

Chapter 4

4.I Index of methods used in Chapter 4 86
4.II Growth and bioconversion performances of *Acetobacter* sp. CIP 58.66 during extraction bioconversion 89

Chapter 5

5.I Model nomenclature 107
5.II Overview of the stepwise parameter optimisation 113
5.III Parameter estimations resulting from stepwise optimisation 117

Conclusion and perspectives

CP.I Comparison of the different approaches towards 3-HP production from 1,3-PDO by acetic acid bacteria 132

Appendices

A.I Mix composition for PCR amplification 155
B.II Obtained k_La values 161
B.III Results of the k_La model's parameter estimation 162

INTRODUCTION

The beginnings of industrial biotechnologies – also known as white biotechnologies – date back to the mid 19th century, when the scientific basis of modern microbiology was established, through the pioneering works of Louis Pasteur. In particular, it was during this period that fermentation processes were proven to be biological phenomena, due to specific microorganisms [29, 166, 165]. With this new paradigm and with the emergence of biochemistry, ancient fermentation technologies, such as wine-making, were better understood, and could be rationally improved. Innovations were however not limited to traditional processes, and fermentation was also used for new applications. The best known example is the Acetone-Butanol-Ethanol (ABE) fermentation, that was developed from the 1910s, for rubber or explosives production. Interestingly, biotechnological production of organic acids for industrial use was first performed at this period. For example, in 1919, Pfizer commercialised citric acid produced through fermentation [29, 230]. Yet, biotechnological production of bulk chemicals remained limited throughout the 20th century. This might be attributed to the simultaneous rise of petrochemistry, which offered a great variety of chemical products, through more competitive processes. Meanwhile, biomanufacturing got more focused on higher value-added products, such as antibiotics (penicillin is the best-known example), enzymes, hormones, flavourings or fragrances [230].

With the soaring of petrochemistry during the 20th century, the chemical industry turned away from the promises of the early industrial biotechnologies, and it is now largely reliant on fossil feedstocks (*i.e.* crude oil, coal, and natural gas), both as energy source and as raw material. For instance, in 2011, crude oil and natural gas represented respectively 74 and 21 % of the feedstock sources for chemicals (*e.g.* plastics, lubricants or fertilisers) worldwide production [62]. Moreover, petrochemistry is the largest industrial oil consumer: in 2017, it accounted for 14 % of the world's demand for oil – half for use as feedstock, and half for process energy [89]. Consequently, the chemical industry is also a significant greenhouse gas emitter: in 2017, it represented 13 % of the industrial emissions in the European Union (EU) [67]. Today, the chemical industry is faced with growing concerns about its environmental impact, and about the forecasted petroleum shortage. Environmental concerns have been on the rise since the 1970s, but they are now more pressing than ever: despite an ever-increasing demand for manufactured goods, it is estimated that direct industrial CO_2 emissions need to be reduced by a third by 2050 (compared to 2014) in order to limit the mean temperature increase to 2 °C above preindustrial levels (with a 50 % chance) [121]. Regarding oil supply, the discovery of new oilfields and the exploitation of new sources (such as shale oil) have

delayed the unavoidable petrol depletion. However, uncertainties in the supply and in the economic growth, as well as the global geopolitical context, have resulted in high volatility and uncertainty in the global oil market [143]. Given these considerations, it appears as inevitable for the chemical industry to make the transition towards processes that consume less oil and emit less greenhouse gases. The main means towards these objectives are: increasing energy and material efficiencies, substituting fuels and raw materials, and using new technologies for carbon capture and storage [121]. These various goals are notably included in the twelve ground principles of Green Chemistry, that were introduced in order to provide a guiding framework towards more virtuous chemical products and processes [9].

In this context, biorefinery has been drawing an increasing interest for production of bulk chemicals from biomass resources [47]. The concept of biorefinery can be defined in an analogous manner to petroleum refinery, as the gathering of "a wide range of technologies able to separate biomass resources [...] into their building blocks [...] which can be converted to value added products, biofuels and chemicals" [46]. Closely related to the development of biorefinery, biotechnological processes have gained renewed attention for the production of bio-based chemicals. Indeed, they are versatile processes, that also offer great opportunities for cost and environmental footprint reduction [78, 161]. Research and innovation on the topic of bio-based chemical commodities – notably through biotechnological processes – are now being fostered by public policies. In the EU, only 6.8 % of the overall chemicals manufacture was bio-based in 2015 [168], so the EU has set itself ambitious objectives through the Bio-based Industries Consortium: the proportion of bio-based chemicals should reach 30 % by 2030 [18]. Moreover, the USA Department of Energy (DoE) has listed in 2004 and 2010 the most promising value-added chemicals that can be obtained from biomass [220, 25]. Criteria underlying these listings were mainly focused on the feedstocks from which the considered chemical can be obtained, on its potential as platform chemical, and on the technical complexity of the processes (from the feedstock to the building-block, and from the building-block to its derivatives) [220]. Interestingly, among the 28 chemicals that were selected in the original 2004 list, 20 of them are organic acids, making them a key group of platform chemicals. Until recently, the outlets of the organic acid market were confined to the food and feed, pharmaceutical, and cosmetic industries, but given their potential as building-blocks, it is expected that this market will significantly expand in short and medium terms [186, 42]. A prime example of this is microbially-produced succinic acid: its potential was foreseen in the 2004 DoE list, notably as a substitute of petrochemically-produced maleic anhydride [220]; and between 2014 and 2017, industrial-scale biotechnological production of bio-based succinic acid was achieved by several chemical companies [93]. However, many challenges still need to be overcome before industrial production of other promising organic acids can be considered, such as low yields and productivities, product toxicity to the microorganisms, or downstream product recovery, to name but a few [25, 139]. As a result, biotechnological production of bio-based organic acids remains an important research field.

*

The present thesis focuses on the case study of 3-hydroxypropionic acid (3-HP) microbial production: 3-HP is one of the top value-added chemicals from the original DoE list, but

– as will be presented later – many challenges still remain and commercial 3-HP production is not yet achieved in large volumes. This thesis is part of one of the research topics of the joint research unit for Microbiology and Food Process Engineering (UMR 782 GMPA, AgroParisTech, INRA, Thiverval-Grignon, France). Indeed, the project was initiated in 2012, in collaboration with the Research and Development Unit *AgroBiotechnologies Industrielles* (AgroParisTech, Pomacle, France). In a first instance, 3-HP production was achieved with a lactic acid bacterium, *Lactobacillus reuteri* [31]. In the meantime, a liquid-liquid in stream product recovery (ISPR) strategy was also designed for reactive extraction of 3-HP from the fermentation broth, using amines [32, 154]. A first attempt of extractive bioconversion was then carried out (*i.e.* 3-HP is bioproduced, while being continuously extracted from the medium, thanks to the ISPR system), and the key challenges to the improvement of that integrated process were identified. In particular, the microbial activity was dramatically inhibited because the toxicity of the organic phase used for the reactive extraction, but also because of the products toxicity [33]. Later works were dedicated to the understanding and the control of the mechanisms involved in the reactive extraction of 3-HP [37]. Today, research is aiming at optimising 3-HP production by *L. reuteri*, and at further optimising the ISPR performance and biocompatibility.

These works have highlighted two major features of the considered integrated process: (i) 1,3-propanediol (1,3-PDO) is an obligate by-product of 3-HP production by *L. reuteri* in quasi-equimolar proportions [31], thus significantly impairing the final yield; (ii) if the pH of the bacterial medium is above the pKa of 3-HP (4.51, [130]), the reactive extraction performances remain very limited. In order to tackle these challenges, both at once, a new approach was proposed and is the subject of the present thesis. Acetic acid bacteria are well-known for their ability to oxidise alcohols into the corresponding acids, and for their high resistance to acidic conditions [173]. Implementing an acetic acid bacterium within the integrated process that was initially conceived could thus be a way of converting the residual 1,3-PDO into 3-HP, while continuously removing 3-HP from the medium, using reactive extraction.

More specifically, the present thesis studies the **potential of this acetic acid bacterium for the development of a unitary process, in a context of integrated bioprocess development towards 3-HP production**. Several acetic acid bacteria strains were previously screened (unpublished work) and *Acetobacter* sp. CIP 58.66 was selected as the most promising one.
The objectives of the thesis are the following:

- **identifying the operating conditions ensuring efficient 3-HP production by the acetic acid bacterium**
- **identifying the challenges in integrating the bioconversion process with continuous product extraction**
- **assessing the impact of extraction on the strain's production performances**
- **understanding the key mechanisms involved in 3-HP production by the acetic acid bacterium (at cell and process levels)**

The different studies composing the current thesis will be successively described in the fol-

lowing chapters. First, a literature review is provided in Chapter 1, where the potential of 3-HP as platform molecule is presented, as well as an extensive review of the various strategies that were already implemented for 3-HP bioproduction – both from cell- and process-scale point of view. This chapter also includes an overview of the downstream processes that were developed for 3-HP recovery, with a special focus on the potential of reactive liquid-liquid extractive fermentation processes. Then, descriptions of the overall methodology of the thesis and of the experimental materials and methods are gathered in Chapter 2. The two following chapters (3 & 4) present and discuss the results thus obtained. Chapter 3 covers, on the one hand, the preliminary tests that were performed, in order to design an efficient process for 3-HP production; and, on the other hand, the results of the fed-batch process thus tested. Chapter 4 is dedicated to the experimental demonstration of a non-dispersive extractive bioconversion for 3-HP production. In order to gain more insights in the biological production of 3-HP by the strain, a mechanistic model was developed using data from Chapters 3 and 4. The modelling approach is detailed in Chapter 5, along with the main results and conclusions that were derived from this study. Finally, the conclusive section summarises the main findings of the present thesis, and offers a global discussion, as well as perspectives for future works.

CHAPTER 1

LITERATURE REVIEW

This chapter seeks to describe the overall context of microbial production of 3-hydroxypropionic acid (3-HP). First, the attractiveness of 3-HP for the chemical industry is explained. Then, the various approaches towards microbial 3-HP production are reviewed, in order to identify the main potentialities and challenges of each strategy. To this end, present understanding of the different possible metabolic pathways is also reviewed in order to highlight how an understanding of the metabolism can help develop more efficient processes. This study also includes a review of available *in situ* product recovery (ISPR) processes and highlights the questions addressed by these methods. Finally, the main conclusions are drawn and some outlooks are discussed.

Most parts of this chapter were published as a review paper:

> de Fouchécour, F., Sánchez-Castañeda, A.K., Saulou-Bérion, C., Spinnler, H.E. Process engineering for microbial production of 3-hydroxypropionic acid. *Biotechnology Advances* **36**, 4, 1207-1222 (2018).

Chapter's table of contents

1.1 Attractiveness of 3-hydroxypropionic acid for the chemical industry 7
1.1.1 Properties of 3-hydroxypropionic acid 7
1.1.2 Numerous potential applications of 3-hydroxypropionic acid 7
1.1.3 Chemical *versus* biotechnological production 9
1.2 3-hydroxypropionic acid as microbial product: various routes with various hurdles 10
1.2.1 Metabolic pathways for 3-HP production 11
1.2.1.1 Glycerol oxidation through a coenzyme A-dependent pathway 11
1.2.1.2 Glycerol oxidation through a coenzyme A-independent pathway . . . 13
1.2.1.3 Malonyl-coenzyme A pathway 15
1.2.1.4 β-Alanine pathway 16
1.2.1.5 Aerobic 1,3-propanediol oxidation 17
1.2.1.6 3-hydroxypropionitrile hydrolysis 18
1.2.1.7 Autotrophic CO_2 assimilation through the 3-hydroxypropionate / 4-hydroxybutyrate cycle and the 3-hydroxypropionate bi-cycle 18

1.2.1.8 Other pathways 19
1.2.2 Optimizing 3-HP production through metabolic engineering 20
1.2.3 Microbial agents for 3-HP production 22
1.3 Overcoming hurdles to 3-hydroxypropionic acid commercial production through process engineering 26
1.3.1 Operationnal strategies for 3-HP-producing fermentative processes . 26
1.3.1.1 Fermentation mode 26
1.3.1.2 Process parameters 28
1.3.2 Multi-step and integrated approaches 29
1.4 Downstream processes for 3-hydroxypropionic acid recovery 33
1.4.1 Challenges in the recovery of organic acids from fermentation broth . 33
1.4.2 A promising approach for 3-HP recovery: reactive liquid-liquid ISPR . 34
1.4.2.1 Principle 34
1.4.2.2 The progress made so far for 3-HP reactive liquid-liquid ISPR 37
1.4.3 Other approaches towards 3-HP recovery 40
1.5 Conclusion and outlooks 40

1.1 Attractiveness of 3-hydroxypropionic acid for the chemical industry

1.1.1 Properties of 3-hydroxypropionic acid

3-hydroxypropionic acid (3-HP) is a three-carbon carboxylic acid and a primary alcohol, thus being a non-chiral positional isomer of lactic acid. As a consequence of the hydroxyl group being in β position, 3-HP is a slightly stronger acid (pKa $= 4.51$) than propionic acid (pKa $= 4.87$), but it is a weaker acid than lactic acid (pKa $= 3.86$), whose hydroxyle group is in α position [37]. Due to its bi-functionality, the molecule displays a high reactivity and tends to dimerise at high concentrations. This is the reason why 3-HP is primarily found in concentrations around 30 % (w/v) when bought from chemical companies such as Sigma-Aldrich or T.C.I.. It might also explain why only a few of the 3-HP physico-chemical properties have been quantified yet. Finally, the bi-functionality and high reactivity of 3-HP are the reasons for the molecule's great versatility and potential as platform chemical.

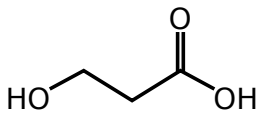

Figure 1.1: Skeletal formula of 3-hydroxypropionic acid (3-HP)

CAS Number	503-66-2	
Molar Mass	90.08 g mol^{-1}	
Density at 25 °C	1.449 g mL^{-1}	[130]
pKa at 25 °C	4.51	[130]
Solubility in water	very soluble	[130]
$\log K_{OW}$	-0.89	[154]
Boiling point	decomposes before vaporisation	[86]

Table 1.I: Physico-chemical properties of 3-hydroxypropionic acid (3-HP)

1.1.2 Numerous potential applications of 3-hydroxypropionic acid

The main applications of 3-HP can be divided into three main categories: (i) direct used; (ii) polymerisation; (iii) conversion into other platform chemicals. When used directly, 3-HP might serve as an additive or as a preservative agent in the food and feed industry [80]. The 3-HP homopolymer, denoted as poly(3-HP), was shown to be a promising alternative to petroleum-based plastics: it displays a low melting temperature (77 °C), good flexibility and high stability [11]. In addition, poly(3-HP) is also biodegradable and biocompatible. Furthermore, it was observed that other 3-HP-containing co-polymers (such as poly(3-hydroxybutyrate-*co*-3-HP)) shared the same ductility and flexibility characteristics. Thanks to their properties, these polymers may be considered for a wide range of processes (such as

film blowing, injection, thermoforming, lamination, *etc.*). Moreover, biodegradability and biocompatibility of poly(3-HP) also allow considering medical applications, such as use in drug capsules or as scaffold for tissue engineering [11].

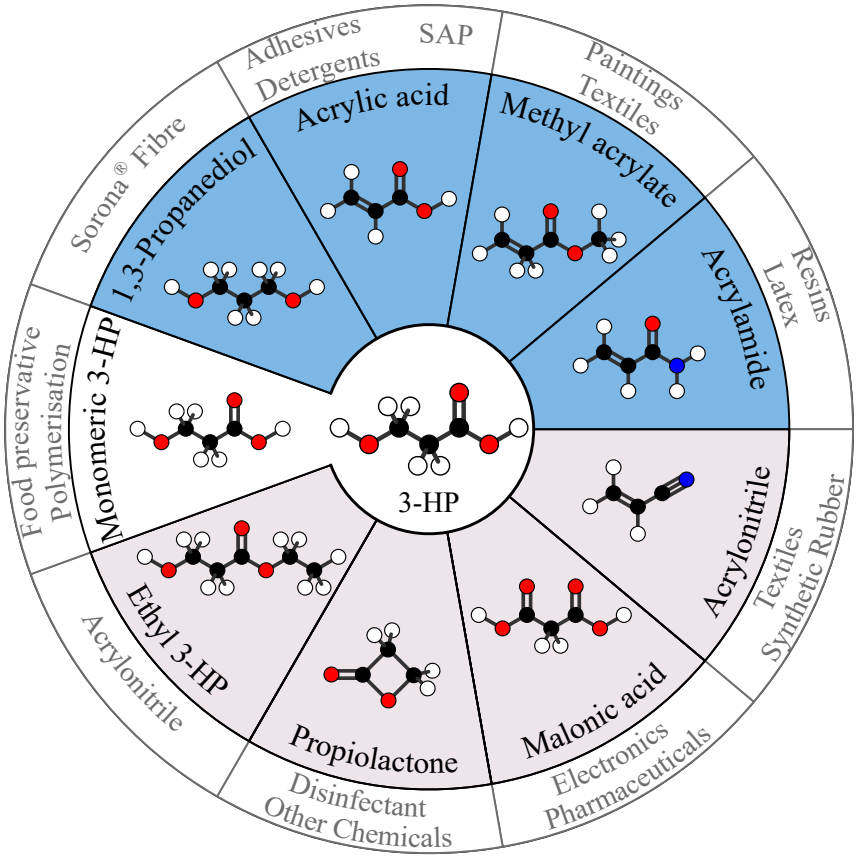

Figure 1.2: The potential of 3-HP as building-block
This figure shows the main derivatives and secondary chemicals that can be obtained from 3-HP, according to the US Department of Energy [220]. Chemicals that are already being produced in commodity (*i.e.* large) volumes are indicated in blue, in opposition to chemicals produced only in specialty volumes (light purple on the figure). Until now, these various compounds (commodity and specialty chemicals) are being produced from other precursors than 3-HP. For each compound, some of their most prominent possible end-uses are shown in grey (non-exhaustive list). SAP: super absorbent polymer (used in diapers, for example).

Apart from direct use or polymerisation, 3-HP also holds an important potential as building-block for the chemical industry (Fig. 1.2), which is the main reason for 3-HP beeing listed in the DoE (US Department of Energy) Top 12 value-added chemicals that can be obtained from biomass [220]. All possible applications presented in Fig. 1.2 will not be fully detailed here, but a noteworthy feature is that 3-HP may be converted either into chemicals that are already produced in commodity (*i.e.* large) volumes, or into chemicals that are – until now – only produced in specialty (*i.e.* more limited) volumes. It means that 3-HP can be used as an intermediate when considering switching from fossil feedstocks to biomass feedstocks for the production of commodities that are already widely used in the chemical industry (notably for acrylic acid, methyl acrylate and acrylamide); but it also means that 3-HP offers

the opportunity to bring new products to the market, whose production has remained limited until now due to high costs or hazardous chemical processes.

To this day, acrylic acid production from 3-HP (often advertised as bio-acrylic acid) has been the application drawing the most attention from chemical companies. In 2013, the worldwide capacity for acrylic acid was estimated around 5 million tonnes, corresponding to a market value over $ 11 billion [70]. Acrylic acid is produced by two-step propylene oxidation (propylene being obtained from oil cracking), and it is mainly used for the production of acrylate esters and of super absorbent polymers (SAP). This market thus appears as the biggest opportunity for 3-HP; and because it is currently only based on petrochemical feedstocks, it is a relevant candidate for the investigation of bio-based alternatives. 3-HP can be converted into acrylic acid in a single catalytic dehydration step [21, 212, 65]. So, when considering acrylic bio-based production, 3-HP appears as a great intermediate, since it can be biotechnologically produced from biomass and only one step is then required for its conversion into acrylic acid. Indeed, several industrial initiatives have already been launched: Cargill and Novozymes started a collaboration towards bio-acrylic acid in 2008, and were joined in 2012 by BASF (which eventually exited the project in 2015); Dow Chemical and OPX Biotechnologies also joined forces to that same goal in 2011 (OPX Biotechnologies was, however, bought by Cargill a few years later). Moreover, an alternative approach towards bio-acrylic acid was considered by Arkema and Nippon Shokubai: they invested in direct acrylic acid production from glycerol, but the project was finally abandoned, due to the increase in the price of glycerol [116]. Finally, a new partnership was announced very recently (september 2019) between the Archer Daniels Midland Company and LG Chem, but it was not specified whether 3-HP was involved in the considered approach. Still, bio-based acrylic acid production through 3-HP seems to remain the dominant approach. Yet, given the low oil prices, it is likely that implementing competitive bio-based processes will be very challenging in the coming years. To the best of our knowledge, commercial production of 3-HP (or of bio-acrylic acid) in large volumes is still unachieved.

1.1.3 Chemical *versus* biotechnological production

Several methods might be considered for the chemical synthesis of 3-HP. First, it can be produced by acrylic acid hydratation, but this route is highly unattractive since acrylic acid is the most interesting application of 3-HP. 3-HP might also be obtained through 3-hydroxypropionitrile hydrolysis or through alkali- and acid-catalysed β-propiolactone hydrolysis [59]. These last two processes, however, require the use of toxic compounds, which is incompatible with the principles of Green Chemistry [9], so their scaling-up seems quite unlikely.

In light of this, it appears that the great potential of 3-HP mostly stands in the fact that it can be obtained through biotechnological processes. Indeed, as will be detailed in the following sections, numerous microbial routes were investigated for 3-HP production. In addition to using bio-based raw materials, microbial processes generally do not require toxic reactants, they are more water-efficient than petrochemical processes, and they usually require milder

conditions (*e.g.* temperature, pressure) and are therefore also more energy-efficient [78, 161]. Fig. 1.3 shows that 3-HP production has been the object of an increasing research and development effort in the past years. In particular, the publication by the DoE of the list of the top 12 chemicals that can be obtained from biomass in 2004 seems to have triggered this trend. As can be expected, many different approaches have been investigated and this diversity will now be reviewed in the next sections.

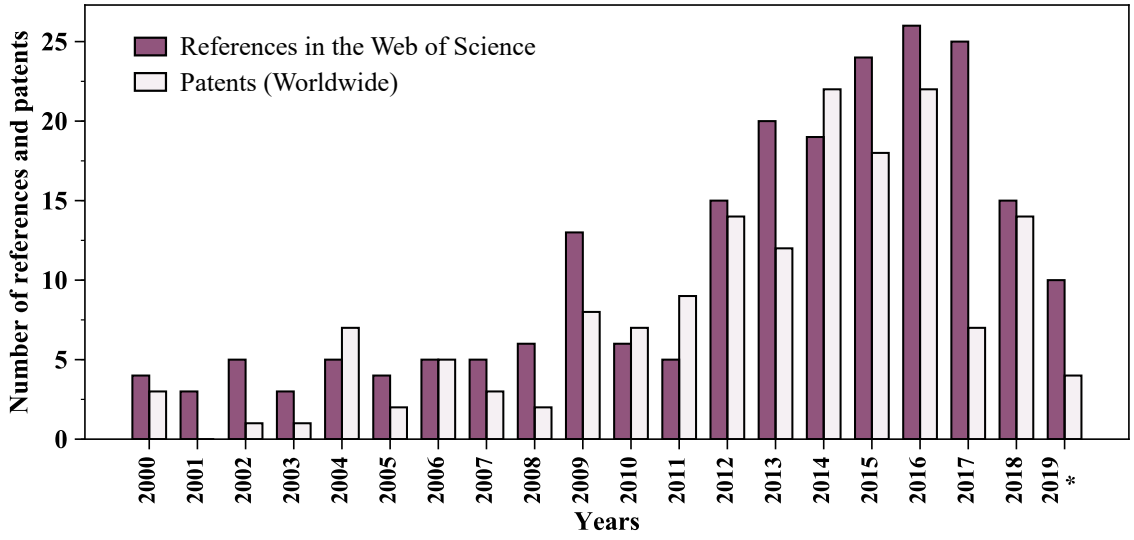

Figure 1.3: Evolution over the years of the number of articles and patents on 3-HP
These results were obtained by searching for "(3-hydroxypropionic acid) OR (3-hydroxypropionate)" in the title of articles and patents respectively in the Web of Science (accessed August, 16th 2019) and on the European Patent Office (accessed September, 29th 2019).
* Only the first six months of 2019 are considered

1.2 3-hydroxypropionic acid as microbial product: various routes with various hurdles

One of the essential strategic choices when designing a new process for biobased chemicals production is to select a relevant microbial agent and an efficient metabolic pathway. Ideally the selected microorganism is an easy-to-use, non pathogenic, genetically-stable microbe, and an efficient producer. In the case of 3-HP production, various approaches have been undertaken in order to develop microbial hosts suitable for such a process. Some of the best 3-HP biosynthesis performances are summed up at Table 1.II. Here, we aim at providing an overview of the possible metabolic routes and of the main strategies that were implemented,

for better understanding the rationale behind the various operational strategies that are being reviewed in this article. Genetic engineering works for the purpose of 3-HP production were already reviewed extensively several times. For details on these, readers are therefore referred to more comprehensive reviews [56, 94, 112, 113, 134, 145].

1.2.1 Metabolic pathways for 3-HP production

1.2.1.1 *Glycerol oxidation through a coenzyme A-dependent pathway*

3-HP is a natural end product of glycerol oxidation in *Lactobacilli*, which are obligate fermentative, Gram-positive bacteria. Glycerol metabolism was notably investigated in detail in *Lactobacillus reuteri*, a heterofermentative species living in human and animal gastrointestinal ecosystems [101]. This species cannot grow on glycerol as sole carbon or energy source [190, 201]. However, both resting (*i.e.* non-growing) cells and cells growing on other substrates (*e.g.* glucose or lactose) are able to consume glycerol. It is first dehydrated into 3-hydroxypropanal (3-HPA) in metabolosomes by a cobalamin (vitamin B_{12})-dependent diol dehydratase [192, 201]. Then, in the case of growing cells of *L. reuteri*, 3-HPA is reduced into 1,3-propanediol (1,3-PDO) with consumption of one mole of reducing equivalent per mole of 1,3-PDO produced. 3-HPA is used as electron acceptor for sugar fermentation. It leads to a fermentative shift from ethanol to the more oxidised product, acetate, thus stimulating cell growth from glucose [202]. On the other hand, when glycerol is supplied to resting cells, there is no such need for electron dissipation. 3-HPA is mainly accumulated in the medium [110, 185, 199]. However, 3-HP and 1,3-PDO are also found as by-products [199]. The reductive pathway (from 3-HPA to 1,3-PDO) remains the same. An oxidative pathway is activated that converts 3-HPA into 3-HP. The aldehyde is converted to 3-HP through a coenzyme A (CoA)-dependent, ATP-producing pathway (see Fig. 1.4.A)[8, 64, 179]. Sabet-Azad *et al.* [179] successfully introduced this pathway into *Escherichia coli*. When resting cells were used, 3-HP was the only product obtained, while 1,3-PDO was found as co-product when growing cells were used instead [179]. 3-HPA oxidation and reduction are in redox balance, thus implying that the theoretical 3-HP yield from glycerol is limited to $Y_{\text{3-HP}} = 0.5$ $\text{mol}_{\text{3-HP}}$ $\text{mol}^{-1}_{\text{glycerol}}$, with 1,3-PDO as an obligate by-product. In practice, yields are even lower due to the accumulation of 3-HPA. Moreover, this aldehyde accumulation is deleterious to cells. When accumulated, monomeric 3-HPA is in equilibrium with its hydrated form and its cyclic dimeric form; the mixture of these with acrolein is called reuterin [68, 200]. Due to the toxicity of reuterin, bioconversion of glycerol by *L. reuteri* in batch mode stops within a few hours [31].

Considering equation 1.1, the overall free energy liberation during conversion of glycerol into 3-HP is $\Delta rG'^{\circ}_{\text{glycerol}\rightarrow\text{3-HP}} = -50$ kJ mol^{-1}. Standard free energies were calculated using a group contribution method, according to Jankowski *et al.*, 2008 [90], and for the following conditions: pH = 7, zero ionic strength and a temperature of 298 K. The pathway thus seems thermodynamically feasible, however, the penultimate step has a positive standard free energy release ($\Delta rG'^{\circ}_{\text{3-HP-CoA}\rightarrow\text{3-HP-P}} = 15$ kJ mol^{-1}). Therefore, some bottlenecks might exist and further investigation would be necessary to identify in which conditions this step be-

Table 1.II: Best 3-hydroxypropionic acid production performances listed by type of metabolic pathway
Abbreviations: 1,3-PDO, 1,3-propanediol; 3-HPN, 3-hydroxypropionitrile; IPTG, isopropyl β-D-1-thiogalactopyranoside (used for induction)

Organism	Carbon Source	Scale	Process Type	Specific requirements	Titre $g\,L^{-1}$	Overall productivity $g\,L^{-1}\,h^{-1}$	Yield $mol_C\,mol_C^{-1}$	Ref.
Glycerol oxidation through a CoA-dependent pathway								
Lactobacillus reuteri	glycerol	3 L bioreactor	Fed-batch	–	14	0.25 [b]	0.49 [b]	[65]
Glycerol oxidation through a CoA-independent pathway								
Escherichia coli [a]	glycerol + glucose	5 L bioreactor	Fed-batch	vitamin B_{12}, IPTG	71.9	1.8	–	[48]
Klebsiella pneumoniae [a]	glycerol	5 L bioreactor	Fed-batch	IPTG	83.8	1.16 [b]	0.60[b]	[127]
Klebsiella pneumoniae [a]	glycerol	5 L bioreactor	Fed-batch	IPTG	102.61	1.07 [b]	0.86	[235]
Corynebacterium glutamicum [a]	glycerol + xylose	5 L bioreactor	Fed-batch	vitamin B_{12}, IPTG	54.8	0.76 [b]	–	[43]
Corynebacterium glutamicum [a]	glycerol	5 L bioreactor	Fed-batch	vitamin B_{12}, IPTG	62.6	0.87 [b]	0.51	[43]
Malonyl-CoA pathway								
Escherichia coli [a]	glucose	1.8 L bioreactor	Fed-batch	IPTG	48.4	–	0.53	[142]
Escherichia coli [a]	glucose	5 L bioreactor	Fed-batch	IPTG	40.6	0.56 [b]	0.19	[135]
β-Alanine pathway								
Escherichia coli [a]	glucose	6.6 L bioreactor	Fed-batch	–	31.1	0.63 [b]	0.423	[191]
Issatechenkia orientalis [a]	glucose	3 L bioreactor	Fed-batch	–	22.8	0.50 [b]	–	[14]
Saccharomyces cerevisiae [a]	glucose	1 L bioreactor	Fed-batch	–	13.7	0.17	0.14	[24]
Other heterotrophic routes								
Gluconobacter oxydans	1,3-PDO	7 L bioreactor	Batch	–	60.5	2.52 [b]	0.94	[234]
Acetobacter sp.	1,3-PDO	10 mL reaction volume	Batch	–	66.95	0.90	0.934	[122]
Comamonas testosteroni	3-HPN	50 mL jacketed vessel	Batch	–	–	23	–	[82]
Escherichia coli[a]	Palmitic acid + HCO_3^-	5 L bioreactor	Fed-batch	L-arabinose	52	–	–	[133]
Autotrophic routes routes								
Synechocystis sp.	$NaHCO_3$	100 mL shake-flask	Fed-batch	cupric ion induction	0.837	–	–	[217]
Pyrococcus furiosus	CO_2	1 L bioreactor	Batch	heat activation	0.366	–	–	[128]

– Value could not be calculated from given data

[a] Engineered microorganisms

[b] Value calculated from data given in the article

comes favourable [94, 147]. Despite the ATP formation accompanying 3-HP production, the metabolic route might not be energy-effective because of thermodynamic bottlenecks and because of the energetic cost for exporting products outside the cell [144]. This CoA-dependent pathway is also present in *Klebsiella pneumoniae*, along with the CoA-independent pathway [113]. 3-HP production in *K. pneumoniae* is however mostly considered through the latter (part 1.2.1.2).

$$\underset{\text{glycerol}}{C_3H_8O_3} + ADP^{2-} + HPO_4^{2-} + NAD^+ \longrightarrow \underset{3-HP}{C_3H_5O_3^-} + ATP^{3-} + H_2O + NADH + H^+ \quad (1.1)$$

1.2.1.2 *Glycerol oxidation through a coenzyme A-independent pathway*

Bacteria from genera *Klebsiella*, *Clostridium*, *Enterobacter* and *Citrobacter* are able to grow on glycerol during anaerobic fermentation. This property has typically been investigated for the purpose of 1,3-PDO production [19]. During glycerol fermentation, different metabolic routes are in redox balance with one another. Part of the glycerol is converted to more oxidised end products, such as lactate, succinate, formate, acetate and CO_2. Biomass production from glycerol also produces reducing equivalents. Glycerol already being a very reduced carbon source (4.67 e^-/C), its fermentation requires efficient routes for the dissipation of reducing equivalents. Possible end products depend on the microbial strain. For species like *Klebsiella pneumoniae* and *Citrobacter freundii*, 1,3-PDO is the main product along with acetate [50], the 1,3-PDO pathway serving as the reducing equivalent dissipation pathway. 1,3-PDO production from glycerol is a two-step route [19, 50], which makes it a quick way of dissipating electrons. The intermediary product between glycerol and 1,3-PDO is 3-HPA (Fig. 1.4.B). In some species, such as *K. pneumoniae*, this first step is catalysed by a vitamin B_{12}-dependent glycerol dehydratase. Despite 3-HPA being present as an intermediate, no significant amount of 3-HP is naturally produced by these microorganisms: 3-HP is not mentioned as an end product of glycerol fermentation [19, 50]. Nevertheless, *K. pneumoniae* was shown to possess a NAD^+-dependent aldehyde dehydrogenase that can use 3-HPA as a substrate and convert it to 3-HP [172]. Aldehyde dehydrogenase overexpression is however required for 3-HP biosynthesis in significant amounts. The two successive reactions leading to 3-HP from glycerol both have negative free energy releases: $\Delta rG'^{\circ}_{\text{glycerol}\rightarrow\text{3-HPA}} = -38$ kJ mol^{-1} and $\Delta rG'^{\circ}_{\text{3-HPA}\rightarrow\text{3-HP}} = -41$ kJ mol^{-1}. The overall free energy release is then $\Delta rG'^{\circ}_{\text{glycerol}\rightarrow\text{3-HP}} = -79$ kJ mol^{-1} (see equation 1.2 for the stoechiometrics), so this pathway is thermodynamically favourable. Despite the standard free energy being negative, it is likely that thermodynamical barriers arise in non-respiratory conditions, due to less efficient NAD^+ regeneration.

$$\underset{\text{glycerol}}{C_3H_8O_3} + NAD^+ \longrightarrow \underset{3-HP}{C_3H_5O_3^-} + NADH + 2\,H^+ \quad (1.2)$$

This CoA-independent pathway in *K. pneumoniae* is the most intensively investigated strategies for 3-HP production from glycerol. Works on engineering *K. pneumoniae* for 3-HP synthesis were recently reviewed by Kumar *et al.* [113]. It was identified that the limiting step

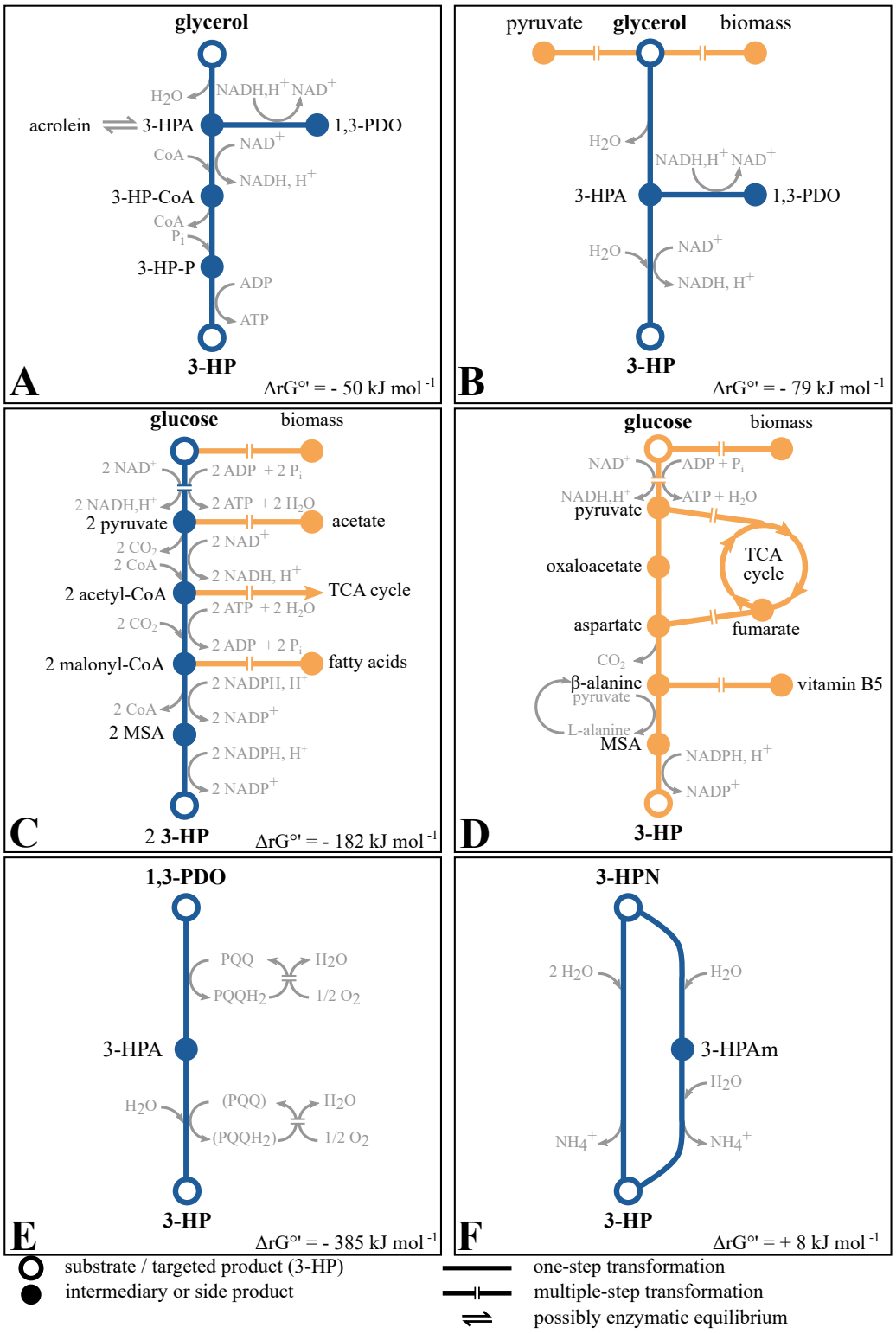

Figure 1.4: Main heterotrophic routes for 3-hydroxypropionic acid synthesis. Reactions presented with stoichiometrics are displayed in blue. Reactions presented without stoichiometrics (only qualitatively) are displayed in orange. Due to the different possible variants of the β-alanine pathway, free energy release was not calculated for this pathway. **A.** Glycerol oxidation through a CoA-dependent pathway. **B.** Glycerol oxidation through a CoA-indpendent pathway. **C.** Malonyl-CoA pathway. **D.** β-Alanine pathway. **E.** Aerobic 1,3-PDO oxidation. The cofactor of the second step is bracketed, because its exact nature is not known with certainty (see part 1.2.1.5). **F.** 3-HPN hydrolysis. Abbreviations: CoA, coenzyme A; P_i, inorganic phosphate (HPO_4^{2-}); 3-HPA, 3-hydroxypropanal; 3-HP-CoA, 3-hydroxypropionyl-coenzyme A; 3-HP-P, 3-hydroxypropionyl-phosphate; 1,3-PDO, 1,3-propanediol; MSA, malonic semialdehyde; TCA, tricarboxylic acid; 3-HPN, 3-hydroxypropionitrile; 3-HPAm, 3-hydroxypropionamide.

of 3-HP production, is the conversion of 3-HPA by an aldehyde dehydrogenase [127]. Efforts have therefore been made in order to engineer more efficient aldehyde dehydrogenases and to make this step more favourable. Li *et al.* [127] carried a systematic optimisation for 3-HP production by *K. pneumoniae*, taking multiple factors into account, such as promoter strength, metabolic pathway modifications, medium composition and operating parameters. Then the mutant strains were tested in a bioreactor, in fed-batch mode. They obtained one of the highest 3-HP titre so far: 83.8 g L^{-1} with a productivity of 1.16 g L^{-1} h^{-1}. A higher 3-HP titre was achieved only in one occurrence: in a recent study, Zhao *et al.* (2019) [235] screened a promoter library in order to overexpress the gene encoding the endogenous aldehyde dehydrogenase. The best performances were obtained when a *K. pneumoniae* strain displaying three tandem *tac* promoters was tested in fed-batch cultures. The final 3-HP titre was 102.61 g L^{-1} and is the highest reported so far in the literature. Interestingly, this approach could also prevent lactic acid formation, which is usually a by-product of glycerol consumption in *K. pneumoniae*.

This two-step, CoA-independent pathway has been implemented in other microbial hosts as well. It is predominantly used when 3-HP production from glycerol is considered with *E. coli* [56]. This approach in *E. coli* led to one of the highest 3-HP titre so far and the highest obtained in this species (71.9 g L^{-1}, see Table 1.II). Chu *et al.* [48] transformed *E. coli* W3110 with gabD4, a gene from *Cupriavidus necator* encoding a highly active aldehyde dehydrogenase. The enzyme activity was then improved by site-directed and saturation mutagenesis. During fed-batch conditions in a 5 L bioreactor, the most efficient mutant *E. coli* could produce 3-HP up to 71.9 g L^{-1} with a productivity of 1.8 g L^{-1} h^{-1} [48]. This CoA-independent pathway was also recently implemented in the industrial chassis *Bacillus subtilis* [100]. *B. subtilis* was transformed with the two-step pathway from *K. pneumoniae*. Further optimisation of medium composition and strain construction led to a stable genetic construction and a maximum 3-HP titre of 10 g L^{-1} in shake-flasks, with a 0.80 mol_C mol_C^{-1} yield.

Interestingly, this pathway was implemented in *E. coli* and *Corynebacterium glutamicum* for 3-HP synthesis from a mix of sugars, using glycerol only as an intermediate. Glucose and xylose were first converted to dihydroxyacetone (DHA) through glycolysis or pentose phosphate pathway, respectively. DHA was subsequently converted to glycerol through a synthetic pathway. 3-HP production was achieved from glycerol through the CoA-independent pathway [43, 99].

1.2.1.3 *Malonyl-coenzyme A pathway*

Among the various metabolic routes for 3-HP production from sugars, such as glucose, the malonyl-CoA pathway was the most studied until now (Table 1.II). The use of this pathway for 3-HP biosynthesis was already extensively reviewed [134]. Glucose conversion to 3-HP through the malonyl-CoA pathway has typically been investigated in model organisms, such as *E. coli*, *Saccharomyces cerevisiae* [134], and more recently in the fission yeast *Schizosaccharomyces pombe* [196]. The first part of the pathway, from glucose to two acetyl-

CoA (Fig. 1.4.C), is achieved through endogenous sugar catabolism, comprising glycolysis. Malonyl-CoA is then obtained from acetyl-CoA using an acetyl-CoA carboxylase. The last two steps, from malonyl-CoA to 3-HP (Fig. 1.4.C), are both catalyzed by a malonyl-CoA reductase (MCR) from the cyanobacterium *Chloroflexus aurantiacus*. The MCR has two distinct functional domains: the first one is C-terminal and catalyses malonyl-CoA's reduction into malonate semialdehyde (MSA), the second one is N-terminal and catalyses MSA's reduction into 3-HP. It was shown that the overall enzymatic activity was increased when MCR was separated in two fragments, MCR-C and MCR-N. The MCR-C step was however found rate limiting, and one of the highest 3-HP titer for the malonyl-CoA pathway (40.6 g L^{-1}, see Table 1.II) was achieved thank to balancing both MCR-C and MCR-N enzyme activities.

The overall transformation of glucose to 3-HP is redox neutral, since both molecules have the same electron equivalent per carbon atom (4 e^-/C). Consequently, this pathway does not require an effective dissipation of excess electrons, like pathways from glycerol do (see sections 1.2.1.1 and 1.2.1.2). In addition, the overall transformation of glucose into 3-HP is thermodynamically favourable, with a negative free energy release $\Delta rG'^{\circ}_{\text{glucose}\rightarrow\text{3-HP}} = -182$ kJ mol^{-1} (see equation 1.3 for stoichiometrics). A further advantage of the malonyl-CoA pathway is that it uses common metabolic intermediates, such as pyruvate and acetyl-CoA. Consequently, a great variety of feedstocks could be considered for 3-HP production. The malonyl-CoA pathway was notably used for 3-HP biosynthesis from a mix of glucose and xylose in *Saccharomyces cerevisiae* [105], from atmospheric carbon dioxide in cyanobacteria *Synechocystis* sp. PCC 6803 [217] and *Synechococcus elongatus* [115], and more recently from methanol in *Methylobacterium extorquens* [224]. However, a downside of resorting to common and central metabolic intermediates lies in the fact that there exist many competitive pathways. It leads to a broad range of by-products, thus limiting the maximal 3-HP yield from the substrate. Notably, acetate overflow is commonly observed when rapidly growing cells of *E. coli* are used. Moreover, malonyl-CoA is involved in the synthesis of fatty acids. It is thus necessary to implement strategies in order to limit the diversion of carbon flux towards other products. The highest performances obtained through the malonyl-CoA pathway were achieved by OPX Biotechnologies. Their work aims both at increasing MCR activity and at decreasing the fatty acid synthesis. They could reach a final 3-HP titre of 48.8 g L^{-1}, with a corresponding yield of 0.53 mol_C mol_C^{-1}[142].

$$\underset{\text{glucose}}{C_6H_{12}O_6} + 4\,NAD^+ + 4\,NADPH \longrightarrow 2\,\underset{\text{3-HP}}{C_3H_5O_3^-} + 4\,NADH + 2H^+ + 4\,NADP^+ \quad (1.3)$$

1.2.1.4 β-*Alanine pathway*

Another strategy for 3-HP production from glucose was proposed in *E. coli* and *S. cerevisiae*, through the β-alanine pathway. This was first patented by Cargill in *E. coli* [129], and by Novozymes in *S. cerevisiae* [91]. Moreover, Novozymes recently patented a β-alanine pathway for various microbial hosts, both bacterial and fungic [14, 204]. Glucose is first oxidised into pyruvate, which is subsequently converted to β-alanine. In turn, β-alanine is converted to malonic semi-aldehyde (MSA). This step also consumes an equivalent of pyru-

vate and releases an equivalent of L-alanine (Fig. 1.4.D). The L-alanine thus produced can be converted back into β-alanine using a 2,3-alanine aminomutase [24]. Finally, MSA is reduced to 3-HP. Borodina *et al.* used a genome-scale metabolic model and showed that the β-alanine route has a higher maximum theoretical 3-HP yield in comparison to the malonyl-CoA pathway, thus making it a more attractive route for an industrial process [24]. The maximal titre achieved in *S. cerevisiae* through this β-alanine pathway was reached in the same study by Borodina *et al* [24]. They further optimised the expression of the critical enzymes and increased aspartate's synthesis. The *S. cerevisiae* strain they developed was implemented in fed-batch and reach a final titre of 13.7 ± 0.3 g L^{-1}, with a yield from glucose of 0.14 ± 0.0 mol_C mol_C^{-1}[24], which remains below the best performances achieved with the malonyl-CoA pathway (Table 1.II). Like the malonyl-CoA pathway, the β-alanine route uses common metabolic intermediates and can thus be used with other substrates than glucose. Indeed, attempt was made to produce 3-HP from xylose by Kildegaard *et al.* They compared *S. cerevisiae* strains harbouring either the malonyl-CoA or the β-alanine pathway. They showed that in batch mode, the β-alanine pathway achieved higher titres than the malonyl-CoA pathway: 6.09 ± 0.33 g L^{-1} versus 2.30 ± 0.09 g L^{-1} [105]. The malonyl-CoA and β-alanine pathways were also compared in the case of 3-HP production from atmospheric CO_2 in *Synechococcus elongatus* [115]. In this case, CO_2 was first assimilated into phosphoenolpyruvate, which subsequently underwent either one of this pathway. In this study, the 3-HP titre was lower through the β-alanine pathway than through the malonyl-CoA pathway: 0.186 g L^{-1} versus 0.665 g L^{-1}.

An alternative β-alanine pathway was developed by Song *et al.* They implemented a route where aspartate is obtained from fumarate instead of oxaloacetate (Fig. 1.4.D). They obtained higher performances than the oxaloacetate-based pathway. Their final engineered *E. coli* strains reached a 31.1 g L^{-1} 3-HP titre in fed-batch mode, with a 0.423 mol_C mol_C^{-1} yield from glucose (Table 1.II) [191]. As for the malonyl-CoA pathway, the fact that the β-alanine pathways uses common metabolic intermediates implies that many side-products are synthesised along with 3-HP. β-Alanine is notably a precursor of vitamin B_5. Free energy release is not calculated here due to difficulties associated with the variety of possible routes and with the recycling of some of the intermediates.

1.2.1.5 *Aerobic 1,3-propanediol oxidation*

Acetic acid bacteria have been known since the beginning of modern microbiology for their ability to transform ethanol into acetic acid during vinegar production [164], but they are among the latest actors to have entered the scene of 3-HP production. These bacteria are Gram-negative, obligate aerobes, and are included in the *Acetobacteraceae* family. They possess various membrane-bound dehydrogenases, which gives them the ability to incompletely oxidise a broad range of alcohols and sugars directly in the periplasm [60]. Of interest here is that some strains from genera *Acetobacter* and *Gluconobacter* were shown to selectively oxidise 1,3-PDO to 3-HP [65, 122]. As first suggested by Dishisha *et al.* [65], the conversion is likely to occur similarly to that of ethanol into acetate, with two membrane-bound dehydrogenases involved (see Fig. 1.4.E). First a pyrroquinoline quinone (PQQ)-dependent

alcohol dehydrogenase oxidises ethanol into acetaldehyde [2, 4, 207]. The aldehyde is then further oxidised into acetic acid by an aldehyde dehydrogenase. It was originally thought that this aldehyde dehydrogenase also had PQQ as cofactor [3, 7]. Yet, later evidence suggested that PQQ was in fact not involved in the aldehyde oxidation [198]. Each step releases two electrons that are transferred to dioxygen through the respiratory chain [207]. Thus, the molar yield $Y_{\text{3-HP/1,3-PDO}}$ is not redox limited and can theoretically reach 1.0 $\text{mol}_{\text{3-HP}}$ $\text{mol}^{-1}_{\text{1,3-PDO}}$ when using resting cells. In the case of a PQQ-dependent aldehyde dehydrogenase, the overall free energy release would be $\Delta rG'^{\circ}_{\text{1,3-PDO}\rightarrow\text{3-HP}} = -385$ kJ mol^{-1} (considering equation 1.4), which suggests that 1,3-PDO oxidation is very favourable.

$$\underset{\text{1,3-PDO}}{\text{C}_3\text{H}_8\text{O}_2} + 4\ \text{PQQ} + 2\ \text{H}_2\text{O} \longrightarrow \underset{\text{3-HP}}{\text{C}_3\text{H}_5\text{O}_3^-} + \text{H}^+ + 2\ \text{PQQH}_2 \tag{1.4}$$

1.2.1.6 *3-hydroxypropionitrile hydrolysis*

Some bacterial genera, such as *Rhodococcus* and *Comamonas*, are able to hydrolyse aliphatic nitriles into corresponding carboxylic acids, in particular 3-hydroxypropionitrile (3-HPN) to 3-HP. The conversion can be carried out in one step using a nitrilase or in two steps by a combination of a nitrile hydratase and an amidase (Fig. 1.4.F). In the latter case, 3-HPN is first dehydrated by the nitrile hydratase to 3-hydroxypropionamide (3-HPAm), which is subsequently converted into 3-HP by the amidase [26, 82]. A nitrile-hydrolyzing activity was recently reported for the first time for the *Meyerozyma* genus. A yeast strain, identified as *Meyerozyma guilliermondii*, was isolated from soil and was found to be able to convert 3-HPN to 3-HP [231]. As highlighted by Bramucci *et al.* [26], carboxylic acids are readily obtained from nitriles through various chemical processes, however these chemical processes require strong acid or base use, or high operating temperatures. Therefore, using a biocatalyst instead should allow a greener and less energetically costly process. This biological pathway has several advantages: (i) its selectivity, 3-HP was each time the only reported product during 3-HPN bioconversion [26, 82, 231], (ii) the fact that no cofactor is required. However, 3-HPN may not be as readily available as other substrates, such as glycerol or glucose. It should also be noted that the overall reaction (see equation 1.5) has a slightly positive standard free energy $\Delta rG'^{\circ}_{\text{3-HPN}\rightarrow\text{3-HP}} = 8$ kJ mol^{-1}, thus indicating that operating conditions of the process have to be carefully chosen, in order to avoid thermodynamic hurdles.

$$\underset{\text{3-HPN}}{\text{C}_3\text{H}_5\text{ON}} + 2\ \text{H}_2\text{O} \longrightarrow \underset{\text{3-HP}}{\text{C}_3\text{H}_5\text{O}_3^-} + \text{NH}_4^+ \tag{1.5}$$

1.2.1.7 *Autotrophic CO_2 assimilation through the 3-hydroxypropionate / 4-hydroxybutyrate cycle and the 3-hydroxypropionate bi-cycle*

3-HP is also involved in carbon dioxide-assimilating metabolic pathways. There are six different CO_2 fixing pathways, as reviewed by Saini *et al.* and by Fuchs [181, 73]. Two of these pathways involve 3-HP as a key intermediary product: the 3-hydroxypropionate/4-hydroxybutyrate (3-HP/4-HB) cycle and the 3-hydroxypropionate bi-cycle. The latter was discovered almost 30 years ago, while the former was discovered ten years ago [17, 85].

Producing 3-HP from carbon dioxide would be very interesting, because it is a cheap, abundant and environmentally relevant carbon source. This would constitute the main advantage of using this kind of pathway. However, 3-HP is not an end product of these pathways and it is not naturally accumulated, or if so only in small amounts [85]. Genetic engineering is therefore required in order to take advantage of these metabolic routes. In fact, research aiming at 3-HP production from CO_2 has already been undertaken, but is still at its early stages [103, 128]. In these studies, part of the 3-hydroxypropionate/4-hydroxybutyrate cycle from the archeon *Metallosphaera sedula* was introduced into the archaeon *Pyroccocus furiosus*. Hence, 3-HP formation was achieved from carbon dioxide as carbon source, dihydrogen as electron donor and maltose as acetyl-CoA and ATP source. At best, the final 3-HP titre reached a few hundreds of milligrams per litre (Table 1.II). Enzymes involved in these autotrophic pathways can also be used for the creation of synthetic heterotrophic pathways. In particular, the malonyl-CoA reductase from the 3-hydroxypropionate bi-cycle of *Chloroflexus aurantiacus* is used for 3-HP production by recombinant *Escherichia coli* or *Saccharomyces cerevisiae* from glucose through the malonyl-CoA route [135] (see section 1.2.1.3).

As mentioned above, inorganic carbon fixation into 3-HP was also attempted photosynthetically, using engineered cyanobacteria *Synechocystis* sp. PCC 6803 or *Synechoccus elongatus* PCC 7942 [115, 217, 215]. CO_2 was assimilated into pyruvate or phosphoenolpyruvate through the ubiquitous Calvin cycle. These intermediates were then further reduced into 3-HP either through the malonyl-CoA pathway [115, 217] or through the β-alanine pathway [115].

1.2.1.8 *Other pathways*

Another metabolic route, the propionyl-CoA pathway, was recently explored for 3-HP production from propionate in *E. coli* [140]. Propionate is first converted to propionyl-CoA, which is subsequently oxidised into acryloyl-CoA using an equivalent of $NADP^+$. Acryloyl-CoA is then hydrated to 3-HP-CoA, whose CoA residue is then transferred to acetate, thus leading to the production of one equivalent of 3-HP and acetyl-CoA. A maximum of 1.60 g L^{-1} was obtained in shake-flasks experiments [140]. Interestingly, it was observed in the same study that in the absence of glucose, 3-HP production was low (0.06 g L^{-1}). Indeed, when propionate serves as sole energy and carbon source for bacterial growth, the flow through the propionyl-CoA pathway decreases. It was also suggested that the quantity of ATP produced from propionate, which is not a preferential energy source for *E. coli*, could not ensure the synthesis of both growth-related and heterologous proteins. 3-HP production was therefore further limited. Glucose addition could help compensate for this energy deficiency [140].

Two new alternative metabolic routes were also recently engineered in *E. coli* for 3-HP from acetate and fatty acid feedstocks, respectively [117, 133]. By addressing the various limitations of 3-HP production from fatty acids (such as low substrate uptake and metabolic fluxes imbalances), Liu *et al.* managed to engineer an efficient pathway: a 52 g L^{-1} final titre was obtained from palmitic acid and HCO_3^- [133]. Fatty acids are highly relevant feedstocks in

the context of biorefinery, because they are a cheap and abundant raw material: examples of such feedstocks are palm fatty acid distillate (by-product of palm oil) or waste cooking oil. Liu *et al.* attempted 3-HP production from waste cooking oil with the *E. coli* strain they had developed: even though 3-HP production was observed, it remained low (3.2 g L^{-1}). This was attributed to the diversity of fatty acids contained in the waste cooking oil, making it challenging for the bacteria to consume all these possible substrates.

Lastly, 3-HP was also found to be an end product of uracil or acrylic acid degradation. This was reported for both prokaryotes and eukaryotes: *Escherichia coli* K-12 and *Saccharomyces kluyveri* were shown to produce 3-HP from uracil [10, 138]; and 3-HP production starting from acrylic acid was observed for fungi [54, 197] and for bacterium *Alcaligenes faecalis* [12]. It was also reported that 3-HP can be produced — through an unknown pathway — by endophytic fungi as a nematicidal agent [189]. However, except for acrylic acid degradation by *Rhodococcus erythropolis* [118], these various pathways were not evaluated as such for 3-HP commercial production.

1.2.2 Optimizing 3-HP production through metabolic engineering

An efficient microbial host is required in order to ensure a commercially relevant process. Therefore, once a metabolic route towards 3-HP is introduced in a non-native producer, further metabolic engineering works are needed to obtain an efficient microbial candidate. This is also true for some native producers, such as *Lactobacillus reuteri*, that do not naturally produce high amounts of 3-HP. Metabolic engineering strategies were already extensively reviewed on several occasions [56, 94, 112, 113, 134, 145]. The key points to understanding the main challenges are presented here along with the most recent works.

In order to improve 3-HP yields, it is necessary that the carbon flux from the substrate is sufficiently channelled through the 3-HP producing pathway. Efforts have thus been made in order to reduce the carbon flow in competitive pathways, which mainly include biomass build-up and efficient ATP-generating pathways. Lactate and acetate are major by-products during 3-HP production from glycerol or from sugars. Final titre of lactate was successfully reduced by Chen *et al.* by knocking out the ldhA gene encoding a lactate dehydrogenase in *Corynebacterium glutamicum* [43]. In shake-flask cultivation, the resulting strain produced almost no lactate (0.4 g L^{-1} *versus* 7.4 g L^{-1} with the control strain) and had an increase of 19.4 % in 3-HP production from glucose [43]. Knockouts of genes encoding enzymes involved in the production of acetate was also proven efficient during 3-HP production through the CoA-independent glycerol pathway in *C. glutamicum* and *E. coli* by Chen *et al.* [43] and Jung *et al.* [98], respectively. A decrease of 52.8 % and 97.2 % in acetate production were observed in *C. glutamicum* and *E. coli* respectively, while 3-HP production was improved by 25.9 % and 27.3 % respectively. Such knockouts had however no significant impact on lactate and acetate production by *K. pneumoniae*. This was attributed to the existence of other lactate- or acetate-producing pathways that were not knocked-out [127]. In the case of acetate, other approaches were also undertaken, such as down-regulating the assimilatory metabolism of glycerol [108, 109, 208], or deleting a gene encoding a TCA cycle repres-

sor (ArcA), so that acetate overflow is prevented [136]. When considering 3-HP production through the malonyl-CoA pathway, an important issue to address is the competition with the fatty acid biosynthesis pathway (see section 1.2.1.3). Attenuating the latter pathway leads to higher intracellular levels of malonyl-CoA, thus improving 3-HP production. The fatty acid synthesis was primarily inhibited by using cerulenin [123, 142, 176, 227]. Due to the cost of adding such an inhibitor to a fermentation broth, alternative approaches were proposed through genetic engineering [41, 142, 227]. Although the disruption of genes involved in central metabolism can improve the 3-HP yield, it was also observed that it can hinder cell growth [109, 127, 142, 208]. A novel approach was recently proposed by Tsuruno *et al.* [210]. They developed a metabolic toggle switch in order to perform conditional repression of genes related to central glycerol metabolism, so that 3-HP is produced while avoiding growth defect. Another promising strategy was proposed by David *et al.* [55], who achieved a dynamic control of the malonyl-CoA node in *S. cerevisiae*. The expression of a fatty acid synthase was subjected to control by a glucose-sensitive promoter. Hence, fatty acid biosynthesis was down-regulated in glucose-limited conditions only. This can ensure that sufficient biomass is produced, before the carbon flux is channelled towards 3-HP synthesis [55].

Another major aspect of pathway optimisation is the balancing of the different steps within the 3-HP producing pathway. Imbalanced pathways can lead to the accumulation of metabolic intermediates, thus hindering the process performances. This is particularly true when 3-HP is produced from glycerol: imbalance between the high glycerol dehydratase activity and the low aldehyde dehydrogenase activity results in detrimental accumulation of the toxic intermediate 3-HPA (see sections 1.2.1.1 and 1.2.1.2). Until now, this issue was mainly addressed by varying the strength of the promoters, or by varying the number of gene copies on the plasmids. A novel technique was recently applied by Lim *et al.* [131]. They used the forward engineering "UTR Designer" software in order to optimise the glycerol dehydratase activity. This software helps predict the translation initiation efficiency of a mRNA sequence, given the 5'-untranslated region (5'-UTR) located upstream. Using this software, Lim *et al.* designed 5'-UTRs with different strength, and showed that the glycerol dehydratase activity was dependent on the 5'-UTR used. Their study resulted in a well-balanced pathway in *E. coli* and a maximum titre of 40.51 g L^{-1} was reached (productivity: 1.35 g L^{-1} h^{-1}; yield: 0.99 mol_C mol_C^{-1}) [131]. Pathway balancing was also achieved in *E. coli* by using a bicistronic synthetic cassette architecture. No 3-HPA accumulation was measured when the aldhyde dehydrogenase activity was 8-fold higher than the glycerol dehydratase activity [184]. As mentioned in section 1.2.1.3, an imbalance also exists between the two functional sites of the malonyl-CoA reductase (MCR) in the malonyl-CoA pathway. Balance between them was achieved by Liu *et al.* by improving the MCR-C fragment by directed evolution and by decreasing the MCR-N activity [135].

Redox cofactors regeneration is a major issue for metabolic pathways optimisation. Indeed, 3-HP generating pathways generally involve at least one redox equilibrium (Fig. 1.4). For instance, when 3-HP is produced from glycerol, 3-HPA is oxidised to 3-HP using NAD^+ as electron acceptor. NAD^+ regeneration is maximal in aerobic conditions, when the electron transport chain is active and electrons are accepted by oxygen. However, aerobic conditions

are incompatible with efficient vitamin B_{12} synthesis (see section 1.2.3). NAD^+ regeneration has typically been ensured by using a NADH oxidase [126]. An alternative strategy was suggested by Li *et al.*, which consists in using a NAD^+-independent aldehyde dehydrogenase from *Pseudomonas* sp. AIU 362 [125]. This enzyme uses O_2 as electron acceptor, so this strategy does not fully resolve the contradiction with anaerobic vitamin B_{12} synthesis. In the malonyl-CoA pathway, the reduction of malonyl-CoA to 3-HP necessitates that two electron equivalents are provided by NADPH. Meanwhile, the upstream part of the pathway consists in the oxidation of glucose to pyruvate, thus generating reducing equivalents (Fig. 1.4.C). Chen *et al.* took advantage of this by engineering *S. cerevisiae*, so that the reducing equivalents generated by the upstream steps of the pathway could be generated as NADPH, instead of NADH, thus ensuring the NADPH supply of the last steps of the pathway [40].

Furthermore, cells' transporting functions were shown to have significant impact on 3-HP production. 3-HP production was successfully increased by 8 % in *C. glutamicum* when the native glucose uptake system was replaced by a route involving inositol permeases and glucokinase. By doing so, glucose uptake was no longer subjected to the need for phosphoenolpyruvate [43]. In *Synechocystis* sp. PCC6803, proteomic and metabolomic approaches led to the identification of 11 genes potentially relevant for 3-HP synthesis. Interestingly, five of them were related to transport functions in cells. Results showed that overexpressing genes putatively involved in cobalt/nickel, manganese and phosphate transports could improve 3-HP production [216].

Lastly, a major concern when designing a bioprocess is the genetic stability of the constructed microbial agent. Genetic engineering in bacteria is mainly achieved using plasmids as vectors because for many species, efficient methods to transfer a plasmid into a cell are known. Yet, they are subjected to major instabilities, such as structural and segregational instabilities [214]. Attempt has thus been made at developing a plasmid-free host for 3-HP production. The proof of concept was provided by Wang and Tian who engineered a plasmid-free, 3-HP-producing strain of *K. pneumoniae* through homologous recombination [214].

1.2.3 Microbial agents for 3-HP production

As illustrated in the previous section, a variety of both microbial species and carbon sources are being investigated for the purpose of 3-HP production. Figure 1.5 sums up the different microorganisms/substrates couples already implemented. Classical microbial chassis are interesting candidates because they are well-known and well-characterised. They are generally easy-to-use fast growing organisms. A lot of tools are already available for their metabolic engineering as well as for their scaling-up. In particular, *E. coli* is one of the most widely used microorganisms for 3-HP production so far. *Bacillus subtilis* and *Corynebacterium glutamicum* are further bacterial model organisms for industrial applications [16, 232]. As reviewed by Zhang and Zhang [232], *B. subtilis* displays interesting advantages such as the Generally Recognised As Safe (GRAS) status, fast growth, low nutrient requirements, and great tolerance to salts and solvents. In addition, the biomass of *B. subtilis* thus produced may be further utilised as a feed additive [178]. Those features are particularly relevant in

the case of 3-HP production. Indeed, it is only a low-value added bioproduct so the process needs to be as cost-effective as possible in order for it to be economically viable. What is more, *B. subtilis* is able to naturally uptake a variety of sugars, including xylose. Xylose is an interesting substrate because it is one of the sugars that can be obtained from lignocellulosic feedstocks. Until now, 3-HP production from xylose was considered in *E. coli*, *C. glutamicum* and *S. cerevisiae* [43, 99, 105], but *B. subtilis* may also be a good candidate for second-generation (*i.e.* using non-food feedstocks) 3-HP production.

From an industrial point of view, yeasts are often preferred over bacteria due to their higher tolerance to low pH values, both facilitating the downstream processes and lowering the overall cost. In addition, *S. cerevisiae* also has the GRAS status (Fig. 1.5). Only a few studies have yet focused on yeasts in comparison to *E. coli*. Several methods for 3-HP production from glucose in recombinant yeasts were patented in recent years by Novozymes and SK Innovation [14, 20, 162]. Interestingly, some yeast species were chosen over *S. cerevisiae* for their greater tolerance to 3-HP [14, 196]. They notably include *Issatechenkia orientalis*, which currently holds the record 3-HP titre in yeast, which is 22.8 g L^{-1} (Table 1.II). Recombinant *I. orientalis* expressed an aspartate 1-decarboxylase from the insect *Aedes aegypti*, and was implemented in a 3 L bioreactor with a glucose feed [14]. However, as explained by the authors of this patent, an important drawback of using yeasts is that their metabolic engineering is typically more complicated than for bacteria. This is notably due to the compartmentalisation of eukaryotic cells, which require that special attention be paid to targeting signals and also to the transportation of intermediates from one cell compartment to another [14]. Nevertheless, efficient tools exist for engineering *S. cerevisiae*. For instance, a toolkit was developed for marker-less integration of genes into *S. cerevisiae* using CRISPR-Cas9 (Clustered Regularly Interspaced Short Palindromic Repeats (CRISPR) and CRISPR-associated endonuclease (Cas9)). This toolkit was used for 3-HP production by enhancing the malonyl-CoA pathway through three different strategies. The most successful strategy consisted in overexpressing a pyruvate dehydrogenase complex and could increase the 3-HP titre by $+23$ % when using the industrial strain Ethanol Red [92]

When considering 3-HP production from glycerol a major limitation of using an industrial chassis is that they generally cannot produce vitamin B_{12} on their own. As explained above, vitamin B_{12} is a necessary cofactor for glycerol's conversion to 3-HPA, both through the CoA-dependent pathway of *Lactobacilli* sp. and through the CoA-independent pathway of *K. pneumoniae* (see sections 1.2.1.1 and 1.2.1.2). Therefore, when microbial chassis such as *E. coli*, *B. subtilis* or *C. glutamicum* are transformed with a glycerol dehydratase from *K. pneumoniae*, costly addition of vitamin B_{12} to the culture medium is required (Table 1.II). Using the vitamin B_{12}-independent glycerol dehydratase from *Clostridium butyricum* [160] could be a way to work around this issue. Another possibility is to use the native species: *Lactobacillus reuteri* and *K. pneumoniae* are indeed prototroph for vitamin B_{12}, so there is no need to supply it to the medium. These species also have further advantages. *L. reuteri* notably has the GRAS status and was even proven to be a probiotic agent [34]. As for it, *K. pneumoniae* was the most studied organism for 3-HP production so far and offers the following advantages: (i) glycerol fermentation pathways have been studied extensively: present

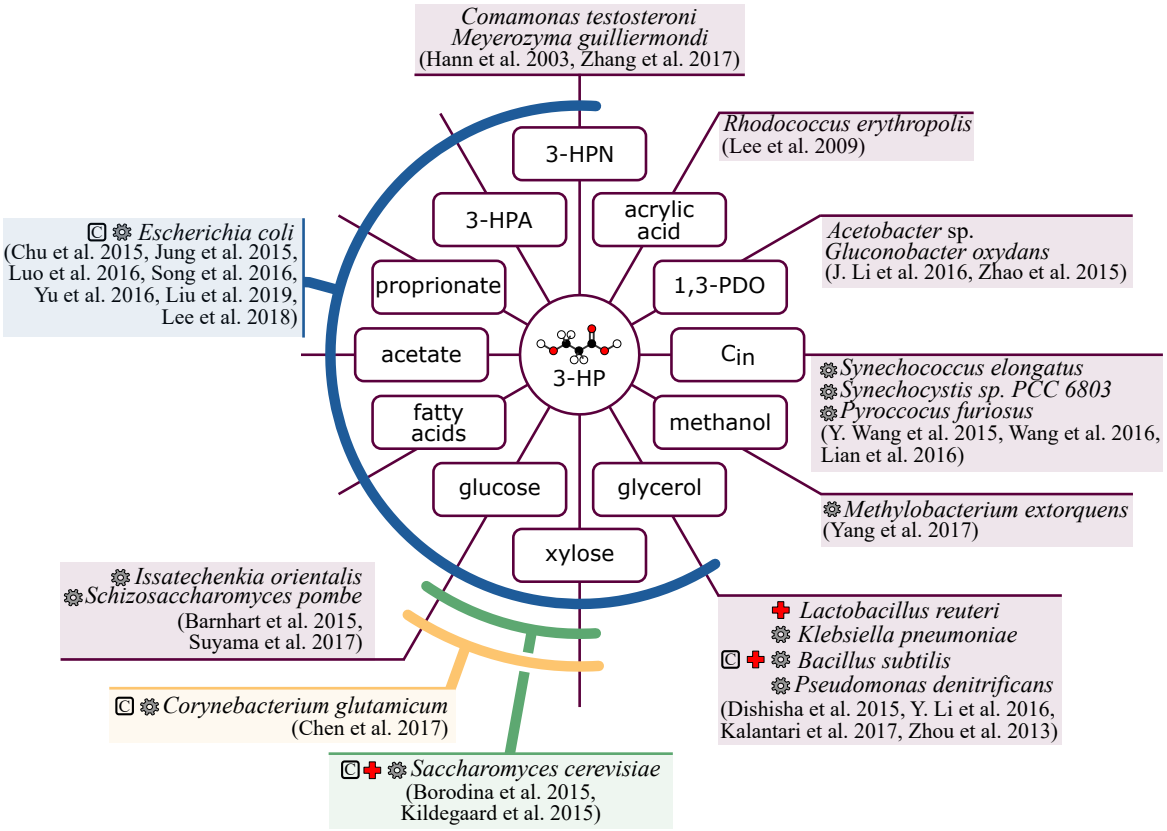

Figure 1.5: Microbial agents under investigation for 3-hydroxypropionic acid production and their carbon source

Non-native 3-HP producers are indicated with a gear icon. Microorganisms that were granted the Generally Recognised As Safe (G.R.A.S.) status are indicated with a red cross. Classical microbial chassis are indicated with the letter C. References are non-exhaustive: at least one reference is given for each microbe/substrate couple. Abbreviations: 3-HPA, 3-hydroxypropanal; 3-HPN, 3-hydroxypropionitrile; 1,3-PDO, 1,3-propanediol; C_{in}, inorganic carbon.

knowledge of glycerol metabolism in *K. pneumoniae* was recently and extensively reviewed [113]; (ii) it can grow directly on glycerol, so the fermentative process could come down to a single step; (iii) *K. pneumoniae* can grow on glycerol both anaerobically and aerobically; and (iv) it has a great glycerol assimilation rate. However, *K. pneumoniae* is pathogenic to humans [169], making a process based on this species unlikely to reach industrial scale. Yet, a new isolate *Klebsiella* sp. AA405 carrying low levels of virulence factors was recently identified as potential host for 3-HP production [124]. Furthermore, an important limitation to efficient 3-HP production remains: there exists a contradiction between vitamin B_{12} synthesis and NAD^+ regeneration. Indeed, maximum NAD^+ regeneration is reached under aerobic conditions, while maximum vitamin B_{12} synthesis is achieved anaerobically. Using the vitamin B_{12}-independent glycerol dehydratase from *C. butyricum* would be subjected to the same limitation, since it is active only in strictly anaerobic conditions [160]. Zhou *et al*. proposed an alternative solution by using *Pseudomonas denitrificans* [236]. The strain is able to produce vitamin B_{12} aerobically, and was transformed with glycerol dehydratase and aldehyde dehydrogenase genes from *K. pneumoniae*. A maximum titre of 4.92 g L^{-1} was reached, corresponding to a 0.67 mol_C mol_C^{-1} yield.

Until now, 3-HP production is primarily achieved from glycerol or glucose, which are both relatively cheap and abundant carbon sources. Glycerol is notably a relevant substrate for biorefinery processes: it is a by-product of first-generation biodiesel production. A large glycerol surplus has been formed, making it a cheap and abundant carbon source [44]. An even cheaper and more abundantly available carbon source would be atmospheric CO_2. 3-HP production was already achieved using inorganic carbon. The proof of concept was provided through an original approaches in archea *Pyrococcus furiosus* and *Metallosphaera sedula* [103, 128], as well as in cyanobacteria *Synechocystis elongatus* and *Synechocystis* sp. PCC 6803 [115, 215, 217] (see sections 1.2.1.7). In contrast, genetic engineering tools are limited for these species as compared to those available for usual microbial chassis. However, cyanobacteria and *Synechocystis* sp. in particular were recently identified as potential next generation chassis for synthetic biology [5, 27]. 3-HP production could therefore benefit from the development of new toolkits for these species, such as CRISPR-Cas systems. Interestingly, a process was recently patented by Verdant Bioproducts Limited for 3-hydroxypropionamide (3-HPAm) production from atmospheric CO_2 and nitrogen, using *Acetobacter lovaniensis* [71]. The patent only mentions the possibility of subsequently converting 3-HPAm to 3-HP through a chemical process. However, a two-step bioprocess could be envisaged: CO_2 and nitrogen are first assimilated by *A. lovaniensis* into 3-HPAm, which is then converted to 3-HP by amidases from *Comamonas testosteroni*, for instance.

Lastly, the combined use of two complementary microorganisms was recently investigated for 3-HP production from glycerol [65, 179, 234] (see section 1.3.2). In particular, acetic acid bacteria were used to oxidise the 1,3-PDO produced either by *K. pneumoniae* or *L. reuteri* into 3-HP. One great advantage of using acetic acid bacteria is their ability to resist organic acids, and grow under acidic conditions [173, 213]. Furthermore, acetic acid bacteria have long been used in the food industry for vinegar production, so they should be suited well for industrial scale-up.

1.3 Overcoming hurdles to 3-hydroxypropionic acid commercial production through process engineering

1.3.1 Operationnal strategies for 3-HP-producing fermentative processes

1.3.1.1 *Fermentation mode*

To this day, 3-HP production is primarily achieved through bench-scale, fed-batch fermentations. Almost all studies reviewed for this paper that carried out 3-HP production in bioreactors used smaller ones (from 1 L to 7 L, see below for exceptions) and most of them were operated under fed-batch mode. An important part of the research effort being focused on genetic engineering, fed-batch fermentations in bioreactors are essentially undertaken in order to confirm a novel strain's potential as a 3-HP producer. During a fed-batch, the medium is gradually supplied with substrate, as cell population grows and products accumulate, which allows higher cell densities and product titres, in comparison with batch mode. Fed-batch cultures are advantageous for the production of both growth-associated and non growth-associated metabolites [137]. In the former case, a continuous exponential substrate supply can control the microbial growth rate in order to make the exponential phase last longer, thus maximizing the metabolite production [137]. This kind of approach, however, requires an in-depth understanding of the strain's physiological needs and does not yet appear to have been applied to 3-HP biosynthesis.

An important feature of fed-batch techniques is that the substrate concentration is kept low throughout the fermentation. This helps limit deleterious phenomena due to high substrate concentrations or due to detrimental intermediates accumulation. Glycerol concentration is typically kept around a relatively low set value, ranging from 5 g L^{-1} to 25 g L^{-1} [87, 127, 234]. Indeed, it was previously reported that glycerol concentrations above 40 g L^{-1} had detrimental effects on the growth of *K. pneumoniae*. Maximal tolerated concentrations were estimated at 110 g L^{-1} and 133 g L^{-1} for aerobic and anaerobic cultures respectively [45]. This rules out the possibility of efficient batch strategies for 3-HP production at high titres from glycerol. Moreover, in conjunction with genetic engineering strategies, fed-batch mode also offers a way to control levels of undesired side products in the final broth. During aerobic cultures, fast-growing cells use fermentation instead of the more energy efficient respiratory chain [15]. This ubiquitous phenomenon is generally referred to as the overflow metabolism. Part of the carbon flux is then diverted from the tricarboxylic acid (TCA) cycle to incompletely oxidised end-products, such as acetate in the case of *E. coli* or ethanol in the case of *S. cerevisiae*. Not only does the production of these metabolites hinder 3-HP yields, but it also has toxic effects on cells. This issue was acknowledged several times during 3-HP

production [106, 136, 171, 183] and was addressed through both fed-batch [106] and genetic engineering [136] strategies. As for wild type *Lactobacillus reuteri*, since it cannot grow on glycerol as sole carbon or energy source, no overflow phenomenon is involved. However, it was demonstrated by Dishisha *et al.* that glycerol dehydration to 3-HPA by resting *L. reuteri* cells is at least 10 times faster than 3-HPA consumption, leading to detrimental 3-HPA accumulation in batch mode [64]. A specific glycerol consumption rate (q_{gly}) of 128.3 $mg_{glycerol}$ per grams of cell dry weight (CDW) was hence identified as maximum value in order to produce only 1,3-PDO and 3-HP from glycerol, without any 3-HPA accumulation. This allowed Dishisha *et al.* to design a fed-batch bioconversion using wild type *L. reuteri* as a biocatalyst that did not produce 3-HPA: the glycerol feed was maintained at 0.75 $g_{glycerol}$ h^{-1}, which is half the maximum rate given the dry weight of biocatalyst used in the experiment. This process achieved a 14 g L^{-1} 3-HP titre with a 0.25 g L^{-1} h^{-1} productivity [65]. This illustrates how process design can be guided by the understanding of the microbial metabolism and how it can help overcome hurdles related to enzymatic kinetics. As pointed out by Li *et al.*, in *K. pneumoniae* too, the aldehyde dehydrogenase is the velocity-limiting enzyme for glycerol conversion to 3-HP [127]. So, similarly to the work of Dishisha *et al.*, fed-batch strategies should allow better 3-HP production using *K. pneumoniae*.

The contradiction between anaerobic vitamin B_{12} regeneration and aerobic NAD^+ regeneration during glycerol conversion to 3-HP (see section 1.2.3) was recently addressed through electro-fermentation for the first time [107]. Electro-fermentation is still an emerging technology and was defined in 2016 as a fermentative process in which polarised electrodes are added and can be used both as a driving tool and for fine redox control [153, 188]. Electro-fermentation relies on the ability some microorganisms have to exchange electrons with solid electrodes, either directly or through redox shuttles. In the case of anodic electro-fermentation, electrons are transferred from microorganisms to the anode. In their study, Kim *et al.* [107] grew a recombinant *K. pneumoniae* overexpressing aldehyde dehydrogenase in the anodic compartment of a bioelectrochemical bioreactor. Electrodes were poised at $+0.5$ V vs. Ag/AgCl and 2-hydroxy-1,4-naphthoquinone (HQN) was added in the medium as an electron shuttle between *K. pneumoniae* and the anode. During anaerobic fermentation, electrons were transferred by the bacteria to the electrode, resulting in current generation in the external circuit and in lower intracellular $NADH/NAD^+$ ratios. The 3-HP to 1,3-PDO ratio thus shifted from 0.84 in fermentative control to 2.26 in electro-fermentative conditions. The process reached a 1.94 g L^{-1} 3-HP titre, with a yield of 0.19 mol_C mol_C^{-1}[107]. This proof of concept demonstrates that NAD^+ regeneration can be significantly improved in anaerobic conditions: it then becomes possible to achieve both high vitamin B_{12} and NAD^+ regeneration. Electro-fermentation gives rise to promising opportunities for overcoming redox limitations of glycerol conversion to 3-HP.

As mentioned at the beginning of this section, 3-HP synthesis is primarily achieved in bench-scale bioreactors and to this date, no industrial production of 3-HP is fully implemented. Two notable exceptions can be found in the scientific literature. The archaeon *Pyroccocus furiosus* that was transformed with part of the 3-HP/4-HB cycle in order to autotrophically produce 3-HP was operated in a 20 L bioreactor [103]. Furthermore, in their 2011 patent,

OPX Biotechnologies demonstrated 3-HP production in a 250 L reactor in fed-batch mode. The *E. coli* inoculum was prepared in two-steps: 1 mL of stock culture was first inoculated into a 100 mL shake-flask, which was subsequently used to inoculate a 14 L bioreactor. This latter culture was then used to inoculate the 250 L bioreactor. IPTG was used for the malonyl-CoA pathway induction. The glucose feed rate was adjusted in order to maintain its concentration between 10 and 15 g L^{-1}. In these conditions, a maximal 3-HP titre of 20.7 g L^{-1} was reached, with a 0.43 g L^{-1} h^{-1} productivity [142].

1.3.1.2 *Process parameters*

Influence of operating parameters, such as aeration rate and medium composition, on the microbial production of 3-HP were studied. Yet, those aspects have been the object of less intense attention, in comparison to metabolic engineering issues. As previously mentioned, 3-HP production from glycerol is an oxidative process; consequently the level of aeration has an impact on final metabolite profile. A first study was conducted by Raj *et al.* [171] on an *E. coli* strain expressing the CoA-independent glycerol pathway (Fig. 1.4.B). By decreasing the liquid-to-flask volume ratio from 0.4 to 0.2 to improve the aeration level, 3-HP titer was enhanced 2.2-fold (0.54 instead of 0.24 mg L^{-1}) while 1,3-PDO production was slightly reduced (from 0.14 to 0.10 mg L^{-1}). However, a 2.5-fold higher accumulation of acetate and formate was observed under aerobic condition. This was attributed to the changes in aeration conditions and to an undefined metabolic overflow phenomenon [171]. To understand the response of *K. pneumoniae* to oxygen supply, Huang *et al.* measured the transcription levels of genes coding for enzymes of the CoA-independent glycerol oxidation pathway and of the formate hydrogen lyase pathway during aerobic, microaerobic, and anaerobic growth in a 5 L bioreactor [88]. Aeration led to a decrease in the glycerol dehydratase transcription level and to an increase in that of aldehyde dehydrogenase. Simultaneously, hydrogenase- and formate dehydrogenase-encoding genes were upregulated. Authors hypothesised that excess NADH formed by overexpressed aldH is consumed through the pathway comprising these enzymes, while producing dihydrogen. To overcome the issue of NAD^+ regeneration while preserving glycerol dehydratase activity and vitamin B_{12} synthesis, Ko *et al.* worked on aeration conditions during *K. pneumoniae* growth on glycerol [109]. After disrupting enzymes of competing pathways (see section 1.2.2), they observed that deletion of the pta-ackA gene responsible for acetate production led to degradation of cell growth, decrease in glycerol uptake, and reduction of 3-HP production. To reduce acetate production without modifying this gene, various aeration rates were tested in a 1-L bioreactor by applying agitation speed between 200 and 600 rotations per minute (rpm), at an air flow rate of 1 vessel volume minute (vvm). Increase in oxygen transfer enhanced cell growth 2.8-fold. 3-HP production yield was improved from 0.18 to 0.38 $mol_{3\text{-HP}}$ $mol^{-1}_{glycerol}$ at 200 and 600 rpm, respectively. In the same time, a drastic decrease in 1,3-PDO yield, from 0.36 to 0.01 $mol_{1,3\text{-PDO}}$ $mol^{-1}_{glycerol}$, was observed. With this strategy, acetate production was minimised at 600 rpm but never totally suppressed [109]. It is also important to keep in mind that high energy needs linked to high aeration and agitation rates contribute to expand production costs at the industrial scale. Simultaneous 3-HP and 1,3-PDO production allows performing process under low-aeration conditions as the pathway is redox balanced.

The influence of the fermentation medium composition was also assessed in several studies. Notably, part of the record-holder study of Li *et al.* was dedicated to this issue [127]. 3-HP production from glycerol by *K. pneumoniae* was tested on different media in shake-flasks. Individual variation of each component of the medium was tested at six different levels: 0 %, 25 %, 50 %, 100 %, 150 %, 200 % (in comparison to their previous study). The optimised medium that was selected led to 1.8-fold increase in 3-HP production. Ten different levels of IPTG concentrations were also tested. Surprisingly, IPTG concentration showed no impact on growth and 3-HP production. pH was also showed to be a critical factor to 3-HP production by *K. pneumoniae*. The adequate pH value that was chosen was 7.0, because it corresponded to the highest glycerol conversion to 3-HP [127]. A study on medium optimisation of growth medium for *Lactobacillus reuteri* was also carried out by Couvreur *et al.* [52]. They screened 30 different media, varying by their concentrations of carbon source (sugar beet and wheat processing coproducts), yeast extract, tween 80 and vitamin B_{12}. In the case of *L. reuteri*, bacterial growth is separated from glycerol conversion in two distinct steps (see section 1.3.2, Fig. 1.6). Couvreur *et al.* studied the impact of the medium composition of the growth step on the performances of the second step. They showed that the optimal medium could lead to an increase of 70 % in subsequent 3-HP production, with reduced 3-HPA titre [52].

1.3.2 Multi-step and integrated approaches

Recently, process approaches to 3-HP bioproduction have been diversifying. In order to improve the yield and selectivity of the overall process, multiple-step integrated processes are being designed. This is especially true for 3-HP production from glycerol. The first step consists of the conversion of glycerol into either 3-HPA or a mix of 3-HP and 1,3-PDO. The undesired product (3-HPA or 1,3-PDO) is subsequently converted into 3-HP (Figure 1.6).

Sabet-Azad *et al.* implemented a two-step process involving both wild-type and recombinant organisms [179]. Glycerol was first supplied in fed-batch mode to wild-type *Lactobacillus reuteri*, which converted it into 3-HPA mostly (56 % of the amount of products), along with 3-HP (22 %) and 1,3-PDO (22 %). By coupling this step with an *in situ* 3-HPA complexation with bisulfite and an extractive module, a 3-HPA solution free of 3-HP and 1,3-PDO, could be obtained. 3-HPA was then converted in fed-batch mode either by growing cells or by resting cells of a recombinant *E. coli*. When using resting cells, this second step reached a 1.1 g L^{-1} 3-HP titre, with a 0.06 g L^{-1} h^{-1} productivity. Interestingly, no by-product was obtained along with 3-HP.
This approach provides another way to circumvent the contradiction between the optimisation of cobalamin availability and NAD^+ regeneration (see section 1.2.3). By using the 3-HPA accumulating bacterium *L. reuteri*, it is possible to separate the anaerobic, cobalamin-dependent step (from glycerol to 3-HPA) from the aerobic NAD^+-dependent step (from 3-HPA to 3-HP-CoA). Then, each step can be optimised separately, according to its specificities.

Zhao *et al.* and Dishisha *et al.* implemented two step processes during which glycerol was first converted respectively into 1,3-PDO by growing *Klebsiella pneumoniae* in batch mode or into a mix of 1,3-PDO and 3-HP by resting *Lactobacillus reuteri* in fed-batch mode [65, 234]. Then, resting cells of acetic acid bacterium *Gluconobacter oxydans* were used to convert 1,3-PDO to 3-HP. In the first study, *G. oxydans* was implemented in the same bioreactor as *K. pneumoniae*, after the latter was heat inactivated at 65 °C during 30 min. The overall process reached a 60.5 g L^{-1} 3-HP titre, corresponding to a 0.52 mol_C mol_C^{-1}yield on glycerol and a 0.94 mol_C mol_C^{-1}yield on 1,3-PDO [234]. The second process implemented *G. oxydans* in a separate batch from *L. reuteri*. Glycerol bioconversion by *L. reuteri* produced an equimolar mix of 1,3-PDO and 3-HP. The supernatant was given as bioconversion medium to *G. oxydans*, which quantitatively and selectively oxidised 1,3-PDO to 3-HP in less than 5 hours. The process reached a final 3-HP titre of 23.6 g L^{-1} [65]. This additional bioconversion step allows an increase in the maximal theoretical 3-HP yield to 1 $mol_{3\text{-HP}}$ $mol_{glycerol}^{-1}$, which is not achievable when using *K. pneumoniae* or *L. reuteri* alone (see section 1.2.2).

Despite the attractiveness multi-step processes may have, particularly regarding overall yields, their economic feasibility is questionable. Indeed, their practical implementation is likely to prove too constraining, with higher associated costs, in comparison to a single-step fermentation. Still, these studies open up new perspectives, notably towards integrated continuous processes. Continuous processes have great industrial interest due to reduced operating costs. Moreover, dual-microbe strategies may be seen as a first step towards implementation of both pathways into a single microbial chassis, or towards mixed cultures for 3-HP production.

An important characteristic of these studies is that at least one step is performed by resting cells (Figure 1.6). Resting cells are also used for 3-HP production from 3-HPN, which is carried out by *Comamonas testosteroni* or recombinant *E. coli* [82, 228]. Generally speaking, when resting cells are used for bioconversions, a preliminary step is required in order to produce the necessary biomass of whole cell biocatalyst. It is thus beneficial to recycle resting cells through several batches: the more bioconversion batches can be carried out from a single biomass production, the more cost-effective the process gets. Cell recycling in the context of 3-HP production was reported in several studies and was achieved by cell immobilisation on alginate beads [82, 122, 228], by cryostructured cross-linking [229], or by microfiltration [63].

Hann *et al.* [82] and Yu *et al.* [228] used *C. testosteroni* and *E. coli* respectively for 3-HPN conversion to 3-HP, while Li *et al.* [122] implemented the acetic acid bacteria *Acetobacter* sp. CGMCC 8142 for 3-HP production from 1,3-PDO. *C. testosteroni* and *E. coli* cells were recycled many times: up to 100 cycles for the former, and up to 74 cycles for the latter. As for it, the study on *Acetobacter* sp. CGMCC 8142 focused on a more restricted number of cycles: 5 consecutive batches were performed. In each study, significant enzymatic activities were retained after the successive cycles, for instance *E. coli* retained 70 % of its enzymatic activity after 74 batches. When compared to suspended cells, it was shown that immobilised cells could retain their ability to produce 3-HP over a greater number of cycles. Suspended cells of *E. coli* could not produce 3-HP after the tenth batch, while immobilised

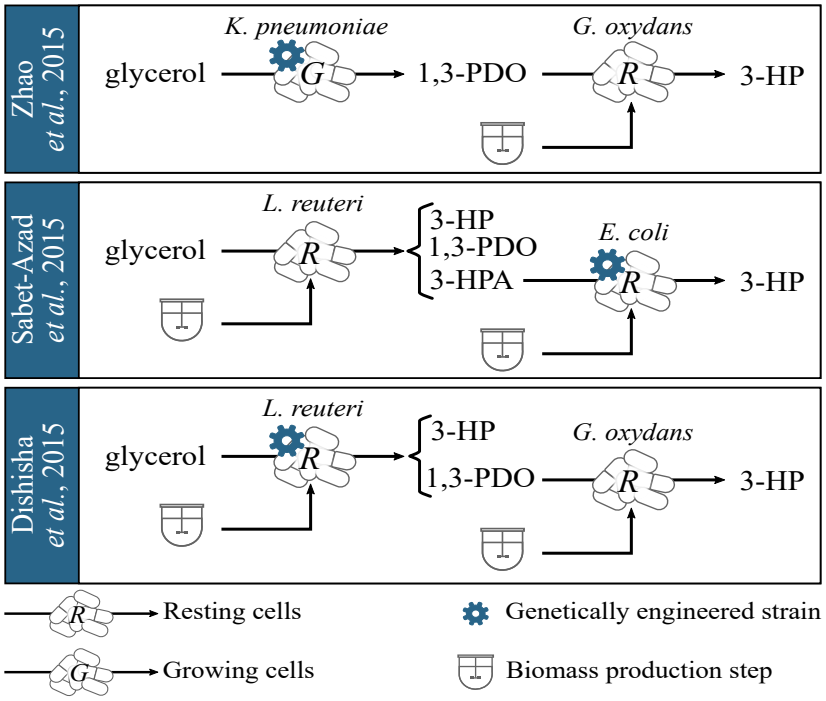

Figure 1.6: Multi-step strategies for 3-hydroxypropionic acid production from glycerol
Abbreviations: 1,3-PDO, 1,3-propanediol; 3-HPA, 3-hydroxypropanal.

cells could still convert 3-HPN to 3-HP after the 60th batch with a molar yield ranging from 0.4 to 0.9 $mol_{3\text{-HP}}$ $mol^{-1}_{3\text{-HPN}}$, depending on the immobilisation material [228]. After 5 cycles, *Acetobacter* sp. CGMMCC 8142 still achieved a 0.81 $mol_{3\text{-HP}}$ $mol^{-1}_{1,3\text{-PDO}}$ yield (final titre: 47.8 g L^{-1}; productivity: 0.8 g L^{-1} h^{-1}), while the yield of suspended cells was already below 0.60 $mol_{3\text{-HP}}$ $mol^{-1}_{1,3\text{-PDO}}$ (final titre: 35.5 g L^{-1}; productivity: 0.6 g L^{-1} h^{-1}) [122]. In the Hann *et al.* [82] study, molar yields are not given, but productivities are remarkably high: 23 g L^{-1} h^{-1} for the first batch and 7 g L^{-1} h^{-1} for the last one. These 3-HP productivities are the highest ones reported so far for a single-step microbial process (Table 1.II). This can be attributed, at least partly, to the high biocatalyst density that was used: given the data available in the paper, the cell load can be estimated around 19 g_{CDW} L^{-1}. In comparison, J. Li *et al.* [122] used a 5 g_{CDW} L^{-1} cell load. Yu *et al.* [228] reached a 36.9 g L^{-1} h^{-1} productivity, but this value accounts for 3-HP obtained after isolation and purification of the production of the first 30 cycles.

Interestingly, it was also shown that cell immobilisation improved their tolerance to the substrate (1,3-PDO or 3-HPN). Like this, higher 3-HP titres can be reached with immobilised cells, in comparison to suspended cells. For instance, immobilised *Acetobacter* sp. CGMCC 8142 were able to produce 67.0 g L^{-1} 3-HP from 70 g L^{-1} 1,3-PDO compared to 50.4 g L^{-1} 3-HP in the case of suspended cells, which corresponds to a 1.32-fold higher molar yield [122]. In the same manner, immobilised *E. coli* cells reached a complete hydrolysis of 497 g L^{-1} HPN within 24 h while free cells were not able to cope with more than 320 g L^{-1}. Thus, cell immobilisation appears as a suitable solution to one of the issues pointed out by Kumar *et al.* in 2013 [112]. Indeed, they identified that metabolite toxicity (3-HPA and 3-HP in particular, but it also applies to substrates) is one of the key issues to address before commercial 3-HP bioproduction can be considered. Another advantage of using cell immobilisation techniques is that they facilitate subsequent downstream processes. Indeed, the filtration step usually needed for cell removal, can be skipped. In case of *in situ* product recovery (ISPR), cell immobilisation could help reduce the toxic effect of the extractant phase (see section 1.4). In order to allow a scale up of immobilisation techniques, special attention should be paid to the bioreactor design, so that process performances are not hindered by mass transfer limitations. The issue of mass transfer was recently addressed by Zaushitsyna *et al.* [229] who evaluated a novel immobilisation technique by direct aggregation of recombinant *L. reuteri* cells for the conversion of glycerol into 3-HPA, 3-HP and 1,3-PDO. Dry cell pellets were mixed with glutaraldehyde, oxidised dextran or a mix of activated polyethyleneimine(PEI)/modified polyvinyl alcohol (PVA) used as various crosslinkers. After freezing at −12 °Cfor 3 days, these cryogels were characterised in terms of structural and mechanical stability, elastic strength, and porosity. Cell load and retaining, preservation of cell viability, and maintenance of metabolic and catalytic activities were also assessed to compare impacts of crosslinkers. On the basis of these results, the PEI/PVA (0.55/0.35 % w/v) mix was retained for glycerol conversion. After packing into cylindrical glass column, embedded resting cells were used for 3-HP production performed in fed-batch mode. At a very low glycerol feeding rate of 3 mg h^{-1}, 3.3 g L^{-1} 3-HP were produced (productivity: 0.09 g L^{-1} h^{-1}; molar yield: 0.48 $mol_{3\text{-HP}}$ $mol^{-1}_{glycerol}$) with 1,3-PDO as obligate co-product [229]. These results are three times lower than that reported earlier for free cells [64]. This

was explained by adverse conditions encountered by cells during cryostructuration process and conversion step by itself. In spite of these low performances, this study offers interesting perspectives in order to overcome mass transfer limitations in cell immobilisation processes. Several improvements were suggested by the authors: limiting oxygen exposure during cryogel preparation, increasing biocatalyst load, and optimising column packing [229].

1.4 Downstream processes for 3-hydroxypropionic acid recovery

1.4.1 Challenges in the recovery of organic acids from fermentation broth

Once the targeted organic acid has been produced through a fermentation process, its separation and purification are still required before it can be used for one of its various possible applications. Along with raw material costs, downstream processes account for a significant cost of the whole production chain: their contribution to the overall cost is typically comprised between 20 % and 60 % [86, 195]. Final product recovery is therefore a critical step for the commercialisation of bio-based compounds. As listed by López-Garzón [139], downstream processes include distinct steps, that may or may not be necessary, depending on the desired final product:

(i) Clarification: the largest particles (such as cells) are removed;

(ii) Primary recovery: the targeted product is removed from the fermentation broth, and is thus separated from the major impurities;

(iii) Counterion removal: if the targeted product is the protonated form instead of the salt, it is necessary to replace the cation with H^+;

(iv) Concentration;

(v) Purification;

(vi) Upgrading: the product obtained thus far might be converted into one of its derivatives if this latter is the targeted end-product of the process;

(vii) Formulation: the final product is prepared for storage.

Clarification is generally achieved using centrifugation or filtration techniques, and this step is generally independent from the nature of the targeted product. On the contrary, various techniques might be considered for the subsequent steps depending on the product's physicochemical properties. Quite complete reviews on carboxylic acid recovery are given by

López-Garzón and Straathof (2014) and Murali *et al.* (2017) [139, 156], where the main primary recovery processes described are: adsorption, liquid-liquid extraction, salt precipitation, filtration, and electrodialysis.

Several aspects make 3-HP recovery in high concentrations and purity especially challenging:

(i) when produced by bioconversion, 3-HP is dissolved in a complex culture medium, at a relatively low concentration;

(ii) being a carboxylic acid of low molecular weight, it is very soluble in aqueous media and has only low affinity for organic solvents ($\log K_{OW} = -0.89$);

(iii) traditional distillation techniques are not effective because 3-HP decomposes at high temperatures and easily dimerises at high concentrations [86].

Yet another important feature of 3-HP is its toxicity to cells, that might be detrimental to the bioproduction performances. As a consequence, irrespective of the chosen recovery technique, achieving 3-HP continuous removal during its production could help improving the overall process performances.

1.4.2 A promising approach for 3-HP recovery: reactive liquid-liquid ISPR

1.4.2.1 *Principle*

The various techniques that might be used for continuous product removal during the production are referred to with the generic term *In Situ* (or In Stream) Product Removal (ISPR). Several setups can be considered for ISPR and they can be grouped in categories, based on two independent criteria [211, 37]:

(i) Location of the separation process: separation can either take place inside the bioreactor (*in situ* product recovery) or outside the bioreactor (in stream product recovery). In the latter case, the fermentation medium is continuously circulated in the separation unit.

(ii) Nature of the contact between microorganisms and the recovery process: it can be either direct (*e.g.* two-phase partitioning bioreactors) or indirect (*e.g.* through membranes).

The best-suited setup depends on the separation technique that is being considered: for example, an *in situ* configuration can be considered for liquid-liquid product recovery, while an in stream configuration is required for electrodialysis, due to practical reasons.

The most appropriate separation technique is selected depending on the product's properties (Fig. 1.7). As reviewed by Van Hecke *et al.* (2014) [211], ISPR was already performed with organic acids: mostly with lactic acid, but also with glycolic, perillic, clavulanic, mandelic

and itaconic acids. The recovery of lactic acid from fermentation broths has been widely studied, and the ISPR approach was proven to enhance lactic acid production processes: for example, Boonmee *et al.* and Gao *et al.* respectively observed 5.9 and 1.8-fold increases in productivities, as well as 1.2 and 2.5-fold increases in total lactic acid productions [22, 76]. In most of the studies on ISPR for organic acids recovery, the fermentation was performed at pH values above the respective pKa of the acids; consequently, electrodialysis and ion exchange were the most often selected techniques. In the few studies with low fermentation pH, sorption or extraction techniques were investigated. According to López-Garzón and Straathof, extraction has been the most studied technique for primary recovery of organic acids (generally speaking, not considering only ISPR) [139]. Several mechanisms can be used for organic acid extraction: for example, solvation with aliphatic and aromatic hydrocarbons, or interactions with amine-based compounds [139]. When either a complex or a chemical compound is formed between the extracted product and the extractant, the term "reactive extraction" is generally used.

Reactive liquid-liquid extraction stands out from the other approaches studied, because it can selectively remove acids from diluted solutions, even at low concentrations. As will be discussed later, this technique was notably considered in the specific case of 3-HP, using aliphatic amines. This method is performed in two stages (a schematic representation is provided in Fig. 1.8, with tertiary amines as an illustration):

(i) First, the solute (3-HP) is extracted from the fermentation (aqueous) medium into the extractant (organic) phase, through an organic acid-base interaction. At the interface between the two phases, a complex is formed between 3-HP and the aliphatic amine. This complex being hydrophobic, 3-HP is thus extracted into the organic phase. The acid-base interaction only occurs between the amine and the carboxylic acid. This is the reason why this technique is mostly relevant when the pH of fermentation is under the targeted product's pKa, so that the carboxylate form is not predominant.

(ii) Then, the extractant phase is regenerated by stripping the solute from the organic complex using another aqueous phase that contains a stronger base (NaOH, typically). This second step is also known as back-extraction [53].

Reactive liquid-liquid extraction using amines for ISPR of organic acids – and including both extraction and back-extraction – was already demonstrated in three occasions (Table 1.III). In these experiments, the aqueous phases (fermentation medium and back-extraction phase) were brought in contact with the organic phase using hollow fibre membrane contactors (HFMC). This experimental configuration displays advantages that make it a good candidate for extractive fermentation [37, 66, 75]:

(i) dispersion between phases is avoided, as well as a subsequent separation step between organic and aqueous phases (through centrifugation, for example);

(ii) direct contact with microorganisms is significantly reduced, thus enhancing the biocompatibility of the process;

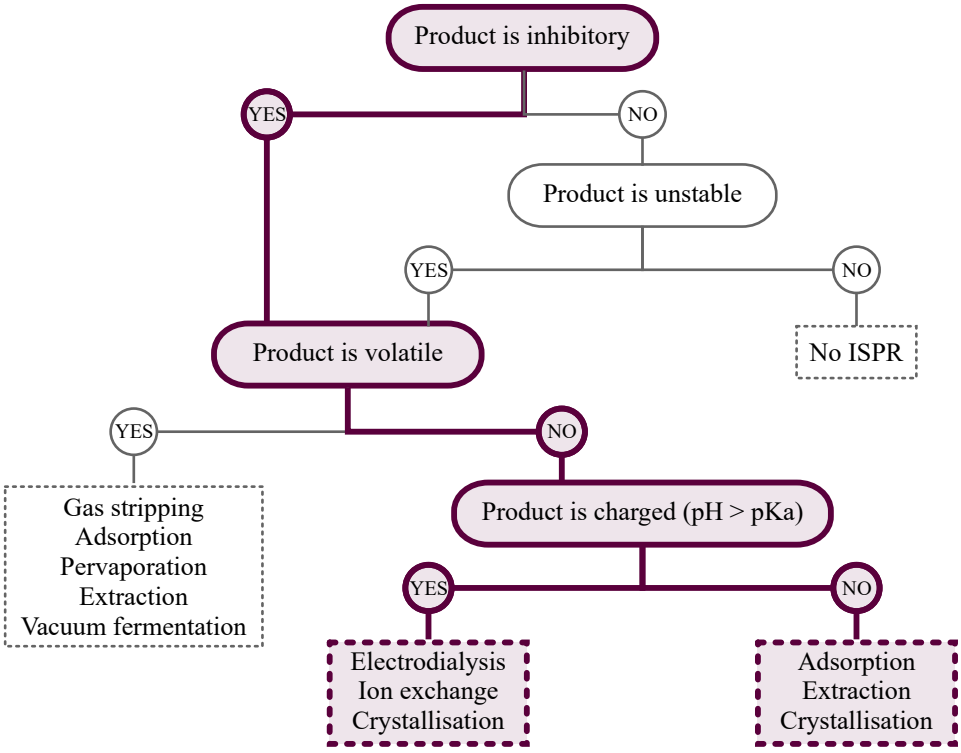

Figure 1.7: Selection of the appropriate ISPR technique for 3-HP recovery. The global heuristics is adapted from Van Hecke *et al.* (2014) [211]. The specific path for 3-HP is highlighted with thick purple lines. Regarding the last criterion ("Product is charged"), the answer might depend on the fermentation pH.

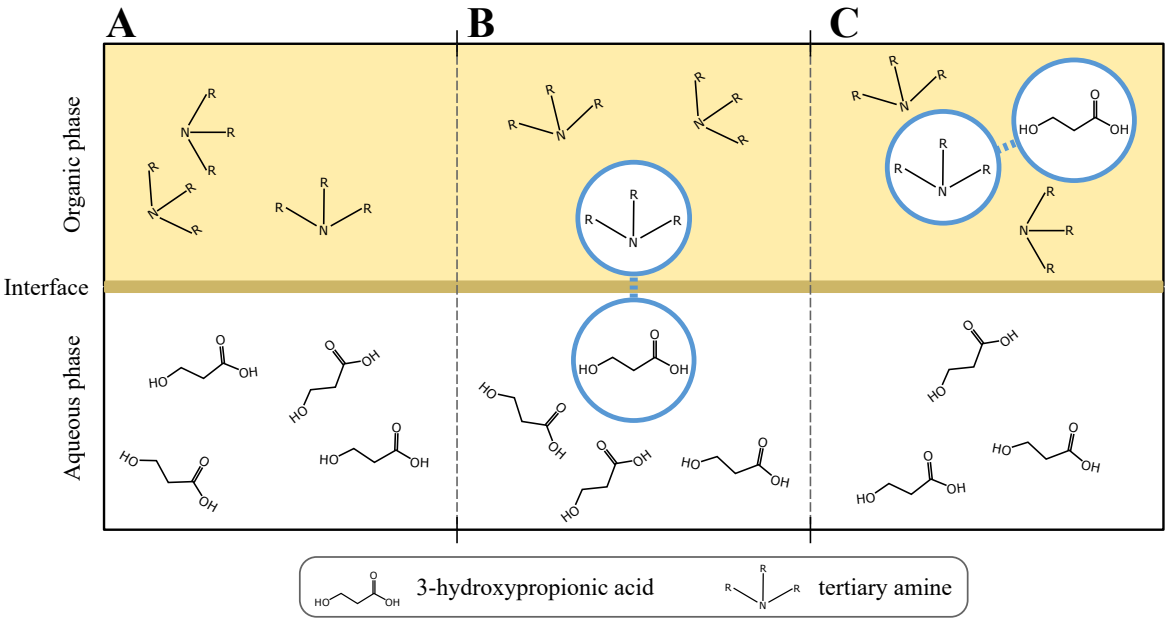

Figure 1.8: Schematic representation of reactive liquid-liquid extraction of 3-HP using tertiary amines. Initially, 3-HP is diluted in the aqueous phase and the amine in the organic phase (**A**). Then, a complex is formed between 3-HP and the tertiary amine at the interface between the phases (**B**). This complex is soluble in the organic phase, so the 3-HP molecule is extracted from the aqueous phase into the organic phase (**C**).

(iii) hollow fibre configuration offers a high interfacial area, which generally improves both the product transfer to the extractant phase and the process compactness.

As illustrated in Table 1.III, these studies showed promising results: when comparing the extractive fermentations with non-extractive controls, it could be observed that the productivity was enhanced. This observation was mainly attributed to the microorganisms being less inhibited by the produced organic acid, thanks to its continuous removal. Results gathered in Table 1.III reveal that reactive liquid-liquid ISPR of organic acids can still be beneficial when the fermentation pH is slightly above the pKa of the products: in these studies, pH was only controlled by the balance between production and extraction rates, and in some cases, pH stabilised above the pKa value. The study of Jin and Yang (1998) [97] also highlights another important process parameter, namely the specific contact area between the two phases. Indeed, by reducing the volume of the fermentation medium from 2.2 to 0.3 L, they increased 7.3-fold the specific contact area and observed that the extraction rate of propionic acid was improved, and consequently the overall productivity was further increased in comparison to the control (Table 1.III).

1.4.2.2 *The progress made so far for 3-HP reactive liquid-liquid ISPR*

Until just recently, there was no study in the literature dedicated to ISPR techniques for 3-HP. Moussa *et al.* made a comparative study of 3-HP and lactic acid behaviour during reactive extraction [154]. They used different concentrations of tri-*n*-octylamine (TOA) and tri-*n*-octylmethylammonium chloride (Aliquat 336) as extractants, since they have exhibited good extraction performances on lactic acid [219, 226]. Both compounds were diluted in *n*-decanol. Solutions of 1 g L^{-1} of each acid were extracted with organic phases. pH of these solutions was 2.9 and 3.2 for lactic acid and 3-HP, respectively. Lactic acid was better extracted than 3-HP for all extractant concentrations, from 0 to 60 % v/v: it had higher partition (or partition) coefficients, K_D, at equilibrium for all conditions. K_D is defined as the ratio between the product's concentration in the organic phase over its concentration in the aqueous phase. This was related to the stronger acidity of lactic acid (pKa $= 3.86$) compared to that of 3-HP (pKa = 4.51), since the interaction between the acid and the extractant is stronger [203]. However, results obtained for 3-HP were encouraging with high distribution coefficients over a wide range of experimental conditions, including 3-HP dissolved in real bioconversion broth. In the latter case, the highest performances were achieved using a mix of TOA (10 % v/v) and Aliquat 336 (10 % v/v) in *n*-decanol: the extraction yield reached 62 % [154].

Afterwards, Burgé *et al.* evaluated the reactive extraction of 3-HP in a HFMC, using the organic phase composition as mentioned above [32]. They obtained higher distribution coefficients (K_D) and yields in comparison to reactive extraction of the same 3-HP solutions in separatory funnels: $K_D = 3.05$ versus $K_D = 2.44$ and $Y = 75.3$ % versus $Y = 71.0$ % respectively, thus demonstrating the potential of this configuration. Further optimisation studies were reported and consisted in a screening of solvents used as extractant phase, and of a detailed study of 3-HP extraction mechanism. It has been found that tertiary amines like TOA have a better extraction performance when diluted in active solvents like long chain

Table 1.III: Extractive fermentations for microbial production of organic acids, using reactive liquid-liquid ISPR

Product	Species	Culture	pH[a]	pKa[b]	Organic phase	Back-extraction phase	Fermentation productivity	Comparison with control	Ref.
Butyric and Hexanoic acid	*Megasphaera elsdenii*	Fed-batch (1 L)	6.3	4.81 4.88	10 % TOA[c]; 90 % Oleyl alcohol	1.0 N NaOH	0.26 g L^{-1} h^{-1}	no control	[159]
Propionic acid	*Propionibacterium acidipropionici*	Repeated batch (0.3 L)	5.2	4.87	4 % Adogen 283[d]; 96 % Oleyl alcohol	6.0 N NaOH	*ca* 0.98 g L^{-1} h^{-1}	5-fold increase	[97]
		Batch (2.2 L)	4.8				0.25 g L^{-1} h^{-1}	2-fold increase	
Butyric acid	*Clostridium tyrobutyricum*	Repeated batch (2 L)	5.5	4.81	10 % Alamine 336[e]; 90 % Oleyl alcohol	6.0 N NaOH	7.37g L^{-1} h^{-1}	1.4-fold increase	[221]

[a] of the bioconversion medium

[b] of the targeted acid

[c] tri-*n*-octylamine

[d] commercial name of ditridecylamine

[e] commercial name of N,N-dioctyl-1-octanamine

alcohols, since they act as proton donors, which improves the acid-amine complex solvation in the organic phase [36]. Also, mathematical models that take into account complexation-solvation mechanisms of 3-HP extraction have been developed [35, 37]. This approach is a promising tool for its use for the development and optimisation of reactive extraction of organic acids.

Biocompatibility is a key factor for ISPR systems that are integrated with fermentation processes: finding a biocompatible organic phase with good extraction performances is challenging. For example, it was shown that Aliquat 336 addition to the extractant phase improved the reaction performance: the degree of extraction increased from 54 % for a 15 % v/v concentration to 64 % for a 60 % v/v concentration; it was, however, found to be very toxic to bacteria, even at low concentrations [111]. Therefore, Aliquat 336 cannot be considered as a suitable candidate for extractive bioconversion. Because of the promising results mentioned above, extraction with TOA (20 % v/v) diluted in decanol was evaluated in a HFMC, for the extraction of 3-HP produced by *Lactobacillus reuteri*. Unfortunately, the ISPR system significantly inhibited the bioproduction of 3-HP, resulting in lower titres compared to the bioconversion alone [33]. This was attributed to the high toxicity of the organic phase, despite the use of the membrane contactor. This is why it is important to find a compromise between the extraction performance and the biocompatibilty of the ISPR being used. Recently, Sánchez-Castañeda *et al*. screened various extracting phase compositions in order to find the most adequate trade-off between extraction performances (assessed by extraction yield and viscosity measurements) and biocompatibility with *L. reuteri* (assessed by flow cytometry analysis of the physiological state of cells) [182]. The main outcomes of this study were the following:

(i) Adding an inert diluent, such as dodecane, to a TOA-decanol mix decreased the viscosity (lower viscosities correspond to higher transfer rates [51]) and improved the biocompatibility, but the extraction yield was impaired (it was *ca.* 15 %, instead of *ca.* 75 % in the control).

(ii) When comparing alcohols used as active diluents, it was observed that alcohols with a greater number of carbon atoms (like dodecanol, compared to decanol) could improve the biocompatibility, at the expense of lower extraction yields.

(iii) Using N,N-didodecylmethylamine (DDMA) instead of TOA improved both biocompatibility and extraction performances.

Overall, the extracting phase formulation that was eventually selected contained 20 % (v/v) DDMA, 47 % (v/v) dodecanol and 33 % (v/v) dodecane. The extraction yield obtained with this organic phase was 49 % and its viscosity was 6.8 mPa s. Furthermore, 3-HP production from glycerol was tested with *L. reuteri* in a medium saturated with the soluble fraction of this organic phase: the total 3-HP production corresponded to 88 % of the total production in the control experiment (without any organic phase contact).

1.4.3 Other approaches towards 3-HP recovery

Currently, several patents describe purification processes applied to 3-HP [1, 86, 148, 205]. They include an initial clarification of the aqueous phase to remove cells and other solids of the bioconversion medium, so they do not include ISPR. 3-HP primary recovery consists of different strategies that combine classical separation processes like salt precipitation and liquid extraction with solvents, and is followed by evaporation and/or distillation. The compositions resulting from the methods used may deliver a highly pure 3-HP, from 70 % up to 99.5 % (w/v); and in concentrations that vary from 30 % up to 95 % (w/v).

However, reaching the maximal concentration and purity represents high energetic costs and makes the economic viability of the overall process questionable. This is why, obtaining an aqueous solution of 3-HP that already has both high purity and high concentration could significantly reduce the cost of further purification steps, and *in situ* or in stream reactive extraction may play an important role in delivering this objective. One of the most appealing advantages over traditional processes is that, with the adequate back-extraction strategy, the product can be recovered in the form of the acid and not as a salt. Studies with other similar organic acids showed that it was possible to obtain the acid form (instead of the salt) through the use of temperature swings, diluent swings, or of a volatile base (such as trimethylamine) in the stripping phase [104]. These approaches might thus be interesting perspectives for the recovery of 3-HP. Further research is still needed in order to integrate the constraints of both microbial production and downstream steps.

1.5 Conclusion and outlooks

In recent years, important progress in 3-HP bioproduction has been made, thanks to ever-increasing research and industrial interest. Research efforts are mainly dedicated to the metabolic engineering of the various metabolic pathways and microbial hosts. Given the great variety of possible substrates, metabolic pathways, microbial agents, and process techniques, it can be expected that the future of 3-HP production is likely to be diverse. Recent studies have notably benefited from the development of synthetic biology tools, such as metabolite sensors, CRISPR-Cas systems for genetic editing, dynamic flux control, and omics and *in silico* techniques. Yet, research is now also focusing on process engineering and downstream processes. Various fermentation strategies are currently under investigation, including one-step fed-batch, electro-fermentation, multi-step and integrated processes. Regarding downstream processes, the main focus is currently on *in situ* product recovery. These fermentation and extractive strategies form a complementary approach to metabolic engineering, towards sustainable and economically viable 3-HP production.

Industrial manufacturers' attention is essentially drawn by the possibility of converting 3-HP into acrylic acid in one step only. Indeed, acrylic acid is one of the most produced commodities and its production currently relies on petro-chemical processes. Bio-based acrylic acid production through 3-HP is a very promising strategy toward greener and less petrol-dependent processes. This is, in any case, the approach that was initiated by the industrial consortia (Novozyme/Cargill and Dow Chemical/OPX Biotechnologies). Other companies, such as BASF and P&G, have recently been patenting catalytic methods for dehydrating 3-HP to acrylic acid, thus proving their interest for bio-based acrylic acid [21, 212]. However, it is still unknown to what extent bio-based acrylic acid production is less energy consuming and less greenhouse gas emitting in comparison to petrochemically-based acrylic acid. Still, a study published in 2014 assessed the life-cycle fossil energy consumption and greenhouse gas emissions of acrylic acid produced from bioproduced 3-HP in comparison to fossil-based acrylic acid [6]. It was estimated that bio-based acrylic acid led to a 53 % reduction in greenhouse gas emissions and to 58 % less fossil fuel consumption. It can be expected in the coming years that the production of bio-based chemicals through biotechnological processes will continue to develop, encouraged by public policies. For instance, the European Commission has designated bio-based chemical production and bioprocesses as priority areas for investments [69]. However, when assessing the commercial feasibility of a new process, one has to take into account the risk of the investment, which mostly relies on the prices of raw materials. Given the low price of petrol and the volatility of substrate prices such as glycerol or glucose, it can be expected that bio-based 3-HP will not be competitive with fossil-based acrylic acid in the next years. Furthermore, because of this volatility of carbon substrates prices, it is difficult to make reliable forecasts and investing in biotechnological processes remains risky. These limitations might hinder the commercial development of 3-HP in the coming years. Nevertheless, the company Verdant Bioproducts Limited built the first biorefinery plant aiming at producing 3-HP – among other commodities – from waste CO_2.

Despite this context, significant progress has been made in the production of 3-HP. Due to some of these improvements, the results of certain process indicators are getting closer to industrial relevance, notably in terms of final titres, the highest so far being 102.61 g L^{-1}. Since most studies are essentially proofs of concept for new recombinant strains, processes are not fully optimised and productivity in particular remains relatively low. In the report published in 2004 by the US DoE, it was estimated that a minimal productivity of 2.5 g L^{-1} h^{-1} is required for 3-HP production to be economically competitive. To this day and according to the scientific literature, this threshold has rarely been crossed. The progress made to date has been possible thanks to intensive efforts in genetic engineering. Physiology of the different 3-HP-producing strains now needs to be characterised in detail for processes to be further optimised. As such, modelling works that have already been carried out have been of great help for better understanding microbial metabolisms for 3-HP production. Process approaches, such as multi-stepping, are now being developed, which should enable better performances. Immobilisation technologies may mark a step toward continuous processes, which might be preferred in industry due to their cost efficiency. With the combination of genetic engineering and process approaches, some of the metabolic hurdles, such as toxicity of some products or redox limitations, are being overcome. Some approaches are however

still in their infancy: electro-fermentation, in particular, offers exciting possibilities for enhancing 3-HP synthesis, but it still requires intensive research efforts before it can be scaled up.

Until now, 3-HP production was mostly attempted from glycerol or glucose as a carbon source. However, some recent studies also achieved 3-HP production from other carbon sources of interest, such as CO_2 and xylose, although performances are still low. It should however be noted that almost no attempt has been made at producing 3-HP from crude industrial by-products, even though it could be very interesting to develop in the context of biorefinery. Only a recent study focused on *L. reuteri*'s growth on wheat and sugar beet by-products [52]. 3-HP production has not yet been attempted using crude glycerol: it is however an important issue to address before commercial production can be considered. Indeed, crude glycerol may contain some impurities that are toxic to cells. Finally, downstream processes for 3-HP extraction and purification will benefit from the experience gained with other organic acids, such as lactic acid in particular. The specificities of 3-HP extraction were already addressed in the case of reactive liquid-liquid extraction, but alternative strategies are still to be explored for 3-HP recovery. Downstream processes hold a central place of the overall process because they are indispensable and they account for an important part of the total cost. In this respect, integrating *in situ* or in stream extraction with the fermentation or bioconversion step is promising.

*

As mentioned in the general introduction, the present thesis studies the implementation of an acetic acid bacterium, *Acetobacter* sp. CIP 58.66, in an integrated strategy towards 3-HP production and primary recovery. The main objectives are to investigate the potential of an acetic acid bacterium as 3-HP producer and to develop an integrated strategy towards ISPR. The following chapter will now cover the various experimental methods that were used.

CHAPTER 2

MATERIAL AND METHODS

This chapter presents the overall methodology of the works presented in this thesis, as well as the detailed materials and methods.

Chapter's table of contents

2.1 Overall methodology . . . 44
2.2 Materials . . . 46
2.2.1 Bacterial strain and storage conditions . . . 46
2.2.2 Chemicals . . . 47
2.2.3 Bioreactor and instrumentation . . . 47
2.2.4 Hollow Fibres Membrane Contactors . . . 48
2.3 Batch cultures in shake-flasks (Chapter 3) . . . 50
2.3.1 Inoculum . . . 50
2.3.2 Cultures conditions . . . 50
2.4 Fed-batch bioconversion of 1,3-propanediol in bioreactor (Chapter 3) . . . 52
2.4.1 Inoculum . . . 52
2.4.2 Single-step, pH control-based fed-batch . . . 52
2.4.3 Sequential pH control-based fed-batch . . . 52
2.4.3.1 Primary growth phase on glycerol . . . 52
2.4.3.2 Fed-batch bioconversion . . . 54
2.5 Extractive bioconversion of 1,3-propanediol (Chapter 4) . . . 54
2.5.1 ISPR system setup and preparation . . . 54
2.5.1.1 Extraction and back-extraction phases composition . . . 54
2.5.1.2 Interface stabilisation . . . 54
2.5.2 Batch production of the biocatalyst . . . 56
2.5.3 Extractive bioconversion initiation and follow-up . . . 57
2.6 Analytical methods . . . 58
2.6.1 Biomass concentration estimation . . . 58
2.6.2 Flow cytometry analysis for physiological state assessment . . . 59
2.6.3 HPLC analyses . . . 60
2.6.3.1 Analysis of bacterial broth samples . . . 60

2.6.3.2 Analysis of organic phase samples 61
2.6.3.3 Analysis of back-extraction phase samples 61
2.7 Calculations 61
2.7.1 Working volume correction for experiments in a bioreactor 61
2.7.2 Kinetic analysis 62
2.7.3 Model simulation for extraction and back-extraction dimensioning . . . 62
2.7.4 Statistical analysis 63
2.8 Modelling approach (Chapter 5) 63

2.1 Overall methodology

The overall methodology of the works presented in the current thesis is illustrated in Figure 2.1. In a first instance, preliminary tests were carried out in shake-flasks, in order to determine growth characteristics of *Acetobacter* sp. CIP 58.66 on 1,3-propanediol (1,3-PDO) or on glycerol. In particular, the study of the impact of initial 1,3-PDO concentration on bioconversion performances showed that a fed-batch approach would be suitable for preventing detrimental accumulation of 3-hydroxypropionaldehyde (3-HPA). Based on these results, a pH control-based feeding strategy was implemented in a bioreactor for fed-batch 3-HP production from 1,3-PDO: substrate was fed along with the pH control solution. Yet, 1,3-PDO could only ensure limited bacterial growth, and cell densities remained low. Consequently, a sequential process was adopted: cells were first grown on glycerol, before the pH control-based fed-batch bioconversion was launched. High process performances could be reached: conversion of 1,3-PDO into 3-HP was almost quantitative, with high productivities. All these results are gathered and discussed in Chapter 3.

Based on these results, process integration could be envisaged. Efforts were mainly focused on the downstream integration of the process: a proof-of-concept for extractive bioproduction of 3-HP was successively performed. Discontinuous bioconversion of 1,3-PDO into 3-HP was performed, while 3-HP was being continuously extracted using a reactive liquid-liquid in stream product recovery (ISPR) technique. In particular, the strain's performances did not seem to be significantly affected by the potential stresses related to continuous ISPR The extraction rate was, however, quite lower than the biological production rate and was identified as the rate-limiting step of the process. Results thereof are presented and discussed in Chapter 4.

Then, using the sequential fed-batcg data (Chapter 3) a first kinetic model could be implemented, in order to better understand the different phenomena involved in the process. The model's validity was then estimated for extractive bioconversions and single-step fed-batch bioconversions. This study puts together all results obtained in previous chapters, and opens

the way towards to process simulation and a more efficient process design. The model implementation is described in Chapter 5.

Finally, key aspects and key results of Chapters 3, 4 and 5 will be put into perspective with one another and within the broader context of these works in a final discussion.

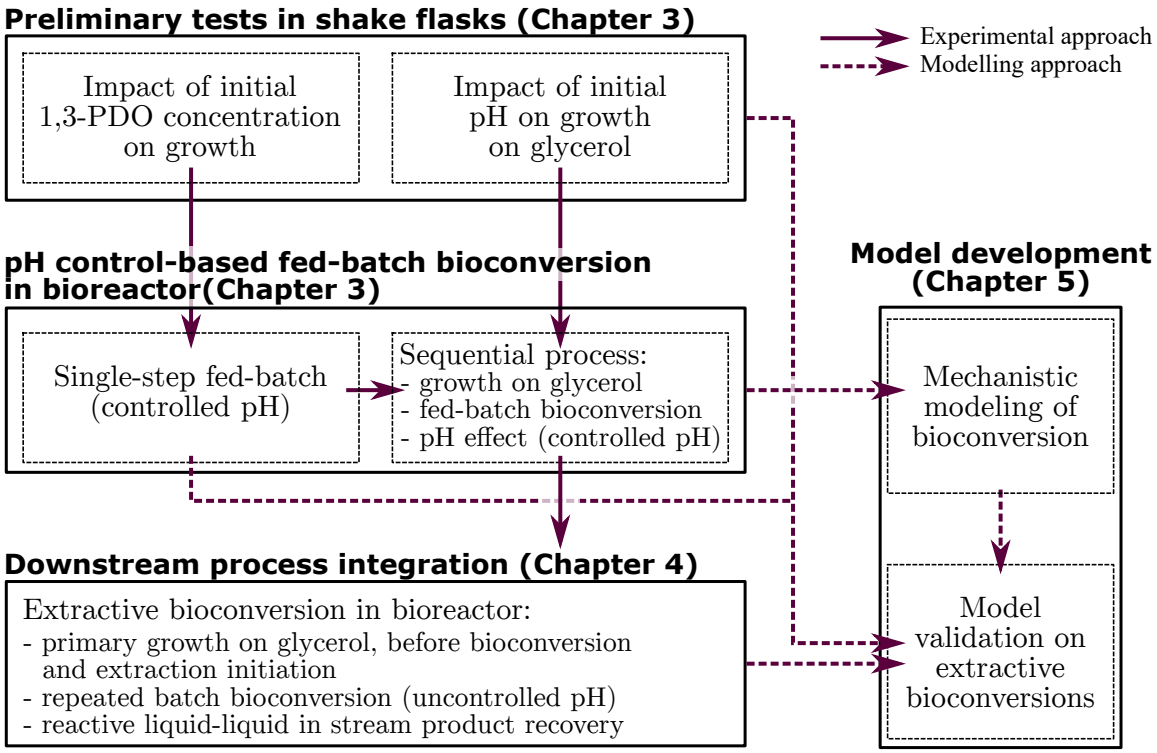

Figure 2.1: **Schematic representation of the overall methodology implemented in the present thesis**

2.2 Materials

2.2.1 Bacterial strain and storage conditions

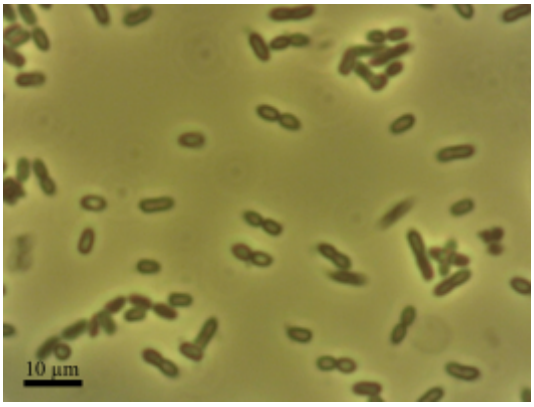

Figure 2.2: Picture of *Acetobacter* sp. 58.66 (Phase contrast microscope)

A lyophilisate of strain was purchased as *Acetobacter aceti* CIP 58.66 (pictured in Fig. 2.2) from the Biological Resource Center of Pasteur Institute (Paris, France). The lyophilisate was inoculated into 50 mL of medium in a 250 mL baffled shake-flask (25 g L^{-1} mannitol, 5 g L^{-1} yeast extract, 3 g L^{-1} peptone; pH ajusted to 6.5 with a 5.5 mol L^{-1} sulfuric acid solution). The culture was incubated one week at 25 °C and 200 rotation per minute (rpm). After one week, 2 mL of this culture were used to inoculate 100 mL of fresh medium in a 500 mL baffled shake-flask (20 g L^{-1} ethanol, 5 g L^{-1} yeast extract, 3 g L^{-1} peptone; pH ajusted to 6.5). This second culture was incubated one week in the same conditions. Then glycerol was added to the medium (20 % (w/v)), as cryoprotectant. The broth was aliquoted in 1 mL tubes and stored at −80 °C, with a cell density around $9.5 \cdot 10^8$ cell mL^{-1}. These cryotubes were used as starters for inoculum preparation of all experiments presented in this thesis (see following sections).

Two of the cryotubes thus prepared were thawed and used for Sanger sequencing (Eurofins Genomics, Les Ulis, France) of the 16S rRNA gene, in order to check the strain purity and the species assignment. The detailed experimental approach for 16S rRNA gene analysis is described in Appendix A.1. The 16S rRNA nucleotide sequences obtained from two samples were all the same, which allowed considering the stored cultures as pure cultures. The corresponding 1377 bp sequence is indicated in Appendix A.2. Subsequently, a phylogenetic analysis based on 16S rRNA gene was established using 57 sequences belonging to genus *Acetobacter* (Appendix A.3, Figure A.1). Results revealed that the strain used in this study is not included in the *aceti* cluster, but in a *syzygii/okinawensis/lambici* cluster. Consequently, this strain was renamed *Acetobacter* sp. CIP 58.66 in this thesis.

2.2.2 Chemicals

All chemicals that were used are listed in Table 2.I, with their suppliers and their purities.

Table 2.I: List of chemicals with suppliers and purities

Chemical	Formula	Supplier	Purity
1,3-propanediol (1,3-PDO)	$C_3H_8O_2$	Sigma-Aldrich (St Louis, USA)	98 %
3-hydroxypropionic acid (3-HP)	$C_3H_6O_3$	TCI Europe (Zwijndrecht, Belgium)	$\simeq$ 30 % [a]
3-hydroxypropanal (3-HPA)	$C_3H_6O_2$	URD ABI (Pomacle, France)[b]	– [b]
Acetone	C_3H_6O	Fisher Scientific (Loughborough, UK)	$>$ 99.5 %
Ammonium hydroxyde	NH_4OH	Sigma-Aldrich (St Louis, USA)	28-30 %
Chemchrom V8 [c]	–	Biomérieux (Marcy l'Étoile, France)	–
ChemSol B24 Buffer	–	Biomérieux (Marcy l'Étoile, France)	–
N,N-Didodecylmethylamine (DDMA)	$C_{25}H_{53}N$	TCI Europe (Zwijndrecht, Belgium)	$>$ 85 %
Di-potassium hydrogen phosphate	K_2HPO_4	Sigma-Aldrich (St Louis, USA)	$\geq$ 99 %
Dodecane	$C_{12}H_{26}$	TCI Europe (Zwijndrecht, Belgium)	$>$ 99.5 %
Dodecanol	$C_{12}H_{26}O$	TCI Europe (Zwijndrecht, Belgium)	$>$ 99 %
Glycerol	$C_3H_8O_3$	VWR Chemicals (Leuven, Belgium)	$\geq$ 97 %
Isopropanol	C_3H_8O	TCI Europe (Zwijndrecht, Belgium)	$>$ 99.5 %
Monohydrate citric acid	$C_6H_8O_7, H_2O$	Acros Organics (Geel, Belgium)	$\geq$ 99.5 %
Peptone	–	BD-France (Le-Pont-de-Claix, France)	–
Propidium iodide (PI)	$C_{27}H_{34}I_2N_4$	Sigma-Aldrich (St Louis, USA)	$\geq$ 94.0 %
Sodium hydroxyde	$NaOH$	VWR Chemicals (Leuven, Belgium)	35 %
Sulfuric acid	H_2SO_4	Sigma-Aldrich (St Louis, USA)	95 %
Trichloroacetic acid	$C_2HCl_3O_2$	VWR Chemicals (Leuven, Belgium)	$\geq$ 96 %
Yeast Extract	–	Organotechnie (La Courneuve, France)	–

[a] Exact purity was retrieved for each lot number from certificates of analysis (available on TCI Europe's website).
[b] 3-HPA is not commercially available. It was synthesised according to Burgé et al. [30], in URD AgroBiotechnologies Industrielles (ABI), located in Pomacle-Bazancourt, France. It was considered as a pure product.
[c] Carboxyfluorescein diacetate (cFDA) solution

2.2.3 Bioreactor and instrumentation

For all experiments carried out in a bioreactor, a 3.6 L Labfors 4 bioreactor was used (Infors, Bottmingen, Switzerland), with its associated software (Iris v.5), for data acquisition and process control. The bioreactor was notably equiped with a single Rushton turbine for broth stirring, and a mass air flowmeter for aeration.

Partial pressure of dioxygen (pO_2) and pH were monitored with InPro 6800 and 405-DPAS-SC probes, respectively (Mettler Toledo, Colombus, USA). The pO_2 probe was calibrated in the medium at 30 °C, just before inoculation. 100 % and 0 % values were calibrated by successively saturating the medium with dry air at 4 normal litres per minute (NL min^{-1}) and with N_2 ($>$ 99 %) at 1.5 bar, with a constant agitation speed of 400 rotations per minute (rpm), during 20 min each. The pH probe was calibrated at room temperature with pH 7 and pH 4 buffers, successively.

Temperature was continuously measured in the medium, and it was controlled by circulating water in a double jacket.

The O_2 transfer in the bioreactor were characterised by measuring the k_La over a relevant range of stirring and air flow rates. This characterisation can be found in Appendix B.

2.2.4 Hollow Fibres Membrane Contactors

For 3-HP extraction and back-extraction, two identical Hollow Fibres Membrane Contactors (HFMC) were used, and included a 2.5×8 Liqui-Cel® module containing X50 fibres (Membrana, USA). Characteristics of the HFMC are presented in Table 2.II, and the working principle of the contactor is illustrated in Fig. 2.3. Two distinct fluids are circulated inside the HFMC in countercurrent flows: one (here, the aqueous phase) in the fibres compartment, and the other (here, the organic phase) in the shell compartment (Fig. 2.3A). The central baffle forces a radial flow in the shell compartment, between the fibres that are woven together (Fig. 2.3B). After the central baffle, the organic phase flow is centralised into the collection pipe. The membrane being hydrophobic, the pores are filled with the organic phase, which is therefore in direct contact with the aqueous phase.

Before each use, the modules were washed by circulating an isopropanol solution (60 %, v/v) during two hours in the two compartments (shell and fibres). The modules were then drained and rinsed with sterilised Reverse Osmosis (RO) water. Finally, modules were dried overnight with compressed air.

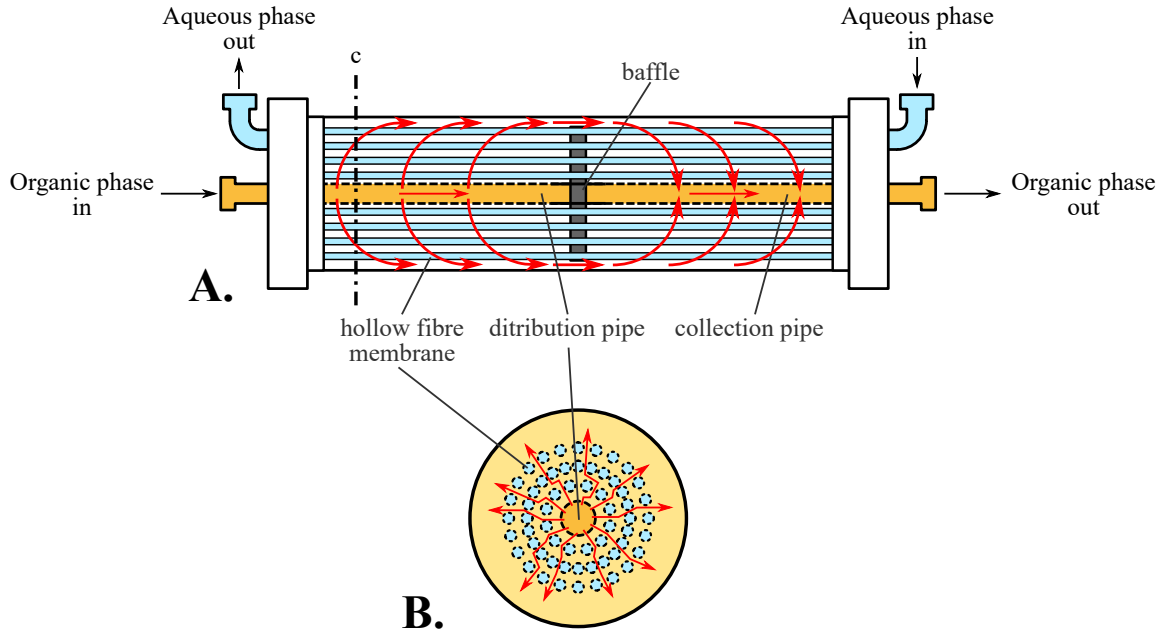

Figure 2.3: Schematic representation of a hollow fibre membrane contactor (HFMC)
A. Longitudinal section of the HFMC. **B.** Transveral section of the HFMC, following axis c. For a transversal section after the central baffle, this subfigure would be the same, but with reversed arrows (from the shell compartment to the collection pipe). Red arrows show the organic phase flow in the shell side.

Table 2.II: Characteristics of the membrane contactor modules

Liqui-Cel® module characteristics	
Material	Polypropylene
Internal diameter	58.4 mm
Internal length	203 mm
Number of fibres	$\simeq$ 9800
Shell side volume	400 mL
Fibres side volume	150 mL
Contact area	$\simeq$ 0.4 m^2

X50 fibres characteristics	
Material	Polypropylene
Internal diameter	220 µm
External diameter	300 µm
Effective length	146 mm
Wall thickness	40 µm
Porosity	40 %
Average pore size	0.03 µm

2.3 Batch cultures in shake-flasks (Chapter 3)

2.3.1 Inoculum

For inocula preparation, 1 mL of stock cultures was added to 25 mL of sterile, basal medium I1 (Table 2.III), in a 250 mL baffled shake-flask. The culture was incubated between 62 and 63 h in an incubator shaker (Multitron, Infors, Bottmingen, Switzerland) at 30 °C and 200 rpm. As shown in Fig. 2.4, this duration of incubation corresponded to early stationnary phase.

2.3.2 Cultures conditions

Preliminary tests in batch cultures were carried out in 500 mL baffled shake-flasks, containing 50 mL of medium. Flasks were inoculated with 1 mL of inoculum, reaching an initial cell dry weight (DW) of 0.04 g_{CDW} L^{-1}. Cultures were inoculated at 30 °C and 200 rpm. In order to perform kinetic analyses, samples were taken all along the cultures, for optical density (OD) measurements and metabolites quantification.

When growth on 1,3-PDO was tested, medium SF1 was used (Table 2.III). Prior to inoculation, the medium was supplied with filter-sterilised 1,3-PDO, in order to reach 5, 10 or 20 g L^{-1} concentrations. A control condition was also tested, where no 1,3-PDO was added to the medium. Each condition was tested in two replicates.

When initial pH effect was tested for growth on glycerol, medium SF2 was used (Table 2.III). This medium included a citrate-phosphate buffer, and the initial pH was adjusted to 4.0, 4.5, 5.0 or 6.5, using H_2SO_4 (5.5 mol L^{-1}). Each condition was tested in three replicates.

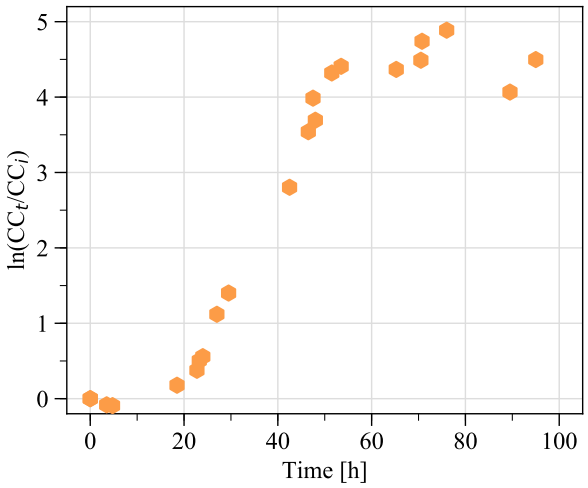

Figure 2.4: Follow up of the growth of *Acetobacter* sp. CIP 58.66 from stock cultures, for inoculum preparation ($n = 2$)
Cell Count (CC, cells mL^{-1}) varied from $1.77 \cdot 10^7$ cells mL^{-1} at $t = 0$ h up to $9.77 \cdot 10^8$ cells mL^{-1} in the end.

Table 2.III: Media composition for cultures of *Acetobacter* sp. CIP 58.66
Sterility was assured by autoclaving the medium-containing shake-flasks or bioreactor at 120 °C for 20 min.

	I1	I2	SF1	SF2	B1	B2
Yeast extract (g L^{-1})	5.0	5.0	5.0	5.0	5.0	5.0
Peptone (g L^{-1})	3.0	3.0	3.0	3.0	3.0	3.0
K_2HPO_4 (g L^{-1})	8.7	8.7	8.7	9.0	–	–
citric acid (g L^{-1})	–	–	–	4.4	–	–
Glycerol (g L^{-1})	–	10.0	–	10.0	–	10.0
1,3-propanediol (g L^{-1})	–	–	A.C.[a]	–	5.0	–
pH [b]	6.5	6.5	6.5	A.C.[a]	5.0	5.0

[a] According to condition: four different levels were tested
[b] Adjusted with a 5.5 mol L^{-1} H_2SO_4 solution

2.4 Fed-batch bioconversion of 1,3-propanediol in bioreactor (Chapter 3)

2.4.1 Inoculum

Inocula were prepared in two successive pre-cultures. The first one was carried out as previously described (section 2.3.1). Then, a volume expansion step was performed: 1 mL of the first pre-culture was used to inoculate 50 mL of medium I2 (Table 2.III), in a 500 mL shake-flask. This second pre-culture was incubated in the same conditions during 24 h (30 °C and 200 rpm). By the end of this incubation duration, the bacterial population is still in mid-exponential phase.

2.4.2 Single-step, pH control-based fed-batch

Single-step, pH control-based fed-batch experiments were carried out in a 3.6 L Labfors 4 bioreactor (section 2.2.3). 1 L of medium B1 (Table 2.III) was inoculated inside the bioreactor, at 120 °C, during 20 min. The temperature was controlled at 30 °C all along the experiments, and pO_2 was kept above 40 % by automatic control of stirring speed (between 100 and 800 rpm) and air flow rate (between 1 and 4 NL min^{-1}). The medium was inoculated using the preculture prepared as described in section 2.4.1, so that the initial cell dry weight (CDW) was around 0.02 g_{CDW} L^{-1}. The pH value was maintained at 5.0 by automatic addition of an equimolar solution of ammonium hydroxide (NH_4OH) and 1,3-PDO, at 6 mol L^{-1}, thus also serving as substrate input. The Pipe and Instrumentation Diagram (PID) of the process is displayed on Figure 2.5. These experiments were carried out in four replicates, and samples were taken all along the cultures, for optical density (OD) measurements and metabolites quantification.

2.4.3 Sequential pH control-based fed-batch

The PID of the process is the same as for the single-step process (Fig. 2.5).

2.4.3.1 *Primary growth phase on glycerol*

Biocatalyst production was performed in batch mode, with glycerol as growth substrate, in a 3.6 Labors 4 bioreactor (part 2.2.3). An initial 1 L volume of medium B2 (Table 2.III) was inoculated with the pre-culture, so that the initial biomass concentration reached 0.02 g_{CDW} L^{-1}. Due to the inoculum addition, initial pH rose from 5.0 to 5.2. During growth, pH was left uncontrolled, but agitation speed (from 100 to 800 rpm, Rushton turbine) and airflow rate (from 1 to 4 NL min^{-1}) were automatically controlled in order to maintain pO_2 above 40 %.

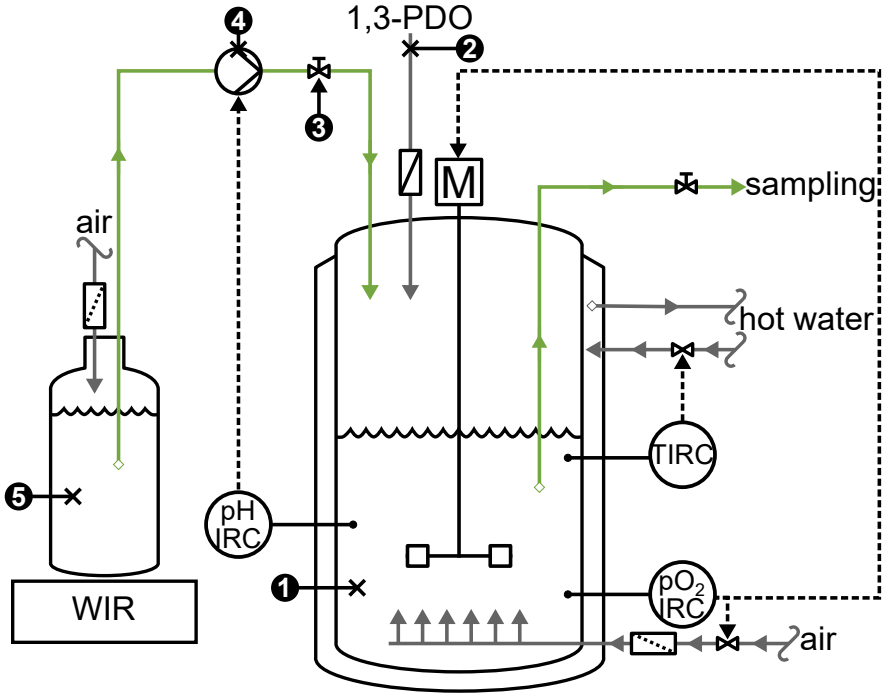

Figure 2.5: Process and Instrumentation Diagram of the pH control-based fed-batch process
1. Bacterial medium. 2. If applicable, addition of filter-sterilised 1,3-PDO to launch the bioconversion, after a preliminary growth phase. 3. Manual valve opened when the bioconversion is launched. 4. Feed pump, activated depending on pH measurements. 5. Base (NH_4OH) and substrate (1,3-PDO) mix, for pH control and bioreactor feeding. Solid arrows indicate fluid streams, while dotted arrows indicate electronic signals. Abbreviations: M, stirring motor; IRC, indicator, recorder and controller of the concerned parameter (pH, pO_2, or Temperature (T)); WIR, weight indicator and recorder.

2.4.3.2 *Fed-batch bioconversion*

When late exponential phase was reached, pH was adjusted to 4.0, 4.5, or 5.0 using H_2SO_4 (5.5 mol L^{-1}). 5 mL of filter-sterilised 1,3-PDO were then added to the medium in order to trigger bioconversion, and the equimolar solution of NH_4OH and 1,3-PDO was plugged to the bioreactor, for both pH contro and 1,3-PDO feeding purposes. Samples were taken all along the growth phase and the bioconversion phase, for OD measurements and metabolites quantification.

2.5 Extractive bioconversion of 1,3-propanediol (Chapter 4)

2.5.1 ISPR system setup and preparation

2.5.1.1 *Extraction and back-extraction phases composition*

The extraction phase consisted of 20 % (v/v) of didodecylmethylamine (DDMA) diluted in 40 % (v/v) dodecanol and 40 % (v/v) dodecane. DDMA was purified as described for trioctylamine (TOA) in a previous study [36]. The corresponding partition coefficient [1] and viscosity were determined as previously described [182] and were equal to 0.78 and 4.7 mPa s, respectively This formulation was adapted from a previous study, which established that a very similar composition (20 % (v/v) DDMA, 47 % (v/v) dodecanol and 33 % (v/v) dodecane) constituted an adequate trade-off between extraction performance and biocompatibility with a 3-HP producing strain [182]. The present organic phase had a similar distribution coefficient, but a lower viscosity. Therefore, a higher mass transfer rate was expected for the complex formed by DDMA and 3-HP in the organic phase [51], as well as a better biocompatibility due to the lower dodecanol to decane ratio [223, 111, 218].

For back-extraction, a solution of NaOH 0.5 mol L^{-1} was used as the stripping solution.

2.5.1.2 *Interface stabilisation*

The pertraction system (Fig. 2.6) consisted in two Hollow Fibres Membrane Contactors (HFMC, section 2.2.4) for 3-HP extraction and back-extraction. Before each experiment, the modules were washed by circulating a 60 % (v/v) isopropanol solution for two hours through the fibres and the shell side, then drained and rinsed with sterilised Reverse Osmosis (RO) water and finally dried overnight by flushing compressed air.

[1] The partition coefficient is the ratio, at equilibrium, between the 3-HP concentration in the organic phase and in the aqueous phase.

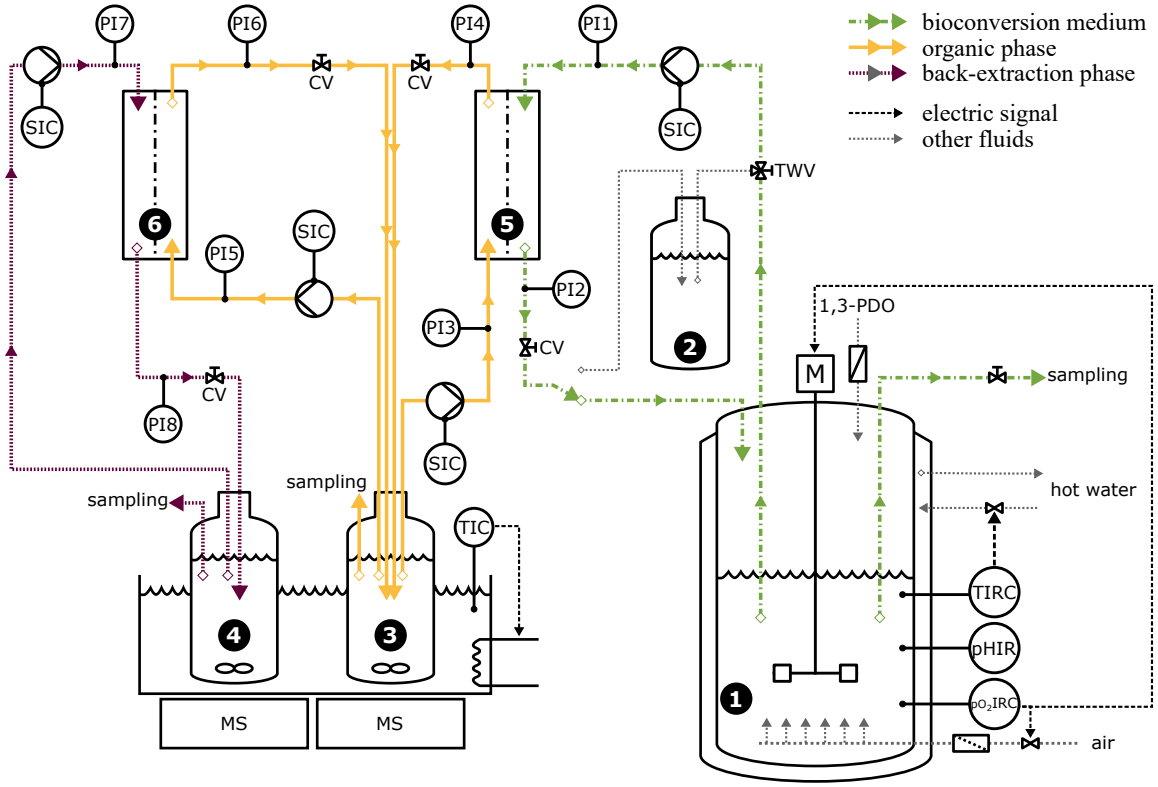

Figure 2.6: Process and instrumentation diagram of the extractive bioconversion
1. Bioconversion broth, where 1,3-PDO is converted into 3-HP. 2. Sterile RO Water for interface stabilisation. 3. Organic phase. 4. Back-extraction phase. 5. Membrane contactor for 3-HP extraction from bioconversion broth into organic phase. 6. Membrane contactor for 3-HP back-extraction into aqueous phase. Abbreviations: CV, control valve; M, motor; MS, magnetic stirrer; pHIR: pH indicator and recorder; PI: pressure indicator; pO2IRC, pO2 indicator, recorder and controller; SIC, speed indicator and controller; TIC, temperature indicator and controller; TIRC, temperature indicator, recorder and controller; TWV, three-way valve.

Table 2.IV: Operating conditions of the membrane contactor modules

Fibres (aqueous phases)			**Shell side** (organic phase)		
Pressure (bar)		Flow rate (mL min^{-1})	Pressure (bar)		Flow rate (mL min^{-1})
Inlet (PI 1&7)[a]	Outlet (PI 2&8)[a]		Inlet (PI 3&5)[a]	Outlet (PI 4&6)[a]	
0.80	0.70	450	0.45	0.45	430

[a] Pressure Indicator numbers are matching numbers on Fig. 2.6.

The large amount of air bubbles in the bioconversion broth, due to air sparging, made it impossible to correctly stabilise the interface with the organic phase in the hydrophobic membrane pores. Interface stabilisation in the extraction module was first performed by circulating 1 L of sterilised RO water inside the fibres and 1.5 L of the extraction phase in the shell side. A three-way valve (TWV on Fig. 2.6) was installed at the fibres inlet to switch the feed from the RO water to the bioconversion medium. For the back-extraction module, 1 L of a NaOH 0.5 mol L^{-1} solution was circulated inside the fibres, while the extraction phase was circulated on the shell side. Both modules were fed with extraction phase from the same container, allowing extractant regeneration. Liqui-Cel modules operating conditions are shown in Table 2.IV.
Due to sampling, the volumes of organic and back-extraction phases decreased over time during the experiments (finally reaching 1.42 and 0.86 L, respectively). These volume variations were taken into account in the mass balances equations.

2.5.2 Batch production of the biocatalyst

The inoculum consisted in two successive pre-cultures (as already described in section 2.4.1): (i) in a 250 mL shake-flask, 25 mL of medium I1 (Table 2.III, page 51) was inoculated with 1 mL of stock culture and incubated for 62 to 63 h at 30 °C and 200 rpm; (ii) then 1 mL of this culture was used to inoculate 50 mL of medium I2 (Table 2.III, page 51) in a 500 mL shake-flask, that was then incubated 24 h at 30 °C and 200 rpm (final dry weight concentration: 0.4 g L^{-1}).

Then, biocatalyst production was performed on glycerol as substrate, in the same conditions as previously described (Section 2.4.3.1). The cultivations were carried out in a 3.6 L Labfors 4 bioreactor, with a 1.2 L initial working volume of medium B2 (Table 2.III, page 51). Sterility of the medium-containing bioreactor was obtained by autoclaving at 120 °C, during 20 min. Medium was then inoculated with the preculture, in order to reach an initial CDW load of 0.02 g_{CDW} L^{-1} (approx. $4.1 \cdot 10^7$ cell mL^{-1}). Due to inoculum addition, the initial pH rose up to 5.2. During growth on glycerol, pH was left uncontrolled, while partial pressure of dioxygen (pO_2) was automatically controlled at a minimal value of 40 % of saturation. This was performed with a cascade of stirring rate (from 100 to 800 rpm, Rushton turbine) and air flow rate (from 1 to 4 NL min^{-1}). Biocatalysts production on glycerol lasted for 32 h, until the late exponential phase was reached. The growth medium was sampled over time, in

order to verify growth reproducibility among the replicates, and with previous experiments (section 2.4.3.1). This is necessary to guarantee that this biomass production step provides a consistent basis for subsequent bioconversion comparison.

2.5.3 Extractive bioconversion initiation and follow-up

After the late exponential phase was reached by *Acetobacter* sp. CIP 58.66 growing on glycerol, bioconversion was triggered by adding 6 mL of filter-sterilised 1,3-PDO (98 %, w/v), reaching an initial concentration close to 5 g L^{-1}. At the end of this primary growth on glycerol (32 h of culture), pH was close to 7. Because pH was left uncontrolled, medium acidification occurred after the 1,3-PDO addition, due to 3-HP production. Reactive liquid-liquid extraction with amines remains very limited when pH is above the pKa of the targeted acid. Consequently, the bacterial medium was brought in contact with the extracting phase only after pH reached 4.6, which is close to the pKa of 3-HP (4.51, [130]). No base was added for pH control, and pH varied freely according to production and extraction rates. RO water was replaced in the extraction module with the bioconversion broth, by switching the three-way valve (TWV on Fig. 2.6). Then the fibres' outlet was manually plugged to the bioreactor. After 4.6 h of bioconversion, a new 6 mL addition of 1,3-PDO in the bioconversion broth was performed. All along the bioconversion, pO_2 was controlled at a minimal value of 40 %, using the same control cascade as during the preliminary growth step (section 2.5.2). Samples were taken from the bioconversion medium, the organic phase and the back-extraction NaOH solution, for components quantification. Biomass evolution was also monitored in the bioreactor, by off-line optical density measurements (see 2.6.1). The extractive bioconversion was carried out in triplicates.

2.6 Analytical methods

2.6.1 Biomass concentration estimation

Cell growth was monitored by off-line optical density (OD) measurements at wavelength 600 nm using an Evolution 201 spectrophotometer (ThermoScientific, Madison, USA). Sterile medium was used as blank. OD was correlated to cell dry weight (CDW, g_{CDW} L^{-1}) using five dedicated shake-flask cultures on glycerol. At 8, 24, 30 and 48 h of culture, 10 mL broth samples were taken and filtered on pre-dried PES filters (pore size: 0.2 µm). These filters were then dried in an oven at 90 °C for at least 24 h. Filters were weighed just before filtration and after drying, on a precision scale (Sartorius ED224S, Goettingen, Germany). CDW was derived from the difference between the two weightings. Measurements were also performed in triplicates with sterile medium. The correlation that was obtained is given by Equation 2.1 and shown in Figure 2.7.

$$\text{CDW} = 0.59 \cdot \text{OD} \qquad (R^2 = 0.96, \text{p-value} < 0.005) \tag{2.1}$$

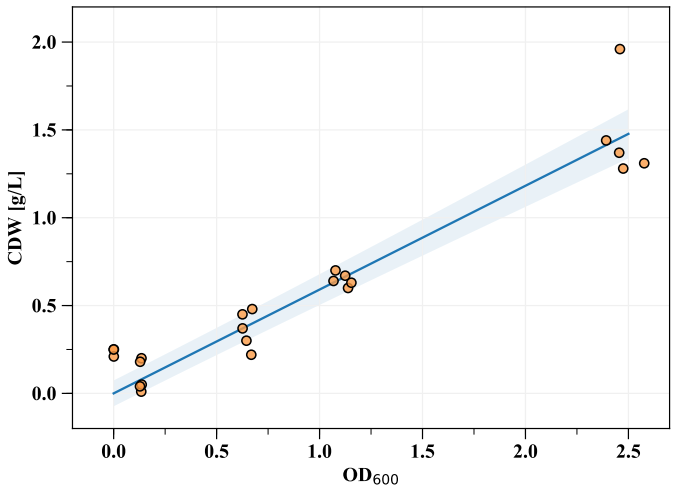

Figure 2.7: Correlation between optical density and cell dry weight of *Acetobacter* sp. CIP 58.66

$R^2 = 0.96$; p-value $= 1.47 \cdot 10^{-16}$. The blue area represents the 95 % confidence interval.

In the case of extractive bioconversions, some coloured compounds were extracted from the bacterial broth to the extractive phase. In this case, OD was measured for the native sample, as well as for its filtrate (PES filter, pore size: 0.22 µm). The filtrate's OD was deducted from the native sample's OD, so that variation of the medium colour would be taken into account. Yet, no significant difference could be evidenced with measurements using only

sterile medium as blank. Therefore, Eq. 2.1 was also used in this case.

When necessary, biomass concentration was expressed in carbon mol per litre (Cmol L^{-1}). The elemental composition of cell dry weight was assumed to be $C_4H_7O_2N$ [152]. Therefore, the molar weight of one Cmol was considered equal to 25.268 g mol^{-1}.

2.6.2 Flow cytometry analysis for physiological state assessment

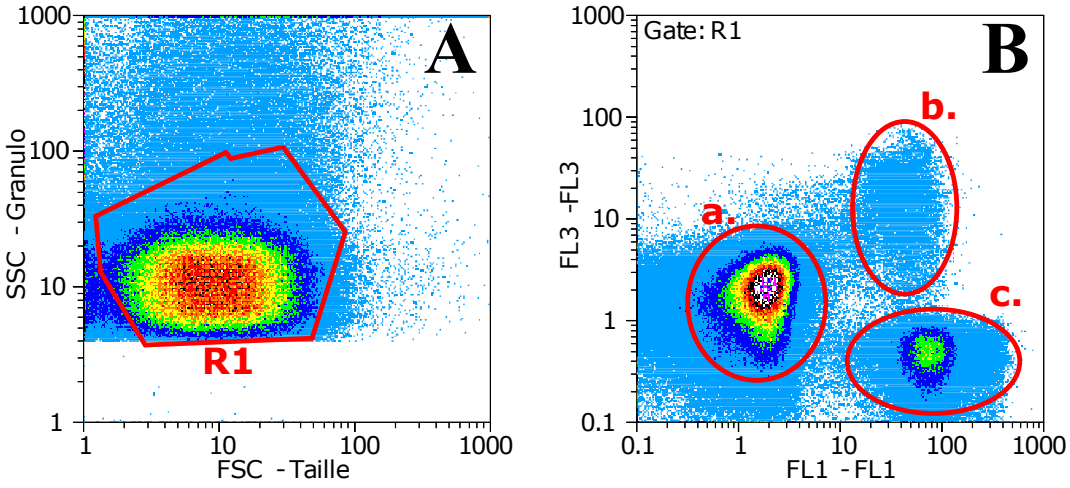

Figure 2.8: Example of a cytogram of dual cFDA/PI staining for a sample from extractive bioconversions

A. SSC against FSC density plot. Each point represents an individual particle. Particles located in region R1 are considered as bacteria. **B.** PI fluorescence intensity (FL3) against cFDA fluorescence intensity (FL1). On this plot, only events from region R1 on the SSC/FSC plot are displayed. The red circles shows the three distinct bacterial sub-populations: a. PI-stained cells (dead cells), b. both PI- and cFDA-stained cells (altered cells), c. cFDA-stained cells (enzymatically active cells)

Evaluation of the physiological state of bacteria was performed by dual fluorescent staining and subsequent analysis with a Cyflow® Space cytometer (Sysmex-Partec, Villepinte, France). The protocol was adapted from Rault *et al.*, (2007) [174]. Carboxyfluorescein diacetate (cFDA) contained in the commercial solution Chemchrom V8 was diluted in acetone at 10 % (v/v) and used to assess the esterase activity of cells, reflecting their basal enzymatic activity. The propidium iodide dye (PI) was diluted at 1 mg mL^{-1} in Milli-Q® water (Merck Millipore, Burlington, USA) and used for membrane integrity assessment. Cell samples were diluted in ChemSol B24 buffer in order to reach a concentration about 10^6 particles mL^{-1}. Dual staining was done by adding 100 µL of the cFDA solution and 5 µL of the PI solution to 1 mL of the diluted bacteria solution. After thorough mixing, samples were incubated 15 min in a bath at 40 °C, and then centrifuged for 90 s at $14,100$ g. Next, the supernatant was discarded and the cell pellet was resuspended in 1 mL of ChemSol B24 buffer before flow cytometry analysis. Data were acquired and analysed with the FlowMax software (Sysmex-Partec, Villepinte, France). The detected particles were gated based on forward scatter (FSC) and side scatter (SSC) values, in order to select only those corresponding to bacteria and to

reduce background noise (see Region R1 on Fig. 2.8.A).

Figure 2.8 provides an example of cytogram. cFDA and PI are respectively markers of esterase activity and of cell membrane integrity loss. Each bacteria can either be stained by one of the two dyes, or by both of them, depending on its esterase activity and on its membrane integrity. PI-stained bacteria (a. on Fig. 2.8.B) were considered as dead cells, while cFDA-stained bacteria (c. on Fig. 2.8.B) were considered as enzymatically active Bacteria stained with both PI and cFDA (b. on Fig. 2.8.B) have both an esterase activity and an altered membrane integrity, so they were considered as altered cells.

2.6.3 HPLC analyses

Table 2.V: Conditions of analysis for HPLC quantifications

	Set A	Set B
Column temperature	35 °C	65 °C
Mobile phase flow rate	0.6 mL min^{-1}	0.4 mL min^{-1}
H_2SO_4 concentration in mobile phase	5 mmol L^{-1}	0.5 mmol L^{-1}

Substrate and metabolites concentrations in aqueous samples were determined by High Performance Liquid Chromatography (HPLC) with an Aminex HPX-87H exchange column (300 mm × 7.8 mm; Bio-Rad, Richmond, VA, USA), and a refractive index detector (Waters, Guyancourt, France). Two different sets of analysis conditions were used (Table 2.V). Chromatograms were analysed using Empower 3 software (Waters).

2.6.3.1 *Analysis of bacterial broth samples*

For samples from the bioconversion medium, protein were first precipitated by diluting 750 µL of sample in 750 µL of a 6 % (w/v) solution of trichloroacetic acid, and putting the mix at 0 °C during at least 45 min. Samples were then centrifuged at 10,000 *g* during 4 min at 4 °C. Similarly to stripping solution samples, supernatants were finally filtered through nylon filters. 3-HPA was always analysed using conditions from Set A (Table 2.V), because its detection limit with conditions from Set B was too high. Glycerol, 3-HP and 1,3-PDO of glycerol-containing samples were always analysed with Set B of conditions (Table 2.V), because the resolution between 3-HP and glycerol was not sufficient when using Set A. However, 3-HP and 1,3-PDO from glycerol-free samples could be analysed with either set of conditions.

Regarding 3-HP and 3-HPA, no high purity, analytical-grade product can be found commercially (Table 2.I, page 47). In particular, 3-HPA was chemically synthesised according to Burgé *et al.* [30], and the final product was not perfectly pure. Their quantifications are therefore likely to be subjected to higher measurement errors, which could explain why the overall carbon recovery of some experiments is found slightly above 1.00.

2.6.3.2 *Analysis of organic phase samples*

Organic phase samples were back-extracted using an equal volume of a NaOH 0.5 mol L^{-1} solution. Mixtures were vortexed for 3 min and left overnight to reach equilibrium, then separated by centrifugation at $8,228$ *g* and 25 °C, for 15 min. Aqueous phase was recovered and filtered before HPLC analysis, using conditions from Set B (Table 2.V).

2.6.3.3 *Analysis of back-extraction phase samples*

Samples from the back-extraction phase were filtered, in order to remove traces of organic phase, before analysis with a nylon membrane filter (pore size: 0.2 µm). These samples were analysed using conditions from Set B (Table 2.V).

2.7 Calculations

2.7.1 Working volume correction for experiments in a bioreactor

During fed-batch experiments, the feeding solution was continuously weighted on a scale with a 0.01 g resolution (PCB6000-1, Kern, Balingen, Germany). The cumulative mass of solution that had been fed to the bioreactor was continuously calculated by deducting the current value to the initial solution mass. The corresponding volume was estimated assuming a 1.0 g mL^{-1} density.

The overall sampled volume (for off-line analyses) was estimated by weighting each sample on an identical scale (also assuming a 1.0 g mL^{-1} density for mass-to-volume conversions).

Furthermore, despite the use of a condenser on the gas outlet pipe, a volume loss still occurred due to dry air sparging and to long culture times. It was thus necessary to take this phenomenon into account in the analysis. For each experiment, the final working volume was measured and the overall volume loss was calculated by deducting the final from the initial working volume. Moreover, the air flow rate (on-line measurements) was time-integrated, so that the overall air volume that had passed through the bioreactor could be estimated. Finally, evaporation was considered to be proportional to the cumulated air volume. Thus, the volume loss due to evaporation could be estimated over time.

2.7.2 Kinetic analysis

Kinetics were analysed using the Gompertz model, as modified by Zwietering *et al.* (1990) [238] (Eq. 2.2).

$$G(t) = a \cdot \exp\left(-\exp\left[\frac{b \cdot e}{a}(c - t) + 1\right]\right) \tag{2.2}$$

$$G'(t) = b \cdot \exp\left(2 + \frac{b \cdot e}{a}(\lambda - t) - \exp\left[1 + \frac{b \cdot e}{a}(\lambda - t)\right]\right) \tag{2.3}$$

Where e represents exp(1), t is the time (h) and a, b, c are the parameters to be fitted. The model was first fitted to the natural logarithm of the relative population size $\ln(\text{CDW}_t/\text{CDW}_0)$: in this case, parameter b corresponds to the maximal growth rate μ_{max} (h^{-1}). The same model was also fitted to 3-HP concentrations. The time derivative of this model (Eq. 2.3) against time is the volumetric productivity $r_{\text{3-HP}}$ ($\text{g}_{\text{3-HP}}\ \text{L}^{-1}\ \text{h}^{-1}$). Specific 3-HP productivities, $q_{\text{3-HP}}$ ($\text{g}_{\text{3-HP}}\ \text{g}_{\text{CDW}}^{-1}\ \text{h}^{-1}$), were estimated by first fitting Gompertz models to 3-HP and CDW amounts in grams, in order to take the volume variations into account. Then, using both fitted models, $q_{\text{3-HP}}$ could be computed using Equation 2.4, with a 0.01 h time step:

$$q_{\text{3-HP}} = \frac{1}{\text{CDW}(t)} \cdot \frac{d\text{3-HP}}{dt} \tag{2.4}$$

The highest value reached was considered to be $q_{\text{3-HP,max}}$, while the average $q_{\text{3-HP}}$ was calculated as the mean of all values of the considered time span.

Parameter optimisation was performed with the Levenberg-Marquardt least-squares method, using Python (Python Software Foundation, version 3.6) and the "curve_fit" function from package scipy.optimize. A characteristic time τ_{90} (h) could then be calculated as the duration during which $q_{\text{3-HP}}$ is greater than or equal to 90 % of its maximal value.

Because of a biphasic exponential growth, maximal growth rates of *Acetobacter* sp. CIP 58.66 on glycerol were estimated for both phases separately by performing linear regression of logarithmic growth values ($\ln(\text{CDW}_t/\text{CDW}_0)$) against time. These regressions were carried out in Python 3.6, with function "OLS" from package "statsmodel.api".

Moreover, number of generations N_g of a growth phase were computed as $\log_2(\text{CDW}_f/\text{CDW}_i)$, where CDW_i and CDW_f are respectively the initial and final CDW values of the considered growth phase.

2.7.3 Model simulation for extraction and back-extraction dimensioning

In order to explore various optimisation strategies for the integrated process, a previously developed mathematical model was adapted to the experimental conditions of this study and used as a simulation tool. The model was written in Matlab (The MathWorks Inc., Natick, USA) and satisfactorily describes 3-HP reactive extraction with an organic phase containing a tertiary amine and back-extraction with a NaOH solution, assisted by a HFMC [37].

2.7.4 Statistical analysis

Results are given as mean $\pm$ sample standard deviation, and the sample size is reminded as "$n =$". When $n = 2$, results are given as mean $\pm$ half the amplitude between the replicates.

Given the low number of replicates, means were compared using the Fisher-Pitman permutation test, for which no distribution hypothesis is needed. These tests were carried out with the "oneway_test" function (with "distribution" option set to "asymptotic") from "coin" package on R 3.3.1 software. Results are given as "p-value = ; $n_1 =$, $n_2 =$", where n_1 and n_2 are the respective sizes of the two compared groups. Differences were considered significant for p-values lower than 0.05.

2.8 Modelling approach (Chapter 5)

Details of the modelling strategy of bioconversion data are provided step by step in the corresponding chapter (Chapter 5). The whole model development was carried out in software Python 3.6.

Page left blank intentionally

CHAPTER 3

AN EASY FEEDING STRATEGY, BASED ON PH CONTROL, FOR HIGHLY EFFICIENT PRODUCTION OF 3-HYDROXYPROPIONIC ACID BY *Acetobacter* SP. CIP 58.66

This chapter describes the development of a feeding strategy, based on pH control, for semi-continuous bioconversions of 1,3-propanediol (1,3-PDO) into 3-hydroxypropionic acid (3-HP) by *Acetobacter* sp. CIP 58.66. First shake-flasks cultures are described, for preliminary growth and bioconversion characterisation. Then, based on these results, the pH control-based feeding strategy was implemented in bioreactor.

This chapter will be submitted to *Bioresource Technology*, after the patent is published.

Chapter's table of contents

3.1 Introduction . . . 66
3.2 Experimental approach . . . 67
3.3 Results and discussion . . . 69
3.3.1 Effect of the initial 1,3-propanediol concentration in batch cultures . . . 69
3.3.2 Single-step, pH-based fed-batch bioconversion of 1,3-propanediol . . . 71
3.3.2.1 Growth performances . . . 71
3.3.2.2 Bioconversion performances . . . 73
3.3.2.3 pH and substrate control . . . 73
3.3.3 Biocatalyst production on glycerol for subsequent use within a sequential bioconversion strategy . . . 74
3.3.3.1 Growth characteristics and effect of initial pH . . . 74
3.3.3.2 Batch production of *Acetobacter* sp. CIP 58.66 on glycerol in bioreactor 75
3.3.4 Sequential, pH-based fed-batch bioconversion . . . 77
3.3.4.1 Secondary growth during the bioconversion phase . . . 77
3.3.4.2 Enhanced bioconversion performances . . . 78
3.3.4.3 pH effect on bioconversion performances . . . 78
3.4 Conclusion . . . 81

3.1 Introduction

As described in Chapter 1, one of the dominant approaches so far has been 3-HP biosynthesis from glycerol, either through a coenzyme A-dependent or -independent metabolic route. In both cases, glycerol is first converted into 3-hydroxypropionaldehyde (3-HPA), which is subsequently oxidised into 3-HP or reduced into 1,3-propanediol (1,3-PDO). These oxidative and reducing pathways are in redox balance with one another. 1,3-PDO is therefore an obligate co-product of 3-HP biosynthesis from glycerol. Consequently, it is of interest to implement a subsequent step for its conversion to 3-HP, so that the yield and the selectivity of the overall process are improved.

Interestingly, the potential of acetic acid bacteria for selective oxidation of diols into hydroxycarboxylic acids was demonstrated by Füchtenbusch *et al.* (1998) [74]. In this light, 1,3-PDO conversion into 3-HP using acetic acid bacteria was recently investigated on three occasions [65, 122, 234]. By analogy with ethanol oxidation into acetate, 3-HP synthesis from 1,3-PDO by these bacteria is thought to be a two-step pathway, set on the outer side of the membrane, with 3-HPA as an intermediate [65, 237] (Fig. 3.1). *Gluconobacter oxydans* was notably implemented, as part of multi-step processes, where 1,3-PDO was first produced from glycerol by *Klebsiella pneumoniae* [234] or *Lactobacillus reuteri* [65]. The performances of immobilised *Acetobacter* sp. CGMCC 8142 for 3-HP production from 1,3-PDO were also evaluated [122]. In these studies, resting bacteria were operated in batch mode and showed promising results: 1,3-PDO was quantitatively converted to 3-HP, with little to no by-products, and high titres could be reached (up to 66.95 g L^{-1}), thanks to their tolerance to acidic conditions. Acrylic acid was the only reported by-product of 1,3-PDO oxidation [234]. These studies mainly focused on pH, temperature, and substrate and biocatalyst concentrations as main parameters for process optimisation. Yet, in their study, Dishisha *et al.* (2015)[65] also reported transient 3-HPA accumulation, with a peak around 2 g L^{-1}, which could be explained by an imbalance between the two enzymatic steps [237]. This is above the minimum inhibitory concentrations (MIC) estimated on *Escherichia coli*, which range from 0.56 to 1.11 g L^{-1} [49].

This chapter investigates the potentialities of *Acetobacter* sp. CIP 58.66 for 3-HP production from 1,3-PDO. Preliminary tests were first carried out in shake flasks, in order to identify the key limitations and the best suited operational conditions. Only low substrate levels could ensure sub-inhibitory 3-HPA concentrations. A fed-batch process was thus designed in order to keep low 1,3-PDO levels. Since 1,3-PDO consumption ultimately leads to medium acidification due to 3-HP accumulation, a simple feeding strategy based on pH control was implemented: 1,3-PDO was mixed with the base used for pH control in equal proportions. By doing so, 1,3-PDO is continuously being added to the broth in the same amount than

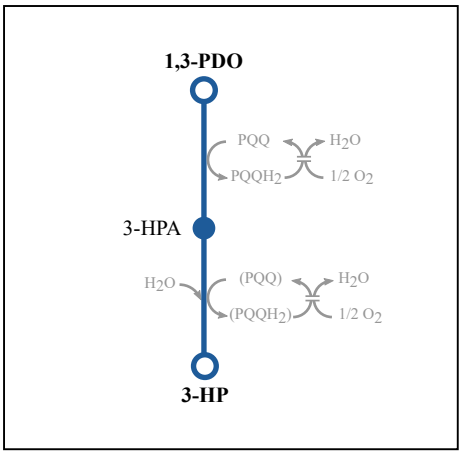

Figure 3.1: Putative metabolic pathway of 1,3-PDO oxidation into 3-HP by acetic acid bacteria
The cofactor of the second step is bracketed, because its exact nature is not known with certainty (see section 1.2.1.5).

the base needed for 3-HP neutralisation. A similar approach was already proven successful for lactic acid production by *Lactobacillus lactis* [233]. The process was then improved by developing a sequential strategy, including two growth steps, first on glycerol alone and then on glycerol and 1,3-PDO. This is also the first report of 3-HP production by growing cells of acetic acid bacteria, rather than resting cells.

3.2 Experimental approach

The experimental approach for process development included several successive steps that are presented on Figure 3.2. For detailed methods, the reader is referred to Chapter 2 (Materials and Methods). An index of the methods that were used is provided in Table 3.I.

First, growth and bioconversion on 1,3-PDO by *Acetobacter* sp. CIP 58.66 was characterised in 500 mL shake-flasks, with complex media containing several levels of initial 1,3-PDO. Then, a feeding strategy was tested in bioreactor (1 L initial working volume), where the strain was inoculated in a 1,3-PDO-containing medium (initially 5 g L^{-1}). An equimolar (6 mol L^{-1}) solution of base (NH_4OH) and 1,3-PDO was used for both substrate feeding and pH control. In order to improve cell densities, a sequential strategy was considered: bacteria were first grown on glycerol, before the bioconversion was triggered. To that aim, growth on glycerol of *Acetobacter* sp. CIP 58.66 was tested in 500 mL shake-flasks containing complex media, with different initial pH. Batch growth on glycerol was then evaluated in bioreactor, with 1 L initial working volume. Finally, the pH control-based feeding strategy was tested in bioreactor after this initial growth step on glycerol. After the late exponential phase was reached on glycerol in batch mode (32 h of culture), the bioconversion was triggered by

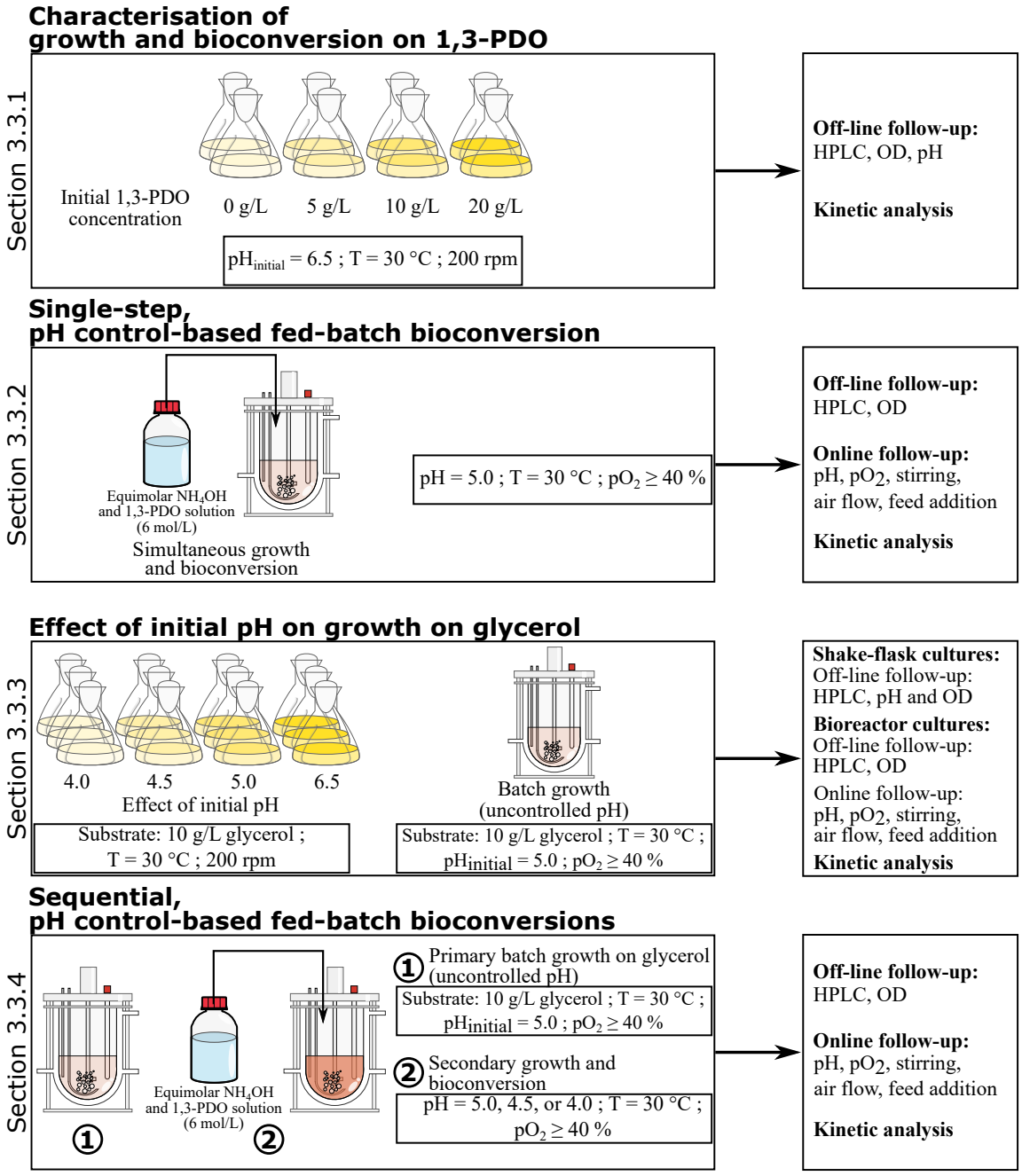

Figure 3.2: Experimental design of Chapter 3

Table 3.I: Index of methods used in Chapter 3

Shake-flasks cultures	Section 2.3	page 50
Fed-batch bioconversions	Section 2.4	page 52
Biomass quantification	Section 2.6.1	page 58
HPLC analyses	Section 2.6.3	page 60
Kinetic analysis	Sections 2.7.1 & 2.7.2	page 61
Statistical analysis	Section 2.7.4	page 63

adjusting the pH at the setpoint value, and by adding 5 mL of filter-sterilised 1,3-PDO. Then, the equimolar 1,3-PDO and NH_4OH solution is used for pH control and substrate feeding. These bioconversions were tested at pH 5.0, 4.5, and 4.0.

3.3 Results and discussion

3.3.1 Effect of the initial 1,3-propanediol concentration in batch cultures

In the first instance, *Acetobacter* sp. CIP 58.66's ability to perform growth-coupled 1,3-propanediol (1,3-PDO) bioconversion was investigated. Its growth was thus tested in shake-flasks on a complex medium containing either 0, 5, 10 or 20 g L^{-1} of 1,3-PDO. First of all, it could be observed that, to some extent, the resources available in the basal medium were sufficient to support the strain's growth. Indeed, in absence of 1,3-PDO, bacterial growth could be observed, reaching a final cell dry weight (CDW) concentration of 0.18 g_{CDW} L^{-1} (Table 3.II). This growth was accompanied by a slight pH increase (from 6.5 to 6.7) that may be attributed to the consumption of amino acids from the complex medium for the anabolism, or to ammonia release due to late cell lysis. When 1,3-PDO was added to the initial medium, changes in growth patterns could be observed. Maximal growth rate μ_{max} was found significantly higher in presence of 1,3-PDO (p-value $= 0.01$; $n_1 = 2$, $n_2 = 6$), but it appeared to be independent from initial concentration. For 5 and 10 g L^{-1} initial 1,3-PDO concentrations, final cell densities were also higher in comparison to control, whereas they were lower for 20 g L^{-1} initial 1,3-PDO (Table 3.II). These results suggest that *Acetobacter* sp. CIP 58.66 is able to use 1,3-PDO for its growth as either carbon or energy source. Yet, seeing as the highest cell density was achieved for the lowest initial 1,3-PDO concentration, it seems that substrate or product inhibition phenomena arise, for higher substrate levels. Previous studies on 1,3-PDO bioconversion into 3-HP using acetic acid bacteria focused on using resting cells, and biomass evolution was not measured over time [65, 234]. This is therefore the first time 1,3-PDO is reported to have an impact on an acetic acid bacterium growth.

The condition with the best growth performances (5 g L^{-1} initial 1,3-PDO) was also the one displaying the best bioconversion performances. Indeed, 1,3-PDO was fully depleted only in the case of 5 g L^{-1} initial 1,3-PDO concentration. For 10 and 20 g L^{-1} initial concentrations, consumption dropped to 53.7 % and 14.4 % respectively. This trend is consistent with the observations made by Dishisha *et al.*, (2015) [65] in their study, resting cells of *Gluconobacter oxydans* consumed 95.3 %, 86.1 % and 31.3 % of 5, 10 and 20 g L^{-1} initial 1,3-PDO respectively. Furthermore, full substrate depletion was also associated with the highest 3-HP yield and titre, as well as with the lowest 3-HPA titre (Table 3.II). On the contrary, for 10 and 20 g L^{-1} initial 1,3-PDO, final 3-HP yields were lower, due to higher

Table 3.II: Comparison of growth and bioconversion for different initial 1,3-PDO concentrations in shake-flasks cultures

Finals values are calculated at 30 h of culture. For each condition, $n = 2$.

	Initial 1,3-PDO concentrations (g L^{-1})			
	0	5	10	20
Final CDW (g L^{-1})	0.18 ± 0.01	0.33 ± 0.02	0.22 ± 0.03	0.12 ± 0.02
Final N_g	2.21 ± 0.06	3.17 ± 0.03	2.58 ± 0.09	1.72 ± 0.02
μ_{max} (h^{-1})	0.21 ± 0.00	0.28 ± 0.00	0.29 ± 0.01	0.27 ± 0.01
Final 1,3-PDO consumption (%)[a]	ND[b]	99.4 ± 0.7	53.7 ± 1.3	14.4 ± 1.4
Final 3-HP titre (g L^{-1})	ND[b]	6.02 ± 0.06	3.77 ± 0.61	2.14 ± 0.06
Final 3-HP yield (mol_C mol_C^{-1})	ND[b]	1.07 ± 0.03	0.59 ± 0.10	0.59 ± 0.01
Final 3-HPA titre (g L^{-1})	ND[b]	0.16 ± 0.00	1.06 ± 0.06	0.55 ± 0.03
Final 3-HPA yield (mol_C mol_C^{-1})	ND[b]	0.04 ± 0.00	0.21 ± 0.01	0.19 ± 0.01
Final pH	6.7 ± 0.1	4.3 ± 0.1	4.4 ± 0.2	5.1 ± 0.2
$q_{3\text{-HP,max}}$ ($g_{3\text{-HP}}$ g_{CDW}^{-1} h^{-1})	ND[b]	2.14 ± 0.12	2.24 ± 0.24	1.82 ± 0.03
τ_{90} (h)	ND[b]	3.97 ± 0.29	2.87 ± 0.28	2.19 ± 0.01

[a] Calculated as the percentage of 1,3-PDO initially supplied

[b] Was not calculated because no 1,3-PDO was supplied to the medium

3-HPA accumulation. Such a drop in 3-HP yield was not reported in the previous studies using resting cells of *G. oxydans* [65, 234]. However, immobilised resting cells of *Acetobacter* sp. CGMCC 8142 showed an important drop in 3-HP yield too, but only for substrate concentrations above 50 g L^{-1} [122]. A recent study on *Gluconobacter oxydans* DSM 2003 suggested that the aldehyde dehydrogenase was the rate limiting enzyme of 1,3-PDO oxidation into 3-HP [237]. This could explain the 3-HPA accumulation when 10 or 20 g L^{-1} of 1,3-PDO is initially supplied: in these cases, substrate excess might have led to detrimental 3-HPA levels. Indeed, for 10 and 20 g L^{-1} initial 1,3-PDO, final 3-HPA concentrations were within the range of the minimal inhibitory concentrations that were measured for 3-HPA on *Escherichia coli*, from 0.56 to 1.11 g L^{-1} [49]. Interestingly, even though the data suggest no clear-cut difference in maximal specific productivities ($q_{\text{3-HP,max}}$) between 5 and 10 g L^{-1} of initial 1,3-PDO, it seems that the characteristic time τ_{90} decreases for higher initial 1,3-PDO concentration (Table 3.II). This suggests that the inhibitory phenomena due to high 1,3-PDO or 3-HPA levels impact not only the growth and bioconversion performances, but also deteriorate the physiological state of cells.

In summary, these results show that the best growth and 3-HP production performances were achieved with a 5 g L^{-1} initial 1,3-PDO concentration. In particular, in this case, 1,3-PDO was quasi-quantitatively converted into 3-HP. Substrate and intermediary 3-HPA inhibitions were thus prevented. Given its low minimal inhibitory concentration, 3-HPA is likely to play a major role in the process inhibition. However, further study would be needed to accurately identify the contribution of each factor (1,3-PDO, 3-HPA, 3-HP, pH) in the inhibition or enhancement of growth and 1,3-PDO conversion by *Acetobacter* sp. CIP 58.66.

3.3.2 Single-step, pH-based fed-batch bioconversion of 1,3-propanediol

In light of these results, a pH control-based fed-batch strategy was implemented in a 3.6 L bioreactor, in order to keep a constant 1,3-PDO concentration of 5 g L^{-1} in the medium. As a first approach, an equimolar (6 mol L^{-1}) solution of NH_4OH and 1,3-PDO was prepared and used for pH control (at pH $= 5$). By doing so, 1,3-PDO was supplied in the same amount as the base used for 3-HP neutralisation.

3.3.2.1 *Growth performances*

For all four replicates of single-step, pH control-based fed-batch, growth of *Acetobacter* sp. CIP 58.66 was observed (Fig. 3.3A). Final cell density reached 0.14 ± 0.07 g_{CDW} L^{-1}, with a maximal growth rate of 0.27 ± 0.04 h^{-1}. The final number of generations was 2.95 ± 0.69. No significant difference in number of generation nor in μ_{max} appeared when comparing with previous experiment with 5 g L^{-1}initial 1,3-PDO (section 3.3.1, Table 3.II): p-values were respectively 0.65 and 0.59 ($n_1 = 2$, $n_2 = 4$). This suggests that pH and 1,3-PDO control, at 5.0 and 5 g L^{-1} respectively, were not enough to overcome all possible limitations arising during the process.

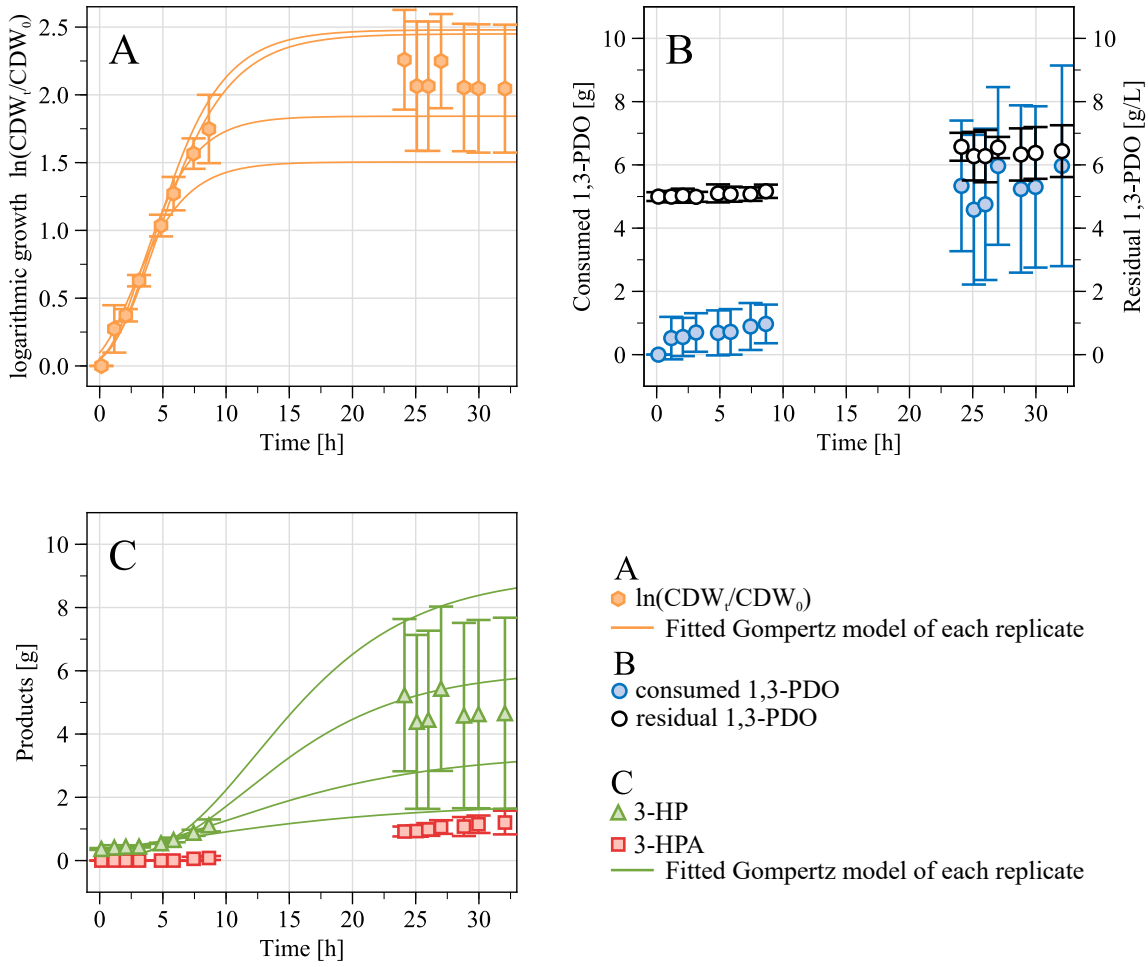

Figure 3.3: Single-step, pH control-based fed-batch of *Acetobacter* sp. CIP 58.66 on 1,3-propanediol ($n = 4$)

A. Logarithmic growth of the bacterial population. B. Residual substrate and overall substrate consumption. C. 3-HP and 3-HPA production. The initial working volume was 1.02 L, and the final volumes varied between 0.90 and 0.95 L, depending on replicates.

3.3.2.2 *Bioconversion performances*

As expected based on previous results (section 3.3.1), bioconversion of 1,3-PDO into 3-HP occurred during growth of *Acetobacter* sp. CIP 58.66 in fed-batch mode (Fig. 3.3). Even though 1,3-PDO was kept around 5 g L^{-1}, its overall consumption remained low (5.97 ± 3.18 g), and final 3-HP titre (5.01 ± 3.16 g L^{-1}) was similar to preliminary shake-flasks batch experiments (Table 3.II). 3-HP yield was however significantly decreased to 0.57 ± 0.18 mol_C mol_C^{-1} (p-value $= 0.047$; $n_1 = 2$, $n_2 = 4$), as compared to shake-flasks cultures during which 1,3-PDO was almost quantitatively converted to 3-HP. This low yield was due to the accumulation of the intermediary 3-HPA, whose final concentration rose up to 1.30 ± 0.39 g L^{-1}. This value is within the inhibitory range of 3-HPA that was measured for *E. coli* [49]. Accumulation of 3-HPA therefore appears as a likely limiting factor to the process performances.

Interestingly, kinetic analysis showed that high specific productivities were achieved during single-step fed-batchs: $q_{\text{3-HP,max}}$ was equal to 3.80 ± 0.33 $g_{\text{3-HP}}$ g_{CDW}^{-1} h^{-1}, which is higher than $q_{\text{3-HP,max}}$ found in batch cultures (p-value $= 0.032$; $n_1 = 2$, $n_2 = 4$). Higher specific productivities can be explained by several factors linked with the process being implemented in a bioreactor instead of shake-flasks (*e.g.* pH and pO_2 control), and in fed-batch mode instead of batch mode (substrate concentration control) All these factors might contribute to a better physiological state of the bacteria.

3.3.2.3 *pH and substrate control*

Since 1,3-PDO was expected to be quantitatively converted into 3-HP (section 3.3.1) and because no buffer solution was added to the medium, the feeding solution was prepared with a 1:1 molar ratio between 1,3-PDO and ammonium hydroxide. By doing so, it was expected that 1,3-PDO would be supplied at the same rate it is consumed by *Acetobacter* sp. CIP 58.66, while pH would remain at the setpoint value. On the one hand, only a slight increase in 1,3-PDO occurred in the bioreactor: final 1,3-PDO concentration reached 6.43 ± 0.82 g L^{-1} (Fig. 3.3B). This accumulation could be partly due to a concentration phenomenon caused by water evaporation. On the other hand, for two of the four replicates, pH was not correctly controlled at the beginning of the culture: in these two occurrences, pH peaked at 6.0 and 6.3 respectively, between the third and fourth hour of culture. This could be due to the lack of temperature control in the feeding solution, resulting in NH_3 exhaust from the feeding system to the bioreactor. This difference in pH control between replicates might explain the high variability of the results.

As a conclusion to this experiment, it appeared that, as designed, the process could successfully keep 1,3-PDO concentrations close to 5 g L^{-1}, while also controlling the pH (at least after 7 h of culture). Yet, the implemented process could not ensure high biomass densities: final cell density was 0.14 ± 0.07 g L^{-1}. 3-HP production therefore remained relatively low: the overall production was equal to 4.49 ± 3.27 g, and the maximal volumetric productivities ($r_{\text{3-HP,max}}$) ranged from 0.06 to 0.32 $g_{\text{3-HP}}$ L^{-1} h^{-1} in the four replicates. The main identified limitation was 3-HPA accumulation up to detrimental levels. Also, it remains unclear

Table 3.III: Growth comparison of *Acetobacter* sp. CIP 58.66 with glycerol as substrate, at different intial pH

For each condition in shake-flasks, $n = 3$; for biocatalyst production in bioreactor (last column), $n = 6$.

	Shake-flasks cultures [a]				Biocatalyst production [b]
Initial pH	4.0	4.5	5.0	6.5	5.0
Final CDW (g L^{-1})	0.14 ± 0.01	0.33 ± 0.04	1.14 ± 0.04	0.43 ± 0.02	0.88 ± 0.05
$\mu_{max,1}$ (h^{-1})	0.10 ± 0.01	0.15 ± 0.01	0.18 ± 0.01	0.11 ± 0.01	0.24 ± 0.03
$\mu_{max,2}$ (h^{-1})	0.03 ± 0.01	0.06 ± 0.01	0.09 ± 0.01	0.07 ± 0.00	0.18 ± 0.02
Glycerol consumption (%) [c]	1.0 ± 0.8	4.6 ± 1.9	16.9 ± 0.7	5.8 ± 0.6	18.6 ± 1.7
Biomass yield (g_{DW} $g^{-1}_{glycerol}$)	ND[d]	0.83 ± 0.28	0.69 ± 0.05	0.76 ± 0.06	0.40 ± 0.05
Final pH	4.1 ± 0.1	4.6 ± 0.1	5.4 ± 0.1	6.6 ± 0.1	6.9 ± 0.2

[a] Comparison at 30.5 h of culture

[b] Values at 31 h of culture in bioreactor

[c] Calculated as the percentage of glycerol initially supplied

[d] Could not be calculated because no significant glycerol consumption occurred

whether 1,3-PDO can be used as carbon source by *Acetobacter* sp. CIP 58.66, or only as additional energy source. Indeed, it is hypothesised that 1,3-PDO is oxidised into 3-HP by acetic acid bacteria through a similar pathway to ethanol oxidation into acetate [65, 237]. Furthermore, it was shown that ethanol as the only carbon source could not support growth of *Acetobacter aceti* and could support only limited growth of *Acetobacter methanolicus* [72, 114]. In this case, the observed impact of 1,3-PDO on growth of *Acetobacter* sp. CIP 58.66 could be due to 1,3-PDO serving as additional energy source only.

3.3.3 Biocatalyst production on glycerol for subsequent use within a sequential bioconversion strategy

3.3.3.1 *Growth characteristics and effect of initial pH*

Previous experiments showed that despite 1,3-PDO having a positive impact on *Acetobacter* sp. CIP 58.66's growth, it could not ensure high biomass density (section 3.3.1). The strain's growth was thus investigated on a separate substrate, namely glycerol. Glycerol was chosen because it was used as growth substrate in other studies on 3-HP production using acetic acid bacteria [65, 122, 170, 234], even though only few details are generally given on this step. Growth of *Acetobacter aceti* was however described by Kylmä *et al.* (2004) [114] and Frébortová *et al.* (1997) [72]. In this paper, we tested four different initial pH in shake-flasks, batch culture of *Acetobacter* sp. 58.66 on 10 g L^{-1} glycerol (Table 3.III).

When pH was initially set to 4.0, glycerol remained unconsumed and biomass density remained low (0.14 g_{CDW} L^{-1}). This condition was therefore considered too stressful and could not ensure high biocatalyst concentration. In the other conditions (*i.e.* initial pH equal to 4.5, 5.0 and 6.5), glycerol consumption occurred and higher levels of biomass were

reached (Table 3.III). The highest concentration (1.14 g L^{-1}) was achieved for an initial pH of 5.0. Even though glycerol consumption remained low at the time of comparison (30.5 h), it could be observed on one replicate that after 115 h, glycerol was fully depleted in all these conditions. In all instances, two distinct exponential growth phases were identified: a slope break would appear between 4 and 8 h of culture. The condition where pH was initially set to 5.0 showed the highest growth rates for both phases (0.18 and 0.09 h^{-1} respectively), and was the only one reaching late-log phase by 30.5 h of culture. This condition showed the best characteristics (highest cell density, growth rates and biomass yield), and was thus chosen for biocatalyst production in bioreactor, prior to bioconversion (section 3.3.3.2).

Surprisingly, no product of glycerol catabolism could be detected in our conditions of analysis. This is in contradiction with previous observations by Kylmä *et al.* (2004) [114], who detected lactate and succinate (up to *ca.* 1.1 and 0.1 g L^{-1}, respectively), when *Acetobacter aceti* was grown on 10 g L^{-1} glycerol. In these concentrations, lactate and succinate would have been detected in our conditions of analysis. Besides, no medium acidification occurred in our experiments (Table 3.III). It was thus hypothesised that glycerol was fully oxidised to CO_2, which was the main product from glycerol oxidation in the study of Kylmä *et al.* (2004) [114]. Moreover, maximal growth rates were lower than the ones determined in the presence of 1,3-PDO with the same initial pH (Table 3.II). This would suggest that glycerol and 1,3-PDO are metabolised in two distinct metabolic pathways by *Acetobacter* sp. CIP 58.66. This is consistent with studies of Kylmä *et al.* (2004) [114] and Zhu *et al.* (2018) [237]: the former proposed two different pathways for glycerol and ethanol metabolism in *Acetobacter aceti*, while the latter showed that acetic acid bacterium *Gluconobacter oxydans* oxidises 1,3-PDO through a pathway similar to the one of ethanol (*i.e.* two successive oxidations, with an intermediary aldehyde, and catalysed by two membrane-bound enzymes).

3.3.3.2 *Batch production of Acetobacter sp. CIP 58.66 on glycerol in bioreactor*

Based on the previous experiments, we tested whether *Acetobacter* sp. CIP 58.66 could grow on 10 g L^{-1} glycerol in a bioreactor controlled at pH 5.0, while simultaneously converting 1,3-PDO fed similarly to experiments from section 3.3.2 (data no shown). At time $t = 27$ h, only 0.68 g of glycerol was consumed, and bioconversion results were similar to from those described in section 3.3.2. Therefore, a sequential strategy was designed, where biomass of *Acetobacter* sp. 58.66 was first produced on glycerol in batch mode. Then, when late exponential phase is reached, cells are supplied with 1,3-PDO in fed-batch mode. This section deals with the first step of the overall process (*i.e.* biomass production), which was the same for all sequential experiments.

Biomass of *Acetobacter* sp. CIP 58.66 was produced from 10 g L^{-1} glycerol in a 3.6 L bioreactor. Initially, pH was set to 5.0 and it was then left uncontrolled. Results are shown in Table 3.III and Figure 3.4. Except for one of the six replicates, bacterial growth started without any latency phase. In all instances, late exponential phase was reached by 31 h of culture, with a 0.88 g L^{-1} CDW concentration. Similarly to preliminary shake-flasks experiments (section 3.3.3.1), two distinct growth rates could be estimated, respectively 0.24

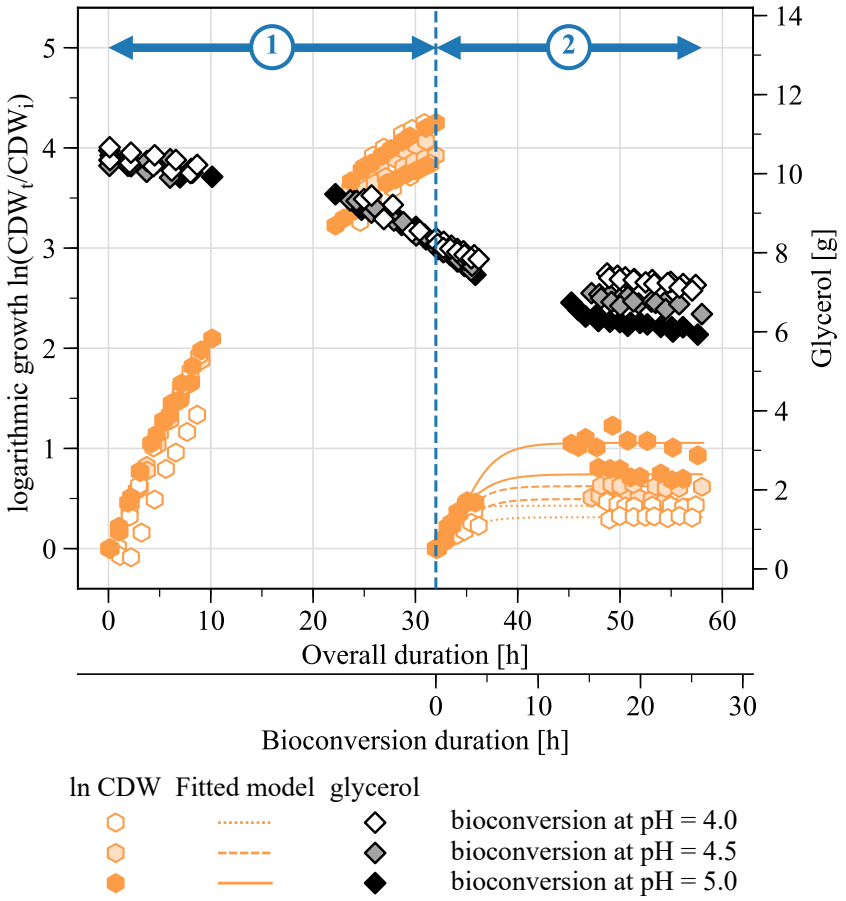

Figure 3.4: Growth of *Acetobacter* sp. CIP 58.66 and glycerol consumption during the sequential process

1. Primary, batch growth on glycerol; this step is performed in the same conditions for all experiments. 2. Secondary growth during 1,3-PDO fed-batch bioconversion, at different pH (4.0, 4.5 or 5.0). For each growth phase, logarithmic growth is calculated on the basis of the initial CDW of the concerned phase: so, at the beginning of phase (2), the logarithmic growth is 0 again, even though there is no CDW change when going from (1) to (2). For each pH condition, $n = 2$. The initial working volume was 1.02 L, and the final estimated volumes varied between 0.83 and 0.91 L, depending on replicates.

and 0.18 h^{-1}. Furthermore, by 31 h of culture, glycerol consumption remained low (18.6 % of initial glycerol) and, again, no by-product could be detected. Indeed, because no buffer solution was added to the medium, pH rose up to 6.94. This rise in pH may be the cause for of the slowing down of growth before full substrate depletion. To a large extent, these results are comparable with those of Kylmä *et al.* (2004), who tested *Acetobacter aceti*'s growth on mineral medium, at pH 5.8, with glycerol as only substrate. In their experiment, a $t = 32$ h, about 20 % of initial glycerol was consumed, and CDW was approximately around 0.5 g L^{-1}. However, they observed lower growth rate (0.15 h^{-1}) and biomass yield (0.16 g_{DW} $g^{-1}_{glycerol}$), which could be due to nutrient limitations in their minimal medium.

Future works on this biomass production step, notably including pH control and medium optimisation, could improve the process in terms of final CDW and growth rates. Yet, the final CDW we obtained were still significantly higher than the ones in the single-step fed-batch bioconversion from section 3.3.2 (p-value $= 0.003$; $n_1 = 6$, $n_2 = 4$). Furthermore, growth on glycerol also showed greater reproducibility: for instance, the coefficient of variation for final CDW was 6 % instead of 47 % for the single-step fed-batch. It was thus considered that these six growth replicates constitute a consistent basis for comparison of the subsequent bioconversions.

3.3.4 Sequential, pH-based fed-batch bioconversion

Once produced as described in section 3.3.3.2, biomass of *Acetobacter* sp. CIP 58.66 was used as biocatalyst for 1,3-PDO selective oxidation into 3-HP. After growth on glycerol, pH was adjusted to the desired value with H_2SO_4 (5.5 mol L^{-1}), and fed-batch bioconversion was launched by adding 5 mL of 1,3-PDO as starter, and by plugging the feeding solution to the bioreactor. The latter solution was a 1:1 molar mix of ammonium hydroxide and 1,3-PDO, in order to ensure both pH and substrate feed control (Fig. 2.5, page 53). In the first instance, bioconversion was tested at pH 5, for comparison with the single-step fed-batch strategy described in section 3.3.2.

3.3.4.1 *Secondary growth during the bioconversion phase*

After bioconversion was launched at pH 5, a secondary exponential growth phase could be identified, without any latency phase (Fig. 3.4). CDW concentration further increased to 2.08 ± 0.04 g L^{-1}, at a maximal growth rate of 0.18 ± 0.04 h^{-1}. No significant differences in growth rates could be evidenced when comparing with growths on glycerol or on 1,3-PDO. Yet, glycerol was further consumed during 1,3-PDO oxidation (Fig. 3.4): by 25 h of bioconversion, 42.1 % of initial glycerol was consumed, instead of 18.6 % at the beginning of bioconversion. It was thus hypothesised that glycerol served as main carbon source for the strain's growth. However, as shown in section 3.3.1, presence of 1,3-PDO has an impact on growth of *Acetobacter* sp. CIP 58.66. Therefore, the exact contribution of each substrate to this secondary growth remains unknown. Moreover, two more factors are likely to have contributed to triggering the new growth phase: (i) pH adjustment prior to bioconversion; and (ii) ammonium hydroxide addition as pH-control agent, also serving as nitrogen source.

3.3.4.2 *Enhanced bioconversion performances*

Consumption of 1,3-PDO began as soon as it was added to the medium, without any latency (Fig. 3.5A). At 25 h of bioconversion, a total of 51.45 ± 6.63 g of 1,3-PDO was consumed and converted almost stoechiometricaly into 61.58 ± 5.88 g of 3-HP (Table 3). Within the first three hours, a transient 3-HPA accumulation occurred, that peaked at 0.10 ± 0.01 g L^{-1}. This accumulation is consistent with aldehyde dehydrogenase being the limiting enzyme of 3-HP production from 1,3-PDO by acetic acid bacteria [237]. In one of the two replicates, 3-HPA was later accumulated again, reaching a final concentration of 0.78 g L^{-1}, which is above the minimal inhibitory concentrations. Kinetic analysis of the bioconversion revealed that specific productivities remained lower than during single-step fed-batch: 2.00 versus 3.80 $g_{3\text{-HP}}$ g_{CDW}^{-1} h^{-1}. However, the characteristic time τ_{90} was increased 2.8-fold. This indicates that environmental conditions were compatible with the population's maximum performances for a longer time span. These results show that after it is grown on glycerol, *Acetobacter* sp. CIP 58.66 is well fitted for 1,3-PDO: no delay in 1,3-PDO consumption, high 3-HP yield, long bioconversion time. This might be surprising since glycerol and 1,3-PDO are hypothesised to be metabolised in distinct pathways (section 3.3.3.1). Yet, Frébortová *et al.* (1997) [72] demonstrated that membrane-bound alcohol dehydrogenases were constitutively produced in *Acetobacter aceti* growing on glycerol. Furthermore, they showed that the alcohol dehydrogenase activity in the membrane fraction was increased 1.8-fold when *A. aceti* was grown on both glycerol and ethanol. By analogy between ethanol and 1,3-PDO oxidations, the 1,3-PDO supply to *Acetobacter* sp. CIP 58.66 might have led to an increased alcohol dehydrogenase activity within the first hours of bioconversion.

Contrary to previous single-step, fed-batch experiments (section 3.3.2), pH was successfully controlled during these bioconversions: no initial rise occurred. However, 1,3-PDO concentration was not kept at 5 g L^{-1} as intended: a slight decrease happened and the final concentration was 2.96 ± 0.79 g L^{-1}. After end of secondary growth, cell lysis might have occurred, thus releasing ammonia. This would have decreased the need in feeding solution for base control, consequently supplying less 1,3-PDO than what was consumed. However, 1,3-PDO was never fully depleted, so it was not considered as a limiting factor. In addition to 3-HPA reaching inhibitory levels for one replicate, two likely limiting factors could be identified: (i) high 3-HP concentrations, and (ii) oxygen limitation. Indeed, from 4.4 h of bioconversion, a drop in pO_2 below the setpoint could be observed, despite maximal stirring and air flow conditions. In one instance pO_2 even dropped to 4 % for 4 h.

3.3.4.3 *pH effect on bioconversion performances*

Given the promising results obtained for sequential fed-batch bioconversions at pH 5, the process was further tested for lower bioconversion pH values (4.5 and 4.0). Again, a secondary growth phase happened (Fig. 3.4). Yet, the lower the pH was, the lower were growth rates, final CDW concentration, and final glycerol consumption (Table 3.IV). This is consistent with previous results (section 3.3.3.1) which showed more limited growth on glycerol with initial pH equal to 4.5 or 4.0, compared to pH 5.0. Concomitantly to this secondary growth phase, 1,3-PDO was consumed in all pH conditions and was quasi-quantitatively

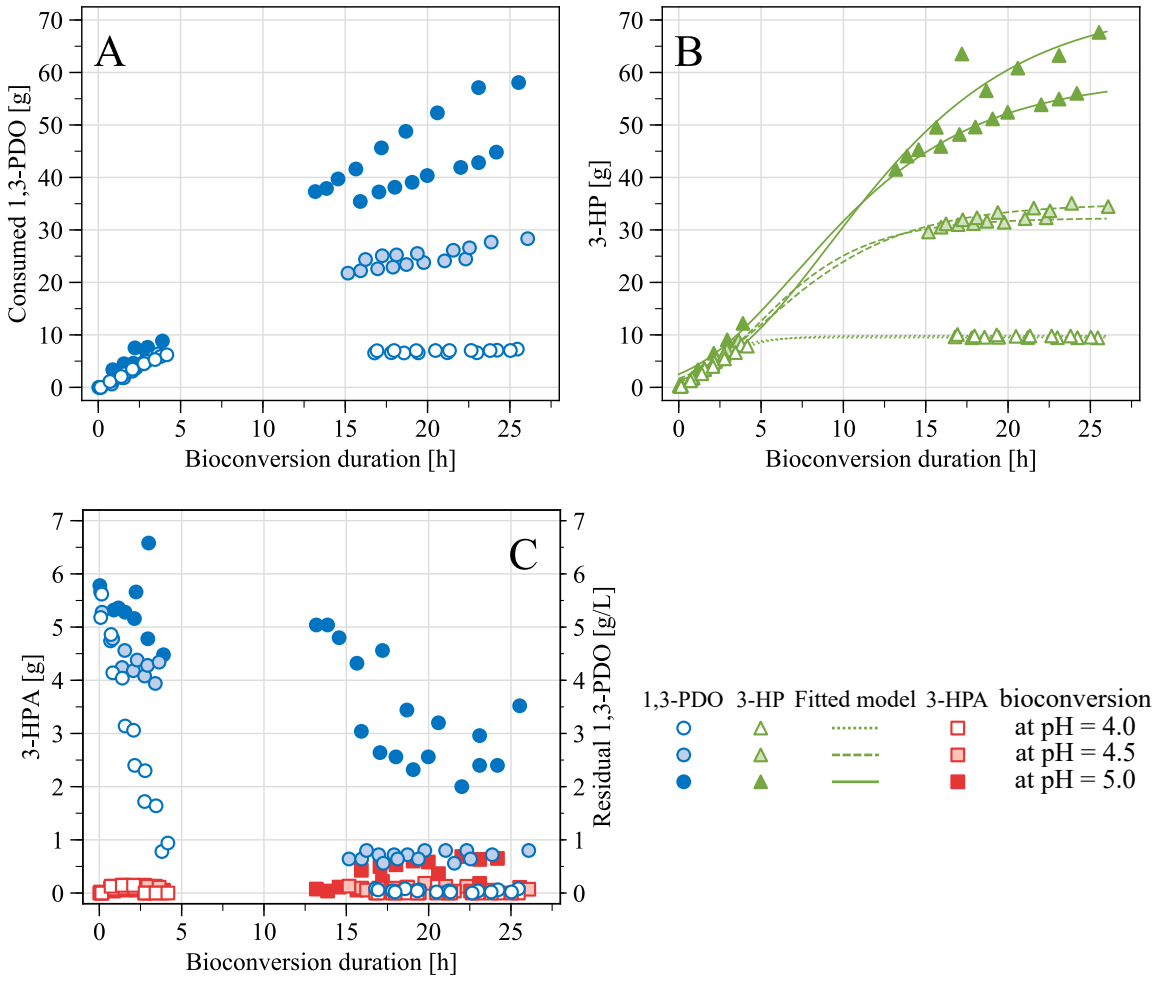

Figure 3.5: Bioconversion of 1,3-PDO into 3-HP by growing cells of *Acetobacter* sp. CIP 58.66 in a pH-based fed-batch, preceded by a first growth step on glycerol in batch mode

A. Overall 1,3-PDO consumption. B. Overall 3-HP production. C. 3-HPA production and residual 1,3-PDO in the bioconversion broth. These bioconversions were launched after a 32 h-long growth on glycerol. Therefore $t = 0$ h on these graphs is equivalent to $t = 32$ h on Fig 3.4. For each pH condition, $n = 2$. Depending on replicates, initial working volumes were estimated to be between 0.91 and 0.96 L, and final volumes between 0.83 and 0.91 L.

Table 3.IV: Bioconversion characteristics of *Acetobacter* sp. CIP 58.66, after its growth on glycerol
For each pH condition, $n = 2$

	pH of bioconversion		
	5.0	4.5	4.0
Final CDW (g L^{-1})	2.08 ± 0.04	1.58 ± 0.06	1.51 ± 0.04
Final N_g [a]	1.21 ± 0.14	0.70 ± 0.03	0.54 ± 0.09
μ_{max} (h^{-1})	0.18 ± 0.04	0.13 ± 0.02	0.12 ± 0.05
Final glycerol consumption (%) [b]	42.1 ± 0.6	36.0 ± 2.1	32.3 ± 1.8
Overall 1,3-PDO consumption (g)	51.45 ± 6.63	25.53 ± 1.07	7.15 ± 0.14
Final 3-HP titre (g L^{-1})	69.76 ± 6.00	36.48 ± 0.8	10.89 ± 0.65
Final 3-HP yield (mol_C mol_C^{-1})	1.02 ± 0.04	1.06 ± 0.05	1.11 ± 0.02
$q_{3\text{-HP,max}}$ ($g_{3\text{-HP}}$ g_{CDW}^{-1} h^{-1})	2.00 ± 0.01	2.22 ± 0.22	2.31 ± 0.06
τ_{90} (h)	8.39 ± 1.00	4.45 ± 0.68	1.24 ± 0.13
$r_{3\text{-HP,max}}$ (g L^{-1} h^{-1})	4.16 ± 0.25	2.94 ± 0.22	2.67 ± 0.13

[a] Number of generations of the secondary growth phase

[b] Calculated as the percentage of glycerol initially supplied

converted to 3-HP (Table 3.IV). Similarly to bioconversions at pH 5, a slight 3-HPA accumulation occurred and peaked around 2 h of bioconversion, at subinhibitory levels, but no later 3-HPA accumulation occurred. Overall bioconversion performances were however lower for lower pH: less 1,3-PDO was consumed and therefore less 3-HP was produced (Fig. 3.5). In particular, at pH 4.0, 3-HP production was only slightly higher than during single-step fed-batch. Consequently, volumetric productivities were also decreased for lower pH (Table 3.IV).

3-HP having a pKa of 4.51 [130], the undissociated and dissociated forms are present in almost equal proportions for pH 4.5. For pH 5.0 (resp. 4.0), however, the dissociated (resp. undissociated) form is predominant over the other. Therefore, even though 3-HP production was quite similar for all pH within the first five hours of bioconversion (Fig. 3.5B), the lower the pH was, the more predominant was the undissociated, protonated form. Because of its higher lipophilicity, the protonated form is usually considered as more toxic to cells than the anionic form [209]. It enters the cell through passive diffusion in the membrane, thus leading to cytosolic acidification and to disruption of the membrane electro-chemical gradient. Resistance mechanisms are then triggered in acetic acid bacteria, including efflux pumps [157]. In particular, *Acetobacter aceti* IFO 3283 was shown to possess a proton motive force-dependent efflux system for acetic acid resistance [146]. Despite a relative specificity for acetic acid, this system seemed to work with short-chain organic acids, and the presence of a respiratory substrate could enhance its activity. Existence of such an efflux system in *Acetobacter* sp. CIP 58.66 — with 1,3-PDO as respiratory substrate — could con-

tribute to explaining the apparently paradoxical increase in specific productivities for lower pH: $q_{\text{3-HP,max}}$ was 2.00 ± 0.11 $g_{\text{3-HP}}$ g_{CDW}^{-1} h^{-1} at pH 5.0, as compared to 2.22 ± 0.22 and 2.31 ± 0.06 $g_{\text{3-HP}}$ g_{CDW}^{-1} h^{-1} for pH 4.5 and 4.0, respectively (Table 3.IV).

Furthermore, consumption of one equivalent of 1,3-PDO would lead to less important proton release for lower pH, due to the predominance of undissociated 3-HP. Consequently, smaller volumes of feeding solution are needed for pH control. In our case, this means that there is also less 1,3-PDO supplied than consumed: the lower the pH, the greater the imbalance. This explains why 1,3-PDO could not be kept at 5 g L^{-1} as desired, and was even completely depleted within the first ten hours of bioconversion at pH 4.0 (Fig. 3.5C). Also, cell lysis might have occurred: this could have released ammonia, thus further decreasing the need for pH control solution and contributing to substrate depletion. These results suggest that the ammonia to 1,3-PDO ratio in the feed should be determined specifically for each pH condition, in order to prevent the slowing down of the process. Adequate base-to-substrate ratio might help taking advantage of the strain's great potentialities, even at low pH.

3.4 Conclusion

The designed process using *Acetobacter* sp. CIP 58.66 achieved high productivities and titres, with a quasi-quantitative molar yield, thus limiting accumulation of detrimental 3-HPA. These performances were comparable to those of the most efficient engineered 3-HP producers [57]. The strain therefore appears as an attractive agent for implementation within an integrated process for 3-HP production from glycerol. Moreover, this is the first report of (i) 1,3-PDO impacting growth of an acetic acid bacteria; and (ii) 3-HP production by growing (instead of resting) acetic acid bacteria. Key limitations could be identified: dioxygen availability, low pH, and feeding solution composition.

Page left blank intentionally

CHAPTER 4

INTEGRATED PRODUCTION OF 3-HYDROXYPROPIONIC ACID USING NON-DISPERSIVE EXTRACTION DURING BIOCONVERSION WITH *Acetobacter* SP. CIP 58.66

This chapter presents the achievement of a proof-of-concept of extractive bioconversion for 3-hydrowypropionic acid (3-HP) production using *Acetobacter* sp. 58.66. The different aspects of the process are considered: bioproduction performances, biocompatibility and extraction performances.

This chapter will be submitted to *Bioresource Technology*, after the patent is published.

The work presented in the current chapter was carried out in collaboration with the PhD project of Ana Karen Sánchez-Castañeda.

Chapter's table of contents

4.1 Introduction . . . 84
4.2 Experimental approach . . . 85
4.3 Results and discussion . . . 87
4.3.1 Bacterial growth and physiological state during extractive bioconversion 87
4.3.1.1 Biocatalyst production prior to extractive bioconversion . . . 87
4.3.1.2 Secondary growth, after 1,3-propanediol addition . . . 87
4.3.1.3 Biocompatibility of the extractive system . . . 89
4.3.2 Bacterial production of 3-HP during extractive bioconversion . . . 91
4.3.2.1 Bioconversion performances . . . 91
4.3.2.2 Medium acidification and aeration . . . 93
4.3.3 In stream reactive pertraction of 3-HP . . . 94
4.3.3.1 Extraction performance of the in stream reactive pertraction system . 94
4.3.3.2 Prospects for improving the extraction performance . . . 96
4.3.4 Integrated approach: the art of compromise . . . 97
4.4 Conclusion . . . 98

4.1 Introduction

The literature review from Chapter 1 has highlighted how important hurdles to 3-hydroxypropionic acid (3-HP) bioproduction still remain and that industrial scale was not reached yet. In particular, significant challenges still lie in downstream processes for 3-HP recovery. Indeed, 3-HP is very soluble in aqueous media, it breaks down at high temperatures and dimerises at high concentrations [86]. Downstream processes for carboxylic acids recovery typically account for 20 % to 60 % of the total cost of production [195]. Several strategies have been considered in order to overcome these issues. Among them, *in situ* and in stream product recovery (ISPR) is one of the most promising, because it offers great potentialities for primary product purification, and for cost reduction [139, 175]. One of the most studied ISPR methods for carboxylic acids is the reactive liquid-liquid extraction, assisted by a hollow fibres membrane contactor (HFMC), also known as reactive pertraction, because of its advantages:

(i) an adequate integration of this method with fermentation can reduce end product inhibition and improve productivity [76, 97, 159, 221],

(ii) pH can be self-regulated by continuous acid removal from the fermentation broth, avoiding base addition,

(iii) the HFMC reduces the toxicity of the solvents used for reactive extraction thanks to the non-dispersive liquid-liquid contact [225],

(iv) a concentrated aqueous solution of the purified acid can be obtained after back-extraction [39].

Regarding 3-HP bioproduction, one of the dominant approaches so far has been its production from glycerol (Chapter 1). Yet, 1,3-propanediol (1,3-PDO) is an obligate by-product of glycerol conversion to 3-HP, and multi-step approaches have thus been undertaken for subsequent 1,3-PDO conversion into 3-HP [65, 234], in order to maximise the overall 3-HP yield from glycerol. This last conversion step was notably performed with acetic acid bacteria (Chapter 3; [65, 234, 122]), which are well known for their ability to incompletely oxidise alcohols. Acetic acid bacteria were shown to quantitatively oxidise 1,3-PDO into 3-HP, through a two-step pathway, with 3-hydroxypropanal (3-HPA) as intermediate. Both steps are catalysed in the periplasm by membrane-bound enzymes, the second one being the rate limiting [237]. In particular, a sequential fed-batch strategy was developed in Chapter 3 with strain *Acetobacter* sp. CIP 58.66: cells were first grown on glycerol in batch mode, then fed-batch bioconversion of 1,3-PDO was initiated, using a pH control-based feeding strategy.

This study explores the feasibility of integrating a similar bioconversion process – but with a discontinuous substrate feed – with an in stream reactive extraction system, assisted by a HFMC. Various bacterial stresses might arise during such a process, such as solvent toxicity and shear stresses [97]. In addition, contrary to strains used in previous HFMC-assisted ISPR works, acetic acid bacteria are obligate aerobes. This raises potential new challenges for process integration, such as lack of oxygen during bacteria circulation through the extraction circuit and interface stabilisation issues, due to the presence of air bubbles. The present chapter provides a first experimental demonstration of 3-HP microbial production associated with a continuous pertraction system, based on reactive liquid-liquid product recovery in a HFMC. Both aspects, microbial production and product recovery, were studied here in order to identify the main associated hurdles to future process scale-up.

4.2 Experimental approach

The experimental setup of this chapter is presented on Figure 4.1, and the methods that were used are referred to in Table 4.I. This chapter focuses on the proof-of-concept of extractive bioconversion by *Acetobacter* sp. CIP 58.66, for 3-HP production. The experiment – as described in section 2.5 (page 54) – was performed in three replicates.

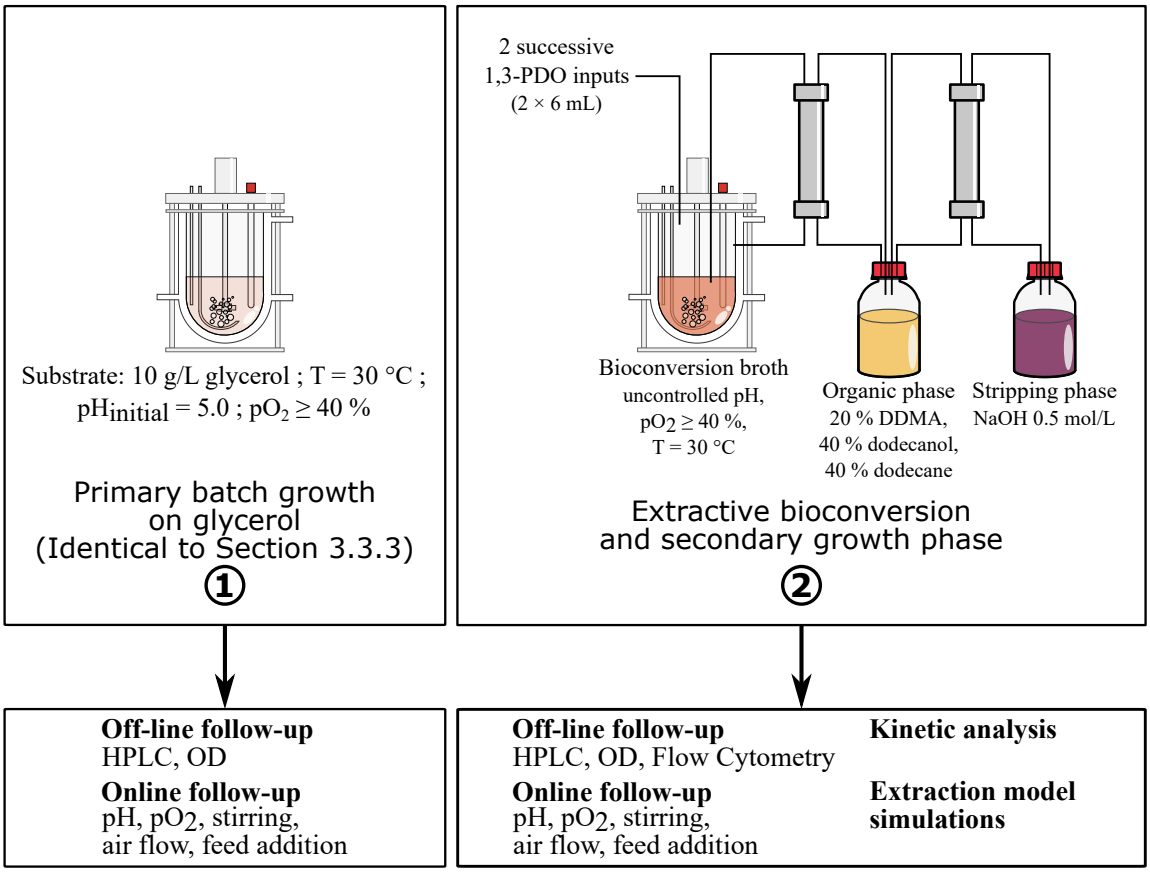

Figure 4.1: Experimental design of Chapter 4

Table 4.I: Index of methods used in Chapter 4

Extractive bioconversions	Section 2.5	page 54
Biomass quantification	Section 2.6.1	page 58
Physiological state assessment	Section 2.6.2	page 59
HPLC analyses	Section 2.6.3	page 60
Kinetic analysis	Sections 2.7.1 & 2.7.2	page 61
Model simulations	Section 2.7.3	page 62
Statistical analysis	Section 2.7.4	page 63

4.3 Results and discussion

4.3.1 Bacterial growth and physiological state during extractive bioconversion

4.3.1.1 *Biocatalyst production prior to extractive bioconversion*

Bioconversion of 1,3-PDO into 3-HP was triggered after a preliminary growth phase on glycerol, which was performed in the same conditions as previously described (Chapter 3). Cell dry weight (CDW) concentration reached 0.98 ± 0.12 g_{CDW} L^{-1} at the end of this preliminary growth step, with a corresponding yield of 0.42 ± 0.12 g_{CDW} $g^{-1}_{glycerol}$, which was consistent with Chapter 3 (see section 3.3.3.2, page 75). Moreover, pH rose from 5.2 to 6.9 ± 0.1 during growth, as previously observed. This rise in pH is a likely cause for growth slowing down, since glycerol was not fully depleted: only 21.1 ± 3.3 % of the initial glycerol was consumed. Based on these results, it can be considered that the biocatalyst production step was reproducible enough to constitute a consistent basis for the subsequent extractive bioconversions. A noteworthy feature of this preliminary growth phase is that no by-product of glycerol consumption (such as organic acids) could be detected in the medium. This is in accordance with previous results (Chapter 3). Yet, this observation is in contradiction with an earlier study dedicated to the growth of *Acetobacter aceti* on glycerol [114]. In that study, succinate and lactate were found in concentrations (up to *ca.* 1.1 and 0.1 g L^{-1}, respectively) that would have been detected in the analytical conditions used here. In the present study, glycerol is therefore hypothesised to be fully oxidised into CO_2, which was the main product of glycerol oxidation in the study of Kylmä *et al.* (2004) [114]. Consequently, this preliminary growth phase was considered to be suitable for the subsequent in stream extraction, since no organic acid was accumulated, that could compete with 3-HP.

4.3.1.2 *Secondary growth, after 1,3-propanediol addition*

After the 32 h-long preliminary growth phase, bioconversion was initiated by 1,3-PDO addition. As expected from previous results (Chapter 3), both 1,3-PDO inputs (at 0 h and 4.6 h of bioconversion) could be associated with a new exponential growth phase, in all replicates (Fig. 4.2, Table 4.II). Numbers of generations (N_g) were similar for both growth phases, and overall, CDW increased from 1.01 ± 0.06 to 2.75 ± 0.07 g_{CDW} L^{-1}. However, it could be observed that the maximal growth rate (μ_{max}) following the first 1,3-PDO addition was higher than the one following the second addition (Table 4.II). During this first exponential phase, the pH decreased from 6.9 to 4.2, and it decreased even further, until 3.9, after the second 1,3-PDO addition (Fig. 4.3.B). Therefore the difference in maximal growth rates was attributed to this difference in pH conditions. Indeed, it was previously shown that the

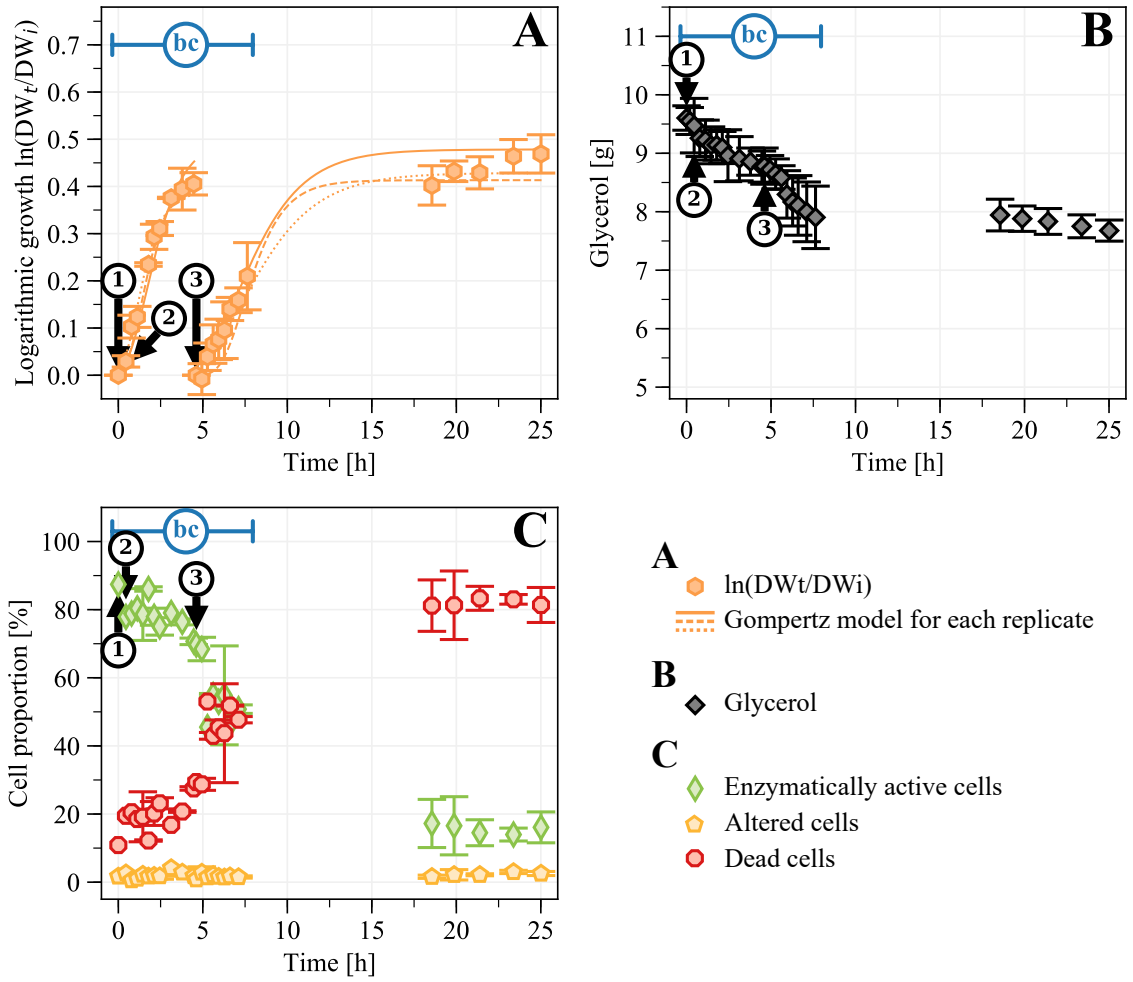

Figure 4.2: Growth characteristics of *Acetobacter* sp. CIP 58.66 during extractive bioconversion A. Logarithmic growth of the successive growth phases, following each 1,3-PDO addition ($n = 3$). For each new growth phase, logarithmic growth is calculated on the basis of the initial CDW of the concerned phase. Each time 1,3-PDO was added, a new growth phase occurred, and logarithmic growth is calculated on the basis of the CDW at the beginning of the new growth phase. **B.** Glycerol in the medium ($n = 3$). Values are given in grams to take into account the volume variations (the working volume varied from 1.12 to 0.96 L). **C.** Flow cytometry analysis of the physiological state of bacteria ($n = 2$, except for values with no error bars, where $n = 1$). 1. Bioconversion is triggered by initial 1,3-PDO addition. 2. The extractive system is connected to the bioreactor. 3. Second 1,3-PDO addition. The horizontal rules marked "bc" indicate the time span corresponding to the bioconversion: after that, 1,3-PDO was fully depleted.

strain's growth on glycerol remained very limited at pH 4, in comparison to pH above 4.5 (section 3.3.3.1, page 74). This is also consistent with a previous study in which the optimal pH for *Acetobacter aceti*'s resistence to acetic acid was found around 6 [193]. During these secondary growth phases, glycerol was further consumed, but never fully depleted: at 25 h of bioconversion, 37.9 ± 2.9 % of the glycerol initially supplied was consumed, instead of 21.1 ± 3.3 % at the beginning of the bioconversion (Fig. 4.2.B). While glycerol is likely the main growth substrate, the presence of 1,3-PDO in concentrations under 10 g L^{-1} was also shown to enhance the growth of *Acetobacter* sp. CIP 58.66 on complex medium (section 3.3.1, page 69). The respective roles of glycerol and 1,3-PDO as growth substrates during the bioconversion phase remain unclear, and further studies would be required in order to better understand the strain's catabolism (for instance, through enzymatic activities assessment or metabolomic analysis). However, in contrast to the previous chapter where 1,3-PDO was continuously fed to *Acetobacter* sp. CIP 58.66 during the bioconversion, here, 1,3-PDO was added discontinuously. The fact that each 1,3-PDO addition was associated here with a new growth phase thus substantiates the hypothesis that 1,3-PDO plays a significant role in this secondary growth phases.

Table 4.II: Growth and bioconversion performances of *Acetobacter* sp. CIP 58.66 during extraction bioconversion

	1st 1,3-PDO addition		2nd 1,3-PDO addition		End of growth
Time	0 h	4.46 h	4.61 h	7.63 h	25.01 h
Growth					
Growth phase	1st exponential phase		2nd exponential phase		late stationnary phase
CDW (g L^{-1})	1.01 ± 0.06	1.57 ± 0.07	1.56 ± 0.06	1.99 ± 0.05	2.75 ± 0.07
N_g [a] of the growth phase	0	0.57 ± 0.04	0	0.30 ± 0.11	0.68 ± 0.06 [b]
μ_{max}	0.17 ± 0.01		0.08 ± 0.03		-
Bioconversion					
Total 3-HP production (g)	0	6.05 ± 0.48	6.65 ± 0.66	13.09 ± 1.02	13.48 ± 1.07
3-HP yield ($mol_{3\text{-HP}}$ $mol^{-1}_{1,3\text{-PDO}}$)	-	0.83 ± 0.06	0.90 ± 0.07	0.91 ± 0.06	0.90 ± 0.07
Maximal $q_{3\text{-HP}}$ [c] ($g_{3\text{-HP}}$ g^{-1}_{CDW} h^{-1})	2.36 ± 0.15		2.58 ± 0.21		-
Average $q_{3\text{-HP}}$ [c] ($g_{3\text{-HP}}$ g^{-1}_{CDW} h^{-1})	2.36 ± 0.15		2.58 ± 0.21		-

[a] Number of generations
[b] Calculated from the beginning of the second 1,3-PDO addition
[c] Specific productivity

4.3.1.3 *Biocompatibility of the extractive system*

The physiological state of *Acetobacter* sp. CIP 58.66 was monitored during the bioconversion, by dual fluorescent staining and flow cytometry analysis. For each sample, cells could be divided into three sub-populations: (i) enzymatically active cells, (ii) altered cells, that are still enzymatically active, but whose membranes are deteriorated, and (iii) dead cells (see

section 2.6.2, page 59). During the first four hours of bioconversion, the proportion of enzymatically active cells remained between 75 and 87 %, while dead cells represented between 11 and 23 % of the overall population (Fig. 4.2.C).
After 4 h of bioconversion, the proportion of enzymatically active cells decreased during approximately two hours, before reaching values between 46 and 55 % at the end of the bioconversion (approx. 8 h). In the meantime, the proportion of dead cells followed the opposite trend, before stabilising between 43 and 53 % (Fig. 4.2.C). This evolution of the ratio of dead cells to active cells (from approximately 1:5 to 1:1) begins around 0.6 h before the second 1,3-PDO addition, which is consistent with the lower μ_{max} of the last growth phase (Table 4.II). Overall, the biocompatibility of the system is still satisfactory, since half of the bacterial population was still active after 7.63 h of bioconversion, when 1,3-PDO was almost fully depleted. Interestingly, between 18 and 25 h after the bioconversion started, the proportion of enzymatically active cells remained between 14 and 17 %. This suggests that this process setup could be suitable for continuous extractive bioconversion, for at least 25 h.

Several factors might be involved in the gradual decline of the basal enzymatic activity of cells. First of all, 3-HP accumulation in the medium (up to 10.59 ± 1.18 g L^{-1}, Fig. 4.3.A) and low pH (close to 4.0, Fig. 4.3.B) might affect the cells. In particular, pH 4.0 was shown to hinder growth of *Acetobacter* sp. CIP 58.66 on glycerol in shake-flasks (section 3.3.3.1, page 74). In addition to these factors, more specific stresses due to the process integration are described in the literature:

(i) Prolonged exposure to solvent. Solvent toxicity is a common concern for ISPR processes [222]. By minimising direct contact between cells and organic solvents, the use of HFMC was shown to limit toxicity [225], even though it cannot always prevent detrimental effects on bacteria [33]. Yet, the extracting phase used in this study was formulated based on the trade-off determined between extraction performances and biocompatibility with the 3-HP-producing strain *Lactobacillus reuteri* DSM 17938 (Sánchez-Castañeda, submitted). Therefore, a limited solvent toxicity was expected in the present study.

(ii) Nutrient depletion. Indeed, after the extraction was initiated, the initially yellowish medium progressively faded while the organic phase became a bit coloured, suggesting that some coloured nutrients (such as some vitamins) might also have been extracted from the bioconversion broth, thus possibly hindering bacterial growth. This phenomenon was also observed by Jin and Yang (1998) [97], while performing extractive fermentation by *Propionibacterium acidipropionici* for propionic acid production. However, their results suggested that their strain's growth was not impacted.

(iii) Oxygen limitation. Acetic acid bacteria are obligate aerobes and even short (less than 1 min) oxygen deprivation was shown fatal to vinegar production processes with *Acetobacter* spp. [84, 155]. Here, the bioconversion medium was supplied with air inside the bioreactor, but not in the extracting system (pipes and membrane contactor). The overall volume in the extracting system was 200 mL (one sixth of the total working volume), so the average medium residence time in the extraction circuit was 33 s.

Under the assumption that the bioreactor is perfectly stirred, this means that bacteria would experience a 33 s-long aeration limitation every 3.3 min, which could lead to oxygen deprivation phenomena.

In the study from Chapter 3, the strain was similarly grown on glycerol, then bioconversion was performed with a continuous 1,3-PDO feed and at a controlled pH, but no extracting system was implemented. In terms of number of generations (N_g) and maximal growth rates ($\mu_{\max}$), the values presented in this study (Table 4.II) are in the same range than those obtained during those fed-batch bioconversions, when pH was controlled at 4.0 or 4.5: $\mu_{\max}$ were respectively 0.12 ± 0.05 and 0.13 ± 0.02 h^{-1}, while N_g were 0.54 ± 0.09 and 0.70 ± 0.03. Results of the present study cannot be fully compared with those from Chapter 3, due to the differences in experimental setup. This still suggests, however, that the strain is tolerant to the overall impact of the pertraction system, and that the observed decline of the basal enzymatic activity of bacteria was caused by a combination of several of the stress factors described above.

4.3.2 Bacterial production of 3-HP during extractive bioconversion

4.3.2.1 *Bioconversion performances*

Following the growth of *Acetobacter* sp. CIP 58.66 on glycerol (section 4.3.1.1), the bioconversion was triggered by 1,3-PDO addition (reaching 5.36 g L^{-1} in the medium). Its consumption began immediately, without any observable latency (Fig. 4.3.A). This first substrate input was fully depleted after 3.8 h, and additional 1,3-PDO (reaching 5.99 g L^{-1} in the medium) was therefore added at 4.6 h. Again, 1,3-PDO was immediately consumed and almost completely depleted within 3.0 h. This shows that, even though glycerol and 1,3-PDO are assumed to be metabolised through distinct pathways by *Acetobacter* sp. CIP 58.66 (Chapter 3), cells grown on glycerol are well fitted for 1,3-PDO oxidation. For both 1,3-PDO additions, 3-HP was the main product, with an overall yield of 0.91 ± 0.06 $mol_{3\text{-HP}}$ $mol^{-1}_{1,3\text{-PDO}}$. The maximal specific productivities ($q_{3\text{-HP,max}}$) that were reached for each successive phase were similar (Table 4.II). 3-HP was mainly accumulated in the bioconversion medium, even though a slight decrease is noticeable prior to the second substrate input, due to extraction (Fig. 4.3.A). Moreover, a slight and transient 3-HPA accumulation was detected around 1 h after each substrate input, without exceeding 0.20 ± 0.11 and 0.24 ± 0.14 g L^{-1}, respectively. This could be the consequence of a slight kinetic imbalance between the two successive enzymatic steps of the metabolic pathway. Indeed, Zhu *et al.* (2018) [237] showed that the aldehyde dehydrogenase was the rate limiting enzyme for 3-HP production by another acetic acid bacterium, *Gluconobacter oxydans*. As 3-HPA is highly toxic to bacteria, its level has to be carefully monitored during the process. In the present study, its maximum values remained below the minimal inhibitory concentrations estimated for another Gram-negative bacterium, *Escherichia coli*: from 0.56 to 1.11 g L^{-1} [49]. Therefore, 3-HPA was not considered as an inhibiting factor of the designed process.

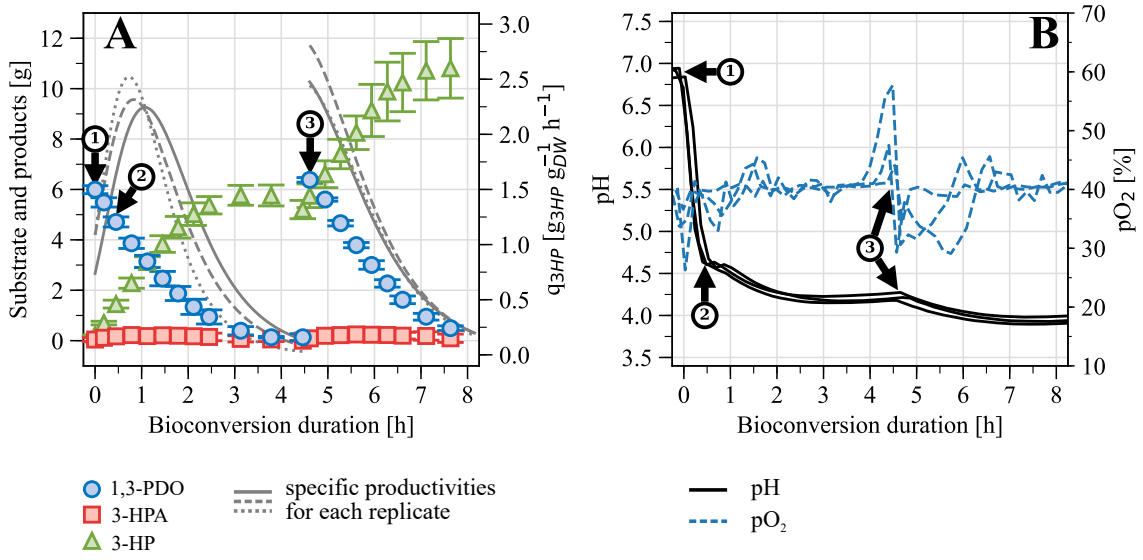

Figure 4.3: Evolution of the medium's composition during extractive bioconversion

A. Substrate and product amounts in the medium. Values are given in grams to take into account the volume variations (the working volume varied from 1.12 to 1.02 L). Each grey line style (*i.e.* solid, dashed, dotted) represents the calculated specific productivities ($q_{3\text{-HP}}$) of one of the three replicates. **B.** Acidification kinetics (solid line, left scale) and partial O_2 pressure (dashed line, right scale) during bioconversion. 1. Bioconversion is triggered by initial 1,3-PDO addition. 2. The extractive system is connected to the bioreactor. 3. Second 1,3-PDO addition.

These results bring out two key features of the implemented extractive bioconversion. Firstly, in spite of the cumulated potential stresses (see section 4.3.1.3), no substantial difference in bacterial performances (yield and specific productivities) could be observed, between the conversion of the first and second 1,3-PDO input (Table 4.II). Similar specific productivities, but higher CDW could explain why the production rate was higher after the second 1,3-PDO addition (Fig. 4.4.C). So it appears that the bacterial population is able to maintain its high capabilities over at least 8 h, which might come as a surprise since a decline in the basal enzymatic activity of cells was observed from 4 h of bioconversion (Fig. 4.2.C). An explanation to this might be the absence of correlation between the 1,3-PDO oxidation ability of acetic acid bacteria, and their basal enzymatic activity. Indeed, it was previously reported that acetic acid bacteria could still oxidise ethanol, even when they had lost their ability to grow [163]. In particular, the basal enzymatic activity was assessed here using the esterase activity as a proxy (section 2.6.2, page 59), while the enzymes for 1,3-PDO oxidation into 3-HP are dehydrogenases [237]. Secondly, the bacterial performances achieved in this study are comparable with the ones obtained during non-extractive, fed-batch bioconversions (section 3.3.4, page 77). During these previous experiments, cells were also grown on glycerol before bioconversion, but 1,3-PDO was continuously fed to bacteria, according to a pH-based strategy, and pH was controlled at 5.0, 4.5, or 4.0. Similarly to the present study, 3-HP yields were always close to the theoretical maximum (1.00 mol mol^{-1}). However, the lower the pH was, the higher the $q_{3\text{-HP,max}}$ was: at pH 4.0, $q_{3\text{-HP,max}}$ was 2.31 ± 0.06 $g_{3\text{-HP}}$ g_{CDW}^{-1} h^{-1}. This is similar to the values from the extractive bioconversion (Table 4.II) during which pH was left

uncontrolled, but remained between 4.6 and 3.9 after a rapid initial decrease (Fig. 4.3.B). All these results show that, as implemented, the extraction system did not substantially affect the oxidation activity *Acetobacter* sp. CIP 58.66. This integrated process therefore shows a promising potential for extractive bioconversion of 3-HP with a continuous 1,3-PDO feeding. However, continuous 3-HP pertraction did not enhance the bioconversion performances for the considered process design and feeding strategy. The main reasons are that: (i) acetic acid bacteria are naturally resistant to organic acids -– most notably to acetic acid — [213], while 3-HP concentrations remained relatively low; and (ii) the extracting rate was much slower than the production rate (see section 4.3.3), so 3-HP accumulation in the medium was not significantly different from a non-extractive bioconversion.

4.3.2.2 *Medium acidification and aeration*

In order to limit the changes in medium composition, which affect the extraction yield [38], the pH was left uncontrolled and no base solution was used. Therefore, the pH rose from 5.0 to 6.9 during growth on glycerol and, after 1,3-PDO was added, it sharply decreased due to 3-HP production (Fig. 4.3.B). The bioconversion medium was put in contact with the organic phase in the HFMC only when pH had reached 4.6, which is close to the pKa of 3-HP (section 2.5.3, page 57). This pH threshold was reached 28 min after the initial 1,3-PDO supply. After pertraction was initiated, the pH further decreased but at a slower rate, until it stabilised at 4.2 (Fig. 4.3.B). When the second 1,3-PDO addition was performed, pH decreased again and stabilised at 3.9 at the end of bioconversion (after that, pH increase again, due to acid extraction). These successive decreases in pH are due to the imbalance between 3-HP production and extraction rates, the latter being much slower than the former. pH values between 4.5 and 4.0 are still compatible with high oxidative activity of *Acetobacter* sp. CIP 58.66 (section 4.3.2.1), and are a good compromise for guaranteeing a satisfactory extraction yield.

Dissolved oxygen is also a key parameter for the process, since acetic acid bacteria are obligate aerobes. Overall, pO_2 was successfully kept at its setpoint (40 % of the saturation value) all along the bioconversion, meaning O_2 availability was not limiting (Fig. 4.3.B). The setpoint was however maintained at the expense of high stirring and air flow rates (800 rpm and 4 NL min^{-1}, respectively). After each 1,3-PDO addition, a transient pO_2 decrease was recorded, before it stabilised at its setpoint again. A brief increase could also be observed between 3.8 and 4.6 h, corresponding to 1,3-PDO depletion. After 8 h of bioconversion, 1,3-PDO was fully depleted, so oxygen uptake decreased and pO_2 rose again, up to 100 %. This suggests that oxygen uptake during the bioconversion was mainly due to 1,3-PDO rather than glycerol oxidation, since the pO_2 rose as soon as 1,3-PDO was depleted while glycerol was still abundant in the medium (Fig. 4.2.B). Therefore, O_2 uptake appears as a convenient indicator of 1,3-PDO availability in the medium for future process control: using online acquisitions of pO_2, stirring rate, and air flow rate, the O_2 uptake rate may be estimated in real-time, and used for automatic control of the 1,3-PDO feeding rate.

4.3.3 In stream reactive pertraction of 3-HP

4.3.3.1 *Extraction performance of the in stream reactive pertraction system*

3-HP distribution among the bioconversion medium, the organic phase and the back-extraction phase is shown in Figure 4.4. During bioconversion (Fig. 4.4.A), extraction started slowly, leading to a progressive 3-HP accumulation in the organic phase. The extraction rate increased progressively with 3-HP production, and back-extraction in the NaOH solution started later: 3-HP was detected in the back-extraction phase only after 1.7 h. Back-extraction rate increased as acid accumulated in the organic phase, eventually exceeding the extraction rate, as shown by the decrease in 3-HP in the organic phase (Fig. 4.4.B). After 8 hours of bioconversion, all the added 1,3-PDO was consumed and 3-HP production stopped. From then on, 3-HP concentration decreased both in the bioreactor and in the organic phase, while the concentration in the back-extraction phase increased. No further 1,3-PDO was added and the system was left running in order to recover all the produced 3-HP. After 114 h, nearly all 3-HP was recovered in the NaOH solution, thus achieving a final concentration of 12.63 ± 0.50 g L^{-1}, while almost no 3-HP was detected in the two other phases (Fig. 4.4.B).

The 3-HP production rate by *Acetobacter* sp. was remarkably higher than the extraction rate of the pertraction system (Fig. 4.4.C). Consequently 3-HP was mainly accumulated in the bacterial broth during its production. Similar studies for other carboxylic acids have reported an adequate extraction performance for maintaining a low acid concentration in the bioreactor, while controlling pH at constant values between 5.2 and 6.3 all along bioconversion [97, 159, 221]. In these cases, pH control was achieved at these relatively high values because extraction and production rates were balanced in most cases: the strains used in these studies performed at production rates between 0.26 and 1.2 g h^{-1}. The present strain displayed a higher production rate (Fig. 4.4.C), so pH stabilised at lower values (3.9 to 4.2, Fig. 4.4.B) using the present extraction system. However, this had a limited impact on the strain's production capacity (section 4.3.2.1).

A further important specificity of this study is the obligate aerobic nature of *Acetobacter* sp. CIP 58.66. Oxygen requirement implies the presence of air bubbles in the bioconversion broth, which circulates inside the contactor fibres. Air bubbles decrease the surface of direct contact between the bioconversion broth and the organic phase and slow down the mass transfer rate of 3-HP to the interface. This could explain the lower extraction performance observed in this study, as compared to the extractive fermentation studies cited above, where the used strains were anaerobic.

An increase in the variability of the 3-HP concentration in each of the three phases can be observed at the end of bioconversion, and it further increases toward the end of extraction (Fig. 4.4.B). This was attributed to the clogging of the fibres inlet, which was revealed during the membrane cleaning step, thus resulting in a decrease in extraction capacity over the successive replicates. This clogging was due to several factors, such as solid particles accumulation and emulsion formation.

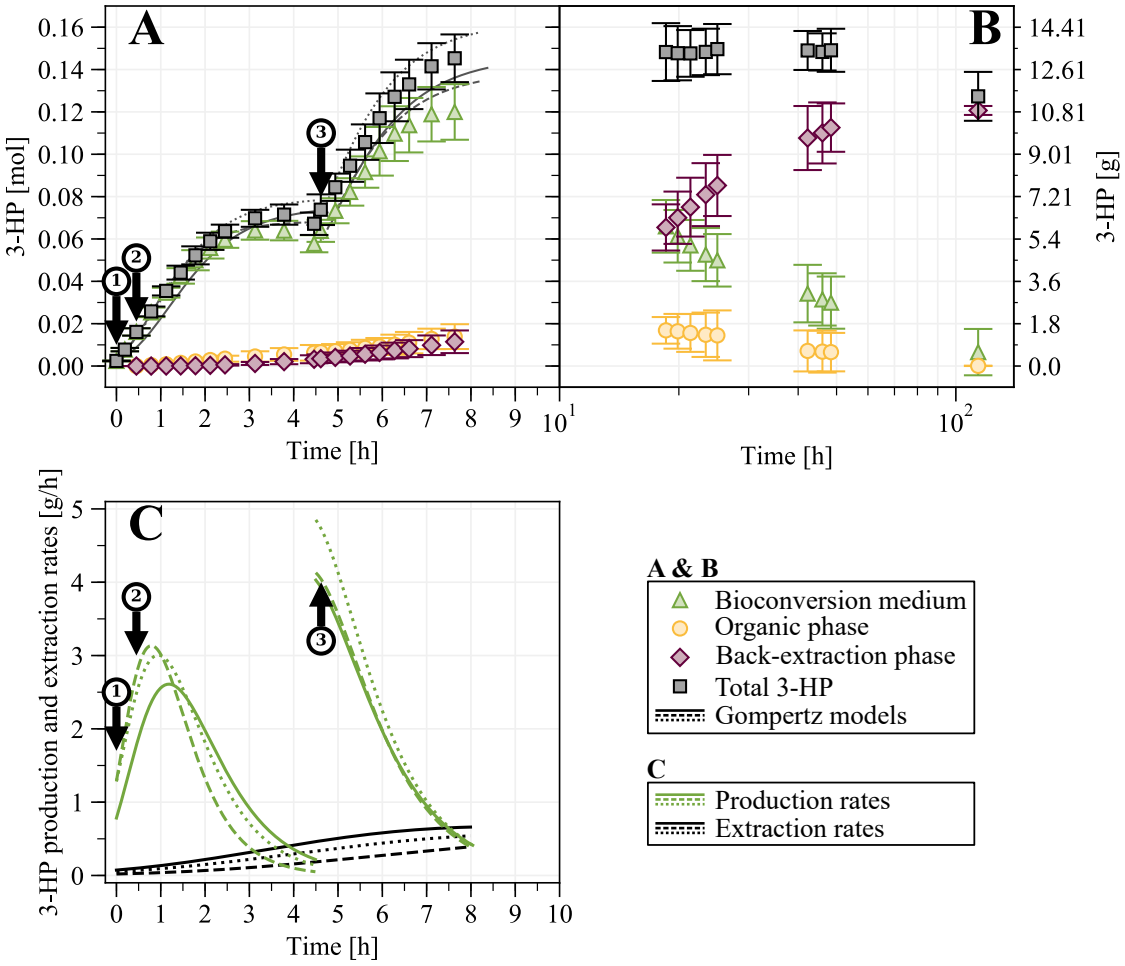

Figure 4.4: Total 3-HP and its distribution among the three phases (bioconversion medium, organic phase and back-extraction phase). A. Focus on the first 8 hours, corresponding to bioconversion duration. **B.** Evolution of the 3-HP distribution, after bioconversion is finished (time is represented in logarithmic scale, due to the longer time scale considered, compared to bioconversion). **C.** Production and extraction rates during bioconversion. Each line style (*i.e.* solid, dashed, dotted) represents one of the three replicates. 1. Bioconversion is triggered by initial 1,3-PDO addition. 2. The extractive system is connected to the bioreactor. 3. Second 1,3-PDO addition.

Lastly, it may be noted that the final 3-HP concentration in the back-extraction phase was 12.63 ± 0.50 g L^{-1}. In other words, 3-HP was not significantly concentrated in this phase in comparison to the bioconversion medium, even though back-extraction is usually considered as an opportunity to reach higher product concentrations from diluted solutions (here, the bioconversion medium). For practical reasons (notably for ease of sampling), the volume of the back-extraction phase was similar to the volume of the bioconversion medium (around 1 L) in the present study. Higher 3-HP concentrations could have been reached easily by reducing the back-extraction phase volume: all other things remaining equal, the present 3-HP production (approximately 13 g L^{-1}) would correspond to a 43 g L^{-1} (0.48 mol L^{-1}) concentration, if the back-extraction volume was 0.3 L. This concentration is close to the maximum value that can be obtained with the present setup: a 0.5 mol L^{-1} $NaOH$ was used for back-extraction, so 3-HP cannot exceed this concentration threshold. For higher 3-HP productions, it would be necessary to increase the $NaOH$ concentration so that it is always is excess.

4.3.3.2 *Prospects for improving the extraction performance*

Optimisation of the pertraction system is required in order to achieve continuous 3-HP production at high productivity, and to obtain a final 3-HP solution at higher concentration and purity than in the bioconversion broth. It was observed that the overall effect of the pertraction system was well tolerated by *Acetobacter* sp. CIP 58.66 during bioconversion. The selected organic phase already showed the best compromise between extraction performance and biocompatibility with a 3-HP producing strain [182]. It is thus necessary to explore alternate strategies other than further optimisation of the organic phase composition.

A first possible approach is to improve extraction performance by increasing the specific contact area (contact area per unit of bioconversion medium) of one of the extraction or back-extraction modules, or both. For example, Jin and Yang (1998) [97] maximised the extraction rate of their system by reducing the volume of the bioconversion broth from 2.2 to 0.3 L, corresponding to a 7.3-fold increase in the specific contact area. They also increased the pH from 4.8 to 5.2, thus improving the global process productivity. In order to assess this effect in the present study, a mathematical model [37] was adapted to the experimental conditions of this work, achieving an adequate description of the process. Simulations with a working volume in the bioreactor of 1.2 L (this study) and 0.3 L were compared, corresponding to 4-fold increase of the specific contact area. A 3-HP productivity of 2.1 g L^{-1} h^{-1} was set, which corresponds to the average productivity observed between 4.5 to 6.6 h of bioconversion in this study. Simulation with 1.2 L showed a 3-HP accumulation in the bioconversion medium up to 71 g L^{-1} after 300 h. This confirms that the extraction performance of the actual pertraction system is not capable of maintaining a low 3-HP concentration in the bioconversion broth during a continuous production by *Acetobacter* sp. Simulation with 0.3 L, however, reached a stationary concentration of 13 g L^{-1} after 30 h of bioconversion. Even though this strain is resistant to 3-HP concentrations of this order of magnitude (Chapter 3), pH in the bioconversion medium would be slightly lower than 4, which will

affect the production performance with time. Alternately, the contact area for extraction and back-extraction can be increased by using several HFMC modules, instead of reducing the volume in the bioreactor. In the present example, in order to maintain a concentration close to 13 g L^{-1} with a 1.2 L working volume, four extraction/back-extraction systems must be used. In practice, both these strategies are limited by the volume of medium required to fill all the extraction circuit. For the bioreactor, this means instrumentation has to be functional with a 1.2 L working volume (during growth phase on glycerol), as well as with 0.4 L (during extractive bioconversion), since 0.8 L are needed to fill the 4 modules. Moreover, this implies a longer residence time without oxygen for the bacterial strain, which may affect its production performance. For the organic and back-extraction phases, this means that higher volumes are required, and that the back-extraction phase will be more diluted in 3-HP. Technical solutions to increase specific contact area thus constitute another point to take into account when searching for compromises in the integrated process.

4.3.4 Integrated approach: the art of compromise

The process described in the present study shows a promising potential, but further optimisation is still required for scaling-up. When designing such an integrated process, the optimal operative conditions are not necessarily the optimum of each process unit. Results presented here highlight some key parameters that have to be considered in future works, for determining an adequate trade-off between production and extraction performances.

To start with, the primary growth phase on glycerol can be further optimised, in order to be shortened. Yet, this has to be done in accordance with constraints from the extraction system, both in terms of medium composition (*e.g.* no addition of pH control solution) and working volume. In particular, pH is a crucial aspect for extractive bioconversion, impacting both the upstream and downstream performances. Here, pH stabilised around 4.0 during bioconversion, which ensured adequate microbial performances (section 4.3.2.1), but lower extraction performances than at even lower pH. However, as pH 4.0 is already below the pKa of 3-HP, only limited improvement of extraction can be expected from lower pH. Another crucial aspect is oxygen availability in the broth: on the one hand oxygen deprivation (for less than 1 min) can be fatal to acetic acid bacteria, which have high oxygen demand, and on the other hand, high aeration rates hindered extraction due to interface instability. Furthermore, critical thresholds have to be determined both for cell residence time in the bioreactor and in the pertraction system. This will impact both the bacterial activity and the extraction system dimensioning: in particular, more insights are needed on the impact of successive oxygen deprivations on the strain's ability to produce 3-HP.

A further key aspect is substrate feeding: adapting the feeding rate is an easy-to-implement strategy, in order to balance the 3-HP production and extraction rates. The feeding rate also needs to guarantee a constant and low (below 5 g L^{-1}) 1,3-PDO concentration in the bioconversion medium, notably in order to prevent deleterious 3-HPA accumulation.

Finally, bacteria immobilisation in the bioreactor would be an interesting strategy to protect

them from the stresses associated with their circulation in the extraction system [97], and it could also help limiting the clogging in the fibres inlet. Interestingly, immobilisation of *Acetobacter* sp. CGMCC 8142 was investigated for 3-HP production from 1,3-PDO, and notably showed promising stability and storability properties [122]. All things considered, extractive bioconversion appears as a complex optimisation problem. As illustrated in section 4.3.3.2, implementing an accurate model for the overall process will constitute a valuable tool for further process development, so that promising designs and operating conditions can be selected prior to their experimental testing.

4.4 Conclusion

This study demonstrates the feasibility of extractive bioconversion for 3-HP production, using *Acetobacter* sp. CIP 58.66. During bioconversion, 3-HP was continuously removed from the bioconversion medium, using a reactive liquid-liquid pertraction technique. This integrated approach was compatible with the high oxidative capacities of the strain. Its resistance to cumulative stresses makes it a great candidate for extractive bioconversion. Yet, a significant imbalance between production and extraction rates could be evidenced. These results pave the way towards continuous extractive bioconversion of 3-HP or other short-chain organic acids, and towards its scaling-up.

CHAPTER 5

KINETIC MODELLING OF 3-HYDROXYPROPIONIC ACID PRODUCTION BY *Acetobacter* SP. CIP 58.66 FOR FURTHER UNDERSTANDING AND OPTIMISATION OF THE PROCESS

The present chapter describes the approach that was undertaken towards the development of a mechanistic model describing the kinetics of 1,3-propanediol (1,3-PDO) conversion into 3-hydroxypropionic acid (3-HP) by *Acetobacter* sp. CIP 58.66. Details of the model development are provided here, as well as the main results: parameter estimation and model validation on independent data sets.

Chapter's table of contents

5.1 Introduction . . . 100
5.2 Experimental methods . . . 101
5.2.1 Available data sets . . . 101
5.2.2 Computation of the model inputs from experimental data . . . 104
5.3 Modelling methods . . . 106
5.3.1 Model description . . . 106
5.3.1.1 Definition of the modelled system and working hypothesis . . . 106
5.3.1.2 Mass balances equations . . . 108
5.3.1.3 Kinetic equations . . . 109
5.3.2 Integration of the ODE system . . . 110
5.3.3 Step-by-step parameter estimation . . . 111
5.4 Results and discussion . . . 114
5.4.1 Model development using sequential fed-batch data . . . 114
5.4.1.1 Estimated model parameters . . . 114
5.4.1.2 Evaluation of the interpolation capacity of the model . . . 120

5.4.2 Model evaluation for extractive bioconversion data 123
5.4.3 Model evaluation for a different initial bacterial state 125
5.5 Conclusion 128

5.1 Introduction

As presented in Chapter 1, the metabolic route for 3-hydroxypropionic acid (3-HP) formation in acetic acid bacteria might appear as quite simple. Indeed, it was shown to be a two-step pathway where the substrate – 1,3-propanediol (1,3-PDO) – is first oxidised into 3-hydroxypropanal (3-HPA), which is in turn oxidised into 3-HP [237]. Quantitative 3-HP production from 1,3-PDO was already achieved in several studies using acetic acid bacteria from genera *Gluconobacter* or *Acetobacter* [234, 65, 122]. In particular, the potential of strain *Acetobacter* sp. CIP 58.66 was demonstrated in Chapter 3: after an initial growth phase on glycerol, the bacterial population was continuously fed with 1,3-PDO. The highest production performances were obtained when pH was controlled at 5.0: the average volumetric productivity was 2.3 g L^{-1} h^{-1}, and the final 3-HP titre reached 70 g L^{-1} (section 3.3.4, page 77). Despite the apparent simplicity and high efficiency of the metabolic pathway, results from Chapter 3 also highlighted that several inhibition and limitation phenomena are involved, and are correlated with one another. The key factors that were identified included product (3-HP and 3-HPA) inhibition, substrate (1,3-PDO) inhibition and limitation, pH inhibition, and oxygen limitation. Determining the extract contribution of each one of these factors to the overall process is a non-trivial issue and would require extensive experimental work. Moreover, results from the extractive bioconversions in Chapter 4 demonstrated the necessity for fine understanding of 3-HP production kinetics by acetic acid bacteria in order to determine the operational conditions for the best trade-off between 3-HP bioproduction and extraction performances. Typically, mechanistic modelling approaches have been implemented for bioprocesses development and improvement: by their simplified representation of the complex underlying biological phenomena, models can be used as a tool for qualitative and quantitative study of the main mechanisms involved. *In silico* simulations can help significantly reducing the process development time by narrowing down the conditions to be tested to the most promising only [79, 28]. Finally, mechanistic models also constitute good tools for on-line process control.

To the best of our knowledge, modelling of the specific case of 3-HP production by acetic acid bacteria has not yet been attempted. The study of Li *et al.* (2016) [122] on *Acetobacter* sp. CGMCC 8142 immobilisation for 3-HP production did include a modelling approach, but it was focused on mass transfer between liquid phase and immobilisation beads. However, several models were already proposed for describing the kinetics of acetic acid bacteria

growth and acetic acid production during industrial vinegar production [95, 81]. Jiménez-Hornero *et al.* published a comprehensive review of the different modelling approaches that were undertaken to that end [95]. In the most complete models that were proposed, growth rate was described as a function of ethanol, acetic acid and oxygen concentrations [95, 81, 177]. Several mechanisms were considered: substrate (ethanol and O_2) limitations, ethanol and acetic acid inhibitions, and also acetic acid activation. Indeed, based on the work of Nanba *et al.* on *Acetobacter* sp. 1-39 Mistukan [158], it was considered that low levels of acetic acid (< 10 g $L^{-1} = 167$ mmol L^{-1}) enhanced the bacterial growth. In one instance, oxygen inhibition was also included in the model [177]. Furthermore, cell death was also accounted for in these different models [95, 81, 177]. The pathway for acetic acid formation is analogous to the one of 3-HP: ethanol is converted into acetic acid in two successive oxidation steps, with acetaldehyde as intermediate. Therefore, it could be possible to adapt these models for 3-HP production. However, in the previous chapters (3 and 4), it was shown that 3-HPA accumulation occured in all culture conditions, either transiently or permanently. Due to its high cell toxicity, 3-HPA is an important variable the model has to account for [49]. Yet, acetaldehyde production is not considered in the models that were implemented for acetic acid production, so they cannot be directly applied in the case of 3-HP production, despite the metabolic pathway analogy.

Based on the experimental results from the previous chapters, this chapter aims at developing a kinetic model for 3-HP production by acetic acid bacteria. As a first approach, the phenomena that were included in the model are: bacterial growth from 1,3-PDO, 3-HPA production from 1,3-PDO, 3-HP production from 3-HPA, and 3-HP inhibition. In particular, 1,3-PDO uptake for 3-HPA production was considered with a distinct kinetic than its uptake for biomass formation. This constitutes a further difference with the previously cited models, in which ethanol uptake was proportional to bacterial growth [95, 81, 177]. First, model parameters were optimised using part of the data from pH control-based fed-batchs (section 3.3.4). Then the model was validated using data the remaining – independent – pH control-based fed-batch experiments, as well as the data from extractive bioconversions (Chapter 4). Finally, perspectives on adding other important phenomena (*e.g.* O_2 uptake, 1,3-PDO and 3-HPA inhibition, cell death) will be discussed.

5.2 Experimental methods

5.2.1 Available data sets

Data from the previous studies (Chapters 3 and 4) were used for model development. Figure 5.1 sums up the different data sets that were available, and how they were used in the modeling strategy.

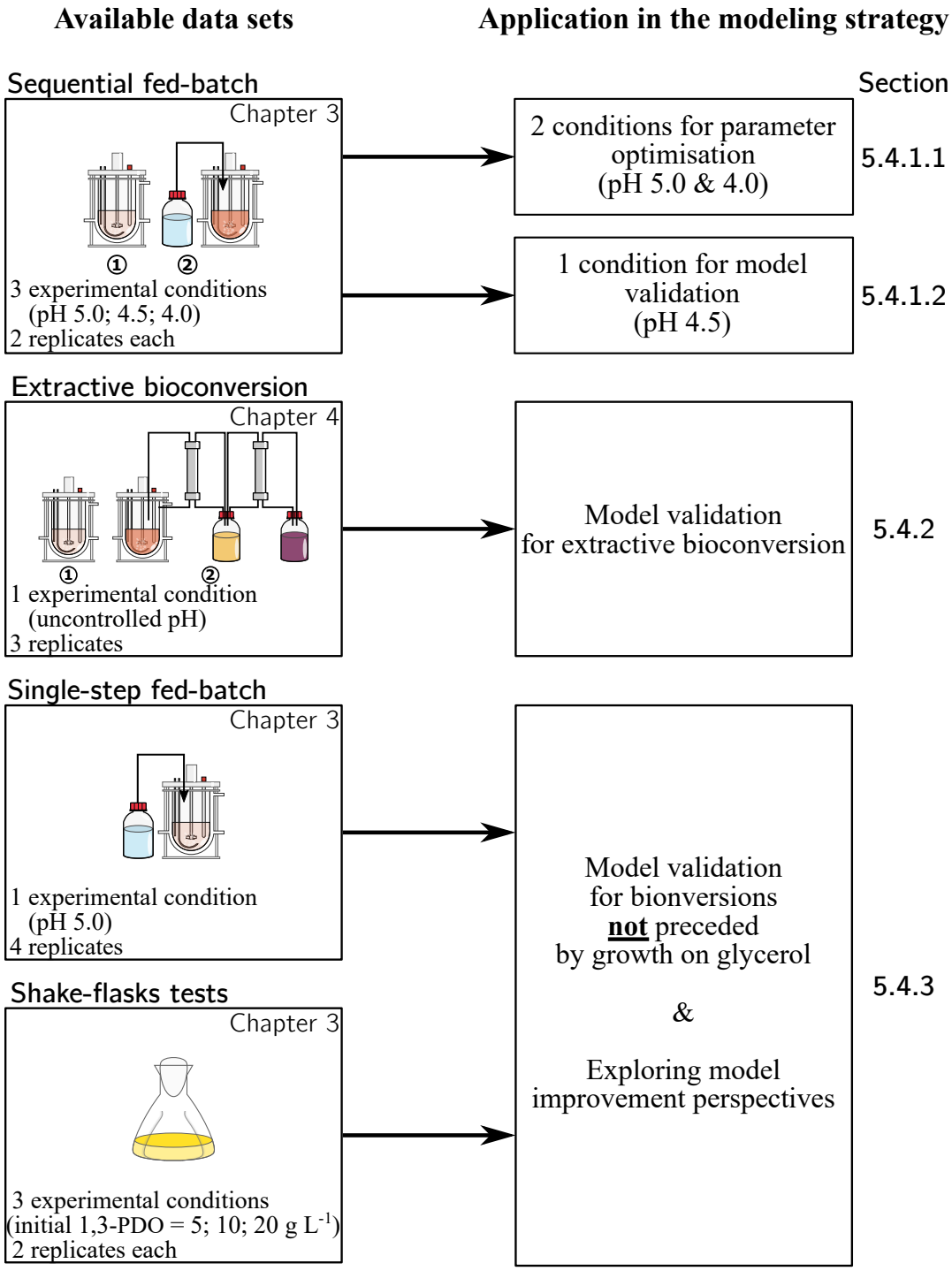

Figure 5.1: Schematic representation of the data sets used for modelling

In a first approach, data from the sequential, pH control-based fed-batch bioconversions were used for parameter estimation. These experiments are detailed in section 2.4.3 (page 52), and their results are presented in Chapter 3 (section 3.3.4, page 77). In summary, *Acetobacter* sp. CIP 58.66 was first grown on glycerol in a bioreactor, during 32 h. This initial growth phase was always performed in the same conditions: the pH was notably left uncontrolled. Then, the bioconversions were triggered *in situ*, by adding 1,3-propanediol (1,3-PDO). The bioreactor was continuously fed with 1,3-PDO, using an equimolar (6 mol L^{-1}) solution of base (NH_4OH) and 1,3-PDO, serving for both pH control and substrate feeding. The feeding rate was automatically controlled, based on pH feedback. Several pH conditions were tested for the bioconversion phases: 5.0, 4.5, or 4.0. In all cases, partial O_2 pressure (pO_2) was controlled through stirring and air flow rates, so that pO_2 was kept above 40 % of saturation. Both pH and pO_2 were monitored with on-line measurements. Each one of these conditions was performed in two replicates. Concentrations of 3-HP, 3-HPA and 1,3-PDO were quantified over time through HPLC (see section 2.6.3, page 60), and cell dry weight (CDW) was quantified through Optical Density (OD) measurements (see section 2.6.1, 58). Each experiment was performed separately from the others: since only one bioreactor was used, they were all carried out at different times, and with their specific inoculum. Therefore, they can be considered as independent experiments. In particular, data from bioconversions carried out at pH 5.0 and 4.0 were used for parameter optimisation, while data from bioconversions at pH 4.5 were used for model validation.

Then, a second model validation was performed using data from the extractive bioconversions, as described in section 2.5 (page 54). Results thereof are described and discussed in Chapter 4. For these experiments, *Acetobacter* sp. CIP 58.66 was first grown on glycerol for 32 h, similarly to the pH control-based fed-batch experiments. Then, the bioconversion phase was triggered with an initial addition of 1,3-PDO (reaching an initial concentration of 5 g L^{-1}). In these cases, the bioconversions were performed in batch mode (no continuous feeding) with a continuous extraction of 3-HP, thanks to the pertraction system. When the initially added 1,3-PDO was fully depleted, a similar second addition was performed. Other important differences with the previous fed-batch bioconversion were (i) that the pH was left uncontrolled during the extractive bioconversions, (ii) and that the initial working volume was 1.2 L, instead of 1 L (because of the volume contained in the pertraction system: pipes and HFMC). The pH therefore varied from 6.9 to 3.9, according to the balance between 3-HP bioproduction and extraction. However, pO_2 was controlled above 40 % in the same way as before. Here again, 3-HP, 3-HPA and 1,3-PDO concentrations were monitored by off-line HPLC analyses, and CDW was derived from off-line OD measurements. Both pH and pO_2 values were monitored on-line. Extractive bioconversions were carried out in three independent replicates. Since the initial growth phase on glycerol was the same as for the non-extractive fed-batchs, it was considered that the system's initial conditions were the same. Therefore, this data set was used for validating the model in a different process setup, but with comparable initial conditions.

Finally, the model's validity was explored with different initial conditions. To that end, two separate data sets were used: batch growth of *Acetobacter* sp. CIP 58.66 on 1,3-PDO in

500 mL shake-flasks; and single-step pH control-based fed-batch bioconversions (Fig. 5.1). These experiments are respectively presented in sections 2.3 (page 50) and 2.4.2 (page 52). Their results are presented and discussed in Chapter 3. In brief, shake-flasks experiments consisted in batch growth of *Acetobacter* sp. CIP 58.66 on different initial concentrations of 1,3-PDO (5, 10, or 20 g L^{-1}). The pH was left uncontrolled, but was monitored by off-line measurements. pO_2 data are not available for these experiments. Each initial 1,3-PDO condition was tested in two replicates.
Single-step fed-batch bioconversions consisted in the strain's fed-batch growth directly on 1,3-PDO, *i.e.* no preliminary growth on glycerol was performed in the bioreactor. The strain was inoculated in a bioreactor with an initial 1,3-PDO concentration of 5 g L^{-1}. Similarly as for the sequential fed-batchs, an equimolar (6 mol L^{-1}) solution of NH_4OH and 1,3-PDO was used for both pH control (at pH 5.0) and substrate feeding. By doing so, 1,3-PDO was fed according to pH feedback. This experiment was carried out in four independent replicates. pH and pO_2 values were monitored by on-line measurements. For both shake-flasks and bioreactor experiments, CDW and metabolites concentrations were monitored through off-line OD measurements and HPLC analyses, respectively.

5.2.2 Computation of the model inputs from experimental data

For each experiment, the experimental values measured at the beginning of the bioconversion were used as initial values for the model's simulations.

Furthermore, in order to successfully establish the mass balances of the bioconversion, the working volume variations have to be taken into account. Inlet and outlet flow rates were passed as arguments to the algorithm used for the model simulations, to that at each time t for which the Ordinary Differential Equations (ODE) system was evaluated, the flow rate values could be interpolated. The identified flows were:

(i) continuous feeding during fed-batch experiments (an equimolar solution of 1,3-PDO and NH_4OH was used for both substrate feeding and pH control);

(ii) medium evaporation, caused by intensive aeration of the broth;

(iii) medium sampling for off-line analyses.

In order to compute each flow rates, volume variations were first experimentally measured, as described in section 2.7.1 (page 61). Then, each cumulative volume (*i.e.* fed, sampled and evaporated volumes) was resampled with a regular and small time step (0.01 h). For the cumulative evaporated and sampled volumes, this was done by linear interpolation (function "interp" from the Numpy library). For the cumulative fed volumed, this was done by fitting function f_A (Eq. 5.1) to the experimental data, using the Levenberg-Marquardt algorithm for sum of squares ("curve_fit" function from package "scipy.optimize" in Python 3.6). Parameters a and b in f_A have no physical meaning and were only used for empirical description of the volume. Using the parameter values thus fitted, the fed volume was computed with the desired 0.01 h time step. Finally, the corresponding flow rates were computed as the ratio of the cumulative volume difference over the time difference, for each time step. The flow

rates thus obtained were passed as arguments to the function used for model simulations, to that at each time t for which the ODE system was evaluated, the flow rate values could be interpolated. An example of this approach is provided in Figure 5.2.

$$f_A(t) = a \cdot (1 - \exp[-b \cdot t]) \tag{5.1}$$

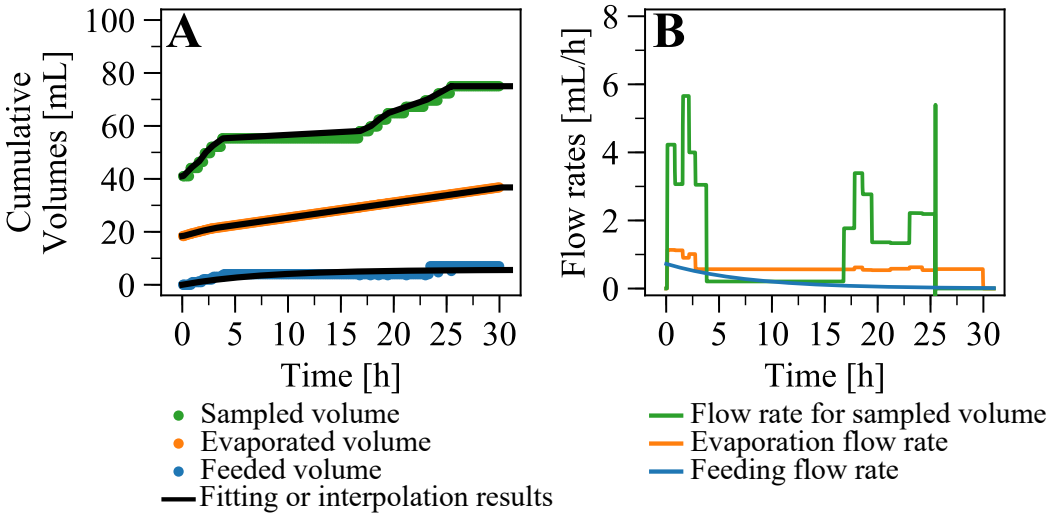

Figure 5.2: **Example of the computation of volumes (A) and flow-rates (B) for one of the fed-batch experiments**

As described below, parameter optimisation was performed in successive steps. For the first steps, biomass and 1,3-PDO evolutions were also required as model inputs, instead of being calculated by mass balances and included in the system of ODEs. In these cases, experimental data of biomass and 1,3-PDO concentrations were also resampled with a regular and small time step (0.01 h), similarly to volume flow rates. For biomass concentrations, the Gompertz model (as modified by Zwietering *et al.* [238], Eq. 2.2) was first fitted to experimental data.

$$G(t) = a \cdot \exp\left(-\exp\left[\frac{b \cdot e}{a}(c - t) + 1\right]\right) \tag{2.2}$$

Regarding 1,3-PDO concentrations, depending on replicates, one of the functions f_B or f_C (Eq. 5.2 & 5.3) was fitted to the experimental data. Similarly to f_A, parameters a, b, c and d have no particular meaning and are only used for data smoothing and interpolation.

$$f_B(t) = a - (b \cdot [1 - \exp(-c \cdot t)]) \tag{5.2}$$

$$f_C(t) = a + b \cdot \left(1 - \frac{1}{1 + \exp[-c \cdot t + d]}\right) \tag{5.3}$$

Both for biomass and 1,3-PDO the models thus fitted were used in order to compute the concentrations with the desired 0.01 h time step.

5.3 Modelling methods

5.3.1 Model description

5.3.1.1 *Definition of the modelled system and working hypothesis*

Given the complexity of the many biological phenomena underlying the bioconversion, it is necessary to first select only some of the phenomena involved, and then proceed to progressive extension of the model. The model proposed in the present chapter was developed based on data from sequential fed-batch bioconversions. Indeed, among the several data sets that were available, this one appeared as the most suited for this early model implementation, because it allowed setting aside some of the phenomena involved:

(i) 1,3-PDO concentration in the medium remained under 5 g L^{-1} during the bioconversions. Results from batch cultures at various initial 1,3-PDO concentrations suggested that this levels of 1,3-PDO are not inhibitory to growth of *Acetobacter* sp. CIP 58.66 (section 3.3.1, page 69). Therefore, 1,3-PDO inhibition was neglected in this study.

(ii) except for one of the six experiments, 3-HPA remained under 0.4 g L^{-1} which is under the minimal inhibitory concentration (0.56 g L^{-1}) that was measured on another Gram-negative bacterium, *Escherichia coli* [49]. Its inhibiting effect was therefore not taken into account.

(iii) for bioconversions at pH 4.0 and 4.5, stirring and air flow rates in the bioreactor ensured sufficient medium aeration to maintain pO_2 at its setpoint (40 % of saturation). For bioconversions at pH 5.0, a pO_2 drop could be observed at the beginning of bioconversion: for one relicate, pO_2 always remained above 25 %, and in the other, it dropped to 4 % during 4 h (before increasing back to its setpoint). In summary, no O_2 limitation was observed in five of the six experiments, and in the sixth one, O_2 limitation lasted only 4 h (compared to 25 h of bioconversion). Therefore, O_2 limitation was not included in the model.

(iv) pH was controlled for all six experiments, so if any, its effect can be considered constant over the whole culture duration. Acetic acid bacteria are known for their high tolerance to low pH [173, 149], so the impact of pH was not included in the model, in a first approach.

To conclude, the system studied was narrowed to four main phenomena: 1,3-PDO (S_1) consumption as growth substrate, 1,3-PDO consumption for 3-HPA (P_0) production, 3-HPA consumption for 3-HP (P_1) production, and finally 3-HP inhibition. The nomenclature used

Table 5.I: Model nomenclature

Symbol	Unit	Definition
μ	h^{-1}	specific growth rate
μ_{max}	h^{-1}	maximal specific growth rate
π_0	h^{-1}	specific 3-HPA production rate
$\pi_{0,max}$	h^{-1}	maximal specific 3-HPA production rate
π_1	h^{-1}	specific 3-HP production rate
$\pi_{1,max}$	h^{-1}	maximal specific 3-HP production rate
D_{in}	h^{-1}	dilution rate due to feeding
D_{out1}	h^{-1}	dilution rate due to volume loss (aeration)
D_{out2}	h^{-1}	dilution rate due to volume loss (sampling)
$f_{I,0}$	*no unit*	3-HP inhibition factor on 3-HPA production
$f_{I,1}$	*no unit*	3-HP inhibition factor on 3-HP production
$f_{I,X}$	*no unit*	3-HP inhibition factor on bacterial growth
$f_{L,0}$	*no unit*	1,3-PDO limitation factor on 3-HPA production
$f_{L,1}$	*no unit*	3-HPA limitation factor on 3-HP production
$f_{L,X}$	*no unit*	1,3-PDO limitation factor on bacterial growth
K_{iX}	$mol\ L^{-1}$	3-HP inhibition constant for biomass formation
K_{i0}	$mol\ L^{-1}$	3-HP inhibition constant for 3-HPA production
K_{i1}	$mol\ L^{-1}$	3-HP inhibition constant for 3-HP production
K_{sX}	$mol\ L^{-1}$	1,3-PDO saturation constant for biomass formation
K_{s0}	$mol\ L^{-1}$	1,3-PDO saturation constant for 3-HPA production
K_{s1}	$mol\ L^{-1}$	3-HPA saturation constant for 3-HP production
n_0	*no unit*	exponent coefficient of the 3-HP inhibition factor on 3-HPA production
n_1	*no unit*	exponent coefficient of the 3-HP inhibition factor on 3-HP production
n_X	*no unit*	exponent coefficient of the 3-HP inhibition factor on bacterial growth
P_0	$mol\ L^{-1}$	3-HPA concentration in the medium
P_1	$mol\ L^{-1}$	3-HP concentration in the medium
Q_{in}	$L\ h^{-1}$	inlet flow rate
Q_{out1}	$L\ h^{-1}$	flow rate of volume loss due to aeration
Q_{out2}	$L\ h^{-1}$	flow rate of volume loss due to sampling
S_1	$mol\ L^{-1}$	1,3-PDO concentration in the medium
$S_{1,in}$	$mol\ L^{-1}$	1,3-PDO concentration in the feeding solution
V	L	volume
w_i	*no unit*	weight attributed to variable i during the model's parameter optimisation
X	$Cmol\ L^{-1}$	biomass concentration in the medium
$Y_{P_0S_1}$	$mol\ mol^{-1}$	3-HPA yield from 1,3-PDO
$Y_{P_1P_0}$	$mol\ mol^{-1}$	3-HP yield from 3-HPA
Y_{XS_1}	$Cmol\ mol^{-1}$	Biomass yield from 1,3-PDO

in the model is available in Table 5.I. The system thus described is presented in Equations 5.4 and 5.5 and in Figure 5.3.

$$S_1 \xrightarrow{\mu(S_1,P_1)} X \tag{5.4}$$

$$S_1 \xrightarrow{\pi_0(S_1,P_1)} P_0 \xrightarrow{\pi_1(P_0,P_1)} P_1 \tag{5.5}$$

Further assumptions were made for the model's implementation. Namely:

(i) thorough mixing of the medium was assumed;

(ii) 1,3-PDO was the only growth substrate;

(iii) the bacterial population was considered homogeneous, and the entire population was supposed active (no cell death or inactivation);

(iv) the evaporation flow (Q_{out2} on Fig. 5.3) was composed only of water vapour: stripping of 1,3-PDO, 3-HPA, 3-HP, or biomass was neglected.

5.3.1.2 *Mass balances equations*

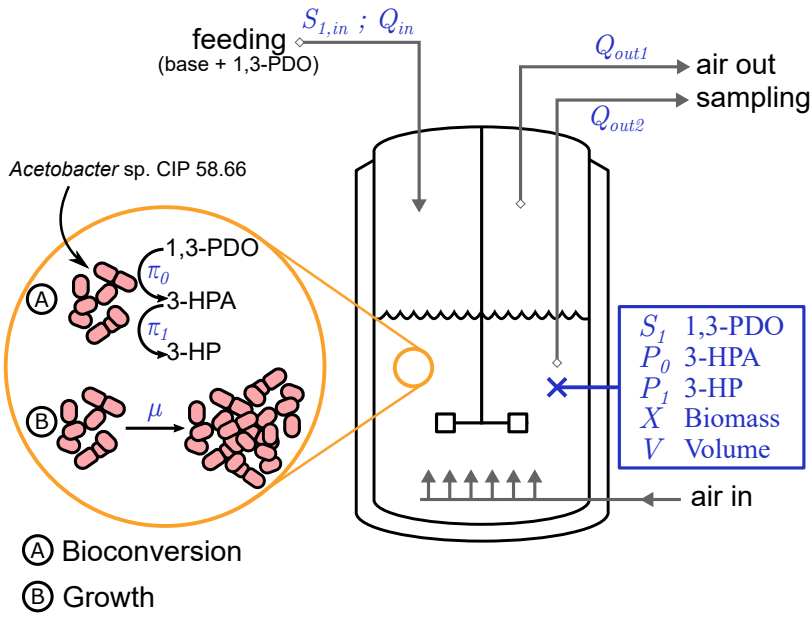

Figure 5.3: Schematic representation of the system being modelled

As illustrated on Fig. 5.3, the different variables of the modelled system may vary according to the production or uptake rate of each constituent, as well as according to volume variations. Therefore, mass balance equations have to account for these different sources of

concentration variation. They can be written as follows:

$$\frac{\mathrm{d}X}{\mathrm{d}t} = \mu \cdot X - (D_{in} - D_{out1}) \cdot X \tag{5.6}$$

$$\frac{\mathrm{d}S_1}{\mathrm{d}t} = -\frac{\pi_0}{Y_{P_0S_1}} \cdot X - \frac{1}{Y_{XS_1}} \cdot \mu \cdot X + S_{1,in} \cdot D_{in} - (D_{in} - D_{out1}) \cdot S_1 \tag{5.7}$$

$$\frac{\mathrm{d}P_0}{\mathrm{d}t} = \left(\pi_0 - \frac{\pi_1}{Y_{P_1P_0}}\right) \cdot X - (D_{in} - D_{out1}) \cdot P_0 \tag{5.8}$$

$$\frac{\mathrm{d}P_1}{\mathrm{d}t} = \pi_1 \cdot X - (D_{in} - D_{out1}) \cdot P_1 \tag{5.9}$$

$$\frac{\mathrm{d}V}{\mathrm{d}t} = (D_{in} - D_{out1} - D_{out2}) \cdot V \tag{5.10}$$

The corresponding nomenclature is available in Table 5.I. The several dilution rates were defined as follows:

$$D_i = \frac{Q_i}{V} \quad \text{for } i \in \{in\ ,\ out1\ ,\ out2\} \tag{5.11}$$

At this stage, four constant parameters appear in the model: $Y_{P_0S_1}$, Y_{XS_1}, $Y_{P_1P_0}$, and $S_{1,in}$. The latter was equal to 6 mol L^{-1}, as described in section 2.4 (page 52). $Y_{P_0S_1}$ and $Y_{P_1P_0}$ were considered equal to 1 mol mol^{-1}, because 1,3-PDO conversion into 3-HP by acetic acid bacteria was experimentally shown to be quantitative in these conditions (see Chapters 3 and 4). The only remaining parameter is Y_{XS_1} and it will be estimated, based on the experimental data, as described below (section 5.3.3).

Furthermore, initial conditions were set for each experiment, using the values measured at the beginning of the bioconversion for 1,3-PDO, 3-HPA, 3-HP, and biomass concentrations, as well as the initial working volume.

5.3.1.3 *Kinetic equations*

The three different specific kinetic rates (for growth, 3-HPA production and 3-HP production) were are all expressed in the same form:

$$r = r_{max} \cdot f_L \cdot f_I \tag{5.12}$$

where r_{max} is the maximal specific rate, and f_L and f_I are respectively limitation and inhibition factors, that vary between 0 and 1. f_L represents the substrate limitation, using Monod's empirical model, while f_I represents the inhibitory effect of 3-HP. For each rate, f_S and f_I

have a similar form, with specific limitation and inhibition parameters:

$$\mu = \mu_{max} \cdot f_{L,X} \cdot f_{I,X} = \mu_{max} \cdot \frac{S_1}{K_{sX} + S_1} \cdot \frac{1}{1 + \left(\frac{P_1}{K_{iX}}\right)^{n_X}} \tag{5.13}$$

$$\pi_0 = \pi_{0,max} \cdot f_{L,0} \cdot f_{I,0} = \pi_{0,max} \cdot \frac{S_1}{K_{s0} + S_1} \cdot \frac{1}{1 + \left(\frac{P_1}{K_{i0}}\right)^{n_0}} \tag{5.14}$$

$$\pi_1 = \pi_{1,max} \cdot f_{L,1} \cdot f_{I,1} = \pi_{1,max} \cdot \frac{P_0}{K_{s1} + P_0} \cdot \frac{1}{1 + \left(\frac{P_1}{K_{i1}}\right)^{n_1}} \tag{5.15}$$

The corresponding nomenclature is available in Table 5.I. Saturation constants (K_s) correspond to the substrate concentration for which the specific rate is equal to half of its maximal value, in absence of inhibition phenomena. Inhibition constants (K_i) correspond to the concentration for which the specific rate is equal to half of its maximal value, in absence of limitation phenomena. The exponent coefficients (n) determine the shape of the inhibition factor as a function of the 3-HP concentration (P_1): the higher the exponent is, the stronger is the threshold effect. An illustration of this is provided on Fig. 5.4.

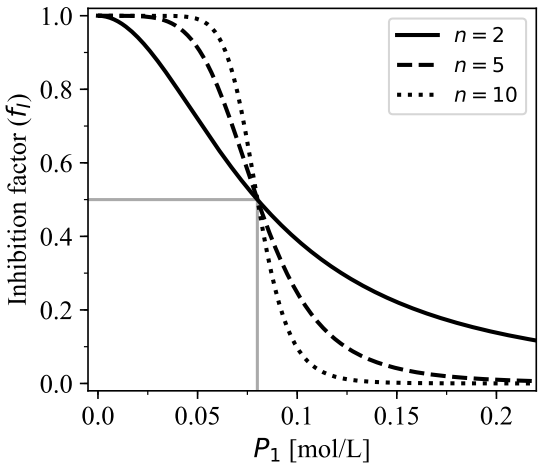

Figure 5.4: Illustration of the variations of the 3-HP inhibition factor depending on the exponent value. Curves are drawn for an arbitrary inhibition constant $K_i = 0.08$ mol L^{-1}

At this stage, 12 constant parameters now appear in the model: the three maximal specific rates (μ_{max}, $\pi_{0,max}$ and $\pi_{1,max}$), the saturation constants (K_{sX}, K_{s0} and K_{s1}), the inhibition constants (K_{iX}, K_{i0} and K_{i1}), and the exponent coefficients (n_X, n_0 and n_1). They will all be estimated from the experimental data, along with Y_{XS_1}, as described in section 5.3.3.

5.3.2 Integration of the ODE system

The Ordinary Differential Equation (ODE) system (Eq. 5.6 to 5.10) was integrated in Python (Python Software Foundation, version 3.6), using the "solve_ivp" function from package

"scipy.integrate". The chosen integration method was 'LSODA', which can automatically detect stiffness, and switch between stiff ('BDF', Backward Differenciation Formula) and non-stiff (Adams) methods [83, 167, 206]. It can be considered as a good universal choice.

5.3.3 Step-by-step parameter estimation

As illustrated on Fig. 5.1, parameter optimisation was performed on bioconversion data from the sequential fed-batch process at pH 5.0 and 4.0. Parameter optimisation is typically a challenging issue in biological non-linear dynamic models. In particular, these models generally involve a great number of parameters that are correlated with one another, potentially leading to non-identifiability problems. Here, in order to work around this issue, parameters were not optimised all at once, but in a stepwise approach, as summarised in Table 5.II.
As a first approach, the overall ODE system was narrowed down to only the volume variations, and the 3-HPA and 3-HP mass balances equations (Eq. 5.8 to 5.10). Biomass and 1,3-PDO concentrations were described with empirical models (see section 5.2.2) and used as model inputs. At this stage, the parameters to be optimised were the ones listed in line 1.a of Table 5.II. Saturation coefficients (K_{s0} and K_{s1}) were fixed to the value found for the ethanol saturation constant (0.08 mol L^{-1}) by Jiménez-Hornero *et al.* (2009) [96].

Since no data was available in the literature for these parameter values, a global optimisation approach was first undertaken. By doing so, no initial guess is required for the different parameters: only the likely variation ranges are to be given. Then, using the evolutionary algorithm of the "differential_evolution" function, from package "scipy.optimize" (Python 3.6) [194, 206], the parameter space was stochastically searched for the parameters values minimising the following cost function – corresponding to a weighted sum of squares of the residuals:

$$C = \frac{1}{2} \cdot \sum_{i} \sum_{j=1}^{j=N_i} \left(\frac{y_{\text{expe},i,j} - y_{\text{pred},i,j}}{w_i} \right)^2 \tag{5.16}$$

where i successively represents the 3-HPA and 3-HP concentrations; N_i is the number of experimental points available for variable i: in the present case, $N_{\text{3-HPA}} = N_{\text{3-HP}} = 56$; $y_{\text{expe},i,j}$ is the j-th experimental point of variable i, and $y_{\text{pred},i,j}$ the corresponding predicted value; w_i is the weight attributed to each variable (Table 5.II). Weights were used so that the contribution of each variable to the overall cost was roughly balanced: in the present case, $w_{\text{3-HP}} = 1$ and $w_{\text{3-HPA}} = 0.1$. An alternate approach would have been to choose w_i as the variation range of the experimental values for each variable, however measured 3-HPA concentrations were close to the limit of quantification (approx. $1 \cdot 10^{-3}$ mol L^{-1}), so the same confidence could not be attributed to these measurements.

For each estimated parameter, variation bounds had to be chosen *a priori* in order to define the parameter space that will be searched by the global optimisation algorithm. They are summarised in Table 5.III. The order of magnitude for 3-HP inhibition constants (K_{i0} and K_{i1}) was determined by analogy with acetic acid, according to Nanba *et al.* (1984) [158]. In their study, their showed that growth of *Acetobacter* sp. 1-39 Mitsukan was negatively impacted by acetic acid concentrations above 20 g L^{-1} (0.333 mol L^{-1}). So the lower bound

for inhibition constants ranges was chosen as the tenth of this value, and the upper bound as ten times this value. Regarding the maximal specific rates values ($\pi_{0,max}$ and $\pi_{1,max}$), lower bounds were set to 0 h^{-1} (or rather $1 \cdot 10^{-6}$ h^{-1}, for numerical reasons). To the best of our knowledge, no data was available in the literature that could help defining the upper bounds, so 20 h^{-1} was arbitrarily chosen as a reasonably high bound. For exponent coefficients (n_0 and n_1), variations were allowed between 1 and 10: this range was considered wide enough to account for different potential forms of inhibition, as illustrated on Fig. 5.4.

Then, estimations obtained from the global optimisation were refined through a local optimisation: they were used as initial guess for a least-square optimisation (Trust Region Reflective algorithm), using function "curve_fit" from package "scipy.optimize" (Python 3.6). The same cost function (Eq. 5.16) was used for all local optimisations. First, local optimisation was carried out on K_{i0} and K_{i1}. Then $\pi_{0,max}$, $\pi_{1,max}$, n_0, and n_1 were successively added pairwise to the optimised parameters pool. Finally, K_{s0} and K_{s1} were also added to the optimisation pool (line 1.b of Table 5.II), with an initial guess set at 0.08 mol L^{-1}. Each time new parameters were added, they were optimised along with the previous ones, using the estimations from the previous step as new initial guess. At this stage, 8 parameters are estimated, using 112 experimental points (3-HPA and 3-HP data, see Table 5.II).

Once parameters concerning 3-HPA and 3-HP production were estimated, the system was successively extended with the 1,3-PDO and biomass mass balance equations (Eq. 5.7 and 5.6). Table 5.II summarises the successive steps of parameter estimation, with the corresponding data sets and variable weights (w_i) that were used.

Based on the results of Luttik *et al.* (1997) [141], it could be considered that the biomass yield of *Acetobacter pasteurianus* from ethanol was 0.52 Cmol mol^{-1}. By analogy, the initial guess for Y_{XS_1} was set to 0.5 Cmol mol^{-1}. Initial guesses for K_{iX}, n_X, and K_{sX} were respectively: 0.3 mol L^{-1}, 4, and 0.08 mol L^{-1}. The initial guess for μ_{max} was the mean of the μ_{max} measured during fed-batch bioconversions (section 3.3.4, page 77). The Python script for this last parameter optimisation step is provided in Appendix C as an illustration of the approach.

Table 5.II: Overview of the stepwise parameter optimisation
For each variable, 56 experimental points are available. Degrees of freedom (DOF) are calculated as the number of experimental points minus the number of optimised parameters.

Optimised parameters		Data used for optimisation				DOF	Equations
	w_i[a] =	Biomass 0.1	1,3-PDO 0.1	3-HPA 0.1	3-HP 1		
(1) Narrowed ODE system							5.8 to 5.10
1.a.	K_{i0}, K_{i1}, $\pi_{0,max}$, $\pi_{1,max}$, n_0, n_1			✓	✓	106	
1.b.	K_{i0}, K_{i1}, $\pi_{0,max}$, $\pi_{1,max}$, n_0, n_1, K_{s0}, K_{s1}			✓	✓	104	
(2) Inclusion of 1,3-PDO mass balance							5.7 to 5.10
2.a.	Y_{XS_1}		✓			55	
2.b.	Y_{XS_1}, K_{i0}, K_{i1}, $\pi_{0,max}$, $\pi_{1,max}$, n_0, n_1, K_{s0}, K_{s1}		✓	✓	✓	159	
(3) Inclusion of bacterial growth							5.6 to 5.10
3.a.	K_{iX}, μ_{max}, n_X, K_{sX}	✓				52	
3.b.	K_{iX}, μ_{max}, n_X, K_{sX}, Y_{XS_1}	✓	✓			107	
3.c.	K_{iX}, μ_{max}, n_X, K_{sX}, Y_{XS_1}, K_{i0}, K_{i1}, $\pi_{0,max}$, $\pi_{1,max}$, n_0, n_1, K_{s0}, K_{s1}	✓	✓	✓	✓	211	

[a] Weight attributed to each variable for cost calculation (Eq. 5.16).

5.4 Results and discussion

5.4.1 Model development using sequential fed-batch data

5.4.1.1 *Estimated model parameters*

Parameter estimation was first carried out on bioconversion data from section 3.3.4, for experiments during which pH was controlled at 5.0 or 4.0. Since each condition was performed in two replicates, this constitutes a pool of four experiments. The resulting parameter estimations are presented in Table 5.III. Maximal specific rates ($\pi_{0,max}$, $\pi_{1,max}$ and μ_{max}), as well as n_0, K_{iX} and K_{sX}, were relatively well estimated, with variation coefficients under 15 %. The estimation of the other parameters was also satisfactory, with variation coefficients comprised between 19 and 26 %. Only n_1 and K_{s1} were found with high coefficients of variation (> 30 %). In particular, it was equal to 51 % for K_{s1}. As will be discussed below, this was attributed to the low concentrations of 3-HPA, compared to the initial guess for this constant.

It can be observed that the simulations adequately represented the variations of the different variables over time (Fig. 5.5). So, even though potentially important phenomena were set aside (see section 5.3.1), the selected phenomena were sufficient for the system's description: notably, this model based on 3-HP inhibition was satisfactory for the two different pH conditions studied here. Analysis of the model's residuals (Fig. 5.6.A) revealed that they were symmetrically and randomly distributed: the mean of all residuals was close to zero (0.008 mol L^{-1}). Moreover, except for a slight heteroscedasticity (*i.e.* residual dispersion increasing for higher predicted values), no clear pattern could be identified. Thus, it was considered that the model provided satisfactorily accurate predictions. It is likely that future model extension – taking into account more phenomena – will correct the observed heteroscedasticity.

Regarding the 3-HP inhibition factors (Fig. 5.7.C), their shapes were relatively different from one another, meaning that 3-HP impacts differentially growth, 3-HPA production and 3-HP production. Bacterial growth appeared to be strongly inhibited for 3-HP concentrations above 0.1 mol L^{-1} (9 g L^{-1}), and above 0.5 mol L^{-1}, growth was completely stopped. 3-HPA production, however, seemed less strongly inhibited by 3-HP: even for 3-HP concentrations as high as 0.8 mol L^{-1}, the inhibition factor did not drop below 0.3. Finally, 3-HP production did not seem affected by 3-HP for concentrations up to approximately 0.2 mol L^{-1}, then the inhibition factor gradually decreased with the increasing 3-HP concentrations, finally reaching 0.1 for concentrations around 0.8 mol L^{-1}. This suggests that despite growth being

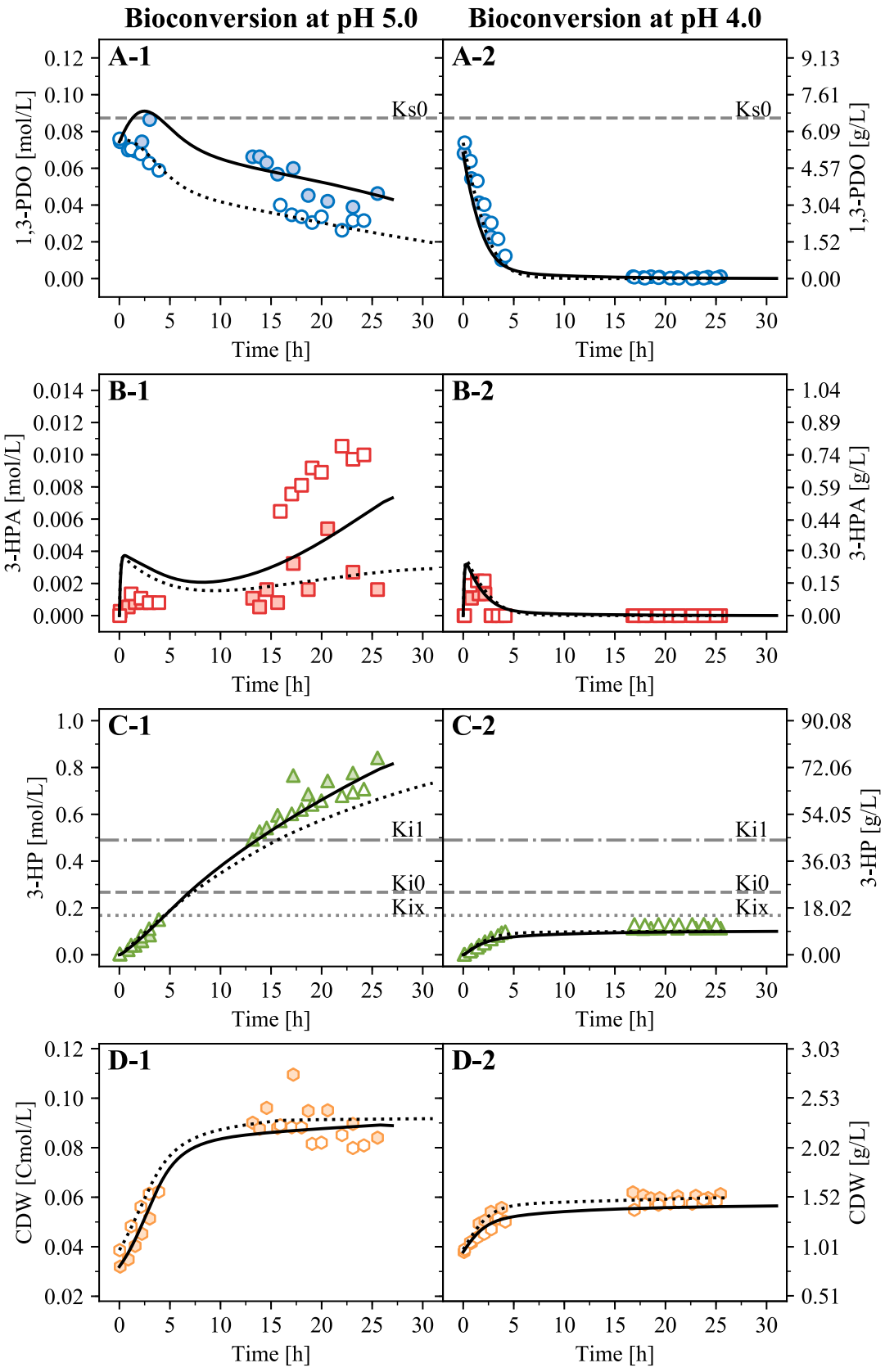

Figure 5.5: Results of the parameter optimisation

Full and empty symbols each represent one of the replicates. The full (respectively dotted) lines represent the fitted model for the full (respectively empty) symbols. The left column (A-1 to D-1) shows results from bioconversion at pH 5.0 and the right column (A-2 to D-2) those from bioconversion at pH 4.0. For all figures, concentrations are given in mol L^{-1} (left scale) and in g L^{-1} (right scale).

inhibited – or even stopped –, bacteria can still perform 1,3-PDO conversion at high 3-HP levels. This behaviour was already demonstrated for vinegar production: growth of acetic acid bacteria is inhibited for acetic acid concentrations ranging from 0.3 to 1 mol L^{-1} [193, 158, 163], and above these concentrations, bacteria are not able to grow but their ethanol oxidation capacity is preserved. Typically, the final acetic acid concentration in vinegar is comprised between 0.7 to 2.5 mol L^{-1} [173].
The form of the 3-HP inhibition factor on bacterial growth (Eq. 5.12 & 5.13) in the present study was the same as the one used for acetic acid inhibition in previous models for vinegar production [177, 95] In these previous studies, only the inhibition constant (denoted K_{iX} here) was considered as a parameter to be estimated, while the exponent coefficient (denoted n_X here) was fixed to 3 and 4 respectively. Interestingly, the n_X estimation in the present study was found between these two values, which means that the threshold effect of 3-HP inhibition on bacterial growth was approximately the same in all cases. On the contrary, the K_{iX} estimation of the present study (0.17 mol L^{-1}) was found lower than those found for acetic acid inhibition: 0.30 mol L^{-1} in the study of Romero *et al.* [177], and 1.67 mol L^{-1} in the study of Jiménez-Hornero *et al.* [95]. The models proposed in these studies include only acetic acid inhibition on bacterial growth, and not on the bioconversion of ethanol into acetic acid. Therefore, comparing the estimations between the present study and the previous ones is questionable. However, it can be noted that the K_{iX} estimation found by Romero *et al.* is relatively close to the ones found for K_{i0} and K_{i1} (Table 5.III). Furthermore, in the study of Jiménez-Hornero *et al.*, the K_{iX} estimation (1.67 mol L^{-1}) was quite high compared to the inhibition constants found in the current study [96]. This could suggest that the organic acid's inhibitory effect occurred for higher concentrations in their study, but in fact, their model also included a cell death rate. In the absence of any ethanol inhibition – which was also included in their model – the cell death rate was doubled for acetic acid concentrations of 0.21 mol L^{-1}. In summary, the present study offers an alternative approach to the one previously implemented: here, the impact of the organic acid on the bacterial growth can be distinguished from its impact on bioconversion. The relevance of this approaches is notably substantiated by the fact that each considered inhibition factor had a different shape (Fig. 5.7.C).

These observed differences in 3-HP inhibition on 3-HPA and 3-HP production rates was mainly responsible for the late 3-HPA accumulation for bioconversions at pH 5.0 (after 15 h, Fig. 5.5.B-1). At this stage, 3-HP had already reached concentrations close to 0.6 mol L^{-1} (Fig. 5.5.C-1), which is the threshold above which 3-HP production is more inhibited than 3-HPA production – all other things being equal. However, even though this late 3-HPA accumulation was qualitatively predicted by the model, the simulations did not accurately fit to the experimental points. This was due to the weight that was attributed to 3-HPA concentrations, for its contribution to the cost function (Eq. 5.16). With the chosen weights, the contribution of 3-HPA was approximately 10 times lower than that the other variables. This choice was made because of the uncertainty of the 3-HPA measurements due to (i) the use of a chemically synthesised standard, that was not perfectly pure; and (ii) the low 3-HPA concentrations that were close to the limit of quantification (approx. $1 \cdot 10^{-3}$ mol L^{-1}). In this light, the model's prediction for 3-HPA variations seems satisfactory, at least qualita-

Table 5.III: Parameter estimations resulting from stepwise optimisation

Parameter	Initial guess	Estimation[a]	Unit	Coefficient of Variation
K_{i0}	$[0.03, 3.3]$	0.27 ± 0.06	mol L^{-1}	22 %
K_{i1}	$[0.03, 3.3]$	0.49 ± 0.10	mol L^{-1}	21 %
$\pi_{0,max}$	$[1.0 \cdot 10^{-6}, 20]$	2.2 ± 0.3	h^{-1}	15 %
$\pi_{1,max}$	$[1.0 \cdot 10^{-6}, 20]$	25 ± 3	h^{-1}	13 %
n_0	$[1, 10]$	0.75 ± 0.09		12 %
n_1	$[1, 10]$	3.9 ± 1.4		35 %
K_{s0}	0.08	0.087 ± 0.022	mol L^{-1}	26 %
K_{s1}	0.08	0.096 ± 0.046	mol L^{-1}	51 %
Y_{XS_1}	0.5	4.4 ± 0.8	Cmol mol^{-1}	19 %
K_{iX}	0.3	0.17 ± 0.02	mol L^{-1}	13 %
K_{sX}	0.04	0.24 ± 0.03	mol L^{-1}	14 %
μ_{max}	0.14	0.77 ± 0.09	h^{-1}	11 %
n_X	4	3.27 ± 0.77		24 %

[a] Given as Estimation $\pm$ Standard Error

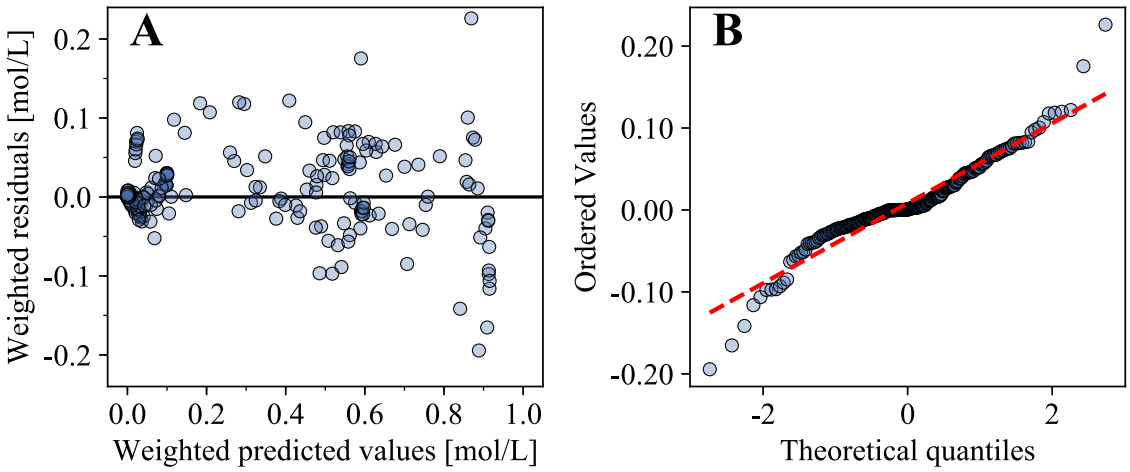

Figure 5.6: Analysis of the residuals. Residuals were calculated as $\frac{1}{w_i} \cdot (y_{\text{expe},i} - y_{\text{pred},i})$, for $i \in \{$3-HPA, 3-HP, 1,3-PDO, CDW$\}$. The same w_i weights were used in this representation as for the cost computation (Eq. 5.16) during parameter estimation. **A.** Plot of the model residuals against predicted values. **B.** Quantile-Quantile (Q-Q) plot of the experimental data against normal distribution.

tively. In particular, the transient 3-HPA accumulation in the first hours (from 0 to 5 h) of bioconversion was predicted in all instances (5.5.B-1 and B-2). Contrary to the late 3-HPA accumulation (after 15 h), this early accumulation was attributed to limitation phenomena, instead of inhibition phenomena. Before 5 h, 3-HP remained below 0.2 mol L^{-1}, meaning that its impact on 3-HPA consumption was negligible (5.7.C), while the 3-HPA limitation factor remained low at all time (< 0.2, Fig. 5.7.B). In the initial conditions, 1,3-PDO was available as substrate (around 0.07 mol L^{-1}, Fig. 5.5.A-1 and A-2), while 3-HPA had not yet been produced. A slight 3-HPA accumulation was necessary for its consumption rate to reach values more balanced with its production rate. In the meantime (from 0 to 5 h), 1,3-PDO was beeing depleted from the medium, almost fully for pH 4.0 bioconversions (Fig. 5.5.A-2), leading to 1,3-PDO limitation phenomena, and consequently to 3-HPA depletion.

Interestingly, the cause for growth slowing down was different for bioconversions at pH 5.0 and 4.0. In the first case (Fig. 5.5.D-1), growth stopped around 10 h of bioconversion. At that time, predictions for 1,3-PDO limitation factors were respectively 0.21 and 0.15 for each replicate, while 3-HP inhibition factors were 0.08 and 0.07, thus suggesting that growth stopped chiefly because of the 3-HP accumulation. In the second case (Fig. 5.5.D-2), growth stopped around 5 h. For each replicate, the corresponding 1,3-PDO limitation factors were 0.018 and 0.00067, while 3-HP inhibition factors were 0.93 and 0.86. In that case, 1,3-PDO depletion was the reason for growth stopping. Overall, it appeared that bacterial growth was well explained by 1,3-PDO consumption. This result might seem surprising since 1,3-PDO was not the only carbon source available to bacteria: in addition to complex sources (*i.e.* yeast extract and peptone), residual glycerol was also present, remaining from the preliminary growth (see section 3.3.3.2, page 75). At the beginning of bioconversion, the remaining glycerol concentration was comprised between 0.09 and 0.10 mol L^{-1} (8.2 and 9.2 g L^{-1}). A slight glycerol consumption was observed during the bioconversions, but it was never fully depleted (Fig. 3.4, page 76). As discussed in Chapter 3, the exact roles of 1,3-PDO and glycerol during the bioconversion-associated growths remained unclear. However, the model predicted that the cause for growth stopping, in the pH 4.0 condition, was 1,3-PDO limitation. Since glycerol was still relatively abundant when growth stopped (between 0.08 and 0.09 mol L^{-1}), it seems that the observed bacterial growth can be primarily attributed to 1,3-PDO and not to glycerol.
Moreover, the Y_{XS_1} final estimation (4.4 Cmol mol^{-1}) might also come as a surprise: one mole of 1,3-PDO represents 3 moles of carbon, so it could be expected that Y_{XS_1} would not exceed 3 Cmol mol^{-1}. However, this is under the assumption that 1,3-PDO is the only growth substrate. So the Y_{XS_1} estimation likely accounts for other growth substrates uptake, glycerol mostly.

Limitation factors corresponding to biomass and 3-HP formation were found almost linear (Fig. 5.7.A and B). In the absence of inhibition phenomena, this means that the corresponding specific rates (μ and π_1) were in fact proportional to 1,3-PDO and 3-HPA concentrations respectively. Indeed 1,3-PDO and 3-HPA concentrations remained small compared to their corresponding saturation constants (K_{sX} and K_{s1}). So the following approximation was verified at all time: $K_s + c \simeq K_s$ (with c the considered substrate concentration), and the

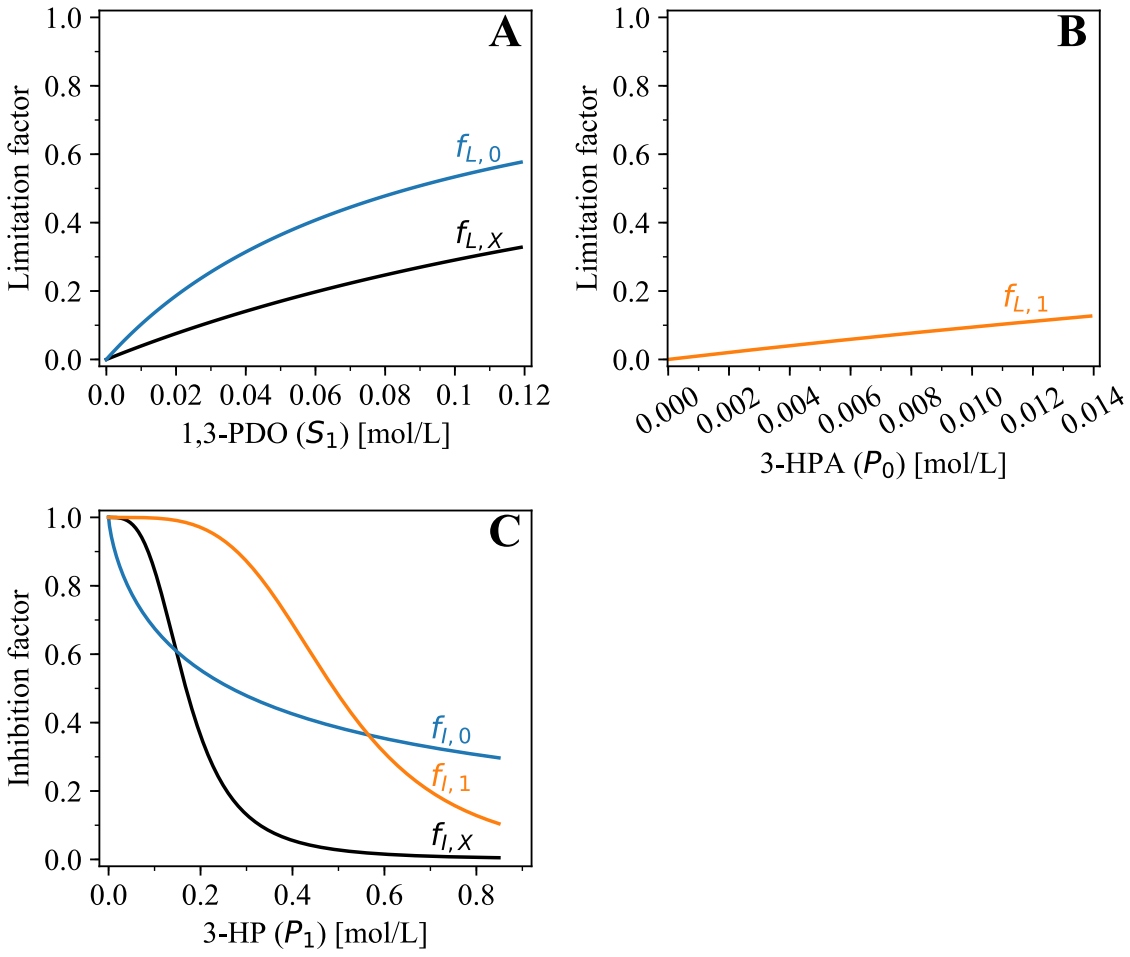

Figure 5.7: Representation of the model's limiting and inhibiting factors.

A. 1,3-PDO limitation factor for 3-HPA production ($f_{L,0}$) and bacterial growth ($f_{L,X}$). **B.** 3-HPA limitation factor for 3-HP production ($f_{L,1}$). **C.** 3-HP inhibition factors for bacterial growth ($f_{I,X}$), 3-HPA production ($f_{I,0}$) and 3-HP production ($f_{I,1}$).

inhibition factors remained in the linearity domain of Monod's expression:

$$f_L(c) = \frac{c}{K_s + c} \simeq \frac{c}{K_s} \tag{5.17}$$

As a consequence, maximal specific rates and saturation constants were not fully distinguishable, and could have been considered as one parameter only. The surprisingly high $\pi_{1,max}$ value, as well as the high coefficient of variation are likely a result of this identifiability issue. Trying to achieve a finer estimation of these parameters is however a non-trivial issue. In particular, experimental data for 3-HPA correspond to the fraction that was present in the bioconversion medium, *i.e.* the extracellular 3-HPA. Yet, the successive steps of 1,3-PDO conversion into 3-HP take place in the bacterial periplasm [237], so it is possible that 3-HPA is locally accumulated in this sub-cellular compartment. Therefore, extracellular 3-HPA may not be the most suitable data for fine description of the enzymatic kinetics, and quantifying intra-cellular 3-HPA overtime would be necessary for a fine understanding of the enzymatic mechanisms. Regarding growth, an important number of mechanisms are involved, which the present model simplifies to the extreme, by considering only biomass formation from 1,3-PDO. The maximal growth rate (μ_{max}) is the only parameter concerning bacterial growth that had a comparable meaning in the present model and in the previous models for vinegar production. The present estimation was close to the one of the study of Jiménez-Hornero *et al.*, who found a μ_{max} equal to 0.61 h^{-1} [96], but these values are higher than the one of Romero *et al.*: 0.22 h^{-1} [177]. Therefore, no reliable conclusion can be drawn from these results, in order to compare the growth of an acetic acid bacterium on ethanol or on 1,3-PDO. In any case, accessing parameter values with a biological significance is highly questionable in the case of bacterial growth, due to the numerous mechanisms at stake.

As a conclusion to this section, results showed that the present model provided simulations in adequacy with the experimental data used for parameter estimation. The simulations thus performed gave new insights for the understanding of 1,3-PDO conversion into 3-HP by *Acetobacter* sp. CIP 58.66. Notably, different situations could be identified where 1,3-PDO limitation or 3-HP inhibition were the main cause for the process slowing down. The model is yet to be validated for independent data sets.

5.4.1.2 *Evaluation of the interpolation capacity of the model*

Once the parameters were estimated, and the adequacy between predictions and experimental data was checked, the model's interpolation capacity was evaluated. To that end, model simulations were performed with the same parameter values and compared with data from the same experimental set, but with an intermediate condition (pH $= 4.5$). Here again, the model's input were the initial conditions of each experiment, and the flow rates of the system's inlet (Q_{in}) and outlets (Q_{out1} and Q_{out2}). Results are presented in Figure 5.8. Evolutions of 1,3-PDO, 3-HPA and 3-HP over time were well predicted by the model. Only the biomass evolution was not adequately represented: biomass formation was overestimated by the model (Fig. 5.8.D). In the simulations, CDW stabilised at 0.082 Cmol L^{-1}, while it stabilised around 0.064 Cmol L^{-1} according to the experimental data. In the simulations, growth stopped around 10 h, and analysis of the growth rate revealed that – and at that time

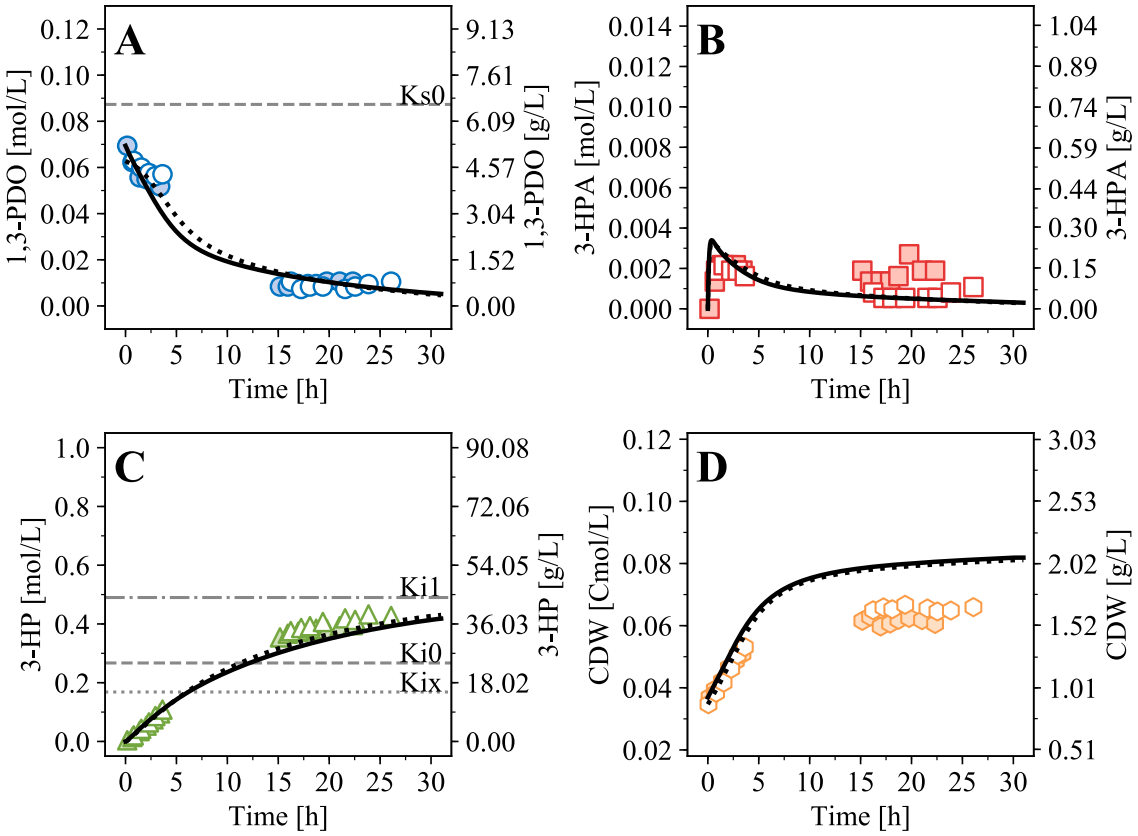

Figure 5.8: Model validation on the data from fed-batch bioconversion at pH 4.5

Full and empty symbols each represent one of the replicates. The full (respectively dotted) lines represent the fitted model for the full (respectively empty) symbols.

– 1,3-PDO limitation factors were 0.073 and 0.082 for each replicate, while 3-HP inhibition factors were respectively 0.25 and 0.22. This suggests that the main driver for growth slowing down in these simulations was 1,3-PDO limitation. 3-HP inhibition might have been underestimated in this case, leading to the observed overestimation. As predicted by the model, the bacterial growth shows an evolution more similar to the one observed for bioconversions at pH 5.0 (Fig. 5.5.D-1), even though the reasons for growth stopping is not the same in both cases. In reality, the measured biomass evolution was closer to the one observed for bioconversions at pH 4.0 (Fig. 5.5.D-2). The model being non-linear, using only two extreme conditions for parameter estimation is not sufficient for an accurate description of all intermediary conditions. Future works have to include the study of a larger set of experimental conditions, in order to address this issue.

Nonetheless, an important feature of the model has to be borne in mind: pH was not explicitly included in the model. So, despite pH 4.5 being an intermediate condition from the biological point of view, this is only reflected in the model through the feeding rates. Indeed, in addition to the difference in pH setpoint, an important difference between the various experimental conditions was also the volume of feeding solution added into the bioreactor. As discussed in section 3.3.4.3 (page 78), the main effects observed in these bioconversions at

pH 5.0, 4.5, or 4.0 was the higher 3-HP production for higher pH values. However, this effect was not directly attributed to pH, but to the design of the feeding strategy. In these experiments, a continuous 1,3-PDO inlet was automatically assured based on pH control: an equimolar (6 mol L^{-1}) solution of base and 1,3-PDO was used as pH-control solution. By doing so, 1,3-PDO was fed according to the acidification due to 3-HP production. Depending on the pH setpoint, the amount of base needed for maintaining the setpoint in the presence of the same amount of 3-HP was not the same. In particular, at pH 4.0 and 4.5, which are below (or close to) the pKa of 3-HP (4.51), significantly less base was needed for pH control, compared to pH 5.0, for an equivalent amount of 3-HP produced. Therefore, the 1:1 molar ratio in the base/substrate inlet solution led to substrate depletion in the case of pH 4.0 because not enough 1,3-PDO was fed, while it was sufficient in the case of pH 5.0 for maintaining 1,3-PDO to non-limiting concentrations. In the present model, this is reflected by the fact that the 1,3-PDO inlet all along the bioconversion is used as an input of the model. It is in that sense that the pH 4.5 bioconversions constitute an intermediary condition between the pH 4.0 and 5.0 bioconversions (Fig. 5.9).

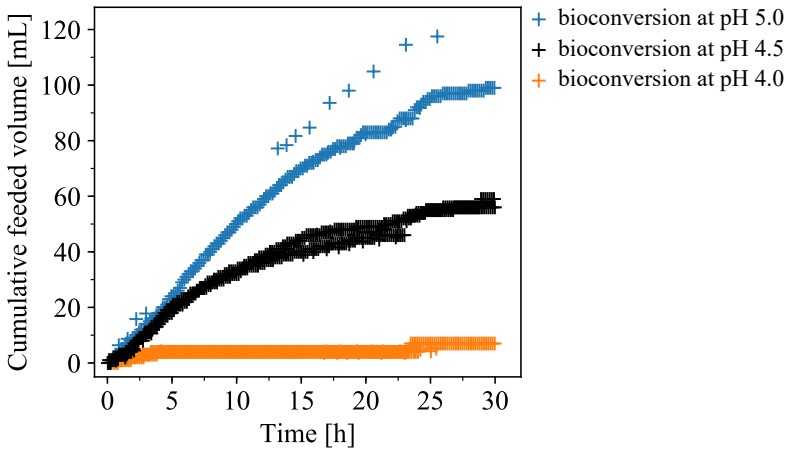

Figure 5.9: Comparison of the cumulative fed volumes of the different experimental conditions of sequential fed-batchs

Except for biomass, evolutions of 1,3-PDO, 3-HPA and 3-HP were well predicted in the case of pH 4.5 bioconversions, thus suggesting that most of the studied system was satisfactorily described using only substrate limitation and 3-HP inhibition. In light of this and of the elements of the previous paragraph, it was considered that the assumptions underlying the present model (section 5.3.1.1) held in most parts. Notably, it seemed that pH was not necessary to predict the kinetics of the pH 4.5 bioconversions, and that bioconversion kinetics, in particular, remained unaffected by the pH within the considered range. At this stage of model development, the interpolation capacity of the present model seemed satisfactory, even though explicit inclusion of pH might be necessary in order to achieve a more accurate description of the bacterial growth. The model's relevance for extrapolation was then evaluated on a different set of experimental data, resulting from a distinct experimental setup.

5.4.2 Model evaluation for extractive bioconversion data

In order to evaluate the extrapolation capacity of the model, simulations were performed and compared to the experimental data obtained during extractive bioconversions. Similarly to the fed-batch experiments used for model development in the previous section, extractive bioconversions were initiated after an initial 32 h-long growth phase on glycerol, which is not studied here but was discussed in sections 3.3.3.2 (page 75) and 4.3.1.1 (page 87). Conditions for this preliminary growth phase were the same in all cases (see section 2.5.2, page 56), so it was considered that at the beginning of the extractive bioconversions, the physiological state of bacteria was comparable to the one at the beginning of fed-batch bioconversions. During extractive bioconversions, 1,3-PDO was added discontinuously: at 0 and 4.6 h of bioconversion, a 6 mL input of 1,3-PDO (98 %, w/v) was performed. pH was left uncontrolled and decreased from 6.9 at the beginning of bioconversion to 3.9 at the end (see section 4.3.2.2, page 93). After 45 min of bioconversion, pH had reached 4.6, and the in stream product recovery (ISPR) process was initiated, so that the 3-HP thus produced was continuously removed from the bioconversion medium. Experimental results of the extractive bioconversion are presented and discussed in Chapter 4.

Figure 5.10 presents the comparison between model predictions and experimental data. Given the differences in the experimental setup compared to the experiments used for model development, the simulations were considered satisfactory for extractive bioconversion also. 1,3-PDO, 3-HPA and 3-HP variations were particularly well predicted and the simulation was located within the experimental standard deviation in most occurrences. Since the pH was uncontrolled during the extractive bioconversion, and varied from 6.9 to 3.9, these results support the observation made previously: the model based on substrate limitation and 3-HP inhibition was sufficient for the system's description, and pH was not required as an explanatory variable, except perhaps for the biomass growth, which was less well predicted. An important remark on 3-HP is that, 3-HP being continuously removed by ISPR, two distinct variables have to be considered: firstly, the actual 3-HP concentration in the medium, and secondly, the overall 3-HP produced. The model simulates the latter, even though only the former should be considered for inhibition. In the present case, the 3-HP extraction rate was significantly lower than its production rate. Therefore, the difference between the total 3-HP production and the 3-HP present in the medium was not large enough to justify adapting the model accordingly by introducing a reactive extraction component (Fig. 5.10.C). However, in future process development, if a better balance between 3-HP production and extraction is achieved, it will be necessary to include 3-HP removal in the model. A compartment model could be proposed in order to differentiate the total 3-HP produced from the residual 3-HP in the bioconversion medium. The 3-HP flow between the two compartments could be simulated with the model that was previously implemented for 3-HP in stream extraction [37].

Again, the bacterial growth was not well predicted by the model (Fig. 5.10.D). This time, the model slightly underestimated the biomass concentration. Since the predicted 3-HP concentrations remained under 0.15 mol L^{-1} (Fig. 5.10.C), the 3-HP inhibition factor on growth was above 0.59 at all time (Fig. 5.7.C). 1,3-PDO limitation was therefore the most important

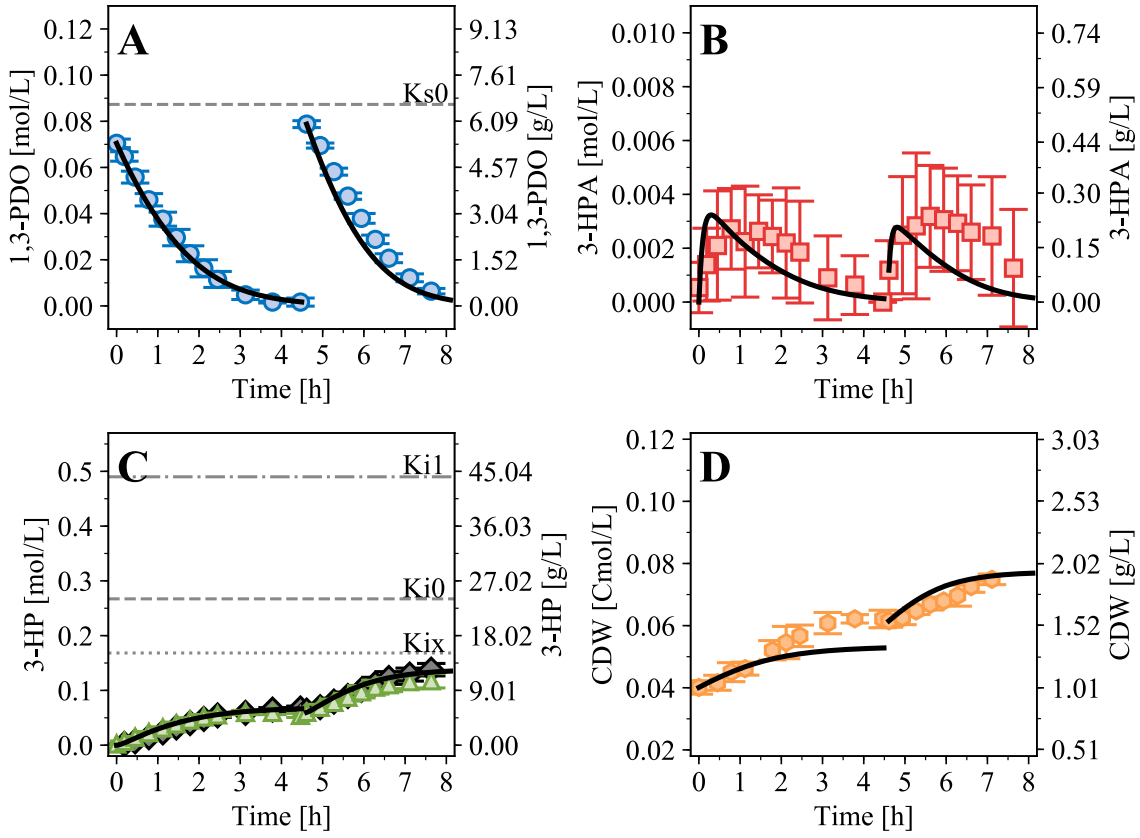

Figure 5.10: Model evaluation on the data from extractive bioconversions

On the figure of 3-HP kinetics (**C.**), green triangles represent the actual 3-HP concentration in the broth, while grey diamonds represent the total 3-HP production: it is the concentration that would have been measured in the medium if no 3-HP had been extracted. For the experimental points: $n = 3$ and results are presented as mean $\pm$ sample standard deviation.

driver for growth slowing down. This underlines again the necessity for parameter estimation on a greater number of experimental conditions, instead of only the two conditions used in section 5.4.1.1. Moreover, contrarily to the 1,3-PDO conversion into 3-HP, bacterial growth is a complex phenomenon, so future model extension with inclusion of more phenomena (such as 3-HPA inhibition, O_2 uptake, pH effect) is expected to allow finer growth predictions.

Yet, despite the inaccuracy in growth prediction, the model showed an interesting potential for bioconversion kinetics prediction. Using the parameters estimated on previous non-extractive experiments, the model's predictions were relevant for 1,3-PDO, 3-HPA and 3-HP, in spite of the differences in experimental conditions, *i.e.* discontinuous 1,3-PDO feeding, uncontrolled pH, and in stream product recovery. However, an important similarity between all experiments studied so far with the model, is that in all cases bioconversion was preceded by an identical 32 h-long growth phase on glycerol. Therefore, the initial state of the biocatalyst population was homogeneous for all bioconversions, no matter the conditions that were then tested during the subsequent bioconversion. The model's extrapolation capacity

for another initial state of the bacterial population will be tested in the next section.

5.4.3 Model evaluation for a different initial bacterial state

In order to evaluate the model's prediction capacity for bioconversions that were not preceded by an initial growth phase on glycerol, two data sets were available: (i) batch growths and bioconversions in shake-flasks, with different initial 1,3-PDO concentrations (as described in section 3.3.1, page 69), (ii) single-step pH-based fed-batch in a bioreactor (as described in section 3.3.2, page 71). Since no preliminary growth phase was performed in these cases, *Acetobacter* sp. CIP 58.66 was directly inoculated on 1,3-PDO as main growth substrate (in a complex medium). Batch bioconversions were performed in shake-flasks, which means that pH and pO_2 were uncontrolled during these experiments: pH was monitored by off-line measurements, but no information on pO_2 evolution is available. Single-step fed-batch bioconversions were carried out similarly to the sequential fed-batch bioconversions at pH 5.0 that were used for parameter estimation in section 5.4.1.1: in particular, pH was controlled at 5.0 with the same equimolar solution of base and 1,3-PDO, also serving as continuous 1,3-PDO feed; pO_2 was also controlled above 40 % of saturation by automatic control of stirring and flow rates. The only difference between sequential and single-step fed-batch was the absence of the preliminary growth on glycerol in the latter case (Fig. 5.1).

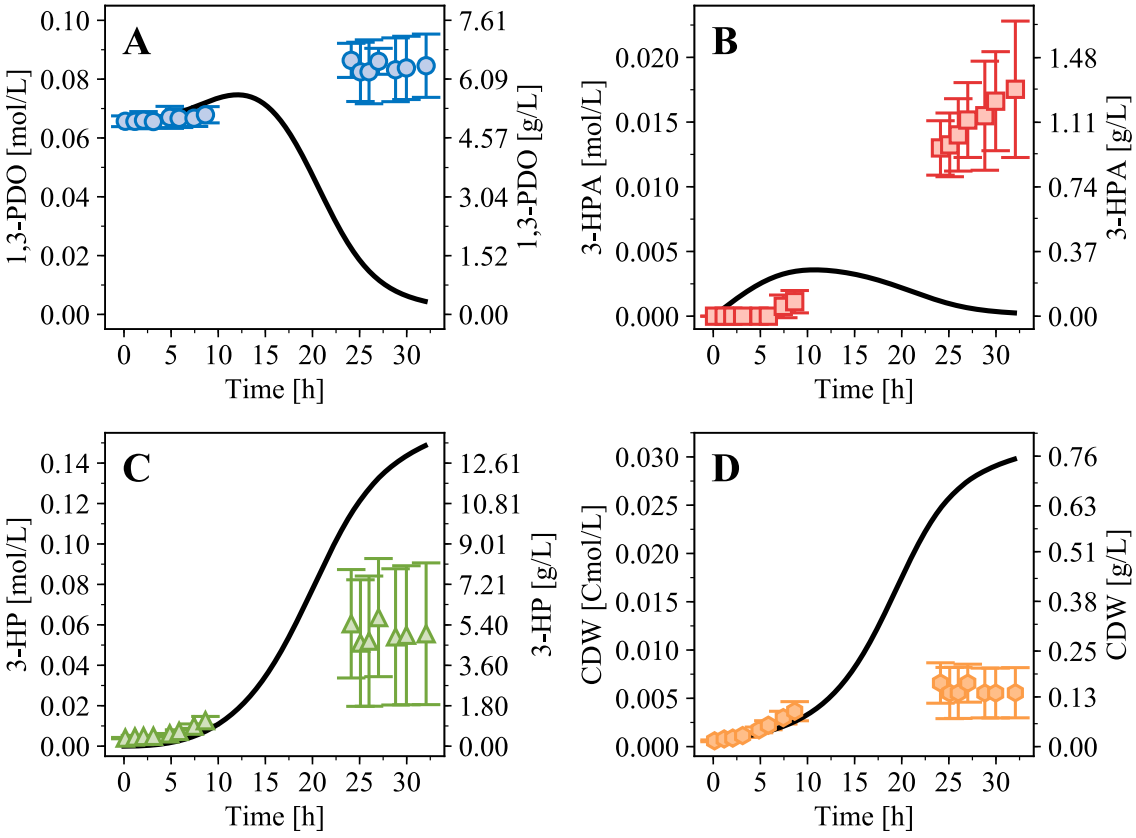

Figure 5.11: Model simulations for single-step fed-batch bioconversions

For the experimental points: $n = 4$ and results are presented as mean $\pm$ sample standard deviation.

Simulations were performed for these different experiments, using the parameter values that were obtained in the previous section (Table 5.III). In all cases, it was observed that simulations did not represent the experimental data adequately (Fig. 5.11 and Fig. 5.12). For single-step fed-batch, the model predicted that 1,3-PDO would be fully depleted, while in reality 1,3-PDO was not fully consumed and even slightly accumulated (Fig. 5.11.A). Consequently, 3-HP and biomass formation were overestimated (Fig. 5.11.C and D, respectively). Furthermore, the predicted 3-HPA concentrations followed a different trend than the experimental data: instead of the initial 3-HPA peak and subsequent depletion predicted by the model, experimental data showed only a continuous 3-HPA accumulation, after a latency phase (Fig. 5.11.B). These trends were similar in batch cultures, when the initial 1,3-PDO concentration was above 10 g L^{-1} (Fig. 5.12). In these cases, simulations also predicted full 1,3-PDO depletion, contrarily to experimental data. Therefore, 3-HP and biomass were also overestimated, and the same differences in 3-HPA trends between simulation and experimental data were observed. For batch cultures with 5 g L^{-1} initial 1,3-PDO, experimental data showed that 1,3-PDO was fully consumed (Fig. 5.12.A). In that case only, the model adequately accounted for 1,3-PDO, 3-HP and biomass evolutions. However, here again, the predictions for 3-HPA were not in line with concentrations measured experimentally.

The two data sets investigated here corresponded to quite different experimental conditions: batch versus fed-batch; uncontrolled versus controlled pH and pO_2; shake-flask versus bioreactor; one-step versus two-step inoculum preparation (Chapter 2). Yet, comparison of predicted and measured values revealed the same pattern in all cases. This consistency among observations suggests that other phenomena than those included in the model are involved when *Acetobacter* sp. CIP 58.66 grows directly on 1,3-PDO, instead of being first grown on glycerol. Notably, inhibition or limitation phenomena that were neglected in a first approach might be responsible here for growth stopping despite 1,3-PDO still being available and 3-HP concentrations remaining at sub-inhibitory levels. Since pO_2 was successfully controlled above 40 % of saturation during the single-step fed-batch, O_2 uptake can still be considered as a non-limiting phenomenon – at least for fed-batch cultures. The most likely relevant phenomena are 3-HPA and 1,3-PDO inhibitions:

(i) on the one hand, 1,3-PDO remained close to its initial value during single-step fed-batch (Fig. 5.11.A), which was the same than during sequential fed-batch. Yet, 3-HPA was accumulated in high concentrations, compared to experiments investigated in the previous section. This suggests that the initial enzymatic activity of the two pathways was different than after growth on glycerol (π_0 was lower or π_1 was higher, or both); but the situation reversed at longer times (> 8 h). The final 3-HPA levels reached here were well above the minimum inhibitory 3-HPA concentrations that were measured for *Escherichia coli*, which were between 0.0075 and 0.015 mol L^{-1} [49]. These observations support the relevance of including 3-HPA inhibition in the model.

(ii) on the other hand, the 3-HPA levels reached in batch cultures were lower when the initial 1,3-PDO concentration was 20 g L^{-1} than when it was 10 g L^{-1}. Yet, growth was also more limited in spite of lower 3-HPA concentrations, thus suggesting that 1,3-PDO had an inhibitory impact on growth.

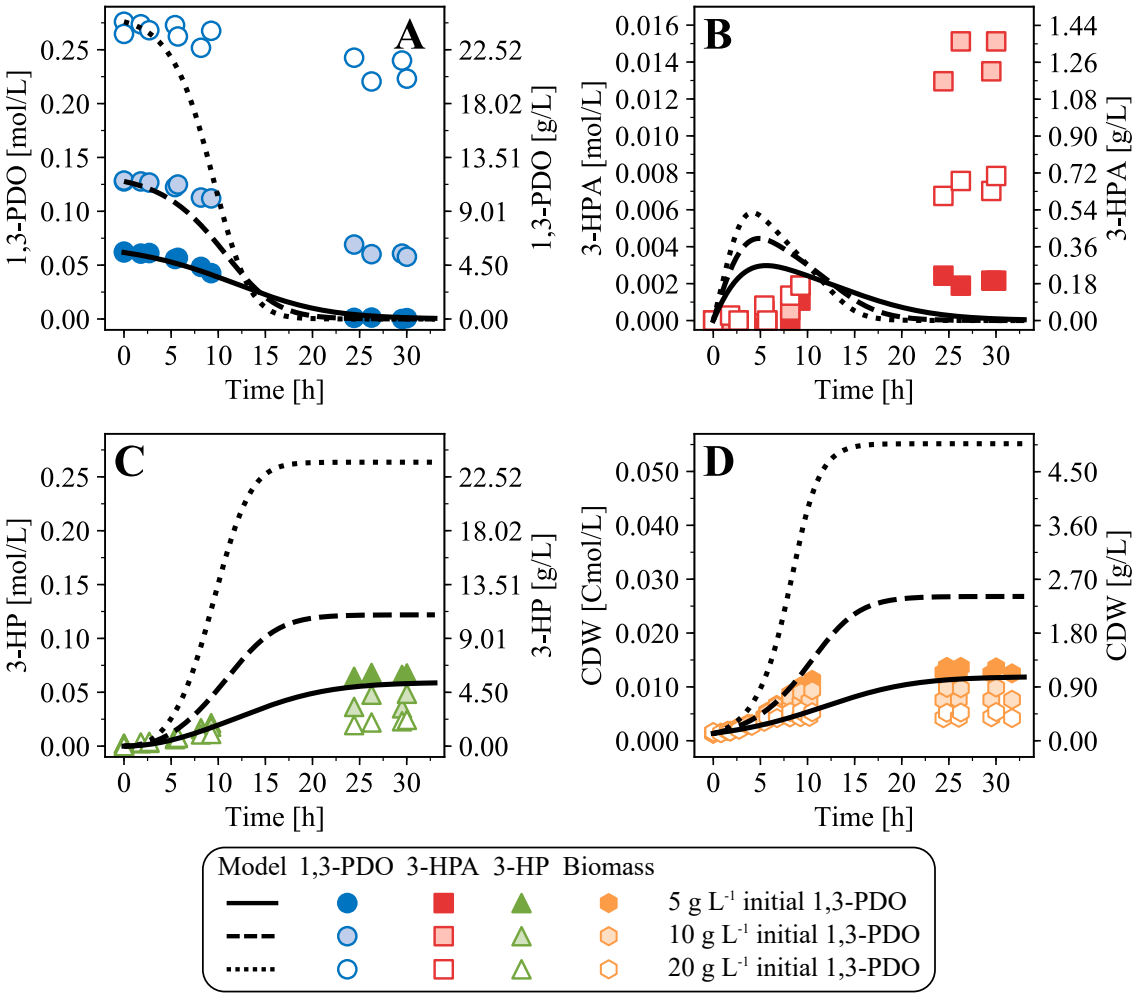

Figure 5.12: Model simulations for batch cultures in shake-flasks with different initial 1,3-PDO concentrations

Details of these experiments are provided in section 2.3 (page 50). They were all tested in two duplicates, so all experimental points from each replicate are displayed.

In addition to 3-HPA and 1,3-PDO inhibitions, it is also likely that bacterial growth kinetics in the absence of residual glycerol are different than those in the presence of residual glycerol. Also, it is likely that growth kinetics vary according to the physiological state of the bacterial population: in the batch and single-step experiments, bacteria were inoculated directly on 1,3-PDO, while in the sequential fed-batch experiments, bacteria had already reached late exponential phase when the bioconversion was initiated; thus it is not surprising that the bioconversion-associated growth could not be explained by the same kinetics in each case. Therefore, in order to expand the model's validity to growth of *Acetobacter* sp. CIP 58.66 in the absence of glycerol, it would be necessary to account separately for glycerol and 1,3-PDO uptake for growth. This would notably require to use separate yields, Y_{XS_1} and Y_{XS_2}, for biomass production from 1,3-PDO and glycerol respectively.

5.5 Conclusion

To conclude, the present chapter lays the groundwork for modelling 1,3-PDO oxidation into 3-HP by *Acetobacter* sp. CIP 58.66, and its associated growth. This preliminary model included 1,3-PDO and 3-HPA limitations, along with 3-HP inhibition on both bioconversion and growth. After parameters were estimated, the model's potential was demonstrated for different (either extractive or non-extractive) bioconversions that were preceded by a preliminary growth phase on glycerol. Analysis of the resulting model gave new insights on the respective contributions of substrate limitation and product inhibition in the final slowing down of the process. Thus, the model appears as a good tool for future works on the optimisation of the sequential fed-batch bioconversions. However, simulation of the bioconversions that were not preceded this preliminary growth revealed that the initial physiological state of the microorganisms and the presence of glycerol in the medium are important, as one might expect, and that further model expansion would be necessary for a good prediction of all experiments.

Future works for model expansion will need to investigate four phenomena in priority: pH effect, 1,3-PDO inhibition, 3-HPA inhibition, and glycerol assimilation. To that end, the experimental setup for pH-based 1,3-PDO feeding in a bioreactor shows a great potential. Indeed, as discussed in section 3.3.4.3 (page 78), designing the right feeding solution (*i.e.* the right base to 1,3-PDO ratio, depending on the targeted pH value) will allow maintaining constant 1,3-PDO concentrations in the medium, while also controlling pH at its setpoint. Then, an adequate experimental design with several 1,3-PDO levels and with several initial glycerol concentrations will allow determining the impact of each phenomenon to the overall system. Regarding the pH effect, the results presented here suggested that it should be

included in order to achieve better growth predictions. This might be an indirect way of refining the 3-HP inhibitory effect: carboxylic acids are generally more toxic to cells than their carboxylate form [209]. Since the proportions of the carboxylic acid and carboxylate forms depends on the pH value, the pH effect on growth might in fact reflect this differential toxicity.

Finally, in a next step, two more phenomena have to be included in the model, before process scale-up through modelling can be considered. First, the bioconversion being a strictly aerobic process, O_2 transfer in the medium will have to be included in the model. Then, it should be considered distinguishing between the bacteria fraction that is still growing and oxidising 1,3-PDO from the fraction that has lost its ability to grow but is still oxidising 1,3-PDO.

Page left blank intentionally

CONCLUSION AND PERSPECTIVES

Achievement of efficient 3-HP production with acetic acid bacteria

3-hydroxypropionic acid (3-HP) production from 1,3-propanediol (1,3-PDO) by acetic acid bacteria was previously reported in four studies, all published between 2015 and 2018 (Table CP.I). Zhu *et al.* (2018) showed that the two enzymes involved in 1,3-PDO oxidation into 3-HP by *Gluconobacter oxydans* were successively an alcohol dehydrogenase and an aldehyde dehydrogenase [237]. This confirmed the hypothesis that was assumed in the other studies: namely, that the metabolic pathway for 3-HP production in acetic acid bacteria is similar to the one of acetic acid production from ethanol (*i.e.* vinegar production). In addition, acetic acid bacteria are known for their great resistance to acetic acid [173], and it could be reasonably considered that they would be resistant also to other short-chain organic acids, such as 3-HP. Thanks to these two key features (a short metabolic pathway and good product resistance) acetic acid bacteria are promising candidates for 3-HP production. Indeed, in the previous studies, it appeared that acetic bacteria could achieve high molar yields (between 0.90 and 1.00 mol mol^{-1}) and productivities (between 0.90 and 2.52 g L^{-1} h^{-1}). As a consequence of these different elements, high 3-HP titres were easily reached with wild-type strains: for example, the final titres were comparable with the ones obtained from glucose using engineered 3-HP producers, such as *Escherichia coli* or *Saccharomyces cerevisiae* (Chapter 1). These works on acetic acid bacteria were already quite promising and laid the basis for subsequent process development. The present thesis provides a new approach towards 3-HP production with acetic acid bacteria, which is complementary to those considered in the previous works on the topic.

The results presented in Chapter 3 showed that growth-associated 3-HP production was possible, and that using resting cells produced separately, as in the four previous studies, was not mandatory. However, low substrate (1,3-PDO) concentrations should be maintained in order to prevent both direct 1,3-PDO toxicity and detrimental accumulation of the metabolic intermediate, 3-hydroxypropanal (3-HPA). Therefore, a fed-batch process was designed in order to maintain low 1,3-PDO levels in the medium: the feeding strategy consisted in using a single solution for both pH control and 1,3-PDO feeding, while using the pH feedback for determining the feeding rate. As illustrated in Table CP.I, this is the first study on fed-batch production of 3-HP using acetic acid bacteria. When the strain was inoculated directly on 1,3-PDO, both growth and 3-HP production remained limited, so it was necessary to perform a primary growth phase. Glycerol was shown to be an adequate substrate for this primary

Table CP.I: Comparison of the different approaches towards 3-HP production from 1,3-PDO by acetic acid bacteria

Strain	V[a] (L)	T[b] (°C)	Cell Load $g_{CDW}\ L^{-1}$	pH	Aeration	Experimental setup	Titre ($g\ L^{-1}$)	Yield ($mol\ mol^{-1}$)	Productivity ($g\ L^{-1}\ h^{-1}$)	Ref.
Gluconobacter oxydans DSM 2003	4.0	28	10	7.0 → 5.5, then controlled at 5.5	constant stirring and air flow rates	Batch (bioreactor); Upstream integration	60.5	0.94	2.52	[234]
Gluconobacter oxydans DSM 50049	1.0	28	3.25	5.5	constant stirring and air flow rates	Batch (bioreactor)	11.84	*ca.* 1	2.4	[65]
						Batch (bioreactor); Upstream integration	23.6[c]	*ca.* 1	–	
Acetobacter sp. CGMCC 8142	0.01	30	5.0	6.0 (buffered)	constant shaking	Batch (flask); Cell immobilisation	66.95	0.934	0.90	[122]
Gluconobacter oxydans DSM 2003/*adhAB* [d] and DSM 2003/*aldh* [d]	0.03	30	5.0	6.0 (buffered)	constant shaking	Batch (flask); 1:2 mix of the strains	44.6	0.94	1.86	[237]
Acetobacter sp. CIP 58.66	1.0	30	0.88 → 2.08	5.0	pO_2 controlled at 40 %	Sequential[e] pH-based fed-batch (bioreactor)	69.76	1.02	2.79	Chp. 3
	1.2	30	1.01 → 2.75	6.9 → 3.9	pO_2 controlled at 40 %	Sequential process[e]; Repeated batch (bioreactor); Downstream integration	10.59	0.90	1.57	Chp. 4

[a] Medium volume
[b] Temperature
[c] The initial 3-HP concentration was already 11.8 $g\ L^{-1}$
[d] Engineered strains (all others are wild type)
[e] A primary growth (on glycerol) is performed before the bioconversion's initiation (no intermediate step between growth and bioconversion)

growth step: bacteria, that were thus produced, performed efficient bioconversions, without any observable latency. The best results were obtained with this sequential pH control-based fed-batch process, when pH was set to 5.0 and when the 1,3-PDO concentration was maintained around 5 g L^{-1}. The bioconversion performances that were achieved in Chapter 3 were slightly higher than the best ones published so far for 3-HP production with acetic acid bacteria (Table CP.I).

An important remark on these results is that they were obtained with relatively low biomass concentrations, as compared to the other studies, that rather resorted to high and constant densities of resting cells (Table CP.I). The present thesis is thus the first report showing that efficient 3-HP production by growing acetic acid bacteria is possible, provided that 1,3-PDO is supplied continuously. This highlights the relevance of estimating the specific productivity ($g_{\text{3-HP}}\ g_{\text{CDW}}^{-1}\ h^{-1}$) in order to compare the performances of the different processes, instead of relying only on the overall volumetric productivity (g L^{-1} h^{-1}). In future process development and optimisation, advantage should be taken of the bioconversion-associated growth, in order to avoid unnecessary costs due to high density biomass production and biomass concentration with centrifugation.

Furthermore, the present study is also the first one addressing the issue of 3-HPA accumulation, depending on the operational conditions. Surprisingly, this issue received only little attention in the previous studies, even though it was notably acknowledged by Dishisha *et al.* [65]. Zhu *et al.* showed that the two-step metabolic pathway is subjected to imbalances in the enzymatic activities: the aldehyde dehydrogenase was shown to be the rate limiting enzyme [237]. Consequently, depending on the culture conditions, 3-HPA might be accumulated either transiently or permanently. Not only might 3-HPA accumulation hinder the final 3-HP yield, but 3-HPA is also a known antimicrobial agent [13]. 3-HPA levels should therefore be carefully monitored during 3-HP production. Zhu *et al.* proposed a workaround in order to mitigate the enzymatic imbalance: they used two different engineered strains of *G. oxydans* that overexpressed the gene coding either for the alcohol dehydrogenase or for the aldehyde dehydrogenase. The optimal 3-HP production was achieved when both strains were mixed in a 1:2 ratio. This approach requires that two mutant strains are cultivated together in a precise ratio, so it might not be the most-suited approach for further process development. Instead, the present thesis showed that an appropriate process design (including a primary growth phase directly followed a fed-batch bioconversion) could prevent detrimental 3-HPA accumulation, even though 3-HPA was still transiently accumulated at sub-inhibitory levels. The kinetic model that was developed based on the results from these sequential fed-batch bioconversions (Chapter 5) could successfully describe the time evolutions of 1,3-PDO, 3-HPA and 3-HP. In particular, the initial transient 3-HPA accumulation was relatively well represented by the model. As a consequence, the model can already be considered as a valuable tool for further process development, since different 1,3-PDO feeding strategies might already be explored *in silico*, and compared based on the 3-HPA levels that are reached. However, in order for the model to give a realistic representation of the growth and bioconversion kinetics once a given 3-HPA level is reached, further study of the 3-HPA toxicity on acetic acid bacteria are still required.

Interestingly, results from Chapter 3 also suggested that the main reason for the bioconversions being less efficient at pH below 5.0 was not so much the impact of pH on the kinetics, but rather an imbalance between the base (NH_4OH) and 1,3-PDO in the solution used for both pH control and 1,3-PDO feeding. Indeed, for pH 4.5 and 4.0 the 1,3-PDO concentration was not kept around 5 g L^{-1}, as during the pH 5.0 bioconversions, instead it decreased relatively quickly. This was mainly attributed to the 1:1 molar ratio between 1,3-PDO and NH_4OH in the inlet solution: this ratio is not adequate for pH setpoints that are close to or under the pKa of 3-HP (4.51). At these pH, the relative proportion of the protonated form of 3-HP is comprised between 50 % (if pH $=$ pKa) and 100 % (if pH $\ll$ pKa), so less base addition is required in order to maintain such a setpoint. In case further optimisation of the pH-based feeding strategy is being considered, the next experiments should focus on defining the right 1,3-PDO-to-base ratio, according to the targeted pH value. Expectedly, the proportion of 1,3-PDO should be increased, relatively to NH_4OH, for lower pH setpoints.
The fact that the bioconversion performances at pH 4.5 and 4.0 were mainly impaired due to substrate limitation, rather than due to a pH inhibitory effect on bacteria, was also supported by the model developed in Chapter 5. Indeed, the model did not take any pH effect into account and it still represented the bioconversion kinetics (*i.e.* time evolutions of 1,3-PDO, 3-HPA and 3-HP) accurately for bioconversions at pH 5.0, 4.5 and 4.0, so this is consistent with the bioconversion remaining unaffected by low pH. Only the biomass evolution was less well predicted by the model, and it was considered that bacterial growth, however, was likely inhibited at low pH. In addition to opening interesting opportunities for model development, this also revealed a certain degree of decorrelation between growth and 1,3-PDO oxidation by acetic acid bacteria.

Achievement of downstream process integration and perspectives towards semi-continuous extractive bioconversions

When the bioconversion was not limited in 1,3-PDO (*i.e.* for pH $= 5.0$), results from the modelling approach revealed that 3-HP inhibition was most likely the main driver for the bioconversion stopping. Overall, it appeared that the designed process was subjected to product inhibition, while being only poorly affected by pH values under the product's pKa. Thus, in stream product recovery (ISPR) using reactive liquid-liquid extraction was considered as a promising strategy for improving the process. A first experimental demonstration thereof was provided in Chapter 4. As a first approach, the bioconversion was performed in a repeated batch mode, with two successive additions of substrate 1,3-PDO. Results suggested that the bioconversion performances were not significantly affected by the extraction system, nor positively nor negatively. Notably, the selected organic phase, used for extraction, had no significant toxic effect on the strain's activity, so this study is also an experimental validation of the biocompatibility of the organic phase with acetic acid bacteria.
Thanks to ISPR, 3-HP was completely removed from the bioconversion medium and was finally found only in the back-extraction phase. However, the 3-HP extraction rate remained much lower than its bioproduction rate, so full 3-HP removal was only achieved long after the bioconversion had ended. The most promising way of better balancing 3-HP produc-

tion and extraction rates is to increase the specific interfacial area between the bioconversion medium and the organic phase, either by decreasing the working volume in the bioreactor or by increasing the number of extraction modules. Better balancing production and extraction will prevent 3-HP accumulation in the bioconversion medium. Then, it will be possible to test whether ISPR can enhance the bioconversion, instead of remaining neutral to the bioconversion performances. To that end, it would be necessary to test it with a continuous 1,3-PDO supply, so that comparisons can be performed with non-extractive bioconversions. Beyond the sole purpose of comparison between extractive and non-extractive bioconversions, achieving an adequate balance between 3-HP production and extraction would also open the way towards a pH feedback-controlled extractive bioconversion. Since the pH of the bioconversion medium is the result of this balance, an automated control of the 1,3-PDO inlet flow rate could be based on the pH variations, similarly to the pH-based feeding strategy from Chapter 3.

Perspectives towards a better understanding of the growth of acetic acid bacteria

Results from Chapter 4 also gave further evidence that 1,3-PDO was involved in the growth of *Acetobacter* sp. CIP 58.66. Similarly to the sequential fed-batch from Chapter 3, the extractive bioconversions were initiated only after a primary growth on glycerol. Then, during the bioconversions, each time 1,3-PDO was added to the medium, a new exponential growth phase was observed and growth slowed down only when 1,3-PDO was fully depleted. Combined with the results of Chapter 3, this strongly suggested that 1,3-PDO might be used as growth substrate by the strain. Nevertheless, results from Chapter 5 suggested that, to some extent, bacterial growth was not completely correlated to 1,3-PDO oxidation; growth being inhibited at lower 3-HP concentrations than 1,3-PDO oxidation. Moreover, residual glycerol remaining from the primary growth step was still present in the medium during the bioconversions, in significant concentrations, and results showed that it was further consumed during secondary growth phases, but never fully depleted (Chapters 3 & 4). At this stage, the respective contributions of 1,3-PDO and glycerol to the growth of *Acetobacter* sp. CIP 58.66 still remain unclear and further experiments are required in order to gain more insight on this question, through enzymatic activity assessment or metabolomic analysis for example. An alternative *in silico* method was however envisaged here: a collaboration was initiated with the Hydrosystems and Bioprocesses Research Unit (UR PROSE, Irstea, Antony, France) in order to apply the "Microbial Transition State" (MTS) theory of growth to the specific system studied in the current thesis.

The MTS theory is a fundamental kinetic theory of bacterial growth that was derived from generic physical principles [61], and that was notably investigated for the modelling of microbial ecosystems [58]. In the MTS theory, statistical physics principles are used in order to derive the bacterial population's growth rate from the probability for a single cell to divide, given the resources that are available (electron donors, electron acceptors, and nutrients). When used to simulate a pure culture growing in a minimal medium, the MTS theory coupled with mass and energy balances could take simultaneously into account all substrates (glucose, dioxygen, and ammonium). Notably, the rule of Liebig – stating that growth is

limited by the scarcest substrate – was found as an emerging property of the MTS theory. The MTS theory is therefore a promising approach to grasp the respective contributions of glycerol, 1,3-PDO and O_2 to the growth kinetics of acetic acid bacteria. Combining this approach with empirical models for inhibition phenomena (such as 3-HP inhibition as presented in Chapter 5) would be a first step towards the establishment of a theoretical basis for modelling 3-HP production by acetic acid bacteria, instead of relying only on less fundamental equations, such as the Monod equation.
As a first approach, the MTS theory is currently being used to describe the growth kinetics of *Acetobacter* sp. CIP 58.66 in a glycerol-containing complex medium, in the absence of 1,3-PDO. To that end, data from the primary growth on glycerol (prior to the bioconversions) are being used for model fitting. Future works should then focus on applying the MTS theory to the strain's growth on 1,3-PDO in the absence of glycerol. Then, the MTS model might be used to study the simultaneous consumption of glycerol and 1,3-PDO, in order to investigate whether the strain favours the consumption of one or the other substrate for optimising its growth rate.

Acetic acid bacteria: versatile whole cell catalysts for integrated approaches

The downstream integration of the process, as presented in Chapter 4, may also be considered as complementary to the upstream integration that was already investigated in previous studies (Table CP.I). *Gluconobacter oxydans* was used in two different studies in order to convert the 1,3-PDO that was first produced by *Klebsiella pneumoniae* [234] or by *Lactobacillus reuteri* [65]. An important difference between the two studies was that, in the case of *K. pneumoniae*, 1,3-PDO was the main product (by-product formation remained limited in comparison to 1,3-PDO: yield = 0.55 $mol_{1,3\text{-PDO}}$ $mol^{-1}_{glycerol}$); however, in the case of *L. reuteri*, 1,3-PDO was produced along with 3-HP in a quasi-equimolar ratio. The extractive bioconversion presented in Chapter 4 may now be considered for adaptation with similar upstream processes, using 1,3-PDO microbially produced in a first step. In that case, it should be noted that 1,3-PDO will likely be far more diluted in the inlet solution, in comparison to the inlet solutions used in the present thesis: here, the feeding solution for the pH-based fed-batch contained 1,3-PDO at 6 mol L^{-1} (approx. 460 g L^{-1}), and for the extractive bioconversions, 6 mL of 1,3-PDO at a 98 % purity were directly added to the medium; on the contrary, in the studies of Zhao *et al.* and Dishisha *et al.*, the 1,3-PDO production steps ended with respective 1,3-PDO concentrations of 54 and 14 g L^{-1} [234, 65]. More generally, when 1,3-PDO is microbially produced, typical final titres range from approximately 40 to 80 g L^{-1} [187]. As a consequence, it can be expected that final 3-HP titres would be lower than those obtained with highly concentrated feeding solutions. Yet, with an adequate back-extraction strategy, the ISPR system is also an opportunity for primary 3-HP concentration, thus compensating for the more dilute 1,3-PDO inlet. Therefore, diluted feeding 1,3-PDO solutions may not be considered as a major drawback, from the overall integrated process point of view.
An important challenge in using a real fermentation broth as 1,3-PDO feed also lies in the diversity of by-products that might be present too. Indeed, if the inlet contains other organic acids, such as acetic or lactic acids, it is likely that they will be extracted along with 3-HP, thus hindering the overall process selectivity, not to mention the potential inhibitory effects

on the bacterial activity. Similarly, if the broth contains other alcohols than 1,3-PDO, such as ethanol, it can be expected that the acetic acid bacteria will also convert them into their corresponding acids.

Getting added-value while producing 3-HP from 1,3-PDO might be questionable, since 1,3-PDO is also a promising platform chemical. However, considering a global integrated approach, 3-HP production from 1,3-PDO might be advantageous. In particular, 1,3-PDO is one of the main by-products of 3-HP production from glycerol, using engineered *Klebsiella pneumoniae* or *Lactobacillus reuteri*. For instance, the highest 3-HP titres achieved so far were 102.6 and 83.8 g L^{-1} (with *K. pneumoniae*), and they were associated with final 1,3-PDO titres comprised between approximately 15 and 20 g L^{-1} [127, 235]. These concentrations are quite significant, and it might be more cost-effective to convert this 1,3-PDO into 3-HP, in order to avoid the necessity for two separate downstream processes: one for 3-HP and one for 1,3-PDO. Instead, the whole added-value of the process might be recovered only in the form of 3-HP. Technico-economic evaluation of such a process is however still required in order to assess its practical feasibility.

Lastly, an interesting feature of acetic acid bacteria is that they are able to oxidise a large range of alcohols into their corresponding carboxylic acids or ketones. This means that, beyond the only purpose of 3-HP production, the present thesis might also be considered as a case study for the integrated production and primary recovery of carboxylic acids from alcohols, using acetic acid bacteria. For example, several valuable organic acids were already produced with acetic acid bacteria, such as 3-hydroxypivalic acid [74], (R)-3-hydroxy-2-methyl propionic acid [150], (S)-2-methylbutanoic acid, (R)-2-hydroxypropionic acid ((R)-lactic acid) and 5-keto-D-gluconic acid [102, 180]. Even though each application is likely to be subjected to specific limitation or inhibition phenomena, valuable experience might be drawn from the present thesis.
One of the important challenges in the development of biorefineries is the capacity of dealing with a broad range of raw materials. In this context, versatile processes, that can be operated similarly for numerous substrate/product pairs, might appear as highly relevant, especially if they also offer a great potential for upstream and downstream integration.

Page left blank intentionally

References

[1] T. W. Abraham, E. Allen, E. C. Bohnert, C. L. Frank, J. J. Hahn, and P. Tsobanakis. "Recovery of 3-hydroxypropionic acid". WO2014144367. 2014.

[2] O. Adachi, E. Miyagawa, E. Shinagawa, K. Matsushita, and M. Ameyama. "Purification and properties of particulate alcohol dehydrogenase from *Acetobacter aceti*". In: *Agricultural and Biological Chemistry* 42.12 (1978), pp. 2331–2340.

[3] O. Adachi, K. Tayama, E. Shinagawa, K. Matsushita, and M. Ameyama. "Purification and characterization of membrane-bound aldehyde dehydrogenase from *Gluconobacter suboxydans*". In: *Agricultural and Biological Chemistry* 44.3 (1980), pp. 503–515.

[4] O. Adachi, K. Tayama, E. Shinagawa, K. Matsushita, and M. Ameyama. "Purification and characterization of particulate alcohol dehydrogenase from *Gluconobacter suboxydans*". In: *Agricultural and Biological Chemistry* 42.11 (1978), pp. 2045–2056.

[5] B. L. Adams. "The Next Generation of Synthetic Biology Chassis: Moving Synthetic Biology from the Laboratory to the Field". In: *ACS Synthetic Biology* 5.12 (2016), pp. 1328–1330.

[6] F. Adom, J. B. Dunn, J. Han, and N. Sather. "Life-Cycle Fossil Energy Consumption and Greenhouse Gas Emissions of Bioderived Chemicals and Their Conventional Counterparts". In: *Environmental Science & Technology* 48.24 (2014), pp. 14624–14631.

[7] M. Ameyama, K. Osada, E. Shinagawa, K. Matsushita, and O. Adachi. "Purification and characterization of aldehyde dehydrogenase of *Acetobacter aceti*". In: *Agricultural and Biological Chemistry* 45.8 (1981), pp. 1889–1890.

[8] H. M. Amin, A. M. Hashem, M. S. Ashour, and R. Hatti-Kaul. "1,2-Propanediol utilization by *Lactobacillus reuteri* DSM 20016, role in bioconversion of glycerol to 1,3-propanediol, 3-hydroxypropionaldehyde and 3-hydroxypropionic acid". In: *Journal of Genetic Engineering and Biotechnology* 11.1 (2013), pp. 53–59.

[9] P. Anastas and N. Eghbali. "Green Chemistry: Principles and Practice". In: *Chem. Soc. Rev.* 39.1 (2010), pp. 301–312.

[10] G. Andersen, O. Björnberg, S. Polakova, Y. Pynyaha, A. Rasmussen, K. Møller, A. Hofer, T. Moritz, M. P. B. Sandrini, A.-M. M. Merico, C. Compagno, H. E. Åkerlund, Z. Gojković, and J. Piškur. "A second pathway to degrade pyrimidine nucleic acid precursors in eukaryotes". In: *Journal of Molecular Biology* 380.4 (2008), pp. 656–666.

[11] B. Andreeßen, N. Taylor, A. Steinbüchel, B. Andreessen, N. Taylor, and A. Steinbuechel. "Poly(3-hydroxypropionate): A promising alternative to fossil fuel-based materials". In: *Applied and Environmental Microbiology* 80.21 (2014), pp. 6574–6582.

[12] J. H. Ansede, P. J. Pellechia, and D. C. Yoch. "Metabolism of acrylate to beta-hydroxypropionate and its role in dimethylsulfoniopropionate lyase induction by a salt marsh sediment bacterium, *Alcaligenes faecalis* M3A." In: *Applied and Environmental Microbiology* 65.11 (1999), pp. 5075–5081.

[13] F. Barbirato, J. P. Grivet, P. Soucaille, and A. Bories. “3-Hydroxypropionaldehyde, an Inhibitory Metabolite of Glycerol Fermentation to 1,3-Propanediol by Enterobacterial Species”. In: *Applied and Enviromental Microbiology* 62.4 (1996), pp. 3–7.

[14] M. Barnhart, A. Negrete-Raymond, J. Frias, G. Barbier, and M. Catlett. “3-Hydroxypropionic Acid Production by Recombinant Yeasts Expressing an Insect Aspartate 1-Decarboxylase”. WO2015017721. 2015.

[15] M. Basan, S. Hui, H. Okano, Z. Zhang, Y. Shen, J. R. Williamson, and T. Hwa. “Overflow metabolism in *Escherichia coli* results from efficient proteome allocation”. In: *Nature* 528.7580 (2015), pp. 99–104.

[16] J. Becker and C. Wittmann. “Bio-based production of chemicals, materials and fuels – *Corynebacterium glutamicum* as versatile cell factory”. In: *Current Opinion in Biotechnology* 23.4 (2012), pp. 631–640.

[17] I. A. Berg, D. Kockelkorn, W. Buckel, and G. Fuchs. “A 3-hydroxypropionate/4-hydroxybutyrate autotrophic carbon dioxide assimilation pathway in Archaea”. In: *Science* 318.5857 (2007), pp. 1782–1786.

[18] BIC. *The Bio-based Industries Vision - Accelerating innovation and market uptake of bio-based products*. Tech. rep. Bio-based Industries Consortium, 2012.

[19] H. Biebl, K. Menzel, A.-P. Zeng, and W.-D. Deckwer. “Microbial production of 1,3-propanediol”. In: *Applied Microbiology and Biotechnology* 52.3 (1999), pp. 289–297.

[20] M. Bindel. “3-Hydroxypropionic Acid Production by Recombinant Yeasts”. WO2014085330. 2014.

[21] T. Blaschke, O. Lang, S. Koch, and M. Hartmann. “Method for the Dehydration of 3-Hydroxypropanoic Acid to Form Acrylic Acid”. WO2016162175 A1. 2016.

[22] M. Boonmee, O. Cotano, S. Amnuaypanich, and N. Grisadanurak. “Improved Lactic Acid Production by In Situ Removal of Lactic Acid During Fermentation and a Proposed Scheme for Its Recovery”. In: *Arabian Journal for Science and Engineering* 41.6 (2016), pp. 2067–2075.

[23] J. D. Borkowski and M. J. Johnson. “Experimental Evaluation of Liquid Film Resistance in Oxygen Transport to Microbial Cells”. In: *Applied Microbiology* 15.6 (1967), pp. 1483–1488.

[24] I. Borodina, K. R. Kildegaard, N. B. Jensen, T. H. Blicher, J. Maury, S. Sherstyk, K. Schneider, P. Lamosa, M. J. Herrgård, I. Rosenstand, F. Öberg, J. Forster, and J. Nielsen. “Establishing a synthetic pathway for high-level production of 3-hydroxypropionic acid in *Saccharomyces cerevisiae* via beta-alanine”. In: *Metabolic Engineering* 27 (2015), pp. 57–64.

[25] J. J. Bozell and G. R. Petersen. “Technology development for the production of biobased products from biorefinery carbohydrates—the US Department of Energy’s “Top 10” revisited”. In: *Green Chemistry* 12.4 (2010), pp. 539–554.

[26] M. G. Bramucci, R. Dicosimo, R. D. Fallon, J. E. Gavagan, F. Herkes, and L. Wilczek. “3-hydroxycarboxylic acid production and use in branched polymers”. WO 2002012530. 2002.

[27] F. Branco dos Santos, W. Du, and K. J. Hellingwerf. “*Synechocystis*: Not Just a Plug-Bug for CO2, but a Green *E. coli*”. In: *Frontiers in Bioengineering and Biotechnology* 2 (2014), p. 36.

[28] J. Brass, F. Hoeks, and M. Rohner. “Application of modelling techniques for the improvement of industrial bioprocesses”. In: *Journal of Biotechnology* 59.1-2 (1997), pp. 63–72.

[29] K. Buchholz and J. Collins. “The roots—a short history of industrial microbiology and biotechnology”. In: *Applied and Environmental Microbiology* 97 (2013), pp. 3747–3762.

[30] G. Burgé, A. L. Flourat, B. Pollet, H. E. Spinnler, and F. Allais. “3-Hydroxypropionaldehyde (3-HPA) quantification by HPLC using a synthetic acrolein-free 3-hydroxypropionaldehyde system as analytical standard”. In: *RSC Advances* 5.112 (2015), pp. 92619–92627.

[31] G. Burgé, C. Saulou-Bérion, M. Moussa, B. Pollet, A. Flourat, F. Allais, V. Athès, and H. E. Spinnler. “Diversity of *Lactobacillus reuteri* Strains in Converting Glycerol into 3-Hydroxypropionic Acid”. In: *Applied Biochemistry and Biotechnology* 177.4 (2015), pp. 923–939.

[32] G. Burgé, F. Chemarin, M. Moussa, C. Saulou-Bérion, F. Allais, H.-E. Spinnler, and V. Athes. “Reactive extraction of bio-based 3-hydroxypropionic acid assisted by hollow-fiber membrane contactor using TOA and Aliquat 336 in *n*-decanol”. In: *Journal of Chemical Technology and Biotechnology* 91.10 (2016), pp. 2705–2712.

[33] G. Burgé, M. Moussa, C. Saulou-Bérion, F. Chemarin, M. Kniest, F. Allais, H.-E. Spinnler, and V. Athès. “Towards an extractive bioconversion of 3-hydroxypropionic acid: study of inhibition phenomena”. In: *Journal of Chemical Technology & Biotechnology* 92.9 (2017), pp. 2425–2432.

[34] I. A. Casas and W. J. Dobrogosz. “Validation of the Probiotic Concept: *Lactobacillus reuteri* Confers Broad-spectrum Protection against Disease in Humans and Animals”. In: *Microbial Ecology in Health and Disease* 12.4 (2000), pp. 247–285.

[35] F. Chemarin, M. Moussa, F. Allais, V. Athès, and I. Trelea. “Mechanistic modeling and equilibrium prediction of the reactive extraction of organic acids with amines: A comparative study of two complexation-solvation models using 3-hydroxypropionic acid”. In: *Separation and Purification Technology* 189 (2017), pp. 475–487.

[36] F. Chemarin, M. Moussa, M. Chadni, B. Pollet, P. Lieben, F. Allais, I. Trelea, and V. Athès. “New insights in reactive extraction mechanisms of organic acids: An experimental approach for 3-hydroxypropionic acid extraction with tri-*n*-octylamine”. In: *Separation and Purification Technology* 179 (2017), pp. 523–532.

[37] F. Chemarin. “Compréhension et maîtrise des mécanismes de l’extraction réactive de l’acide 3-hydroxypropionique au regard d’un procédé intégré couplant bioconversion et exctraction”. PhD thesis. Université Paris-Saclay, 2017.

[38] F. Chemarin, V. Athès, M. Bedu, T. Loty, F. Allais, I. C. Trelea, and M. Moussa. “Towards an *in situ* product recovery of bio-based 3-hydroxypropionic acid: influence of bioconversion broth components on membrane-assisted reactive extraction”. In: *Journal of Chemical Technology & Biotechnology* 94.3 (2019), pp. 964–972.

[39] F. Chemarin, M. Moussa, F. Allais, I. Trelea, and V. Athès. “Recovery of 3-hydroxypropionic acid from organic phases after reactive extraction with amines in an alcohol-type solvent”. In: *Separation and Purification Technology* 219 (2019), pp. 260–267.

[40] S. Chen, A. E. Rotaru, F. Liu, J. Philips, T. L. Woodard, K. P. Nevin, and D. R. Lovley. “Carbon cloth stimulates direct interspecies electron transfer in syntrophic co-cultures”. In: *Bioresource Technology* 173 (2014), pp. 82–86.

[41] X. Chen, X. Yang, Y. Shen, J. Hou, and X. Bao. “Increasing Malonyl-CoA Derived Product through Controlling the Transcription Regulators of Phospholipid Synthesis in *Saccharomyces cerevisiae*”. In: *ACS Synthetic Biology* 6.5 (2017), pp. 905–912.

[42] Y. Chen and J. Nielsen. “Biobased organic acids production by metabolically engineered microorganisms”. In: *Current Opinion in Biotechnology* 37 (2016), pp. 165–172.

[43] Z. Chen, J. Huang, Y. Wu, W. Wu, Y. Zhang, and D. Liu. “Metabolic engineering of *Corynebacterium glutamicum* for the production of 3-hydroxypropionic acid from glucose and xylose”. In: *Metabolic Engineering* 39 (2017), pp. 151–158.

[44] Z. Chen and D. Liu. “Toward glycerol biorefinery: metabolic engineering for the production of biofuels and chemicals from glycerol”. In: *Biotechnology for Biofuels* 9.205 (2016), pp. 1–15.

[45] K.-K. Cheng, H.-J. Liu, and D.-H. Liu. “Multiple growth inhibition of *Klebsiella pneumoniae* in 1,3-propanediol fermentation”. In: *Biotechnology Letters* 27.1 (2005), pp. 19–22.

[46] F. Cherubini. “The biorefinery concept: Using biomass instead of oil for producing energy and chemicals”. In: *Energy Conversion and Management* 51.7 (2010), pp. 1412–1421.

[47] S. Choi, C. W. Song, J. H. Shin, and S. Y. Lee. “Biorefineries for the production of top building block chemicals and their derivatives”. In: *Metabolic Engineering* 28 (2015), pp. 223–239.

[48] H. S. Chu, Y. S. Kim, C. M. Lee, J. H. Lee, W. S. Jung, J.-H. Ahn, S. H. Song, I. S. Choi, and K. M. Cho. “Metabolic engineering of 3-hydroxypropionic acid biosynthesis in *Escherichia coli*”. In: *Biotechnology and Bioengineering* 112.2 (2015), pp. 356–364.

[49] V. Cleusix, C. Lacroix, S. Vollenweider, M. Duboux, and G. Le Blay. “Inhibitory activity spectrum of reuterin produced by *Lactobacillus reuteri* against intestinal bacteria”. In: *BMC Microbiology* 7.101 (2007).

[50] J. M. Clomburg and R. Gonzalez. “Anaerobic fermentation of glycerol: a platform for renewable fuels and chemicals”. In: *Trends in Biotechnology* 31.1 (2013), pp. 20–28.

[51] I. Coelhoso, P. Silvestre, R. Viegas, J. Crespo, and M. Carrondo. “Membrane-based solvent extraction and stripping of lactate in hollow-fibre contactors”. In: *Journal of Membrane Science* 134.1 (1997), pp. 19–32.

[52] J. Couvreur, A. Teixeira, F. Allais, H.-E. Spinnler, C. Saulou-Bérion, and T. Clément. “Wheat and sugar beet Coproducts for the bioproduction of 3-hydroxypropionic acid by *Lactobacillus reuteri* DSM17938”. In: *Fermentation* 3.3 (2017), p. 32.

[53] D. Datta, S. Kumar, and H. Uslu. “Status of the Reactive Extraction as a Method of Separation”. In: *Journal of Chemistry* 2015 (2015), pp. 1–16.

[54] H. Dave, C. Ramakrishna, and J. D. Desai. “Degradation of acrylic acid by fungi from petrochemical activated sludge”. In: *Biotechnology Letters* 18.8 (1996), pp. 963–964.

[55] F. David, J. Nielsen, and V. Siewers. “Flux Control at the Malonyl-CoA Node through Hierarchical Dynamic Pathway Regulation in *Saccharomyces cerevisiae*”. In: *ACS Synthetic Biology* 5.3 (2016), pp. 224–233.

[56] Y. David, Y. Hoon Oh, M. G. Babylon, K.-A. Baritugo, J. C. Joo, C. G. Chae, Y. J. Kim, and S. J. Park. “14. Microbial Production of 3-Hydroxypropionic acid”. In: *Industrial Biotechnology: Products and Processes*. Ed. by L. C. Wittmann and J. C. Liao. Wiley-VCH. Weinheim, Germany, 2017, pp. 411–451.

[57] F. de Fouchécour, A. K. Sanchez-Castañeda, C. Saulou-Bérion, and H. E. Spinnler. “Process engineering for microbial production of 3-hydroxypropionic acid”. In: *Biotechnology advances* 36.4 (2018), pp. 1207–1222.

[58] H. Delattre, E. Desmond-Le Quéméner, C. Duquennoi, A. Filali, and T. Bouchez. "Consistent microbial dynamics and functional community patterns derived from first principles". In: *The ISME Journal* 13.2 (2019), pp. 263–276.

[59] C. Della Pina, E. Falletta, and M. Rossi. "A green approach to chemical building blocks. The case of 3-hydroxypropanoic acid". In: *Green Chemistry* 13.7 (2011), pp. 1624–1632.

[60] U. Deppenmeier and A. Ehrenreich. "Physiology of acetic acid bacteria in light of the genome sequence of *Gluconobacter oxydans*." In: *Journal of molecular microbiology and biotechnology* 16.1-2 (2009), pp. 69–80.

[61] E. Desmond-Le Quéméner and T. Bouchez. "A thermodynamic theory of microbial growth". In: *The ISME Journal* 8.8 (2014), pp. 1747–1751.

[62] M. Dieterle and E. Schwab. "Raw Material Change in the Chemical Industry". In: *Topics in Catalysis* 59.8-9 (2016), pp. 817–822.

[63] T. Dishisha. "Microbial Production of Bio-Based Chemicals: A Biorefinery Perspective". PhD thesis. Lund University, 2013, p. 154.

[64] T. Dishisha, L. P. Pereyra, S.-H. Pyo, R. A. Britton, and R. Hatti-Kaul. "Flux analysis of the *Lactobacillus reuteri* propanediol-utilization pathway for production of 3-hydroxypropionaldehyde, 3-hydroxypropionic acid and 1,3-propanediol from glycerol". In: *Microb Cell Fact* 13.1 (2014), p. 76.

[65] T. Dishisha, S.-H. Pyo, and R. Hatti-Kaul. "Bio-based 3-hydroxypropionic- and acrylic acid production from biodiesel glycerol via integrated microbial and chemical catalysis". In: *Microbial Cell Factories* 14.200 (2015).

[66] E. Drioli, A. Criscuoli, and E. Curcio. *Membrane contactors : fundamentals, applications and potentialities*. Elsevier, 2006, p. 502. ISBN: 9780080457017.

[67] EEA. *Annual European Union greenhouse gas inventory 1990–2017 and inventory report 2019 (Report EEA/PUBL/2019/051)*. Tech. rep. Copenhaguen: European Environment Agency, 2019, pp. 455–480.

[68] C. Engels, C. Schwab, J. Zhang, M. J. A. Stevens, C. Bieri, M.-O. Ebert, K. McNeill, S. J. Sturla, and C. Lacroix. "Acrolein contributes strongly to antimicrobial and heterocyclic amine transformation activities of reuterin". In: *Scientific Reports* 6.1 (2016), p. 36246.

[69] European Commission. *Communication from the Commission of the European Parliament, the Council, the European Economic and Social Committee and the Committe of the Regions for a European Industrial Renaissance*. Tech. rep. Bruxelles, 2014, pp. 1–23.

[70] European Commission. *From the Sugar Platform to biofuels and biochemicals (Final report for the European Commission Directorate-General Energy)*. Tech. rep. 2015, pp. 1–183.

[71] I. Finnegan. "Method for producing 3-hydroxypropanamide employing *Acetobacter lovaniensis*". WO2017130007A1. 2017.

[72] J. Frébortová, K. Matsushita, and O. Adachi. "Effect of growth substrates on formation of alcohol dehydrogenase in *Acetobacter methanolicus* and *Acetobacter aceti*". In: *Journal of Fermentation and Bioengineering* 83.1 (1997), pp. 21–25.

[73] G. Fuchs. "Alternative Pathways of Carbon Dioxide Fixation: Insights into the Early Evolution of Life?" In: *Annual Review of Microbiology* 65.1 (2011), pp. 631–658.

[74] B. Füchtenbusch, M. Wältermann, and A. Steinbüchel. "Biotransformation of 2,2-Dimethyl-1,3-Propanediol to 3-Hydroxypivalic Acid by *Acetobacter acetii* DSMZ3508 and Related Bacteria". In: *Biotechnology Letters* 20.5 (1998), pp. 507–510.

[75] A. Gabelman and S.-T. Hwang. “Hollow fiber membrane contactors”. In: *Journal of Membrane Science* 159.1-2 (1999), pp. 61–106.

[76] M.-T. Gao, T. Shimamura, N. Ishida, E. Nagamori, H. Takahashi, S. Umemoto, T. Omasa, and H. Ohtake. “Extractive lactic acid fermentation with tri-*n*-decylamine as the extractant”. In: *Enzyme and Microbial Technology* 44.5 (2009), pp. 350–354.

[77] F. Garcia-Ochoa and E. Gomez. “Bioreactor scale-up and oxygen transfer rate in microbial processes: An overview”. In: *Biotechnology Advances* 27 (2009), pp. 153–176.

[78] M. Gavrilescu and Y. Chisti. “Biotechnology - A sustainable alternative for chemical industry”. In: *Biotechnology Advances* 23.7-8 (2005), pp. 471–499.

[79] K. V. Gernaey, A. E. Lantz, P. Tufvesson, J. M. Woodley, and G. Sin. “Application of mechanistic models to fermentation and biocatalysis for next-generation processes”. In: *Trends in Biotechnology* 28.7 (2010), pp. 346–354.

[80] R. R. Gokarn, O. V. Selifonova, H. Jessen, S. J. Gort, T. Selmer, and W. Buckel. “3-hydroxypropionic acid and other organic compounds”. WO 02/42418 A2. 2002.

[81] J. Gonzalez-Saiz, C. Pizarro, and D. Garrido-Vidal. “Evaluation of Kinetic Models for Industrial Acetic Fermentation: Proposal of a New Model Optimized by Genetic Algorithms”. In: *Biotechnology Progress* 19.2 (2003), pp. 599–611.

[82] E. C. Hann, A. E. Sigmund, S. K. Fager, F. B. Cooling, J. E. Gavagan, A. Ben-Bassat, S. Chauhan, M. S. Payne, S. M. Hennessey, and R. DiCosimo. “Biocatalytic Hydrolysis of 3-Hydroxyalkanenitriles to 3-Hydroxyalkanoic Acids”. In: *Advanced Synthesis & Catalysis* 345.67 (2003), pp. 775–782.

[83] A. C. Hindmarsh. “ODEPACK, a systematized collection of ODE solvers”. In: *IMACS Transactions on Scientific Computation* 1 (1983), pp. 55–64.

[84] A. Hitschmann and H. Stockinger. “Oxygen deficiency and its effect on the adenylate system in *Acetobacter* in the submerse acetic fermentation”. In: *Applied Microbiology and Biotechnology* 22 (1985), pp. 46–49.

[85] H. Holo. “*Chloroflexus aurantiacus* secretes 3-hydroxypropionate, a possible intermediate in the assimilation of CO2 and acetate”. In: *Archives of Microbiology* 151.3 (1989), pp. 252–256.

[86] C. Hoppe, S. M. Hoyt, R. Tengler, D. DeCoster, B. Harkrader, P. H. Au-Yeung, S. Biswas, P. Vargas, R. P. Roach, and T. C. Frank. “3-hydroxypropionic acid compositions”. US9512057 B2. 2016.

[87] Y. Huang, Z. Li, K. Shimizu, and Q. Ye. “Co-production of 3-hydroxypropionic acid and 1,3-propanediol by *Klebsiella pneumoniae* expressing aldH under microaerobic conditions”. In: *Bioresource Technology* 128 (2013), pp. 505–512.

[88] Y. Huang, Z. Li, and Q. Ye. “Transcriptional regulation of genes involved in 3-hydroxypropionic acid production in response to aeration of recombinant *Klebsiella pneumoniae*”. In: *Applied Biochemistry and Biotechnology* 178.6 (2016), pp. 1129–1140.

[89] International Energy Agency. *The future of petrochemicals: Towards more sustainable plastics and fertilisers*. Tech. rep. 2018, pp. 1–130.

[90] M. D. Jankowski, C. S. Henry, L. J. Broadbelt, and V. Hatzimanikatis. “Group contribution method for thermodynamic analysis of complex metabolic networks.” In: *Biophysical Journal* 95.3 (2008), pp. 1487–1499.

[91] H. Jessen, R. Brian, J. Huryta, B. Mastel, A. Berry, D. Yaver, M. Catlett, and M. Barnhart. “Compositions and methods for 3-hydroxypropionic acid production”. WO2012074818 A2. 2012.

[92] M. M. Jessop-Fabre, T. Jakociunas, V. Stovicek, Z. Dai, M. K. Jensen, J. D. Keasling, and I. Borodina. "EasyClone-MarkerFree: A vector toolkit for marker-less integration of genes into *Saccharomyces cerevisiae* via CRISPR-Cas9". In: *Biotechnology Journal* 11.8 (2016), pp. 1110–1117.

[93] M. Jiang, J. Ma, M. Wu, R. Liu, L. Liang, F. Xin, W. Zhang, H. Jia, and W. Dong. "Progress of succinic acid production from renewable resources: Metabolic and fermentative strategies". In: *Bioresource Technology* 245 (2017), pp. 1710–1717.

[94] X. Jiang, X. Meng, and M. Xian. "Biosynthetic pathways for 3-hydroxypropionic acid production". In: *Applied Microbiology and Biotechnology* 82.6 (2009), pp. 995–1003.

[95] J. E. Jiménez-Hornero, I. M. Santos-Dueñas, and I. García-García. "Optimization of biotechnological processes. The acetic acid fermentation. Part I: The proposed model". In: *Biochemical Engineering Journal* 45.1 (2009), pp. 1–6.

[96] J. E. Jiménez-Hornero, I. M. Santos-Dueñas, and I. García-García. "Optimization of biotechnological processes. The acetic acid fermentation. Part II: Practical identifiability analysis and parameter estimation". In: *Biochemical Engineering Journal* 45.1 (2009), pp. 7–21.

[97] Z. Jin and S.-T. Yang. "Extractive Fermentation for Enhanced Propionic Acid Production from Lactose by *Propionibacterium acidipropionici*". In: *Biotechnology Progress* 14.3 (1998), pp. 457–465.

[98] W. S. Jung, J. H. Kang, H. S. Chu, I. S. Choi, and K. M. Cho. "Elevated production of 3-hydroxypropionic acid by metabolic engineering of the glycerol metabolism in *Escherichia coli*". In: *Metabolic Engineering* 23 (2014), pp. 116–122.

[99] I.-Y. Jung, J.-W. Lee, W.-K. Min, Y.-C. Park, and J.-H. Seo. "Simultaneous conversion of glucose and xylose to 3-hydroxypropionic acid in engineered *Escherichia coli* by modulation of sugar transport and glycerol synthesis". In: *Bioresource Technology* 198 (2015), pp. 709–716.

[100] A. Kalantari, T. Chen, B. Ji, I. A. Stancik, V. Ravikumar, D. Franjevic, C. Saulou-Bérion, A. Goelzer, and I. Mijakovic. "Conversion of Glycerol to 3-Hydroxypropanoic Acid by Genetically Engineered *Bacillus subtilis*". In: *Frontiers in Microbiology* 8 (2017), p. 638.

[101] O. Kandler, K.-O. Stetter, and R. Köhl. "*Lactobacillus reuteri* sp. nov., a New Species of Heterofermentative *Lactobacilli*". In: *Zentralblatt für Bakteriologie: I. Abt. Originale C: Allgemeine, angewandte und ökologische Mikrobiologie* 1.3 (1980), pp. 264–269.

[102] G. Keliang and W. Dongzhi. "Asymmetric oxidation by *Gluconobacter oxydans*". In: *Applied Microbiology and Biotechnology* 70.2 (2006), pp. 135–139.

[103] M. W. Keller, G. J. Schut, G. L. Lipscomb, A. L. Menon, I. J. Iwuchukwu, T. T. Leuko, M. P. Thorgersen, W. J. Nixon, A. S. Hawkins, R. M. Kelly, and M. W. W. Adams. "Exploiting microbial hyperthermophilicity to produce an industrial chemical, using hydrogen and carbon dioxide". In: *Proceedings of the National Academy of Sciences of the United States of America* 110.15 (2013), pp. 5840–5845.

[104] A. Keshav and K. L. Wasewar. "Back extraction of propionic acid from loaded organic phase". In: *Chemical Engineering Science* 65.9 (2010), pp. 2751–2757.

[105] K. R. Kildegaard, Z. Wang, Y. Chen, J. Nielsen, and I. Borodina. "Production of 3-hydroxypropionic acid from glucose and xylose by metabolically engineered *Saccharomyces cerevisiae*". In: *Metabolic Engineering Communications* 2 (2015), pp. 132–136.

[106] K. R. Kildegaard, N. B. Jensen, K. Schneider, E. Czarnotta, E. Oezdemir, T. Klein, J. Maury, B. E. Ebert, H. B. Christensen, Y. Chen, I.-K. Kim, M. J. Herrgard, L. M. Blank, J. Forster, J. Nielsen, and I. Borodina. "Engineering and systems-level analysis of *Saccharomyces cerevisiae* for production of 3-hydroxypropionic acid via malonyl-CoA reductase-dependent pathway". In: *Microbial Cell Factories* 15.5 (2016), pp. 609–620.

[107] C. Kim, M. Y. Kim, M. Iain, B.-H. Jeon, G. C. Premier, S. Park, and J. R. Kim. "Anodic electro-fermentation of 3-hydroxypropionic acid from glycerol by recombinant *Klebsiella pneumoniae* L17 in a bioelectrochemical system". In: *Biotechnology for Biofuels* 10.199 (2017).

[108] K. Kim, S.-K. Kim, Y.-C. Park, and J.-H. Seo. "Enhanced production of 3-hydroxypropionic acid from glycerol by modulation of glycerol metabolism in recombinant *Escherichia coli*". In: *Bioresource Technology* 156.1 (2014), pp. 170–175.

[109] Y. Ko, E. Seol, B. Sundara Sekar, S. Kwon, J. Lee, and S. Park. "Metabolic engineering of *Klebsiella pneumoniae* J2B for co-production of 3-hydroxypropionic acid and 1,3-propanediol from glycerol: Reduction of acetate and other by-products". In: *Bioresource Technology* 244 (2017), pp. 1096–1103.

[110] H. Krauter, T. Willke, and K.-D. Vorlop. "Production of high amounts of 3-hydroxypropionaldehyde from glycerol by *Lactobacillus reuteri* with strongly increased biocatalyst lifetime and productivity". In: *New Biotechnology* 29.2 (2012), pp. 211–217.

[111] S. Kumar, B. V. Babu, and K. L. Wasewar. "Investigations of biocompatible systems for reactive extraction of propionic acid using aminic extractants (TOA and Aliquat 336)". In: *Biotechnology and Bioprocess Engineering* 17.6 (2012), pp. 1252–1260.

[112] V. Kumar, S. Ashok, and S. Park. "Recent advances in biological production of 3-hydroxypropionic acid". In: *Biotechnology Advances* 31.6 (2013), pp. 945–961.

[113] V. Kumar and S. Park. "Potential and limitations of *Klebsiella pneumoniae* as a microbial cell factory utilizing glycerol as the carbon source". In: *Biotechnology Advances* 36.1 (2017), pp. 150–167.

[114] A. K. Kylmä, T. Granström, and M. Leisola. "Growth characteristics and oxidative capacity of *Acetobacter aceti* IFO 3281: implications for l-ribulose production". In: *Applied Microbiology and Biotechnology* 63.5 (2004), pp. 584–591.

[115] E. I. Lan, D. S. Chuang, C. R. Shen, A. M. Lee, S. Y. Ro, and J. C. Liao. "Metabolic engineering of cyanobacteria for photosynthetic 3-hydroxypropionic acid production from CO2 using *Synechococcus elongatus* PCC 7942". In: *Metabolic Engineering* 31 (2015), pp. 163–170.

[116] B. Le. "Bio-based Acrylic Acid: Considerations for Commercial Viability and Success". https://www.nexant.com/resources/bio-based-acrylic-acid-considerations-commercial-viability-and-success. 2014. (Visited on 08/10/2019).

[117] J. Lee, S. Cha, C. Kang, G. Lee, H. Lim, and G. Jung. "Efficient Conversion of Acetate to 3-Hydroxypropionic Acid by Engineered *Escherichia coli*". In: *Catalysts* 8.11 (2018), p. 525.

[118] S.-H. Lee, S. J. Park, O.-J. Park, J. Cho, and J. W. Rhee. "Production of 3-Hydroxypropionic Acid from Acrylic Acid by Newly Isolated *Rhodococcus erythropolis* LG12". In: *Journal of Microbiology and Biotechnology* 19.5 (2009), pp. 474–481.

[119] F. Lemoine, D. Correia, V. Lefort, O. Doppelt-Azeroual, F. Mareuil, S. Cohen-Boulakia, and O. Gascuel. "NGPhylogeny.fr: new generation phylogenetic services for non-specialists". In: *Nucleic Acids Research* 47.W1 (2019), W260–W265.

[120] I. Letunic and P. Bork. “Interactive Tree Of Life (iTOL) v4: recent updates and new developments”. In: *Nucleic Acids Research* 47.W1 (2019), W256–W259.

[121] P. G. Levi and J. M. Cullen. “Mapping global flows of chemicals: from fossil fuel feedstocks to chemical products”. In: *Environmental Science & Technology* 52.4 (2018), pp. 1725–1734.

[122] J. Li, H. Zong, B. Zhuge, X. Lu, H. Fang, and J. Sun. “Immobilization of *Acetobacter* sp. CGMCC 8142 for efficient biocatalysis of 1, 3-propanediol to 3-hydroxypropionic acid”. In: *Biotechnology and Bioprocess Engineering* 21.4 (2016), pp. 523–530.

[123] S. Li, T. Si, M. Wang, and H. Zhao. “Development of a Synthetic Malonyl-CoA Sensor in *Saccharomyces cerevisiae* for Intracellular Metabolite Monitoring and Genetic Screening”. In: *ACS Synthetic Biology* 4.12 (2015), pp. 1308–1315.

[124] Y. Li, X.-Z. Ge, and P.-F. Tian. “Production of 1,3-propanediol from glycerol using a new isolate *Klebsiella* sp. AA405 carrying low levels of virulence factors”. In: *Biotechnology & Biotechnological Equipment* 31.4 (2017), pp. 725–732.

[125] Y. Li, L. Liu, and P. Tian. “NAD(+)-independent aldehyde oxidase catalyzes cofactor balanced 3-hydroxypropionic acid production in *Klebsiella pneumoniae*”. In: *Biotechnology Letters* 36.11 (2014), pp. 2215–2221.

[126] Y. Li, M. Su, X. Ge, and P. Tian. “Enhanced aldehyde dehydrogenase activity by regenerating NAD(+) in *Klebsiella pneumoniae* and implications for the glycerol dissimilation pathways”. In: *Biotechnology Letters* 35.10 (2013), pp. 1609–1615.

[127] Y. Li, X. Wang, X. Ge, and P. Tian. “High Production of 3-Hydroxypropionic Acid in *Klebsiella pneumoniae* by Systematic Optimization of Glycerol Metabolism”. In: *Scientific Reports* 6 (2016), p. 26932.

[128] H. Lian, B. M. Zeldes, G. L. Lipscomb, A. B. Hawkins, Y. Han, A. J. Loder, D. Nishiyama, M. W. W. Adams, and R. M. Kelly. “Ancillary contributions of heterologous biotin protein ligase and carbonic anhydrase for CO2 incorporation into 3-hydroxypropionate by metabolically engineered *Pyrococcus furiosus*”. In: *Biotechnology and Bioengineering* 113.12 (2016), pp. 2652–2660.

[129] H. H. Liao, R. R. Gokarn, S. J. Gort, H. Jessen, and O. V. Selifonova. “Production of 3-hydroxypropionic acid using beta-alanine/pyruvate aminotransferase”. WO2005118719 A2. 2005.

[130] D. R. Lide, ed. *CRC Handbook of Chemistry and Physics, 85th Edition*. CRC Press. 2005.

[131] H. G. Lim, M. H. Noh, J. H. Jeong, S. Park, and G. Y. Jung. “Optimum Rebalancing of the 3-Hydroxypropionic Acid Production Pathway from Glycerol in *Escherichia coli*”. In: *ACS Synthetic Biology* 5.11 (2016), pp. 1247–1255.

[132] P. Lisdiyanti, H. Kawasaki, T. Seki, Y. Yamada, T. Uchimura, and K. Komagata. “Systematic study of the genus *Acetobacter* with descriptions of *Acetobacter indonesiensis* sp. nov., *Acetobacter tropicalis* sp. nov., *Acetobacter orleanensis* (Henneberg 1906) comb. nov., *Acetobacter lovaniensis* (Frateur 19”. In: *The Journal of General and Applied Microbiology* 46.3 (2000), pp. 147–165.

[133] B. Liu, S. Xiang, G. Zhao, B. Wang, Y. Ma, W. Liu, and Y. Tao. “Efficient production of 3-hydroxypropionate from fatty acids feedstock in *Escherichia coli*”. In: *Metabolic Engineering* 51 (2019), pp. 121–130.

[134] C. Liu, Y. Ding, M. Xian, M. Liu, H. Liu, Q. Ma, and G. Zhao. “Malonyl-CoA pathway: a promising route for 3-hydroxypropionate biosynthesis”. In: *Critical Reviews in Biotechnology* 37.7 (2017), pp. 933–941.

[135] C. Liu, Y. Ding, R. Zhang, H. Liu, M. Xian, and G. Zhao. “Functional balance between enzymes in malonyl-CoA pathway for 3-hydroxypropionate biosynthesis”. In: *Metabolic Engineering* 34 (2016), pp. 104–111.

[136] M. Liu, L. Yao, M. Xian, Y. Ding, H. Liu, and G. Zhao. “Deletion of arcA increased the production of acetyl-CoA-derived chemicals in recombinant *Escherichia coli*”. In: *Biotechnology Letters* 38.1 (2016), pp. 97–101.

[137] S. Liu. “Chapter 12 - Cell Cultivation”. In: *Bioprocess Engineering (Second Edition)*. Ed. by S. Liu. Second Edi. Elsevier, 2017, pp. 699–782. ISBN: 978-0-444-63783-3.

[138] K. D. Loh, P. Gyaneshwar, E. M. Papadimitriou, R. Fong, K.-S. S. Kim, R. Parales, Z. Zhou, W. Inwood, and S. Kustu. “A previously undescribed pathway for pyrimidine catabolism”. In: *Proceedings of the National Academy of Sciences of the United States of America* 103.13 (2006), pp. 5114–5119.

[139] C. S. López-Garzón and A. J. Straathof. “Recovery of carboxylic acids produced by fermentation”. In: *Biotechnology Advances* 32.5 (2014), pp. 873–904.

[140] H. Luo, D. Zhou, X. Liu, Z. Nie, D. L. Quiroga-Sánchez, and Y. Chang. “Production of 3-Hydroxypropionic Acid via the Propionyl-CoA Pathway Using Recombinant *Escherichia coli* Strains”. In: *Plos One* 11.5 (2016). Ed. by I. A. Berg.

[141] M. Luttik, R. Van Spanning, D. Schipper, J. P. Van Dijken, and J. T. Pronk. “The Low Biomass Yields of the Acetic Acid Bacterium *Acetobacter pasteurianus* Are Due to a Low Stoichiometry of Respiration-Coupled Proton Translocation.” In: *Applied and environmental microbiology* 63.9 (1997), pp. 3345–51.

[142] M. D. Lynch, R. T. Gill, and T. Warnecke-Lipscomb. “Method for producing 3-hydroxypropionic acid and other products”. WO 2011/038364 A1. 2011.

[143] G. Maisonnier. *Enjeux pétroliers 2019*. 2019. URL: https://www.ifpenergiesnouvelles.fr/article/enjeux-petroliers-2019-croissance-economique-embargo-liran-gestion-opep-shale-oil-normes-imo (visited on 09/27/2019).

[144] A. J. A. van Maris, W. N. Konings, J. P. van Dijken, and J. T. Pronk. “Microbial export of lactic and 3-hydroxypropanoic acid: implications for industrial fermentation processes”. In: *Metabolic Engineering* 6.4 (2004), pp. 245–255.

[145] L. Matsakas, E. Topakas, and P. Christakopoulos. “New Trends in Microbial Production of 3-hydroxypropionic Acid”. In: *Current Biochemical Engineering* 1.2 (2014), pp. 141–154.

[146] K. Matsushita, T. Inoue, O. Adachi, and H. Toyama. “*Acetobacter aceti* possesses a proton motive force-dependent efflux system for acetic acid.” In: *Journal of bacteriology* 187.13 (2005), pp. 4346–52.

[147] M. L. Mavrovouniotis. “Duality theory for thermodynamic bottlenecks in bioreaction pathways”. In: *Chemical Engineering Science* 51.9 (1996), pp. 1495–1507.

[148] X. Meng, P. Tsobanakis, and T. Abraham. “Process for separating and recovering 3-hydroxypropionic acid and acrylic acid”. US20060149100 A1. 2006.

[149] U. Menzel and G. Gottschalk. “The internal pH of *Acetobacterium wieringae* and *Acetobacter aceti* during growth and production of acetic acid”. In: *Archives of Microbiology* 143 (1985), pp. 47–51.

[150] F. Molinari, R. Gandolfi, R. Villa, E. Urban, and A. Kiener. “Enantioselective oxidation of prochiral 2-methyl-1,3-propandiol by *Acetobacter pasteurianus*”. In: *Tetrahedron: Asymmetry* 14.14 (2003), pp. 2041–2043.

[151] C. Monnet, K. Correia, A.-S. Sarthou, and F. Irlinger. “Quantitative detection of *Corynebacterium casei* in cheese by real-time PCR.” In: *Applied and environmental microbiology* 72.11 (2006), pp. 6972–9.

[152] R. Moscoviz, F. de Fouchécour, G. Santa-Catalina, N. Bernet, and E. Trably. “Cooperative growth of *Geobacter sulfurreducens* and *Clostridium pasteurianum* with subsequent metabolic shift in glycerol fermentation”. In: *Scientific Reports* 7 (2017), p. 44334.

[153] R. Moscoviz, J. Toledo-Alarcón, E. Trably, and N. Bernet. “Electro-Fermentation: How To Drive Fermentation Using Electrochemical Systems”. In: *Trends in Biotechnology* 34.11 (2016), pp. 856–865.

[154] M. Moussa, G. Burgé, F. Chemarin, R. Bounader, C. Saulou-Bérion, F. Allais, H.-E. Spinnler, and V. Athès. “Reactive extraction of 3-hydroxypropionic acid from model aqueous solutions and real bioconversion media. Comparison with its isomer 2-hydroxypropionic (lactic) acid”. In: *Journal of Chemical Technology and Biotechnology* 91.8 (2015), pp. 2276–2285.

[155] H. Murakoa, Y. Watabe, and N. Ogasawara. “Effect of oxygen deficiency on acid production and morphology of bacterial cells in submerged acetic fermentation by *Acetobacter aceti*”. In: *Journal of Fermentation Technology* 60.3 (1982), pp. 171–180.

[156] N. Murali, K. Srinivas, and B. K. Ahring. “Biochemical Production and Separation of Carboxylic Acids for Biorefinery Applications”. In: *Fermentation* 3.2 (2017), p. 22.

[157] S. Nakano and M. Fukaya. “Analysis of proteins responsive to acetic acid in *Acetobacter*: Molecular mechanisms conferring acetic acid resistance in acetic acid bacteria”. In: *International Journal of Food Microbiology* 125.1 (2008), pp. 54–59.

[158] A. Nanba, A. Tamura, and S. Nagai. “Synergistic effects of acetic acid and ethanol on the growth of *Acetobacter* sp.” In: *Journal of Fermentation Technology* 62.6 (1984), pp. 501–505.

[159] R. Nelson, D. Peterson, E. Karp, G. Beckham, and D. Salvachúa. “Mixed carboxylic acid production by *Megasphaera elsdenii* from glucose and lignocellulosic hydrolysate”. In: *Fermentation* 3.1 (2017), p. 10.

[160] J. R. O’Brien, C. Raynaud, C. Croux, L. Girbal, P. Soucaille, and W. N. Lanzilotta. “Insight into the Mechanism of the B12-Independent Glycerol Dehydratase from *Clostridium butyricum*: Preliminary Biochemical and Structural Characterization”. In: *Biochemistry* 43.16 (2004), pp. 4635–4645.

[161] OECD. *The Application of Biotechnology to Industrial Sustainability*. Tech. rep. Paris: Organisation for economic co-operation and development, 2001, pp. 1–137.

[162] J. M. Park, J. Y. Park, W. C. Park, S. M. Lee, and Y. B. Seo. “Recombinant Yeast Producing 3-Hydroxypropionic Acid and Method for Producing 3-Hydroxypropionic Acid Using the Same”. WO2016032279. 2016.

[163] Y. Park, K. Toda, M. Fukaya, H. Okumura, and Y. Kawamura. “Production of a high concentration acetic acid by *Acetobacter aceti* using a repeated fed-batch culture with cell recycling”. In: *Applied Microbiology and Biotechnology* 35.2 (1991), pp. 149–153.

[164] L. Pasteur. “Mémoire sur la fermentation acétique”. In: *Annales scientifiques de l’Ecole Normale Supérieure* 1ère série.tome 1 (1864), pp. 113–158.

[165] L. Pasteur. “Mémoire sur la fermentation alcoolique”. In: *Comptes rendus hebdomadaires des séances de l’Académie des sciences* 45 (1857), pp. 1032–1036.

[166] L. Pasteur. “Mémoire sur la fermentation appelée lactique”. In: *Comptes rendus hebdomadaires des séances de l’Académie des sciences* 45 (1857), pp. 913–916.

[167] L. Petzold. “Automatic Selection of Methods for Solving Stiff and Nonstiff Systems of Ordinary Differential Equations”. In: *SIAM Journal on Scientific and Statistical Computing* 4.1 (1983), pp. 136–148.

[168] S. Piotrowski, M. Carus, and D. Carrez. *European Bioeconomy in Figures 2008-2015 - Update, April 2018*. Tech. rep. nova-Institute for Ecology and Innovation, 2018.

[169] R. Podschun and U. Ullmann. “*Klebsiella* spp. as nosocomial pathogens: epidemiology, taxonomy, typing methods, and pathogenicity factors.” In: *Clinical microbiology reviews* 11.4 (1998), pp. 589–603.

[170] S.-H. Pyo, T. Dishisha, S. Dayankac, J. Gerelsaikhan, S. Lundmark, N. Rehnberg, and R. Hatti-Kaul. “A new route for the synthesis of methacrylic acid from 2-methyl-1,3-propanediol by integrating biotransformation and catalytic dehydration”. In: *Green Chemistry* 14.7 (2012), p. 1942.

[171] S. M. Raj, C. Rathnasingh, W.-C. Jung, and S. Park. “Effect of process parameters on 3-hydroxypropionic acid production from glycerol using a recombinant *Escherichia coli*”. In: *Applied microbiology and biotechnology* 84.4 (2009), pp. 649–657.

[172] S. M. Raj, C. Rathnasingh, W.-C. Jung, E. Selvakumar, and S. Park. “A Novel NAD+-dependent aldehyde dehydrogenase encoded by the puuC gene of *Klebsiella pneumoniae* DSM 2026 that utilizes 3-hydroxypropionaldehyde as a substrate”. In: *Biotechnology and Bioprocess Engineering* 15.1 (2010), pp. 131–138.

[173] P. Raspor and D. Goranovič. “Biotechnological Applications of Acetic Acid Bacteria”. In: *Critical Reviews in Biotechnology* 28.2 (2008), pp. 101–124.

[174] A. Rault, C. Béal, S. Ghorbal, J.-C. Ogier, and M. Bouix. “Multiparametric flow cytometry allows rapid assessment and comparison of lactic acid bacteria viability after freezing and during frozen storage”. In: *Cryobiology* 55.1 (2007), pp. 35–43.

[175] S. Roffler, H. W. Blanch, and C. R. Wilke. “Extractive Fermentation of Acetone and Butanol: Process Design and Economic Evaluation”. In: *Biotechnology Progress* 3.3 (1987), pp. 131–140.

[176] J. K. Rogers and G. M. Church. “Genetically encoded sensors enable real-time observation of metabolite production”. In: *Proceedings of the National Academy of Sciences of the United States of America* 113.9 (2016), pp. 2388–2393.

[177] L. Romero, J. Gómez, I. Caro, and D. Cantero. “A kinetic model for growth of *Acetobacter aceti* in submerged culture”. In: *The Chemical Engineering Journal and the Biochemical Engineering Journal* 54.1 (1994), B15–B24.

[178] G. Rychen, G. Aquilina, G. Azimonti, V. Bampidis, M. De Lourdes Bastos, G. Bories, A. Chesson, P. S. Cocconcelli, G. Flachowski, J. Gropp, B. Kolar, M. Kouba, M. López Alonso, S. López Puente, A. Mantovani, B. Mayo, F. Ramos, R. E. Villa, R. J. Wallace, P. Wester, R. Brozzi, and M. Saarela. “Safety and efficacy of *Bacillus subtilis* PB6 (*Bacillus subtilis* ATCC PTA-6737) as a feed additive for sows”. In: *EFSA Journal* 15.5 (2017), pp. 4855–4864.

[179] R. Sabet-Azad, R. R. Sardari, J. A. Linares-Pastén, and R. Hatti-Kaul. “Production of 3-hydroxypropionic acid from 3-hydroxypropionaldehyde by recombinant *Escherichia coli* co-expressing *Lactobacillus reuteri* propanediol utilization enzymes”. In: *Bioresource Technology* 180 (2015), pp. 214–221.

[180] N. Saichana, K. Matsushita, O. Adachi, I. Frébort, and J. Frebortova. “Acetic acid bacteria: A group of bacteria with versatile biotechnological applications”. In: *Biotechnology Advances* 33.6 (2015), pp. 1260–1271.

[181] R. Saini, R. Kapoor, R. Kumar, T. Siddiqi, and A. Kumar. “CO2 utilizing microbes — A comprehensive review”. In: *Biotechnology Advances* 29.6 (2011), pp. 949–960.

[182] A. K. Sanchez-Castañeda, M. Moussa, L. Ngansop, I. C. Trelea, and V. Athès. “Organic phase screening for in stream reactive extraction of bio-based 3-hydroxypropionic acid: biocompatibility and extraction performances”. In: submitted (2019).

[183] M. Sankaranarayanan, S. Ashok, and S. Park. “Production of 3-hydroxypropionic acid from glycerol by acid tolerant *Escherichia coli*”. In: *Journal of Industrial Microbiology & Biotechnology* 41.7 (2014), pp. 1039–1050.

[184] M. Sankaranarayanan, A. Somasundar, E. Seol, A. S. Chauhan, S. Kwon, G. Y. Jung, and S. Park. “Production of 3-hydroxypropionic acid by balancing the pathway enzymes using synthetic cassette architecture”. In: *Journal of Biotechnology* 259 (2017), pp. 140–147.

[185] R. R. Sardari, T. Dishisha, S.-H. Pyo, and R. Hatti-Kaul. “Biotransformation of glycerol to 3-hydroxypropionaldehyde: Improved production by in situ complexation with bisulfite in a fed-batch mode and separation on anion exchanger”. In: *Journal of Biotechnology* 168.4 (2013), pp. 534–542.

[186] M. Sauer, D. Porro, D. Mattanovich, and P. Branduardi. “Microbial production of organic acids: expanding the markets”. In: *Trends in Biotechnology* 26.2 (2008), pp. 100–108.

[187] R. K. Saxena, P. Anand, S. Saran, and J. Isar. “Microbial production of 1,3-propanediol: Recent developments and emerging opportunities”. In: *Biotechnology Advances* 27.6 (2009), pp. 895–913.

[188] A. Schievano, T. Pepé Sciarria, K. Vanbroekoven, H. De Wever, S. Puig, S. J. Andersen, K. Rabaey, and D. Pant. “Electro-fermentation – Merging electrochemistry with fermentation in industrial applications”. In: *Trends in Biotechnology* 34.11 (2016), pp. 866–878.

[189] M. Schwarz, B. Köpcke, R. W. Weber, O. Sterner, and H. Anke. “3-Hydroxypropionic acid as a nematicidal principle in endophytic fungi”. In: *Phytochemistry* 65.15 (2004), pp. 2239–2245.

[190] M. Sobolov and K. L. Smiley. “Metabolism of glycerol by an acrolein-forming *Lactobacillus*.” In: *Journal of bacteriology* 79 (1960), pp. 261–266.

[191] C. W. Song, J. W. Kim, I. J. Cho, and S. Y. Lee. “Metabolic Engineering of *Escherichia coli* for the Production of 3-Hydroxypropionic Acid and Malonic Acid through beta-Alanine Route”. In: *ACS Synthetic Biology* 5.11 (2016), pp. 1256–1263.

[192] D. D. Sriramulu, M. Liang, D. Hernandez-Romero, E. Raux-Deery, H. Lünsdorf, J. B. Parsons, M. J. Warren, and M. B. Prentice. “*Lactobacillus reuteri* DSM 20016 produces cobalamin-dependent diol dehydratase in metabolosomes and metabolizes 1,2-propanediol by disproportionation.” In: *Journal of bacteriology* 190.13 (2008), pp. 4559–67.

[193] P. Steiner and U. Sauer. “Long-term continuous evolution of acetate resistant *Acetobacter aceti*”. In: *Biotechnology and Bioengineering* 84.1 (2003), pp. 40–44.

[194] R. Storn and K. Price. “Differential Evolution – A Simple and Efficient Heuristic for global Optimization over Continuous Spaces”. In: *Journal of Global Optimization* 11.4 (1997), pp. 341–359.

[195] A. J. Straathof. “The Proportion of Downstream Costs in Fermentative Production Processes”. In: *Comprehensive Biotechnology*. Elsvier, 2011, pp. 811–814.

[196] A. Suyama, Y. Higuchi, M. Urushihara, Y. Maeda, and K. Takegawa. “Production of 3-hydroxypropionic acid via the malonyl-CoA pathway using recombinant fission yeast strains”. In: *Journal of Bioscience and Bioengineering* 124.4 (2017), pp. 392–399.

[197] K. Takamizawa, H. Horitsu, T. Ichikawa, K. Kawai, and T. Suzuki. "β-hydroxypropionic acid production by *Byssochlamys* sp. grown on acrylic acid". In: *Applied Microbiology and Biotechnology* 40.2 (1993), pp. 196–200.

[198] H. Takemura, T. Tsuchida, F. Yoshinaga, K. Matsushita, and O. Adachi. "Prosthetic Group of Aldehyde Dehydrogenase in Acetic Acid Bacteria Not Pyrroloquinoline Quinone". In: *Bioscience, Biotechnology, and Biochemistry* 58.11 (1994), pp. 2082–2083.

[199] T. L. Talarico, I. A. Casas, T. C. Chung, and W. J. Dobrogosz. "Production and isolation of reuterin, a growth inhibitor produced by *Lactobacillus reuteri*". In: *Antimicrobial Agents Chemotherapy* 32.12 (1988), pp. 1854–1858.

[200] T. L. Talarico and W. J. Dobrogosz. "Chemical characterization of an antimicrobial substance produced by *Lactobacillus reuteri*". In: *Antimicrobial agents and chemotherapy* 33.5 (1989), pp. 674–679.

[201] T. L. Talarico and W. J. Dobrogosz. "Purification and Characterization of Glycerol Dehydratase from *Lactobacillus reuteri*". In: *Applied and environmental microbiology* 56.4 (1990), pp. 1195–1197.

[202] T. L. Talarico, L. T. Axelsson, J. Novotny, M. Fiuzat, and W. J. Dobrogosz1. "Utilization of Glycerol as a Hydrogen Acceptor by *Lactobacillus reuteri*: Purification of 1,3-Propanediol:NAD+ Oxidoreductase". In: *Applied and Environmental Microbiology* 56.4 (1990), pp. 943–948.

[203] J. A. Tamada and C. J. King. "Extraction of carboxylic acids with amine extractants. 2. Chemical interactions and interpretation of data". In: *Industrial & Engineering Chemistry Research* 29.7 (1990), pp. 1327–1333.

[204] M. Tassone and A. Diano. "Beta-alanine aminotransferases for the production of 3-hydroxypropionic acid". WO2017035270 A1. 2017.

[205] R. Tengler and D. DeCoster. "Purification of 3-Hydroxypropionic Acid from Crude Cell Broth and Production of Acrylamide". US20130345470 A1. 2013.

[206] The SciPy Community. *SciPy Reference Guide, Release 1.3.0*. 2019.

[207] J. Tkac, J. Svitel, I. Vostiar, M. Navratil, and P. Gemeiner. "Membrane-bound dehydrogenases from *Gluconobacter* sp.: Interfacial electrochemistry and direct bioelectrocatalysis". In: *Bioelectrochemistry* 76.1 (2009), pp. 53–62.

[208] K. Tokuyama, S. Ohno, K. Yoshikawa, T. Hirasawa, S. Tanaka, C. Furusawa, and H. Shimizu. "Increased 3-hydroxypropionic acid production from glycerol, by modification of central metabolism in *Escherichia coli*". In: *Microbial Cell Factories* 13.64 (2014), pp. 1–11.

[209] J. Trček, N. P. Mira, and L. R. Jarboe. "Adaptation and tolerance of bacteria against acetic acid". In: *Applied Microbiology and Biotechnology* 99.15 (2015), pp. 6215–6229.

[210] K. Tsuruno, H. Honjo, and T. Hanai. "Enhancement of 3-hydroxypropionic acid production from glycerol by using a metabolic toggle switch". In: *Microbial Cell Factory* 14.155 (2015).

[211] W. Van Hecke, G. Kaur, and H. De Wever. "Advances in in-situ product recovery (ISPR) in whole cell biotechnology during the last decade". In: *Biotechnology Advances* 32.7 (2014), pp. 1245–1255.

[212] J. E. Velasquez, D. I. Collias, and J. E. Godlewski. "Catalytic Dehydration of Hydroxypropionic Acid and its Derivatives". WO2017040386 A1. 2017.

[213] B. Wang, Y. Shao, and F. Chen. “Overview on mechanisms of acetic acid resistance in acetic acid bacteria”. In: *World Journal of Microbiology and Biotechnology* 31.2 (2015), pp. 255–263.

[214] K. Wang and P. Tian. “Engineering Plasmid-Free *Klebsiella pneumoniae* for Production of 3-Hydroxypropionic Acid”. In: *Current Microbiology* 74.1 (2017), pp. 55–58.

[215] Y. Wang, F. Tao, J. Ni, C. Li, and P. Xu. “Production of C3 platform chemicals from CO2 by genetically engineered cyanobacteria”. In: *Green Chemistry* 17.5 (2015), pp. 3100–3110.

[216] Y. Wang, L. Chen, and W. Zhang. “Proteomic and metabolomic analyses reveal metabolic responses to 3-hydroxypropionic acid synthesized internally in cyanobacterium *Synechocystis* sp. PCC 6803”. In: *Biotechnology for Biofuels* 9.209 (2016).

[217] Y. Wang, T. Sun, X. Gao, M. Shi, L. Wu, L. Chen, and W. Zhang. “Biosynthesis of platform chemical 3-hydroxypropionic acid (3-HP) directly from CO2 in cyanobacterium *Synechocystis* sp. PCC 6803”. In: *Metabolic Engineering* 34 (2016), pp. 60–70.

[218] K. L. Wasewar, D. Shende, and A. Keshav. “Reactive extraction of itaconic acid using tri-*n*-butyl phosphate and aliquat 336 in sunflower oil as a non-toxic diluent”. In: *Journal of Chemical Technology & Biotechnology* 86.2 (2011), pp. 319–323.

[219] K. L. Wasewar, A. A. Yawalkar, J. A. Moulijn, and V. G. Pangarkar. “Fermentation of Glucose to Lactic Acid Coupled with Reactive Extraction: A Review”. In: *Industrial & Engineering Chemistry Research* 43.19 (2004), pp. 5969–5982.

[220] T. Werpy and G. Petersen. *Top Value Added Chemicals from Biomass: Volume I – Results of Screening for Potential Candidates from Sugars and Synthesis Gas.* Tech. rep. 2004, p. 69.

[221] Z. Wu and S.-T. Yang. “Extractive fermentation for butyric acid production from glucose by *Clostridium tyrobutyricum*”. In: *Biotechnology and Bioengineering* 82.1 (2002), pp. 93–102.

[222] V. M. Yabannavar and D. I. C. Wang. “Strategies for reducing solvent toxicity in extractive fermentations”. In: *Biotechnology and Bioengineering* 37.8 (1991), pp. 716–722.

[223] T. Yamamoto, K. Kojima, H. Mori, H. Kawasaki, and M. Sayama. “Extraction of Lactic Acid Using Long Chain Amines Dissolved in Non-Polar Diluents”. In: *Journal of Chemical Engineering of Japan* 44.12 (2011), pp. 949–956.

[224] Y.-M. Yang, W.-J. Chen, J. Yang, Y.-M. Zhou, B. Hu, M. Zhang, L.-P. Zhu, G.-Y. Wang, and S. Yang. “Production of 3-hydroxypropionic acid in engineered *Methylobacterium extorquens* AM1 and its reassimilation through a reductive route”. In: *Microbial Cell Factories* 16.1 (2017), p. 179.

[225] S.-T. Yang, H. Huang, A. Tay, W. Qin, L. De Guzman, and E. C. S. Nicolas. “Extractive Fermentation for the Production of Carboxylic Acids”. In: *Bioprocessing for Value-Added Products from Renewable Resources*. Elsevier, 2007, pp. 421–446. ISBN: 9780444521149.

[226] D. Yankov, J. Molinier, J. Albet, G. Malmary, and G. Kyuchoukov. “Lactic acid extraction from aqueous solutions with tri-*n*-octylamine dissolved in decanol and dodecane”. In: *Biochemical Engineering Journal* 21.1 (2004), pp. 63–71.

[227] Z. Ye, X. Li, Y. Cheng, Z. Liu, G. Tan, F. Zhu, S. Fu, Z. Deng, and T. Liu. “Evaluation of 3-hydroxypropionate biosynthesis in vitro by partial introduction of the 3-hydroxypropionate/4-hydroxybutyrate cycle from *Metallosphaera sedula*”. In: *Journal of Industrial Microbiology & Biotechnology* 43.9 (2016), pp. 1313–1321.

[228] S. Yu, P. Yao, J. Li, J. Ren, J. Yuan, J. Feng, M. Wang, Q. Wu, and D. Zhu. "Enzymatic synthesis of 3-hydroxypropionic acid at high productivity by using free or immobilized cells of recombinant *Escherichia coli*". In: *Journal of Molecular Catalysis B: Enzymatic* 129 (2016), pp. 37–42.

[229] O. Zaushitsyna, T. Dishisha, R. Hatti-Kaul, and B. Mattiasson. "Crosslinked, cryostructured *Lactobacillus reuteri* monoliths for production of 3-hydroxypropionaldehyde, 3-hydroxypropionic acid and 1,3-propanediol from glycerol". In: *Journal of Biotechnology* 241 (2017), pp. 22–32.

[230] Y.-H. P. Zhang, J. Sun, and Y. Ma. "Biomanufacturing: history and perspective". In: *Journal of Industrial Microbiology & Biotechnology* 44.4-5 (2017), pp. 773–784.

[231] Q. Zhang, J.-S. Gong, T.-T. Dong, T.-T. Liu, H. Li, W.-F. Dou, Z.-M. Lu, J.-S. Shi, and Z.-H. Xu. "Nitrile-hydrolyzing enzyme from *Meyerozyma guilliermondii* and its potential in biosynthesis of 3-hydroxypropionic acid". In: *Bioprocess and Biosystems Engineering* 40.6 (2017), pp. 901–910.

[232] X.-Z. Zhang and Y.-H. P. Zhang. "One-step production of biocommodities from lignocellulosic biomass by recombinant cellulolytic *Bacillus subtilis*: Opportunities and challenges". In: *Engineering in Life Sciences* 10.5 (2010), pp. 398–406.

[233] Y. Zhang, W. Cong, and S. Shi. "Application of a pH feedback-controlled substrate feeding method in lactic acid production". In: *Applied Biochemistry and Biotechnology* 162.8 (2010), pp. 2149–2156.

[234] L. Zhao, J. Lin, H. Wang, J. Xie, and D. Wei. "Development of a two-step process for production of 3-hydroxypropionic acid from glycerol using *Klebsiella pneumoniae* and *Gluconobacter oxydans*". In: *Bioprocess and Biosystems Engineering* 38.12 (2015), pp. 2487–2495.

[235] P. Zhao, C. Ma, L. Xu, and P. Tian. "Exploiting tandem repetitive promoters for high-level production of 3-hydroxypropionic acid". In: *Applied Microbiology and Biotechnology* 103.10 (2019), pp. 4017–4031.

[236] S. Zhou, C. Catherine, C. Rathnasingh, A. Somasundar, and S. Park. "Production of 3-Hydroxypropionic Acid From Glycerol by Recombinant Pseudomonas denitrificans". In: *Biotechnology and Bioengineering* 110.12 (2013), pp. 3177–3187.

[237] J. Zhu, J. Xie, L. Wei, J. Lin, L. Zhao, and D. Wei. "Identification of the enzymes responsible for 3-hydroxypropionic acid formation and their use in improving 3-hydroxypropionic acid production in *Gluconobacter oxydans* DSM 2003". In: *Bioresource Technology* 265 (2018), pp. 328–333.

[238] M. Zwietering, I. Jongenburger, F. Rombouts, and K. Van't Riet. "Modeling of the Bacterial Growth Curve". In: *Applied and Environmental Microbiology* 56.6 (1990), pp. 1875–1881.

APPENDICES

A 16S rRNA gene analysis of *Acetobacter* sp. CIP 58.66

In order to check the strain's purity in stock cultures, genomic DNA was extracted from two thawed cryotubes for 16S rRNA gene analysis. This appendix describes the main steps that allowed to determine that (i) the stock cultures were not contaminated; and (ii) the strain purchased did not belong to the *aceti* species, contrary to what was expected.

A.1 DNA extraction, amplification and purification

A.1.1 *Genomic DNA extraction and purification*

Genomic DNA was extracted from thawed cryotubes and purified as previously described by Monnet et al. (2006) [151].

A.1.2 *16S rRNA gene amplification and purification*

The 16S rRNA gene was amplified by PCR using the following universal primer pairs (forward 5'-AGAGTTTGATCCTGGCTCAG-3' / reverse 5'-AGAGTTTGATCCTGGCTCAG-3') with a GeneAmp® thermocycler (PE Applied Biosystems). The mix composition is presented in Table A.I. The PCR protocol consisted in: (i) a DNA denaturation step during 5 min at 94 °C; (ii) 25 cycles of denaturation (1 min at 94 °C), hybridation (1 min at 57 °C) and polymerisation (2 min at 72 °C); (iii) an elongation step during 5 min at 72 °C. Finally, samples were cooled at 4 °C. PCR products were purified and sequenced (Sanger sequencing) by the company Eurofins Genomics (Les Ulis, France).

Table A.I: Mix composition for PCR amplification

GoTaq Promega 5x Buffer	10 µL
Sterile milliQ® water	*q.s.* 50 µL
DNA	1 µL at 20 ng µL
Forward primer	2 µL at 0.2 µmol L^{-1}
Reverse primer	2 µL at 0.2 µmol L^{-1}
dNTP	for each: 4 µL (final 0.2 µmol L^{-1})
GoTap Promega polymerase (5 U µL)	0.25 µL

A.2 16S rRNA gene sequence of *Acetobacter* sp. CIP 58.66

Only one 16S rRNA gene sequence was obtained from sequencing of the DNA extracted from the two samples. Stock cultures were therefore considered free from contaminants.

16S rRNA gene sequence of *Acetobacter* sp. CIP 58.66 (1377 bp):

AGTCGCTGACCCGACCGTGGTCGGCTGCGCCCCTTGCGGGTTCGCTCACC
GGCTTAAGGTCAAACCAACTCCCATGGTGTGACGGGCGGTGTGTACAAGGC
CCGGGAACGTATTCACCGCGGCATGCTGATCCGCGATTACTAGCGATTCCA
CCTTCATGCACTCGAGTTGCAGAGTGCAATCCGAACTGAGACGACTTTTTGA
GATCAGCACGATGTCGCCATCTAGCTTCCCATTGTCATCGCCATTGTAGCAC
GTGTGTAGCCCAGGACATAAGGGCCATGAGGACTTGACGTCATCCCCACCT
TCCTCCGGCTTGTCACCGGCAGTCTCTCTAGAGTGCCCACCCAAACATGCTG
GCAACTAAAGATAGGGGTTGCGCTCGTTGCGGGACTTAACCCAACATCTCAC
GACACGAGCTGACGACAGCCATGCAGCACCTGTGCGGTAGGTCCCTTGCGG
GAAATGCCCATCTCTGGACACAGCCTACCCATACAAGCCCTGGTAAGGTTCT
GCGCGTTGCTTCGAATTAAACCACATGCTCCACCGCTTGTGCGGGCCCCCG
TCAATTCCTTTGAGTTTCAACCTTGCGGCCGTACTCCCCAGGCGGTGTGCTT
ATCGCGTTAGCTACGACACTGAGTAACTAAGTTACCCAACATCCAGCACACA
TCGTTTACAGCGTGGACTACCAGGGTATCTAATCCTGTTTGCTCCCCACGCT
TTCGCGCCTCAGCGTCAGTAATGAGCCAGGTTGCCGCCTTCGCCACCGGTG
TTCTTCCCAATATCTACGAATTTCACCTCTACACTGGGAATTCCACAACCCTC
TCTCACACTCTAGTCTGCACGTATTAAATGCAGCTCCCAGGTTAAGCCCGGG
GATTTCACATCTAACTGTACAAACCGCCTACACGCCCTTTACGCCCAGTCAT
TCCGAGCAACGCTAGCCCCCTTCGTATTACCGCGGCTGCTGGCACGAAGTT
AGCCGGGGCTTCTTCTGCGGGTACCGTCATCATCGTCCCCGCCGAAAGTGC
TTTACAATCCGAAAACCTTCTTCACACACGCGGCATTGCTGGATCAGGGTTG
CCCCCATTGTCCAATATTCCCCACTGCTGCCTCCCGTAGGAGTCTGGGCCGT
GTCTCAGTCCCAGTGTGGCTGATCATCCTCTCAGACCAGCTATTGATCATCG
CCTTGGTAGGCCATTACCCCACCAACAAGCTAATCAAACGCAGGCTCCTCCA
CAGGCGACTTGCGCCTTTGACCCTCAGGTATCATGCGGTATTAGCTCCAGTT
TCCCGGAGTTATCCCCCACCCATGGATAGATTCCTACGCGTTACTCACCCGT
CCGCCACTAAGGCCGAAGCCTTCGTGCGACTGCA

The strain was initially purchased from the Biological Resource Center of Pasteur Institute (Paris, France) as *Acetobacter aceti*. The 16R rRNA gene sequence that was obtained, was compared with the bacterial 16S RNA sequences from the NCBI (National Center for Biotechnology Information) database using the BLASTn (nucleotide Basic Local Alignment Tool) online tool (National Institute for Health, USA). BLAST results showed that 15 bacterial 16S rRNA gene sequences of the database had an identity percentage above 99 %, with an E-value [1] equal to 0.0. These 15 sequences all belonged to genus *Acetobacter*, but none of them to species *aceti*. Five different species were represented: *cerevisiae*, *malorum*, *orleanensis*, *persici*, and *farinalis*. A phylogenetic analysis was thus carried out, in order to try to identify the strain used for the experimental works of the present thesis.

A.3 Phylogenetic analysis

In order to get more insights on the strain's taxonomy, a phylogenetic tree was constructed according to the following mehod:

[1] "The Expect value (E) is a parameter that describes the number of hits one can 'expect' to see by chance when searching a database of a particular size. It decreases exponentially as the Score (S) of the match increases. Essentially, the E value describes the random background noise. [...] The lower the E-value, or the closer it is to zero, the more "significant" the match is." (blast.ncbi.nlm.nih.gov/Blast.cgi?CMD=Web&PAGE_TYPE=BlastDocs&DOC_TYPE=FAQ, accessed online August 6, 2019)

(i) 16S rRNA gene sequences from species belonging to genus *Acetobacter* were retrieved from the Reference Sequence (RefSeq, NCBI). When several sequences were available for one specific strain, only one was kept in the dataset. Fifty-four sequences were thus selected, corresponding to 28 different species. Three 16S rRNA gene sequences of *Escherichia coli* strains were used as outgroup, they were also retrieved from the RefSeq database.

(ii) The phylogenetic tree was constructed using the "FastTree One Click Workflow" from the online tool NGPhylogeny.fr [119], with default tools and parameters.

(iii) The final tree was rendered using the iTOL (interactive Tree of Life) tool [120].

The phylogenetic tree thus obtained is shown in Figure A.1. As expected from the BLASTn results, the sequence obtained from our stock-cultures were not included in the same group as *Acetobacter aceti*. More surprisingly, the closest sequences to strain CIP 58.66 did not belong to the same species as the ones that had the highest BLASTn scores. On the phylogenetic tree, strain CIP 58.66 was included in a *syzygii/okinawensis/lambici* cluster. This constitutes another evidence that strain CIP 58.66 does not belong to species *aceti*. Further analysis of the phenotypic characteristics, ubiquinone systems, DNA base compositions, and levels of DNA-DNA relatedness would be required in order to identify accurately the strain [132]. In the works presented here, the strain is thus referred to as *Acetobacter* sp. CIP 58.66.

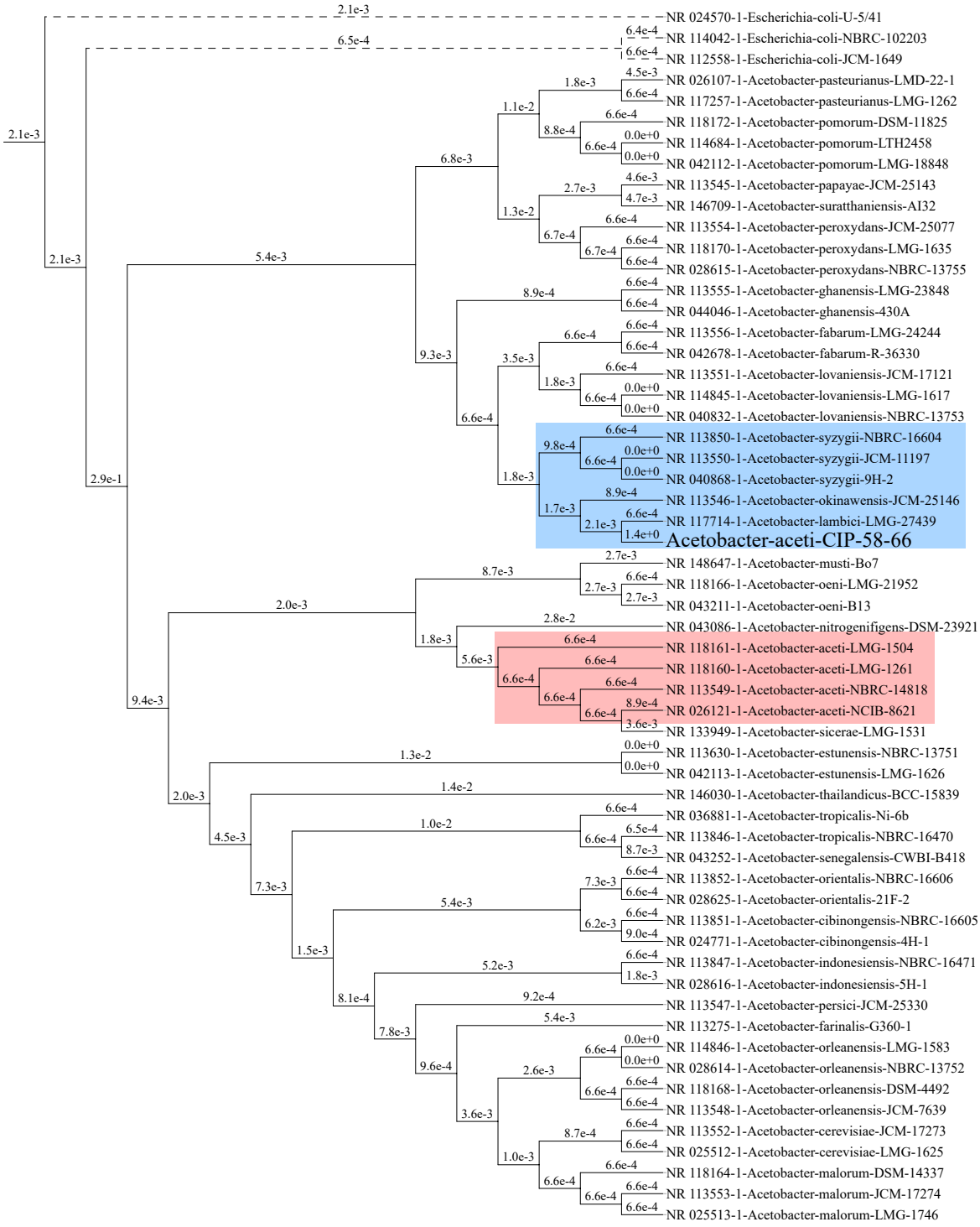

Figure A.1: Phylogenetic tree of genus *Acetobacter* based on 16S rRNA gene sequences
The blue area highlights the group containing the 16S rRNA gene sequence of *Acetobacter* sp. CIP 58.66, and the red area shows the *Acetobacter aceti* group. The tree was rooted using 16S rRNA gene sequences of three *E. coli* strains (dotted lines). Branches are only qualitatively represented, but their actual lengths are shown.

B O_2 transfer characterisation in the bioreactor: k_La estimation

B.1 Notion of k_La and calculation method

B.1.1 *Introducing the k_La parameter*

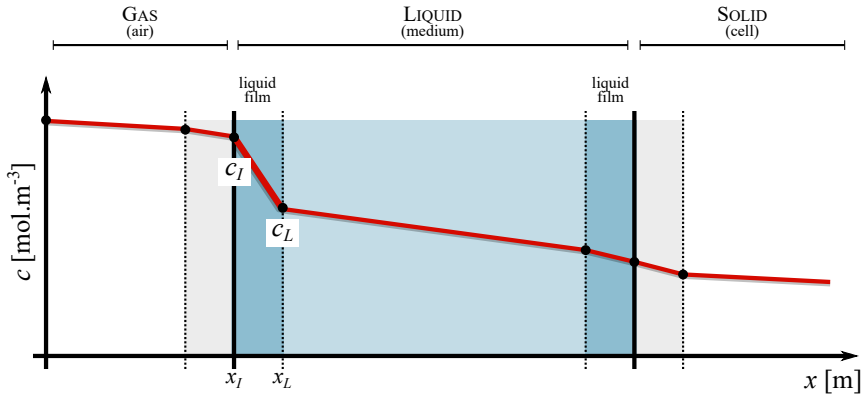

Figure B.2: Schematic representation of the variations of O_2 concentration (c) during its transfer

Among all steps of O_2 transfer from the air to the bacteria (Fig. B.2), its diffusion through the boundary liquid film at the air/medium interface can be considered as the most limiting step [77, 23]. The other steps being neglected, O_2 diffusion is only considered in this film. Under the hypotheses that air and liquid medium are homogeneous phases that are thoroughly mixed, the unidimensional Fick's law can be applied:

$$j = -D\frac{\partial c}{\partial x} \tag{B.18}$$

with j (mol m^{-2} s^{-1}) is the molar diffusion flux of O_2, D (m^2 s^{-1}) is the diffusivity of O_2 in the medium, and c (mol m^{-3}) is the molar concentration of O_2.

Assuming the c decrease in the boundary film to be linear, the previous relationship can be written as:

$$j = -\frac{D}{x_L - x_I}\left(c_I - c_L\right) \tag{B.19}$$

The quantity $\frac{D}{x_L - x_I}$ is noted k_L (m s^{-1}). Moreover, since O_2 diffusion is not limiting in the boundary gas film, c_I is in fact the saturating concentration of O_2 in the medium in equilibrium with air, whiwh is noted c^*. The formula for the O_2 flux from the air to the medium can thus be written:

$$\boxed{j = -k_L\left(c^* - c_L\right)} \tag{B.20}$$

In the absence of O_2 uptake, the mass balance in the bioreactor is as follows:

$$\frac{d(V \cdot c_L)}{dt} = Sj \tag{B.21}$$

where V (m^3) is the working volume of medium, and S (m^2) the gas-liquid exchange surface. Considering a constant working volume, the specific exchange surface $\frac{S}{V}$ is noted a (m^{-1}). Integrating equations B.20 and B.21 leads to the following relationship:

$$\boxed{\frac{\mathrm{d}c_L}{\mathrm{d}t} = -\mathrm{k}_L a \left(c^* - c_L\right)} \tag{B.22}$$

B.1.2 *The "gas out - gas in" calculation method*

For given conditions of aeration flow rate and stirring rate, O_2 is first flushed out of the bioreactor with N_2. Then, from time $t = 0$ s, the medium is sparged with air. In these conditions, $c_L(t = 0)$ is equal to 0 mol m^{-3}. Using this initial condition, the solution to Equation B.22 is the following:

$$c_L = c^* \left(1 - \exp^{-\mathrm{k}_L a t}\right) \tag{B.23}$$

which is equivalent to:

$$\ln\left(\frac{c^* - c_L}{c^*}\right) = \ln\left(1 - \frac{c_L}{c^*}\right) = -\mathrm{k}_L a t \tag{B.24}$$

The polarographic probe used in the bioreactor measures the partial pressure of O_2 in the medium, noted $\%pO_2$ (%), as a percentage of a reference value. A calibration is performed so that a $\%pO_2$ value of 100 % corresponds to O_2 saturation. The O_2 proportion in the inlet air is assumed to be constant, so c^* is a constant parameter. According to Henry's law, the partial pressure of a gas is proportional to its concentration in the liquid phase. Hence, the $\%pO_2$ value is here considered as $100 \cdot \frac{c_L}{c^*}$. Consequently, the $k_L a$ can be estimated as the slope of the following equation:

$$\boxed{\ln\left(1 - \frac{\%\mathrm{p}_{O_2}}{100}\right) = -\mathrm{k}_L a t} \tag{B.25}$$

B.2 Experimental approach

B.2.1 *Experimental design*

5 stirring rates and 4 air flow rates were tested for a model medium The variation ranges of these to parameters were representative of the ranges used during cultures of *Acetobacter* sp. CIP 58.66. The medium was composed of 5 g L^{-1} of yeast extract, 3 g L^{-1} of peptone, and 10 g L^{-1} of glycerol. pH was adjusted to 5.0 with a 5.5 mol L^{-1} solution of sulfuric acid. The working volume was 1 L, and experiments were performed in the same conditions than those used for cultivation of *Acetobacter* sp. CIP 58.66: autoclaving at 120 °C during 20 min, pO_2 probe calibration as described in section 2.2.3 (page 47), and the medium temperature was controlled at 30 °C during the whole duration of the experiments.

All conditions were tested in three replicates. Each set of replicates was performed independently, with a newly prepared medium and a newly calibrated probe. Between each tested condition, O_2 was flushed out of the liquid medium and the new condition was tested only after the $\%pO_2$ had stabilised around 0 %.

B.2.2 $k_L a$ *calculation*

Fig. B.3 provides an illustration of $k_L a$ computation for one replicate of a set of conditions. Using the acquired $\%pO_2$ data, $\ln\left(1 - \frac{\%\mathrm{p}_{O_2}}{100}\right)$ was calculated at each time. Linear regression was performed on this latter variable over time using function "ols" from package "statsmodels.formula.api" from Pyhton 3.6. The slope estimation corresponded to the $k_L a$ parameter.

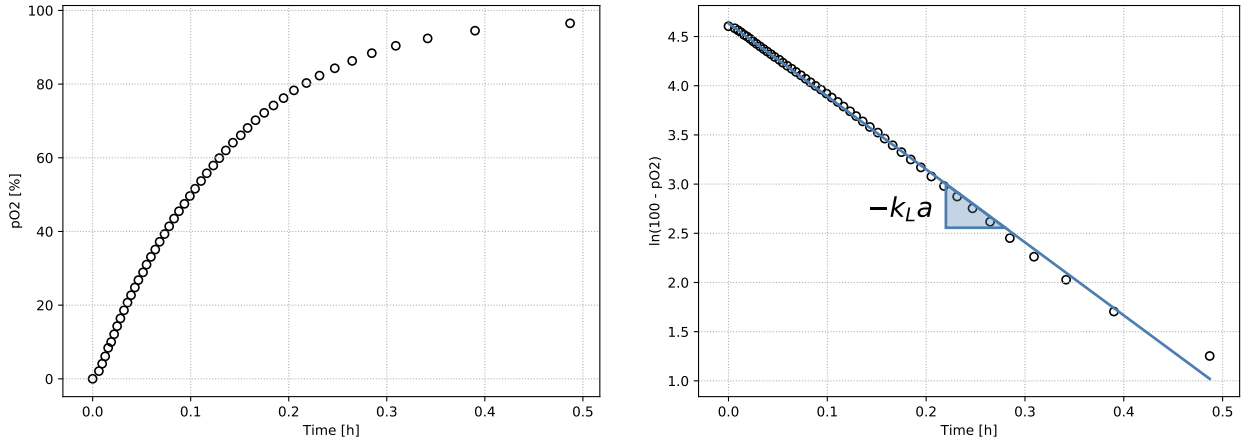

Figure B.3: Illustration of k_La calculation for one set of stirring and air flow conditions
In this example, the tested conditions were respectively 100 rpm and 1 NL min^{-1} for stirring rate and air flow rate. **A.** %p$_{O_2}$ (%) over time (data from the acquisition software). **B.** $ln\left(100 - \mathrm{p}_{O_2}\right)$ over time.

B.3 Results

The k_La values obtained are presented in Table B.II. For all 60 linear regressions (20 sets of conditions in three replicates), R^2 was always found between 0.9737 and 0.9998.

Table B.II: Obtained k_La values

Air flow rate [NL/min] \ Stirring rate [rpm]	100	200	400	600	800
1	$9,13 \pm 1,57$	$11,79 \pm 2,60$	$23,55 \pm 2,75$	$50,37 \pm 4,85$	$69,80 \pm 6,87$
2	$9,10 \pm 6,50$	$19,33 \pm 1,06$	$34,68 \pm 1,25$	$69,52 \pm 1,12$	$103,21 \pm 4,11$
3	$15,16 \pm 8,63$	$26,99 \pm 3,78$	$50,49 \pm 4,64$	$83,88 \pm 4,09$	$141,49 \pm 18,65$
4	$29,00 \pm 5,30$	$26,01 \pm 8,13$	$58,81 \pm 5,41$	$98,34 \pm 10,87$	$151,03 \pm 19,52$

During cultivations of *Acetobacter* sp. CIP 58.66, air flow rate and stirring rate were automatically controlled based on the pO$_2$ measurement, so their values varied over time. Therefore, establishing a relationship between the k_La and the stirring and air flow rates is of interest, so that k_La can be computed at each time of cultivation. Several empirical multivariate linear models were investigated and the one with the best results was selected (*i.e.* a model that includes only significant factors, has a R^2 close to 1, and for which residuals are symmetrically and randomly distributed around 0). The final model was the following:

$$k_La = \beta_0 + \beta_1 N^2 + \beta_2 NF + \epsilon \tag{B.26}$$

where N (rpm) is the stirring rate, F is the air flow rate (NL min^{-1}), β_i the linear model's coefficient, and ϵ the residual error. The results obtained with this model are presented in Table B.III and Figure B.4.

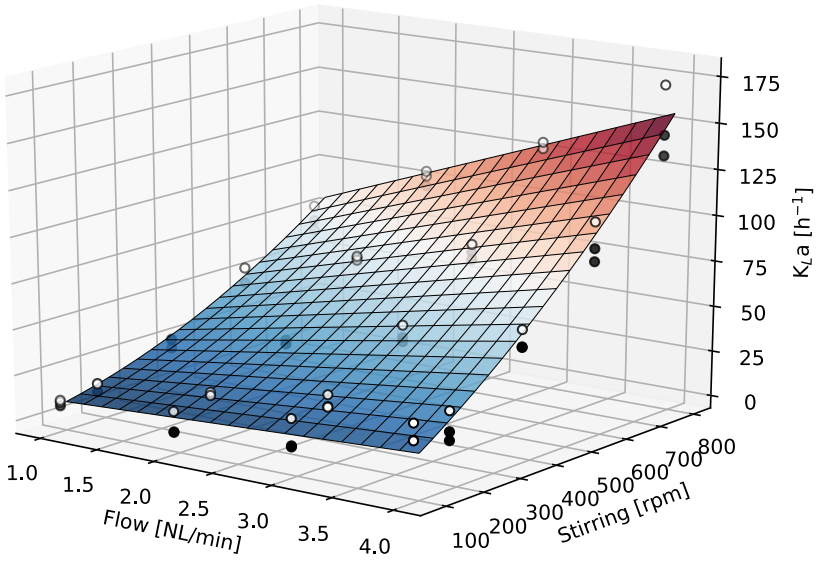

(a) Resulting model

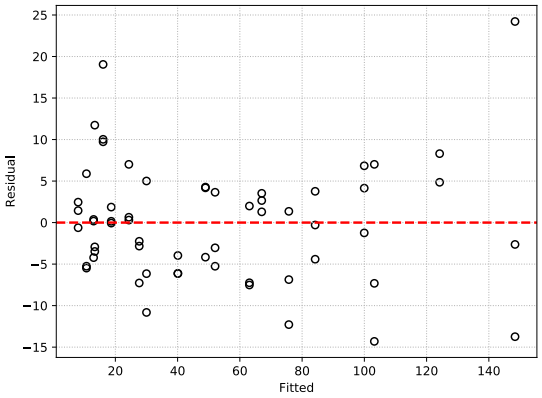

(b) Model residuals versus fitted values

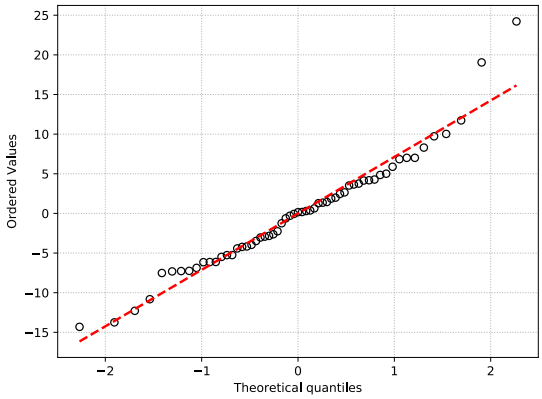

(c) QQ plot of the residuals

Figure B.4: Results of the multivariate linear regression of k_La as a function of stirring and air flow rates

Table B.III: Results of the k_La model's parameter estimation
$R^2 = 0,969$; $p_{value} = 5.70 \cdot 10^{-43}$

	Estimation	Std. Err.	p_{value}	$[0,025$	$0.975]$
β_0	4.8	1.5	$2.1 \cdot 10^{-3}$	1.8	7.8
β_1	$7.9 \cdot 10^{-5}$	$6.5 \cdot 10^{-6}$	$2.1 \cdot 10^{-17}$	$6.7 \cdot 10^{-5}$	$9.2 \cdot 10^{-5}$
β_2	$3.2 \cdot 10^{-2}$	$1.7 \cdot 10^{-3}$	$3.4 \cdot 10^{-25}$	$2.8 \cdot 10^{-2}$	$3.5 \cdot 10^{-2}$

C Python script for parameter estimation

```
# -*- coding: utf-8 -*-
"""
Created on Mon Aug 26 19:35:03 2019

@author: Florence
"""

# Libraries
import pandas              as pd
import numpy               as np
from scipy.optimize        import curve_fit
from scipy.integrate       import solve_ivp

# Useful functions
def gompertz(x, lda, mu_max, A):
    '''Gompertz model, as modified by Zwietering et al. (1990)'''
    return A * np.exp(- 1 * np.exp((mu_max * np.exp(1) * (lda - x) / A) + 1))

def d_gompertz(x, lda, mu_max, A):
    '''Time derivative of Gompertz model'''
    return mu_max * np.exp(1 + (1 + mu_max * np.exp(1) * (lda - x) / A) - np.exp(1 + mu_max * np.
        ↪ exp(1) * (lda - x) / A))

def expo(x, a, b):
    '''Increasing exponential'''
    return a * (1 - np.exp(- b * x))

def expo2(x, a, b, c):
    '''Decreasing exponential function'''
    return a - (b * (1 - np.exp(- c * x)))

def sigmo(x, a, b, c, d):
    '''Decreasing sigmoid function'''
    return a + b*(1-1/(1+np.exp(-c*x+d)))

def debit(V, t):
    '''Take a cumulated volume as argument
       Returns the corresponding flow rate'''
    Q = np.array([0])
    for i in np.arange(1, len(t)-1,1):
        Q = np.append(Q, (V[i+1] - V[i-1])/(t[i+1] - t[i-1]))
    Q = np.append(Q, Q[-1])
    Q[0] = Q[1]
    return Q

def bioreacteur(t,y,InterpData,Ks0,Ks1,pi0_max,pi1_max,Ki0,Ki1,n0,n1,Yxs1,mu_max,Ks1x,Ki1x,nx):
    """
    Function describing the variables in the bioreactor
    """

    # Variables notation for better clarity
    P0 = y[0]
    P1 = y[1]
    V = y[2]
    S1 = y[3]
    X = y[4]

    # Values to be interpolated
    Q_in_interp   = np.interp(t, InterpData['Time'], InterpData['Q_in'])
    Q_out_interp  = np.interp(t, InterpData['Time'], InterpData['Q_out'])
    Q_out2_interp = np.interp(t, InterpData['Time'], InterpData['Q_out2'])

    D_in   = Q_in_interp / V
    D_out  = Q_out_interp / V
    D_out2 = Q_out2_interp / V

```

```
66      # mu calculation
67      mu = mu_max * (S1/(Ks1x + S1)) * (1 / (1+(P1/Ki1x)**nx))
68
69      # pi0 and pi1 calculation
70      pi0 = pi0_max * S1 / (Ks0 + S1) * (1 / (1+(P1/Ki0)**n0))
71      pi1 = pi1_max * P0 / (Ks1 + P0) * (1 / (1+(P1/Ki1)**n1))
72
73      dXdt = mu * X - X * (D_in - D_out)
74
75      # ODE system
76      n = len(y)
77      dydt = np.zeros((n,1))
78      dydt[0] = (pi0 - (pi1/Yp1p0)) * X - P0 * (D_in-D_out)          # 3-HPA
79      dydt[1] = pi1 * X  - P1 * (D_in-D_out)                         # 3-HP
80      dydt[2] = (D_in - D_out - D_out2)*V                            # Working volume
81      dydt[3] = D_in * 5.96 - (pi0/Yp0s1) * X - S1 * (D_in - D_out) - (1/Yxs1) * mu * X   # 1,3-PDO
82      dydt[4] = dXdt                                                 # Biomasse
83
84      return dydt
85
86  def bioreacteurINT(T,Ks1x,Ki1x,mu_max,nx,Yxs1,Ki0,Ki1,pi0_max,pi1_max,n0,n1,Ks0,Ks1):
87
88      Ypred = np.array([])
89
90      for label in ManipFB.keys():
91
92          manip = ManipFB_BIOCONV[label]
93          off_line = ManipFB_OFFLINE[label]
94
95          Y0 = [0, 0, manip['V_U [mL]'][0]/1000, off_line['1,3-PDO [mol/L]'][0], manip['DW [Cmol/L]
                ↪ '][0]] # Initial values
96          T_eval = manip.dropna(subset=['1,3-PDO [mol]'])['Bioconv_Time [h]']
97          t_f = max(T_eval)
98
99          solver = solve_ivp(fun=lambda t, y: bioreacteur(t, y, ManipFB_INTERP[label], Ks0, Ks1,
                ↪ pi0_max, pi1_max, Ki0, Ki1, n0, n1, Yxs1, mu_max, Ks1x, Ki1x, nx), t_span=(0,t_f),
                ↪  y0=Y0, rtol=1E-6, t_eval = T_eval, vectorized=True,method='LSODA')
100
101         Y_cond = np.concatenate((solver.y[0]/wp0, solver.y[1]/wp1, solver.y[3]/ws1, solver.y[4]/
                ↪ wx))
102         Ypred = np.concatenate((Ypred,Y_cond))
103
104     return Ypred
105
106 ###########################################################################
107 ###########################################################################
108 if __name__ == '__main__':
109
110     # Fixed Parameters
111     Yp0s1 = 1
112     Yp1p0 = 1
113
114     # Weightings
115     ws1 = 0.1
116     wp0 = 0.1
117     wp1 = 1
118     wx = 0.1
119
120     ###########################################################################
121     # Data import
122
123     wd = 'ManipFB.xlsx'
124
125     FB_D = pd.read_excel(wd, 'FB_D', header = 0, index_col=0, skiprows=1)
126     FB_H = pd.read_excel(wd, 'FB_H', header = 0, index_col=0, skiprows=1)
127     FB_K = pd.read_excel(wd, 'FB_K', header = 0, index_col=0, skiprows=1)
128     FB_L = pd.read_excel(wd, 'FB_L', header = 0, index_col=0, skiprows=1)
129
130     ManipFB = {'FB_D':FB_D, 'FB_H':FB_H, 'FB_K':FB_K, 'FB_L':FB_L}
131
132     ManipFB_OFFLINE = dict.fromkeys(ManipFB.keys()) # Dict. containing off-line experimental data
            ↪ only of each experiment
133     ManipFB_BIOCONV = dict.fromkeys(ManipFB.keys()) # Dict. containing all experimental data of
            ↪ each experiment
134
135     for label in ManipFB.keys():
```

```
136         manip = ManipFB[label]
137         print('Data prep on Manip_'+manip.index[0][3])
138 
139         Drop = [x[0]=='_' for x in manip.index]
140         manip.drop(manip[Drop].index , inplace=True)
141 
142         manip = manip[(manip['Bioconv_Time [h]']<30)&(manip['Bioconv_Time [h]']>=0)]
143         ManipFB_BIOCONV[label] = manip
144 
145         off_line = manip.dropna(subset=['3-HP [mol]', '1,3-PDO [mol]', '3-HPA [mol]'])
146         ManipFB_OFFLINE[label] = off_line
147 
148     ##########################################################################
149     # Creation of Ymes, the vector containing the experimental data and TIME, its associated time
            ↪ vector
150 
151     Ymes = np.array([]) # initialisation
152     TIME = np.array([])
153 
154     for label in ManipFB.keys():
155         manip = ManipFB_BIOCONV[label]
156         off_line = ManipFB_OFFLINE[label]
157         print('Ymes prep on Manip_'+manip.index[0][3])
158 
159         TIME = np.concatenate((TIME, off_line['Bioconv_Time [h]'], off_line['Bioconv_Time [h]'],
                ↪ off_line['Bioconv_Time [h]']))
160 
161         Ycond = np.concatenate((off_line['3-HPA [mol/L]']/wp0, off_line['3-HP [mol/L]']/wp1,
                ↪ off_line['1,3-PDO [mol/L]']/ws1, off_line['DW [Cmol/L]']/wx))
162         Ymes = np.concatenate((Ymes, Ycond))
163 
164     ##########################################################################
165     # Computation of variables that are fitted or interpolated from experimental data
166     # This includes biomass (X), input flow rate (Q_in) and output low rates (Q_out and Q_out2)
167 
168     ManipFB_INTERP = dict.fromkeys(ManipFB.keys())  # initialisation
169 
170     for label in ManipFB.keys():
171         manip = ManipFB_BIOCONV[label]
172         off_line = ManipFB_OFFLINE[label]
173         print('Data interp on Manip_'+manip.index[0][3])
174 
175         # Creation of a time vector from 0 h to end of bioconversion, with a 0.01 time step
176         t_f = round(np.max(manip['Bioconv_Time [h]']),0)+1
177         Time    = np.arange(0,t_f,0.01)
178 
179         # Gompertz fitting to biomass data
180         Xpopt, Xpcov = curve_fit(gompertz, off_line['Bioconv_Time [h]'], off_line['DW [Cmol/L]'],
                ↪ p0 = (0,0.2,off_line['DW [Cmol/L]'][-1]))
181         X = gompertz(Time, *Xpopt)
182         dXdt = d_gompertz(Time, *Xpopt)
183 
184         # Input and output flow rates computation
185         Temp = manip.sort_values('Bioconv_Time [h]')  # Values have to be sorted in chronological
186         Temp2 = Temp.dropna(subset = ['V_feed [mL]']) # Rows with empty 'V_feed' values are
                ↪ removed
187 
188         V_in_popt, V_in_pcov = curve_fit(expo, Temp2['Bioconv_Time [h]'], Temp2['V_feed [mL]'])
189         V_in = expo(Time, *V_in_popt)
190         V_out2 = np.interp(Time, manip.dropna(subset=['V_sample_Sum [mL]'])['Bioconv_Time [h]'],
                ↪ manip.dropna(subset=['V_sample_Sum [mL]'])['V_sample_Sum [mL]'])
191 
192         Q_in = debit(V_in, Time)/1000
193         V_out = np.interp(Time, manip['Bioconv_Time [h]'], manip['V_evap [mL]'])
194         Q_out = debit(V_out, Time)/1000
195         Q_out2 = debit(V_out2, Time)/1000
196 
197         # Fitted and interpolated data are gathered in a dict.
198         manip_interp = {'Time':Time, 'Biomass':X, 'dXdt':dXdt, 'Q_in':Q_in, 'Q_out':Q_out, '
                ↪ Q_out2':Q_out2, 'V_in':V_in, 'V_out':V_out, 'V_out2':V_out2}
199         ManipFB_INTERP[label] = manip_interp
200 
201     ##########################################################################
202     # Local Optimisation
203     p0 = 0.215495, 0.17923512, 0.67815431, 4.19179422, 2.7315596 , 0.32115771, 0.52910194,
            ↪ 2.06219012, 28.49357468, 0.74193362, 4.29421035, 0.08847711, 0.11685678
```

```
204     POPT, PCOV = curve_fit(bioreacteurINT, TIME, Ymes, p0, bounds=[1E-6,30], diff_step=1E-4,
            ↪ verbose=2)
205
206     Ks1x = POPT[0]
207     Ki1x = POPT[1]
208     mu_max = POPT[2]
209     nx = POPT[3]
210     Yxs1 = POPT[4]
211     Ki0 = POPT[5]
212     Ki1 = POPT[6]
213     pi0_max = POPT[7]
214     pi1_max = POPT[8]
215     n0 = POPT[9]
216     n1 = POPT[10]
217     Ks0 = POPT[11]
218     Ks1 = POPT[12]
219
220     # Fitting evaluation
221     Diag    = np.diag(PCOV)
222     ErStd   = np.sqrt(Diag)                    # Standard Error
223     CoefVar = np.round(ErStd / POPT * 100,1) # Variation Coefficients
224     D       = np.diag(1/ErStd)
225     Corr    = D@PCOV@D                         # Correlation Matrix
```

Titre : Étude et contrôle de la production de l'acide 3-hydroxypropionique par une bactérie acétique dans un contexte de bioconversion extractive
Mots clés : Chimie verte, *Acetobacter* sp., Procédé intégré, Building-block

Résumé : Compte tenu de la nécessité pour les industries de réduire leur dépendance aux ressources fossiles, la demande pour des molécules plateformes bio-sourcées augmente continuellement. En particulier, l'acide 3-hydroxypropionique (3-HP) fait partie des molécules les plus prometteuses pouvant être obtenues à partir de biomasse. Ce n'est que récemment que des procédés intégrés incluant à la fois la production bactérienne et l'extraction *in situ* de la molécule ciblée ont été développés pour produire du 3-HP. L'amélioration du contrôle de ces procédés demeure un enjeu important, passant notamment par une meilleure compréhension du comportement des micro-organismes impliqués. Ainsi, ce projet vise à comprendre les réponses métaboliques et physiologiques d'*Acetobacter* sp. CIP 58.66 lors de son utilisation dans un bioprocédé intégré pour la production de 3-HP. Des cultures semi-continues de la souche ont d'abord été mises en oeuvre et ont montré son potentiel comme agent de production de 3-HP dans différentes conditions opératoires. Par la suite, une bioconversion extractive – c'est-à-dire une bioconversion couplée au procédé d'extraction liquide-liquide réactive sélectionné par ailleurs – a été mise en oeuvre, démontrant ainsi la faisabilité du procédé intégré. Parallèlement, les données de cultures acquises ont été utilisées dans le développement d'un modèle cinétique du procédé. Modèle qui servira ensuite à mieux décrire les phénomènes bactériens et à définir une stratégie efficace pour le contrôle du procédé.

Title: Study and control of the production of 3-hydroxypropionic acid by an acetic acid bacterium in the context of extractive bioconversion
Key-words: Green Chemistry, *Acetobacter* sp., Integrated process, Building-block

Abstract: In a context where industries need to reduce their dependency on fossil feedstocks, demand for bio-based chemicals is steadily increasing. Notably, 3-hydroxypropionic acid (3-HP) has been identified as one of the most promising value-added chemicals that can be obtained from biomass. Integrated bioprocesses comprising up-stream biological production and *in situ* recovery of the targeted molecule have only recently been investigated to produce 3-HP. Challenges still lie in improving these processes' control, through better understanding the behaviour of the involved microorganisms. Thus, this project aims at understanding the metabolic and physiological responses of *Acetobacter* sp. CIP 58.66 during its implementation in an integrated bioprocess producing 3-HP. First, fed-batch cultures were carried out and showed the strain's potential as 3-HP producing agent in several operating strategies. Then, extractive bioconversions (i.e. bioconversions integrated with the selected reactive liquid-liquid downstream process) were successfully performed, thus validating the proof-of-concept. Meanwhile, measured culture parameters were used in the implementation of a kinetic model of the process. The model's outputs will help better understanding the microbial phenomena as well as help designing an efficient process control.

Université Paris-Saclay
Espace Technologique / Immeuble Discovery
Route de l'Orme aux Merisiers RD 128 / 91190 Saint-Aubin, France